University of Alberta

Origin of island dolostones: case study based on Tertiary dolostones from Cayman Brac, British West Indies

by

Hongwen Zhao

A thesis submitted to the Faculty of Graduate Studies and Research
in partial fulfillment of the requirements for the degree of

Doctor of Philosophy

Department of Earth and Atmospheric Sciences

Spring 2013
Edmonton, Alberta

ABSTRACT

Cayman Brac (19 km long, 1.5 to 3 km wide), which is the easternmost of the Cayman Islands, is characterized by a thick Tertiary carbonate succession that has been pervasively dolomitized. The finely crystalline dolostones in the Cayman Formation (Miocene) are fabric-retentive whereas the coarse, sucrosic dolostones in the Brac Formation (Lower Oligocene) are mostly fabric-destructive.

Analyses of these dolostones indicate that (1) the dolostones are formed of various mixtures of low-Ca calcian dolomite (LCD – < 55 mol% $CaCO_3$) and high-Ca Calcian dolomite (HCD – > 55 mol% $CaCO_3$), (2) their geochemical signatures (e.g., $\delta^{18}O$ and Sr) are heavily influenced by the dolomite stoichiometry, (3) the $^{87}Sr/^{86}Sr$ ratios point to two phases of dolomitization with Phase I (Late Miocene, 6-8 Ma) that caused partial dolomitization of the upper part of the Brac Formation and basal part of the Cayman Formation and Phase II (Pliocene to Early Pleistocene, 1-5 Ma), that completed dolomitization of the Cayman Formation. Interpretation of these data indicates that dolomitization was probably linked to sea level fluctuations whereas the distribution of the dolomite and evolution of their textures was controlled largely by permeability pathways that governed circulation patterns of the dolomitizing fluids. The large sucrosic dolomite crystals in the Brac Formation probably developed as a result of repeated cycles of limestone matrix dissolution and dolomite precipitation.

Rare earth elements (REE) and yttrium (Y) concentrations of carbonates from Cayman Brac are characterized by (1) LREE depletion relative to HREE, (2) positive La anomalies, (3) negative Ce anomalies, and (4) superchondritic Y/Ho molar ratios. Dolomitization did not have a major impact on their REE +Y signatures, which indicates that the dolomitization was probably mediated by seawater-like fluids. The variations in Dy_N/Sm_N, La_N/Nd_N, Ce/Ce*, and Y/Ho

with depth reflect the influences of the diagenetic processes (e.g., Dy_N/Sm_N) and possibly, secular changes in the REE+Y composition of seawater (e.g., La_N/Nd_N, Y/Ho, and Sm/Nd) on the REE+Y signature of carbonates.

ACKNOWLEDGEMENTS

A number of people who made my thesis research possible have to be thanked for their support during the project.

Firstly, I am greatly indebted to my supervisor Dr. Brian Jones for his advice, constructive criticism, encouragement, patience, and countless hours of editing the thesis. Without his help, I would never reach the current point to get the thesis in shape.

Secondly, I would also like to express my thanks to Dr. K. Muehlenbachs for providing his laboratory for the stable isotope analyses, Dr. S. Matveev who helped for the Electron Microprobe analyses, Mr. Guangcheng Chen who ran the ICP-MS analyses, Mrs. Diane Caird, who ran the XRD analyses, and Mr. George Braybrook who took the SEM photomicrographs used in this study.

I would also like to thank the Natural Sciences and Engineering Research Council of Canada, which funded this research (grants A6090 to Jones), Hendrik van Genderen, Water Authority, Cayman Islands, who helped collect many of the samples used in this study.

It has been a pleasure to work with various members of the carbonate research group – Breanna Uzelman, Hilary Corlett, Josh Thomas, Alexandra Der, Rong Li, and Ting Liang. It was enjoyable to share the lab with them.

Finally, I would like to thank my wife, Xuefeng Duo, and my parents for their support and encouragement throughout my thesis research.

TABLE OF CONTENTS

LIST OF TABLES

LIST OF FIGURES

CHAPTER 1
INTRODUCTION

1.1. Introduction

Sedimentologists have been puzzled by the “simple” mineral dolomite for more than 200 years since Déodat de Dolomieu first described it in 1791. Although a common mineral in the rock record, dolomite is rare in modern sediments in comparison with aragonite and calcite. In the laboratory, dolomite cannot be synthesized under the earth surface conditions without bacteria being present (e.g., Land, 1998; Vasconcelos et al., 2005). Nevertheless, dolomite is a common component of many ancient carbonate rocks and many thick, aerially extensions ancient platform successions are formed largely of dolostones(Sun, 1994). This is the so-called “dolomite problem”.

Attempts to resolve the dolomite problem have taken both laboratory- and field-based approaches. Since 1960, many laboratory experiments operating under high temperature conditions (Northrop and Clayton, 1966; O›Neil and Epstein, 1966; Clayton et al., 1968; Matthews and Katz, 1977) or in the presence of bacteria (Vasconcelos et al., 2005) have tried to resolve the fundamental factors that are responsible for triggering the formation of dolomite as well as the chemical, crystallographic evolution of dolomite crystals through the dolomitization process. Considerably more research, however, has been focused on the dolomite-bearing sediments or rocks in order to determine their origin through interpretation of their petrographic, crystallographic, geochemical, and biochemical characters (Land, 1980; Morrow, 1982a, b; Machel and Mountjoy, 1986; Hardie, 1987; Budd, 1997; Warren, 2000; Machel, 2004). This approach, however, relies heavily on our understanding of the geochemical features of dolomites (e.g., carbon and oxygen stable isotopes, trace elements). Interpretation

of these geochemical data, however, is commonly hindered by: (1) the behaviour of stable isotopes and trace elements in the dolomitizing system that are poorly constrained because dolomite cannot be grown in the laboratories under ambient conditions, and (2) ancient dolostones have been diagenetically altered (e.g., recrystallization) and no longer have their original geochemical signatures.

In order to minimize the influence of post-depositional diagenesis on the geochemical signatures of dolostones as much as possible, research must focus on dolostone successions that have been carefully selected. Thick successions of Cenozoic dolostones, found on many tropical islands and atolls in the Caribbean Sea and Pacific Ocean, have been referred to "islands dolostones" (Budd, 1997). They are ideal candidates for addressing the "dolomite problem" because the dolomites developed in isolated diagenetic environments, have experienced a short diagenetic history, and have never been buried (cf. Budd, 1997). Theses successions developed on islands that are isolated by the deep ocean waters that surround them.

On Cayman Brac, one of the Cayman Islands located in the Caribbean Sea (Fig. 1-1), there is a thick (> 150 m) Oligocene to Pliocene carbonate succession that has been dolomitized to varying degrees (Jones et al., 1994a, b; MacNeil, 2001; MacNeil and Jones, 2003; Uzelman, 2009). The dolostones on Cayman Brac share many of the traits that are associated with other island dolostones. This location is ideal for research purposes because the carbonate succession is well exposed in cliff faces and quarries and has been penetrated by numerous wells, to a depth of ~ 60 m, across the island. In addition, the stratigraphy and sedimentology of this succession has been well-established by previous research (e.g., Jones and Hunter, 1994; Jones et al., 1994a, b; MacNeil, 2001; MacNeil and Jones, 2003; Uzelman, 2009).

This study focuses on the Tertiary carbonate succession found on Cayman

Brac with a view of deciphering the origin of massive island dolomite, the timing of dolomitization, and the factors that controlled the petrographic, geochemical, and crystallographic features of the dolostones. In order to achieve this goal, a multiple-discipline approach that integrates various aspects of sedimentology, petrography, geochemistry, and crystallography is adopted.

1.2. Study area and methods

1.2.1. Study area

Cayman Brac, which is one of the three Cayman Islands, is 19 km long and 1.5 to 3.0 km wide. The island is located in the Caribbean Sea, approximately 240 km south of Cuba and 290 km northwest of Jamaica (Fig. 1-1). Tectonically, Cayman Brac is located on the Cayman Ridge, which parallels the Oriente Transform Fault that delineates the boundary between the Caribbean Plate and the North American Plate (Fig. 1-2). The Mid-Cayman Rise, which is an active spreading centre, is located off the southwest corner of Grand Cayman (Fig. 1-2). The Oriente Transform Fault extends eastward from the north end of the spreading center, whereas the Swan Islands Transform Fault extends westward from it south end (Fig. 1-2). The Cayman Trench (also known as the Bartlett Trough), located to the south of the Cayman Islands, is a complex transform fault zone pull apart basin with a maximum water depth of 7686 m. Each of the Cayman Islands is probably located on different fault blocks on the Cayman Ridge, which extends from the Sierra Maestra of southern Cuba westward towards Honduras (Fig. 1-2). The transform fault is characterized by left-lateral motion of the North American Plate relative to the Caribbean Plate (Perfit and Heezen, 1978). This area has been tectonically active since the Late Eocene (Rosencrantz and Sclater, 1986; Leroy et al., 2000). Recent GPS measurements and seismic data indicate that this area is still tectonically active (DeMets and Wiggins-Grandison, 2007). The

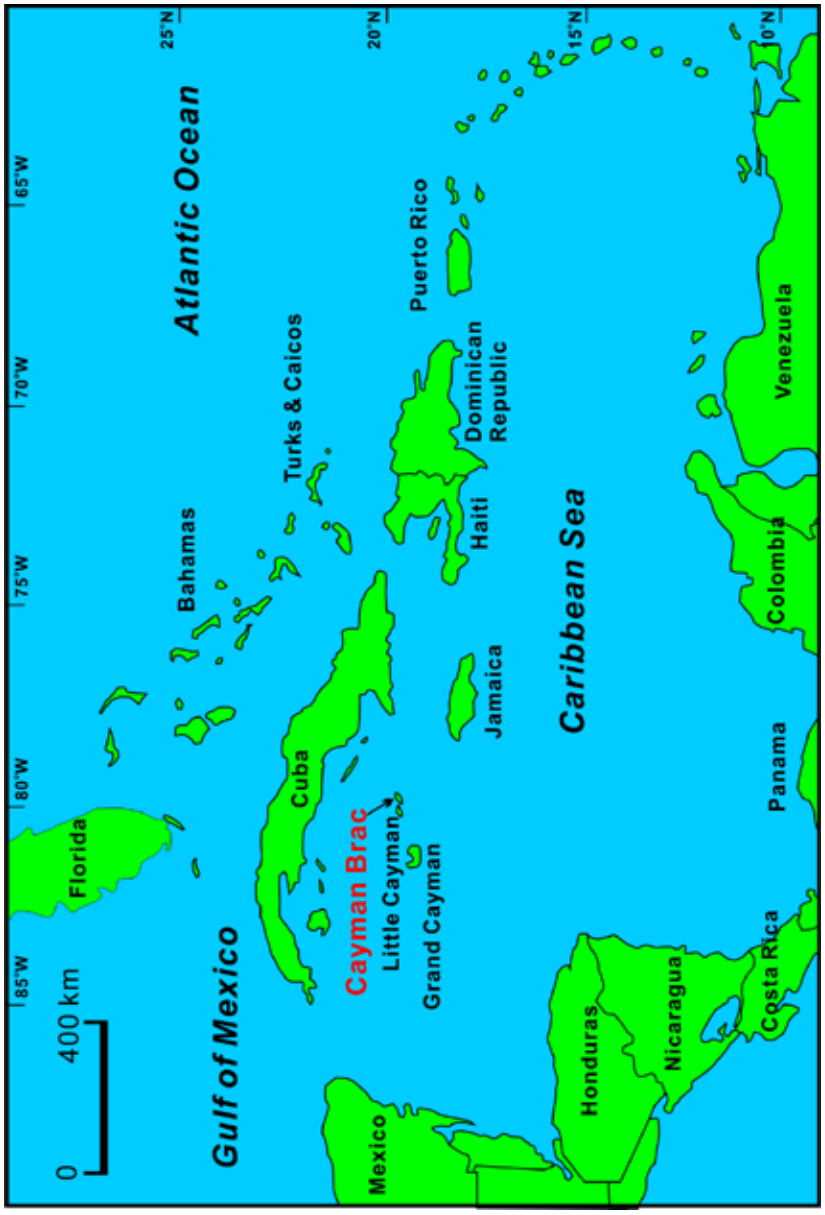

Fig. 1-1. Map of the Caribbean Area showing the location of Cayman Brac

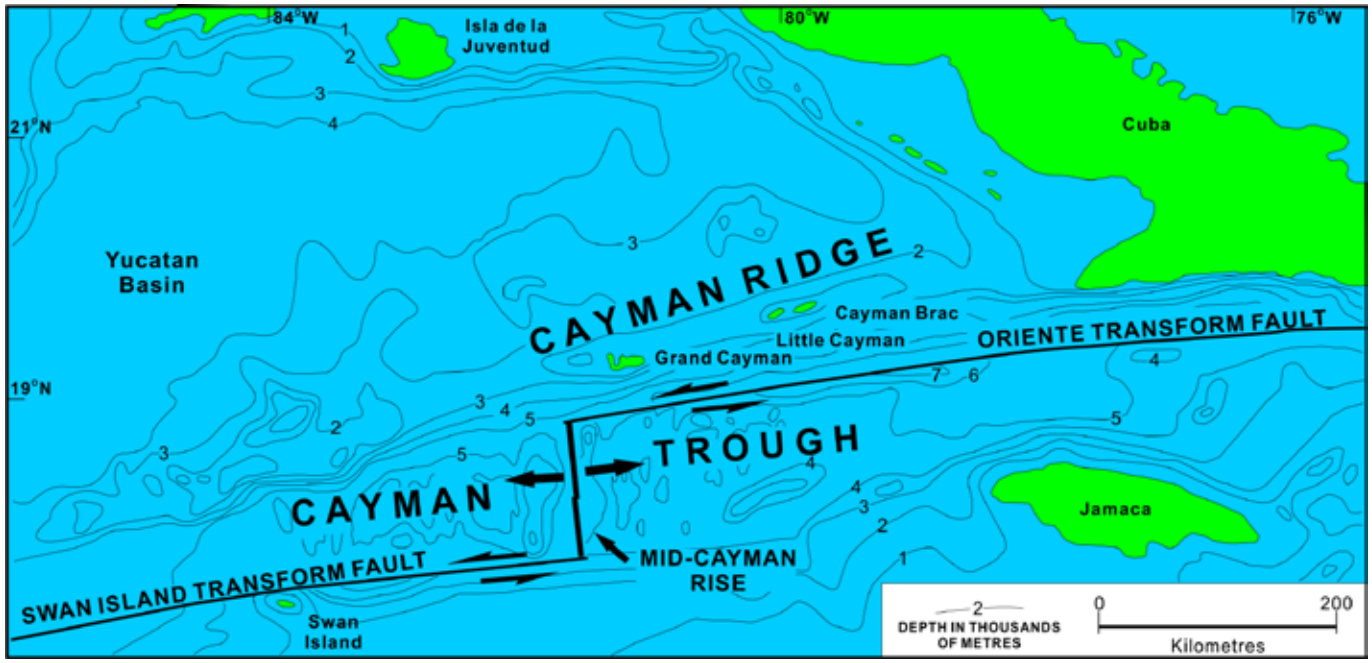

Fig. 1-2. Tectonic and bathymetric setting of the Cayman Islands. Modified from Jones (1994) and based on maps from Perfit and Heezen (1978) and MacDonald and Holcombe (1978)

Mid-Cayman spreading centre is opening at an average rate of ~11-12 mm yr^{-1} (Rosencrantz and Sclater, 1986; Mann et al., 2002).

On Cayman Brac, which rises 1500 – 2000 m above the seafloor, the carbonate succession sits on a foundation formed of igneous rocks (Emery and Milliman, 1980; Stoddart, 1980). Although the thickness of carbonate cap is not known, it is at least 150 m thick (Jones et al., 1994a, b). The carbonate succession is composed of four unconformity-bound packages: the Brac Formation (Low Oligocene), the Cayman Formation (Middle Miocene), the Pedro Castle Formation (Pliocene), and the Ironshore Formation (Pleistocene). The Brac Formation, Cayman Formation, and Pedro Castle Formation collectively form the Bluff Group (Fig. 1-3A). Although dolomite is widespread in the Bluff Group, it has not been found in the limestones of the Ironshore Formation (Fig. 1-3A, B). The carbonate strata were uplifted and tilted after deposition of the Bluff Group but before deposition of the Ironshore Formation so that they now dip at about 0.5^{o} to the west. The surface of the island slopes gradually westward, from about 43 m above sea level at the northeastern end to sea level at the southeastern end (Fig. 1-3C). Late Pleistocene limestones form a low-lying platform that abuts against the limestones and dolostones of the Bluff Group (Fig. 1-3B).

1.2.2. Methods

Samples used in this study were collected from wells BW#1, SQW#1, CRQ#1 and KEL#1 and exposures above CRQ#1 and KEL#1, and outcrops SCD, WOJ#3 and WOJ#7 on the eastern end of the island (Fig. 1-3B, C). Dr. Brian Jones collected the samples from wells, which were drilled between 2003 and 2004. He also collected the samples from section SCD, whereas those from WOJ#3 and WOJ#7 were collected by Mr. Michael Wojcik. These sections are located so that different parts of the carbonate successions can be sampled due to the tilting of the island (Fig. 1-3C). Samples of well cuttings were collected over

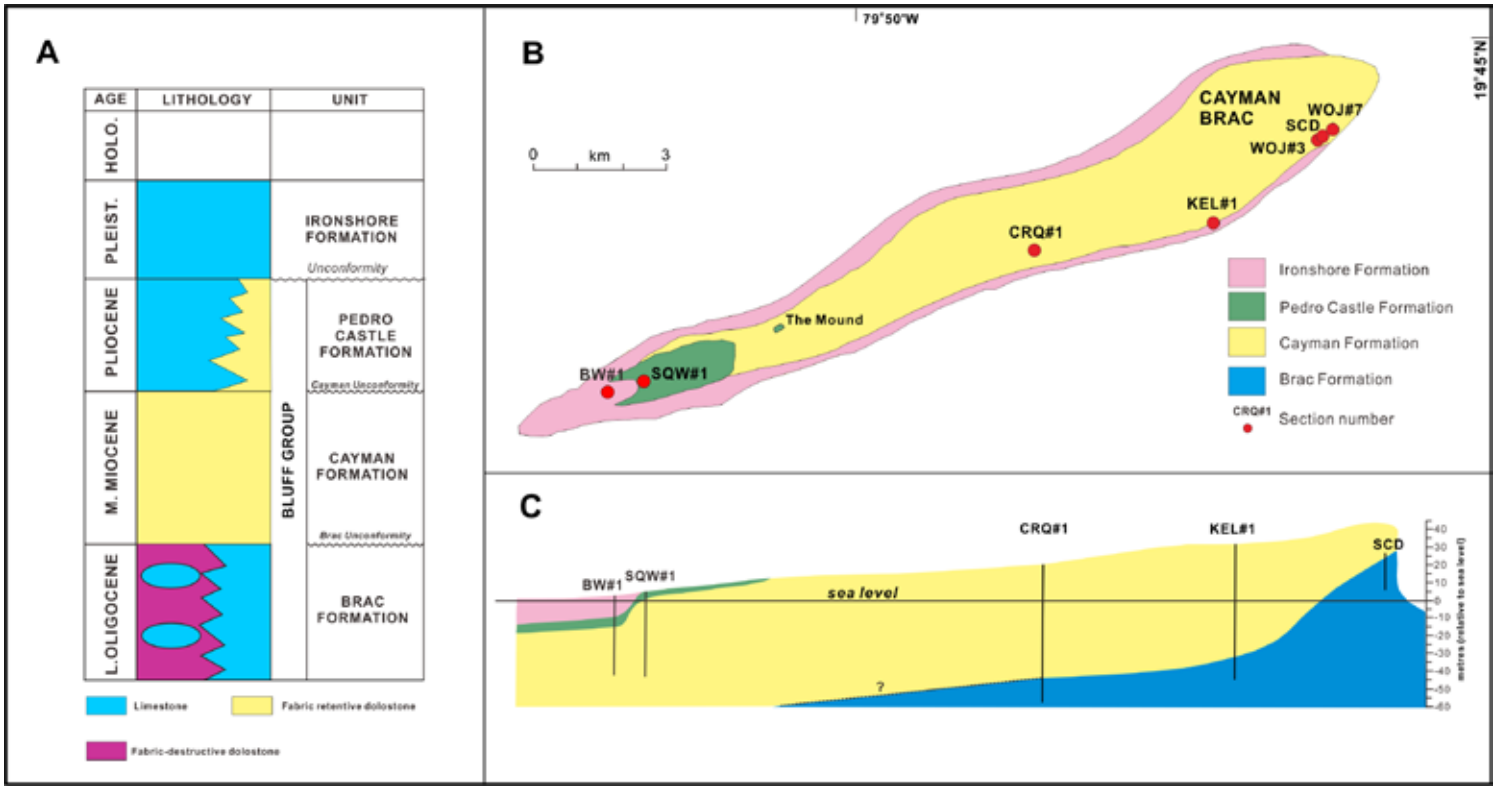

Fig. 1-3. Stratigraphy and geological map of Cayman Brac. (A) Stratigraphic succession on Cayman Brac (modified from Jones, 1994) showing distribution of dolostones and limestones B) Geologic map of Cayman Brac (modified from Jones, 1994) showing locations of wells and outcrops. (C) Cross section through Cayman Brac (modified from Jones, 2005)

0.75 m intervals. Samples collected from outcrop, which are generally hand-sized pieces of unweathered dolostones, were collected at 1 m intervals. Seventy-five samples were used for the Brac Formation whereas 235 samples were used for the Cayman Formation. Little attention was focused on the Pedro Castle Formation because that succession had already been examined in detailed by MacNeil (2001) and MacNeil and Jones (2003). Seven samples were, however, collected from the Pedro Castle Formation and the Iron Formation for rare earth elements (REE) analysis. In addition, for comparison purpose, five samples from the Ironshore Formation (coral and matrix) and two samples of limestone from the Cayman Formation were collected from wells RWP#11 and NSC#1 on Grand Cayman.

The petrography of dolostones were established by standard thin-section techniques, with each thin section being impregnated with blue epoxy and stained with Alizarin Red-S solution. Selected polished samples were also subjected to cathodoluminescent petrography. Scanning electron microscopy (SEM) was used to examine the microstructure of dolomite crystals and backscatter electron images (BSEI) were used to examine the spatial distribution of dolomite crystal populations based on differences in their %Ca (molar Ca/(Ca+Mg) × 100)

The mineralogy of the samples was established by X-ray diffraction analysis (XRD) using the techniques and protocol developed by Jones et al. (2001). For samples containing dolomite, the molar %$CaCO_3$ of the dolomite was determined. Following Jones et al. (2001), the dolomite is divided into low-Ca calcian dolomite (LCD – 50-55 %Ca) and high-Ca calcian dolomite (HCD – 55-62 %Ca). The weight % of LCD, weight % of HCD, and the average %Ca were calculated using the methods outlined by Jones et al. (2001).

The samples formed of 100% dolomite were analyzed for carbon and oxygen stable isotopes by the standard phosphoric acid dissolution method following McCrea (1950). Selected samples were analyzed for their strontium isototpes and

trace element contents (Sr, Mn, Fe, rare earth elements). The detailed technical parameters for each method of analysis are provided in the appropriate chapters.

1.3. Previous researches

1.3.1. Stratigraphy and lithological facies

Until 25 years ago, the geology of Cayman Islands had only been studied in general terms (Matley, 1926; Moore, 1973; Roberts, 1977). Matley (1926) originally named the Bluff Limestone for the massive, crystalline, hard carbonates found on Cayman Brac. Based on Lepidocyclina found in the limestones on the northeast coast of Cayman Brac, he assigned a Middle Oligocene age to the strata. The limestone succession (Pleistocene) that unconformably overlies upon the Bluff Limestone, was named the Ironshore Formation (Matley, 1926). It was subsequently realized, however, that much of the Bluff Limestone had been intensely dolomitized (Jones et al., 1984; Pleydell, 1987; Jones and Hunter, 1989). Jones and Hunter (1989) therefore used the term Bluff Formation in order to remove the lithological connotation that was attached to the Bluff Limestone. Two unconformity-bounded packages in the Bluff Formation found on Grand Cayman were named as Cayman Member and Pedro Castle Member (Jones and Hunter, 1989). After extensive outcrop analysis on Cayman Brac, Jones et al. (1994b) defined the Lepidocyclina-rich limestone and dolostone section exposed along the cliff faces on the eastern end of Cayman Brac as the Brac Formation. Jones et al. (1994a) then elevated the Cayman Member and the Pedro Castle Member to formation status. They also gave the Bluff Formation group status and assigned the Brac Formation, the Cayman Formation, and the Pedro Castle Formation to it. Based on fossils and Sr isotope data, they argued that these formations were early Oligocene, middle Miocene, and Pliocene in age, respectively (Fig. 1-3A). For ease of communication, the unconformity between

the Brac Formation and Cayman Formation is called the Brac Unconformity whereas the unconformity that separates the Pedro Castle Formation from the underlying Cayman Formation is called the Cayman Unconformity. The Brac Unconformity developed during the late Oligocene and early Miocene whereas the Cayman unconformity developed during late Miocene and possibly early Pliocene times (Jones et al., 1994b).

The lithological characteristics and depositional environments of the Tertiary carbonates on Cayman Brac have been outlined by Jones et al., (1994b), Jones and Hunter (1994), MacNeil (2001), and Uzelman (2009). The following descriptions are summarized from those papers.

1.3.1.1 The Brac Formation

The Brac Formation, exposed on the eastern end of Cayman Brac, is also found in wells CRQ#1, KEL#1, APL#1 and EOR#1. The Brac Unconformity, which forms its upper boundary, is a karst surface with a relief of at least 25 m (Jones et al., 1994b). The thickness of the Brac Formation is unknown because its lower boundary is not exposed and has not been reached by drilling (Jones et al., 1994b; Uzelman, 2009). It is, however, at least 20 m thick.

The Brac Formation is lithologically variable. On the northeast coast, the formation is characterized by limestones formed mainly of bioclastic wackestones to grainstones with minor amount of dolomite (Jones et al., 1994b). Large *Lepidocyclina* (up to 32 mm diameter) dominate the biota along with lesser numbers of other foraminifera (e.g., rotalids, milioilids), red algae, and echinoid plates. Corals, bivalves, and gastropods are absent with the exception of scattered *Porites* fragments found in the uppermost part of the formation. In contrast, on the south coast, the Brac Formation is formed largely of coarsely crystalline fabric-destructive sucrosic dolostone (crystals up to 1.5 mm long). In some areas, pods of fossiliferous limestone (up to 10 m long and 2 m) are encased by

the sucrosic dolostones. The limestone in these pods, which contains numerous *Lepidocyclina* with scattered bivalves (Jones et al., 1994b), is similar to the limestone found on the north coast. In the subsurface, the Brac Formation is formed largely of fossiliferous limestones and dolomitic limestones with lesser amounts of finely to medium crystalline fabric destructive dolostones (Uzelman, 2009). The subsurface limestones are lithologically compatible with ones exposed on the eastern end of Cayman Brac.

According to their lithological and paleontological features, Uzelman (2009) divided the Brac Formation into the (1) *Lepidocyclina* Facies, (2) Mollusc Facies, (3) Foraminifera Facies, (4) Fabric Retentive Finely Crystalline Dolomite Facies, (5) Fabric-destructive Finely Crystalline Dolomite Facies, and (6) Sucrosic Dolomite Facies. Most facies, however, in the Brac Formation are isolated and cannot correlated from section to section (Uzelman, 2009). Based on the biotic assemblages and depositional textures, Jones and Hunter (1994) and Uzelman (2009) suggested that carbonate sediments that now form the Brac Formation were deposited on a shallow carbonate bank (< 10 m) under low to moderate energy conditions.

1.3.1.2. The Cayman Formation

The Cayman Formation, ~100 m thick, is bounded by the Cayman Unconformity and the Brac Unconformity. This formation is widely exposed on Cayman Brac in vertical cliff faces, road cuts, and quarries. Due to the regional tilting of Cayman Brac, the exposed Cayman Formation becomes younger from east to west (Jones et al., 1994b). The Cayman Formation is formed largely of finely crystalline, fabric retentive dolostones that are composed of anhedral to subhedral dolomite crystals. The dolostones commonly contain numerous fossils (e.g. corals, bivalves, gastropods, rhodoliths, *Halimeda* plates, echinoid plates, red algae, and foraminifera) with original depositional textures commonly being

evident. Fossils originally formed of aragonite have been mostly leached out. The precursors limestones were formed largely of wackestones and mudstone with some beds and lenses of rudstone, packstone, and grainstone (Jones and Hunter, 1994). Compared to the Brac Formation, the Cayman Formation is characterized by numerous colonial and branching corals (e.g., *Diploria, Montastrea limbata, M. tampaensis, Siderastrea, Leptoseris, Porites, Stylophora*). There is, however, no evidence of reefal development (Jones and Hunter, 1994). By comparing numerous outcrop sections, Jones et al. (1994b) pointed out that there were no significant variations in the biota and lithology of the Cayman Formation across Cayman Brac.

According to the coral-dominated biota and the depositional textures, Jones and Hunter (1994) suggested that the original sediments that formed the Cayman Formation probably accumulated on a shallow bank with a maximum of water depth of 30 m.

1.3.1.3. The Pedro Castle Formation

The Pedro Castle Formation (6 – 20 m thick), which is separated from the underlying Cayman Formation by the Cayman Unconformity (Jones et al. 1994b), is only found on the western end of Cayman Brac (Fig. 1-3B). This formation is formed of limestones, dolomitic limestones, and dolostones (Jones et al., 1994b; MacNeil, 2001). The dolomite content tends to decrease from bottom to top (MacNeil and Jones, 2003). The finely crystalline, fabric retentive dolostones from the Pedro Castle Formation are similar to those found in the underlying Cayman Formation. The biota in the Pedro Castle Formation includes bivalves, gastropods, foraminifera (predominantly *Archaias angulate, Amphistegina sp*., *Globorotalia sp)*, red algae, and scattered corals. Although this biota is similar to that in the underlying Cayman Formation, corals tend to be less numerous. As in the Cayman Formation, there is no evidence of reefal development. Based on

the lithological and paleontological characteristics, MacNeil (2001) divided the carbonates of the Pedro Castle Formation into the Sandy Facies Association and the Coral Facies Association. These associations were divided them into the (1) Echinoid – Red Algae Facies, (2) Algae – Mollusc Facies, (3) Red Algae Facies, (4) Rhodolite Facies, (5) Foram – Mollusc Facies, (6) Foraminifera Facies, and (7) Coral Facies. These facies were probably deposited in a shallow marine environment (< 20 m) with moderate to low energy conditions (MacNeil, 2001).

1.3.1.4. The Ironshore Formation

The Ironshore Formation forms a coastal platform around Cayman Brac (Fig. 1-3B). These limestones, which are commonly coral-rich, are still formed largely of aragonite. No dolomite has been found in this formation. On Cayman Brac, the exposed part of the Ironshore Formation probably belongs to Unit D (Coyne and Jones, 2007), which was deposited ~ 124 ky when sea-level was ~ 6 m higher than it is today. The wave-cut notch that formed at that time is readily apparent in the cliff faces of the island.

1.3.2. Characteristics and origin of Cayman dolomite

Previous studies on the petrographic and geochemical features of Cayman dolostones have been undertaken by Jones et al. (1984), Jones (1989), Ng (1990), Pleydell et al. (1990), Wignall (1995), Montpetit (1998), Willson (1998), Jones et al. (2001), MacNeil (2001), Jones and Luth (2002, 2003b, a), MacNeil and Jones (2003), Jones (2004, 2005, 2007), and Uzelman (2009). Most of those papers focused on the dolostones from in the Cayman Formation and the Pedro Castle Formation found on Grand Cayman. MacNeil (2001), MacNeil and Jones (2003), and Uzelman (2009), however, considered the dolostones in the Pedro Castle Formation and the Brac Formation on Cayman Brac. These studies demonstrated the following main features of the dolostones from the Bluff Group.

1.3.2.1. Dolomite populations in Cayman dolostones

The dolostones from the Cayman Islands are composed largely of Ca-rich non-stoichiometric dolomites with %Ca content ranging from 49 to 63%Ca (Jones et al., 2001). Thus, like most sedimentary dolomite, they are non-stoichiometric (Lumsden and Chimahusky, 1980; Sperber et al., 1984; Sibley, 1990; Sibley et al., 1994; Vahrenkamp and Swart, 1994; Budd, 1997; Wheeler et al., 1999; Schubel et al., 2006; Suzuki et al., 2006). Jones et al. (2001) developed a XRD technique that showed that the Cayman dolomites can be divided into low-Ca calcian dolomite (LCD >55% mol %$CaCO_3$) and high-Ca calcian dolomite (HCD >55% mol %$CaCO_3$). Such analyses showed that most Cayman dolostones are formed of both LCD and HCD (Jones et al., 2001; Jones and Luth, 2002; Jones and Luth, 2003a; Jones, 2004, 2005, 2007). There are, however, some dolostones that are formed solely of LCD or HCD. Dolostones in the Pedro Castle Formation and the Brac Formation, for example, are commonly formed largely of HCD (MacNeil 2001; MacNeil and Jones 2003; Uzelman, 2009) whereas those in the Cayman Formation are formed largely of mixtures of LCD and HCD (Jones et al., 2001; Jones and Luth, 2002).

1.3.2.2. Dolomite Crystal Structure

The dolomite crystals in the Cayman dolostones are typically <100 μm and commonly < 50 μm long. There appears to be no systematic stratigraphic or geographic variation in crystal size (Jones, 2005). Even in crystals < 20 μm long, alternating zones (oscillatory or step-zoned) of LCD and HCD are commonly apparent (Jones, 2004). He argued that both extrinsic and intrinsic factors may have controlled the formation of zoned dolomite crystals on different time scales.

On a microscale, a blocky substructure characterizes LCD crystals whereas HCD typically displays a modulated structure (Jones and Luth, 2002). They argued that the difference in the microstructures supports the contention that LCD

and HCD are crystallographically distinct forms of dolomite. Jones (2004, 2005) argued that the architectural characteristics of dolomite crystals in the Cayman Formation were indicative of multiple phases of dolomitization and diagenesis.

1.3.2.3. Origin of Cayman dolomite

The mechanisms inferred for the formation of Cayman dolomites have been based largely on the interpretation of stable isotope and trace elements data. According to Pleydell (1990), Ng (1990), and Jones and Luth (2002), the oxygen isotope values of dolostones from the Cayman Formation of Grand Cayman range from 2.0 to 3.5 ‰ (PDB) whereas the carbon isotope values are commonly between 2.0 and 4 ‰ (PDB). These values are similar to other "islands dolomites" (cf. Budd 1997). Based on petrographic and geochemical data, Pleydell (1990) argued that dolomitization on Grand Cayman was mediated by normal seawater. Based on various dolomite-water fractionation equations, Ng (1990) argued that the mixed fresh-seawater with 0-75% freshwater was probably responsible for the dolomitization of the Cayman Formation on Grand Cayman. Jones and Luth (2002), however, suggested that seawater that had been slightly-modified by evaporation mediated dolomitization of the Brac Formation. In comparison, the oxygen and carbon isotope values from the Pedro Castle Formation, as reported by MacNeil and Jones (2003), are more depleted with $\delta^{18}O$ ranging from 0.08‰ to 2.16‰, and $\delta^{13}C$ varying from -1.81‰ to 1.42‰. Thus, they suggested that the dolomitization of the Pedro Castle Formation of Cayman Brac was probably mediated by saline water, which is seawater that has been modified by water-rock interaction. The dolostones in the Brac Formation of Cayman Brac have a remarkable wide ranges of $\delta^{18}O$ (-4.64 to +4.73‰) and $\delta^{13}C$ values (-4.53‰ to +3.80‰) (Uzelman, 2009). She attributed these wide ranges to the variations in the %Ca of dolomite, the mixture of different phases of dolomite (e.g., replacive dolomite and dolomite cement), and contamination

by coexisting calcite. Uzelman (2009), however, argued that normal seawater or saline waters were probably responsible for dolomitization of the Brac Formation of Brac Cayman.

1.3.2.4. The timing of dolomitization

The $^{87}Sr/^{86}Sr$ ratios of limestones can be used to determine their age providing they have not undergone later diagenetic processes that have reset the ratio. In the case of dolomitization, it has been argued that the $^{87}Sr/^{86}Sr$ ratio can be used as a geochronometer to date the timing of dolomitization providing dolomitization was mediated by seawater (Saller, 1984; Swart et al., 1987; Ohde and Elderfield, 1992; Fouke et al., 1996). Pleydell et al. (1990) reported that the $^{87}Sr/^{86}Sr$ ratios of the dolostones from the Cayman Formation and the Pedro Castle Formation of Grand Cayman range from 0.70898 to 0.70911 (average 0.70905, n = 16). Based on these $^{87}Sr/^{86}Sr$ ratios, Pleydell et al. (1990) argued that the Cayman Formation and the Pedro Castle Formation on Grand Cayman were dolomitized in a single episode of dolomitization event, 2 to 5 Ma. Ng (1990), however, argued that two phases of dolomitization were responsible for the formation of dolostones from the Cayman Formation and the Pedro Castle Formation on Grand Cayman. He argued that the relative uniform $^{87}Sr/^{86}Sr$ ratios reported by Pleydell et al. (1990) were probably due to the $^{87}Sr/^{86}Sr$ ratios being reset of by the second, younger phase of dolomitization. Jones and Luth (2003b) reported the $^{87}Sr/^{86}Sr$ ratios from dolostones on Grand Cayman ranging from 0.708917 to 0.709139 (average 0.709021). Based on the Neogene seawater $^{87}Sr/^{86}Sr$ curve of Hodell et al. (1991), Jones and Luth (2003b) proposed a three-phase model of dolomitization: Phase I during Miocene to early Pliocene times, Phase II in the Late Pliocene, and Phase III in the Pleistocene. The $^{87}Sr/^{86}Sr$ ratios from dolostones of the Pedro Castle Formation on Cayman Brac, reported by MacNeil and Jones (2003), range from 0.709032 to 0.709108 (average 0.709068, n = 14). According to the $^{87}Sr/^{86}Sr$

curve of Farrell (1995), these $^{87}Sr/^{86}Sr$ ratios were interpreted to indicate that the dolomitization took place 4.4 to 1.2 Ma ago. The $^{87}Sr/^{86}Sr$ ratios from dolomite of the Brac Formation on Cayman Brac, as reported by Uzelman (2009), range from 0.708605 to 0.709155 (average 0.708900, n = 11). The wide spread in the $^{87}Sr/^{86}Sr$ ratios were attributed to a time-transgressive dolomitizing process that started ~18 Ma ago and subsequently involved multiple stages of dolomitization (Uzelman, 2009).

1.4. Rationale and objectives

Although numerous studies have focused on the Cayman dolostones, only a few have systematically dealt with the geochemical and petrographic features of the dolostones found on Cayman Brac (MacNeil and Jones, 2003; Uzelman, 2009). As an isolated island, Cayman Brac provides a relative simple geological setting in which the diagenetic environments that have affected these relatively young dolostones can be reasonably inferred. Furthermore, the thick carbonate succession exposed on Cayman Brac has been dolomitized to varying degrees and the dolostones have various textures. Such variety in the occurrence of dolomite offers us a unique opportunity to examine the factors that underlie the formation of dolostones with various textures. Thus, it is essential to further study these dolostones with new datasets that allow comparison between the dolostones from the different formations.

Deciphering the origin of dolomite relies heavily on the interpretation of their geochemical signatures. Critical to this assessment is the understanding that those signatures may represent subsequent early diagenetic processes as well as the original dolomite. An understanding of the petrographic features of dolostones is therefore critical to deciphering the history of these complex rocks. Fortunately, the succession on Cayman Brac provides samples that allows discussion of many

aspects of this issue, including the relationship between the different geochemical characteristics (especially stable isotope and trace elements) of the dolostones, the stoichiometry of the dolomite, the factors that controlled the textures of dolostones, and preservation of some of the primary geochemical features of the dolostones (e.g., rare earth elements). A thorough understanding of these issues is critically important because it may help to explain how dolostones, of all ages, formed.

The main objectives of this thesis, which is based on the Tertiary succession found on Cayman Brac, are as follows:

- Delineation of the factors that controlled the formation of the finely crystalline dolostones in the Cayman Formation on Cayman Brac with a focus on the relationship between their geochemical signatures (especially stable isotope and trace elements) and dolomite stoichiometry. In so doing, it also proposes techniques that should be used to interpret the geochemical data of dolostones formed of non-stoichiometric dolomite.
- Comparison of the dolostones with fabric-destructive textures found in the Brac Formation and the finely crystalline dolostone with fabric-retentive textures that are found in the Cayman Formation. The reasons for the formation of the different types of dolostones are considered.
- Assessment of the possibility that rare earth elements in the dolostones from Cayman Brac may help to resolve their origin.

This thesis is presented in a paper-based format. Each chapter has been published in a peer-reviewed journal or has been submitted to a journal for possible publication (status indicated in a footnote to each chapter).

Chapter Two: This chapter documents the petrographic and geochemical characteristics of dolostones found in the Cayman Formation of Cayman Brac. Interpretations of various aspects of the dolostones, including their mol %Ca,

cathodoluminescence signatures, carbon and oxygen isotopes, Sr isotopes, and trace element (Sr, Fe, Mn) concentration are integrated into a model that explains the origin of the dolostones in the Cayman Formation. This chapter emphasizes the influence of dolomite stoichiometry on their geochemical signatures and proposes an approach for interpretation of the oxygen isotopic data of dolostones that are composed Ca-rich nonstoichiometric dolomites.

Published as: Zhao, H. and Jones, B. 2012, Origin of dolostones from the Cayman Formation (Miocene), Cayman Brac, British West Indies, Sedimentary Geology, v. 243-244, p. 191-206.

Chapter Three: This chapter uses the petrographic and geochemical characteristics of fabric-destructive dolostones found in the Brac Formation on Cayman Brac to explain the origin of the fabric destructive textures found in these dolostones. Integration of the petrography, luminescence, geochemistry data from the fabric-destructive dolostones indicates that they probably formed in the seawater-like dolomitizing fluids, much like the waters that were responsible for the formation of the fabric-retentive dolostones in the overlying Cayman Formation. This paper also demonstrates that the coarsely crystalline fabric-destructive textures reflect repeated diagenetic cycles that involved dolomitization, dissolution, and cementation.

Published as: Zhao, H. and Jones, B. 2012, Genesis of fabric-destructive dolostones: A case study of the Brac Formation (Oligocene), Cayman Brac, British West Indies, Sedimentary Geology, v. 267-268, p. 36-54.

Chapter Four: This chapter documents the distribution of rare earth elements and yttrium (REE + Y) in the carbonate succession found on Cayman Brac. In so doing, it examines the possible effects of the original depositional environments and post-depositional diagenesis (e.g., dolomitization) on the REE+Y values. This paper points out the limitations of using REE+Y in the study

of dolomitization and considers the possibility of using REE+Y as proxies for delineating carbonate stratigraphy and the evolution of the REE+Y compositions of seawater

In submission as: Zhao, H. and Jones, B. 2012, Distribution and interpretation of rare earth elements and yttrium in Cenozoic dolostones on Cayman Brac, British West Indies, Sedimentary Geology,.

Chapter Five: This chapter summarizes the all of the conclusions that have been reached from the study.

1.5. References

Budd, D.A., 1997. Cenozoic dolomites of carbonate islands: their attributes and origin. Earth-Science Reviews 42, 1-47.

Clayton, R.N., Jones, B.F., Berner, R.A., 1968. Isotope studies of dolomite formation under sedimentary conditions. Geochimica et Cosmochimica Acta 32, 415-424.

Coyne, M., Jones, B., 2007. Highstands during Marine Isotope Stage 5: evidence from the Ironshore Formation of Grand Cayman, British West Indies. Quaternary Science Reviews 26, 536-559.

DeMets, C., Wiggins-Grandison, M., 2007. Deformation of Jamaica and motion of the Gonâve microplate from GPS and seismic data. Geophysical Journal International 168, 362-378.

Emery, K., Milliman, J., 1980. Shallow-water limestones from slope off Grand Cayman Island. The Journal of Geology 88, 483-488.

Farrell, J.W., Clemens, S.C., Gromet, L.P., 1995. Improved chronostratigraphic reference curve of late Neogene seawater 87Sr/86 Sr. Geology 23, 403-406.

Fouke, B.W., Beets, C., Meyers, W.J., Hanson, G.N., Melillo, A.J., 1996. 87 Sr/86 Sr Chronostratigraphy and dolomitization history of the Seroe Domi Formation, Curaçao (Netherlands Antilles). Facies 35, 293-320.

Hardie, L.A., 1987. Dolomitization; a critical view of some current views. Journal of Sedimentary Research 57, 166-183.

Hodell, D.A., Mueller, P.A., Garrido, J.R., 1991. Variations in the strontium isotopic composition of seawater during the Neogene. Geology 19, 24-27.

Jones, B., Lockhart, E., Squair, C., 1984. Phreatic and vadose cements in the Tertiary Bluff Formation of Grand Cayman Island,British West Indies. Bulletin of Canadian Petroleum Geology 32, 382-397.

Jones, B., 1989. Syntaxial overgrowths on dolomite crystals in the Bluff Formation, Grand Cayman, British West Indies. Journal of Sedimentary Research 59, 839-847.

Jones, B., Hunter, I.G., 1989. The Oligocene-Miocene Bluff Formation on Grand Cayman. Caribbean Journal of Science 25, 71-85.

Jones, B., 1994. Geology of the Cayman Islands. In: M.A. Brunt, J.E. Davies (Eds.), The Cayman Islands: Natural history and biogeography. Kluwer, Dordrecht, The Netherlands, pp. 13–49.

Jones, B., Hunter, I.G., 1994. Evolution of an isolated carbonate bank during Oligocene, Miocene and Pliocene times, Cayman Brac, British west Indies. Facies 30, 25-50.

Jones, B., Hunter, I.G., Kyser, K., 1994a. Revised stratigraphic nomenclature for Tertiary strata of the Cayman Islands, British West Indies. Caribbean Journal of Science 30, 53-68.

Jones, B., Hunter, I.G., Kyser, K., 1994b. Stratigraphy of the Bluff Formation (Miocene-Pliocene) and the newly defined Brac Formation (Oligocene), Cayman Brac, British West Indies. Caribbean Journal of Science 30, 30-51.

Jones, B., Luth, R.W., MacNeil, A.J., 2001. Powder X-ray diffraction analysis of homogeneous and heterogeneous sedimentary dolostones. Journal of Sedimentary Research 71, 790-799.

Jones, B., Luth, R.W., 2002. Dolostones from Grand Cayman, British West Indies. Journal of Sedimentary Research 72, 559-569.

Jones, B., Luth, R.W., 2003a. Petrography of finely crystalline Cenozoic dolostones as revealed by backscatter electron imaging: Case study of the Cayman Formation (Miocene), Grand Cayman, British West Indies. Journal of Sedimentary Research 73, 1022-1035.

Jones, B., Luth, R.W., 2003b. Temporal evolution of Tertiary dolostones on Grand Cayman as determined by 87Sr/86Sr. Journal of Sedimentary Research 73, 187-205.

Jones, B., 2004. Petrography and significance of zoned dolomite cements from the Cayman Formation (Miocene) of Cayman Brac, British West Indies. Journal of Sedimentary Research 74, 95-109.

Jones, B., 2005. Dolomite crystal architecture: genetic implications for the origin of the Tertiary dolostones of the Cayman Islands. Journal of Sedimentary Research 75, 177-189.

Jones, B., 2007. Inside-out dolomite. Journal of Sedimentary Research 77, 539-551.

Land, L.S., 1980. The isotopic and trace element geochemistry of dolomite: the state of the art. In: Zenger, D.H., Dunham, J.B., Ethington, R.L. (Eds.), Concepts and Models of Dolomitization, SEPM Special Publication 28, Tulsa, Oklahomano, pp. 87–110.

Land, L.S., 1998. Failure to Precipitate Dolomite at 25°C from Dilute Solution Despite 1000-Fold Oversaturation after 32 Years. Aquatic Geochemistry 4, 361-368.

Leroy, S., Mauffret, A., Patriat, P., Mercier de Lépinay, B., 2000. An alternative interpretation of the Cayman trough evolution from a reidentification of magnetic anomalies. Geophysical Journal International 141(3), 539-557.

Lumsden, D.N., Chimahusky, J.S., 1980. Relationship between dolomite nonstoichiometry and carbonate facies parameters. In: D.H. Zenger, J.B. Dunham, R.L. Ethington (Eds.), Concepts and Models of Dolomitizatioin. SEPM Special Publication 28, Tulsa, Oklahoma, pp. 123–137.

MacDonald, K.C., Holcombe, T.L., 1978. Inversion of magnetic anomalies and sea-floor spreading in the Cayman Trough. Earth and Planetary Science

Letters 40, 407-414.

Machel, H.G., Mountjoy, E.W., 1986. Chemistry and environments of dolomitization–a reappraisal. Earth-Science Reviews 23, 175-222.

Machel, H.G., 2004. Concepts and models of dolomitization: a critical reappraisal, The geometry and petrogenesis of dolomite hydrocarbon reservoirs, pp. 7-63.

MacNeil, A., 2001. Sedimentology, Diagenesis and Dolomitization of the Pedro Castle Formation on Cayman Brac, BWI. Master Thesis, Unversity of Alberta, 128 pp.

MacNeil, A., Jones, B., 2003. Dolomitization of the Pedro Castle Formation (Pliocene), Cayman Brac, British West Indies. Sedimentary Geology 162, 219-238.

Mann, P. et al., 2002. Oblique collision in the northeastern Caribbean from GPS measurements and geological observations. Tectonics 21, 1057.

Matley, C.A., 1926. The geology of the Cayman Islands (British West Indies), and their relation to the Bartlett Trough. Quarterly Journal of the Geological Society 82, 352.

Matthews, a., Katz, A., 1977. Oxygen isotope fractionation during the dolomitization of calcium carbonate. Geochimica et Cosmochimica Acta 41, 1431-1438.

McCrea, J.M., 1950. On the isotopic chemistry of carbonates and a paleotemperature scale. The Journal of Chemical Physics 18, 849-857.

Montpetit, J.C., 1998. Sedimentology, Depositional Architecture, and Diagenesis of the Cayman Formation at Tarpon Springs Estates, Grand Cayman, British West Indies. Master Thesis, University of Alberta, 133 pp.

Moore, C.H., 1973. Intertidal carbonate cementation, Grand Cayman, West Indies. Journal of Sedimentary Research 43, 591-602.

Morrow, D.W., 1982a. Diagenesis, 1. Dolomite–Part 1: The chemistry of dolomitization and dolomite precipitation. Geoscience Canada 9, 5-13.

Morrow, D.W., 1982b. Diagenesis 2. Dolomite-Part 2 Dolomitization Models and Ancient Dolostones. Geoscience Canada 9, 95-107.

Ng, K.C.S., 1990. Diagenesis of the Oligocene-Miocene Bluff Formation of the Cayman Islands - A Petrographic and Hydrogeochemical Approach. Ph.D. Thesis, University of Alberta, 344 pp.

Northrop, D.A., Clayton, R.N., 1966. Oxygen-isotope fractionations in systems containing dolomite. The Journal of Geology 74, 174-196.

O'Neil, J.R., Epstein, S., 1966. Oxygen isotope fractionation in the system dolomite-calcite-carbon dioxide. Science 152, 198-201.

Ohde, S., Elderfield, H., 1992. Strontium isotope stratigraphy of Kita-daito-jima Atoll, North Philippine Sea: Implications for Neogene sea-level change and tectonic history. Earth and Planetary Science Letters 113, 473-486.

Perfit, M.R., Heezen, B.C., 1978. The geology and evolution of the Cayman Trench. Geological Society of America Bulletin 89, 1155-1174.

Pleydell, S.M., 1987. Aspects of Diagenesis and Ichnology in the Oligocene-Miocene Bluff Formation of Grand Cayman Island, British West Indies. Master Thesis, 209 pp.

Pleydell, S.M., Jones, B., Longstaffe, F., Baadsgaard, H., 1990. Dolomitization of the Oligocene-Miocene Bluff Formation on Grand Cayman, British West Indies. Canadian Journal of Earth Sciences 27, 1098-1110.

Roberts, H.H., 1977. Field guidebook to the reefs and geology of Grand Cayman Island, B.W.I. , B.W.I. Third International Symposium on coral Reefs. University of Miami, Miami, pp. 44.

Rosencrantz, E., Sclater, J.G., 1986. Depth and age in the Cayman Trough. Earth and Planetary Science Letters 79, 133-144.

Saller, A.H., 1984. Petrologic and geochemical constraints on the origin of subsurface dolomite, Enewetak Atoll: an example of dolomitization by normal seawater. Geology 12, 217-220.

Schubel, K.A., Veblen, D.R., Malone, M.J., 2006. Microstructures and textures of experimentally altered Bahamian ooids: Implications for reaction mechanisms of dolomitization. Carbonates and Evaporites 21, 1-13.

Sibley, D.F., 1990. Unstable to stable transformations during dolomitization. The Journal of Geology 98, 739-748.

Sibley, D.F., Nordeng, S.H., Borkowski, M.L., 1994. Dolomitization kinetics of hydrothermal bombs and natural settings. Journal of Sedimentary Research 64, 630-637.

Sperber, C.M., Wilkinson, B.H., Peacor, D.R., 1984. Rock composition, dolomite stoichiometry, and rock/water reactions in dolomitic carbonate rocks. The Journal of Geology 92, 609-622.

Stoddart, D.R., 1980. Geology and geomorphology of Little Cayman. Atoll Research Bulletin 241, 11-16.

Sun, S.Q., 1994. A reappraisal of dolomite abundance and occurrence in the Phanerozoic. Journal of Sedimentary Research 64, 396-404.

Suzuki, Y., Iryu, Y., Inagaki, S., Yamada, T., Aizawa, S., Budd, D.A., 2006. Origin of atoll dolomites distinguished by geochemistry and crystal chemistry: Kita-daito-jima, northern Philippine Sea. Sedimentary Geology 183, 181-202.

Swart, P.K., Ruiz, J., Holmes, C.W., 1987. Use of strontium isotopes to constrain the timing and mode of dolomitization of upper Cenozoic sediments in a core from San Salvador, Bahamas. Geology 15, 262-265.

Uzelman, B.C., 2009. Sedimentology, diagenesis, and dolomitization of the Brac Formation (Lower Oligocene), Cayman Brac, British West Indies. Master

Thesis, University of Alberta, 120 pp.

Vahrenkamp, V.C., Swart, P.K., 1994. Late Cenozoic dolomites of the Bahamas: metastable analogues for the genesis of ancient platform dolomites. In: B. Purser, M. Tucker, D. Zenger (Eds.), Dolomites: A Volume in Honour of Dolomieu: International Association of Sedimentologists, Special Publication, pp. 133–153.

Vasconcelos, C., McKenzie, J.A., Warthmann, R., Bernasconi, S.M., 2005. Calibration of the δ18O paleothermometer for dolomite precipitated in microbial cultures and natural environments. Geology 33, 317-320.

Warren, J., 2000. Dolomite: occurrence, evolution and economically important associations. Earth-Science Reviews 52, 1-81.

Wheeler, C.W., Aharon, P., Ferrell, R.E., 1999. Successions of late Cenozoic platform dolomites distinguished by texture, geochemistry, and crystal chemistry; Niue, South Pacific. Journal of Sedimentary Research 69, 239-255.

Wignall, B.D., 1995. Sedimentology and Diagenesis of the Cayman (Miocene) and Pedro Castle (Pliocene) Formations at Safe Haven, Grand Cayman, British West Indies. Master Thesis, University of Alberta, 110 pp.

Willson, E.A., 1998. Depositional and Diagenetic Features of the Middle Miocene Cayman Formation, Roger's Wreck Point, Grand Cayman, British West Indies. Master Thesis, University of Alberta, 103 pp.

CHAPTER 2
ORIGIN OF FABRIC-RETENTIVE DOLOSTONES OF THE CAYMAN FORMATION[1]

2.1. Introduction

Cenozoic "island dolostones", found on isolated islands throughout the Caribbean Sea and Pacific Ocean (Budd, 1997), are critically important for understanding the origin of pervasive dolomitization. In theory, determining the origin of island dolostones should be straightforward because they are geologically young, have not been buried, and have developed under conditions that are known or can be reasonably inferred (Budd, 1997). Consistencies in their $^{87}Sr/^{86}Sr$ ratios, for example, has led to the notion that dolomitization may be controlled by regional events related to eustatic sea level changes (Budd, 1997; Wheeler et al., 1999; Jones and Luth, 2003; MacNeil and Jones, 2003; Suzuki et al., 2006). Nevertheless, interpretations of these dolostones is commonly hindered by their complex textures (Sibley, 1982; Randazzo and Zachos, 1984; Dawans and Swart, 1988; Jones, 1994; Vahrenkamp and Swart, 1994; Budd, 1997; Wheeler et al., 1999; Jones and Luth, 2002; MacNeil and Jones, 2003; Suzuki et al., 2006), multiple populations of dolomite (Wheeler et al., 1999; Jones and Luth, 2002; Jones, 2004, 2005; Suzuki et al., 2006; Jones, 2007), and early diagenetic modifications (Humphrey, 2000, Jones, 2007, Gaswirth et al., 2007).

Even though island dolostones from different locales throughout the world are petrographically and geochemically similar, a diverse array of fluids and processes has been invoked to explain their origin (cf. Budd, 1997). Thus, their development has been attributed to normal seawater (e.g. Saller, 1984; Aharon

---

1 This chapter was published as: Zhao, H and Jones, B. 2012, Origin of dolostones from the Cayman Formation (Miocene), Cayman Brac, British West Indies, Sedimentary Geology, 243-244, 191-206

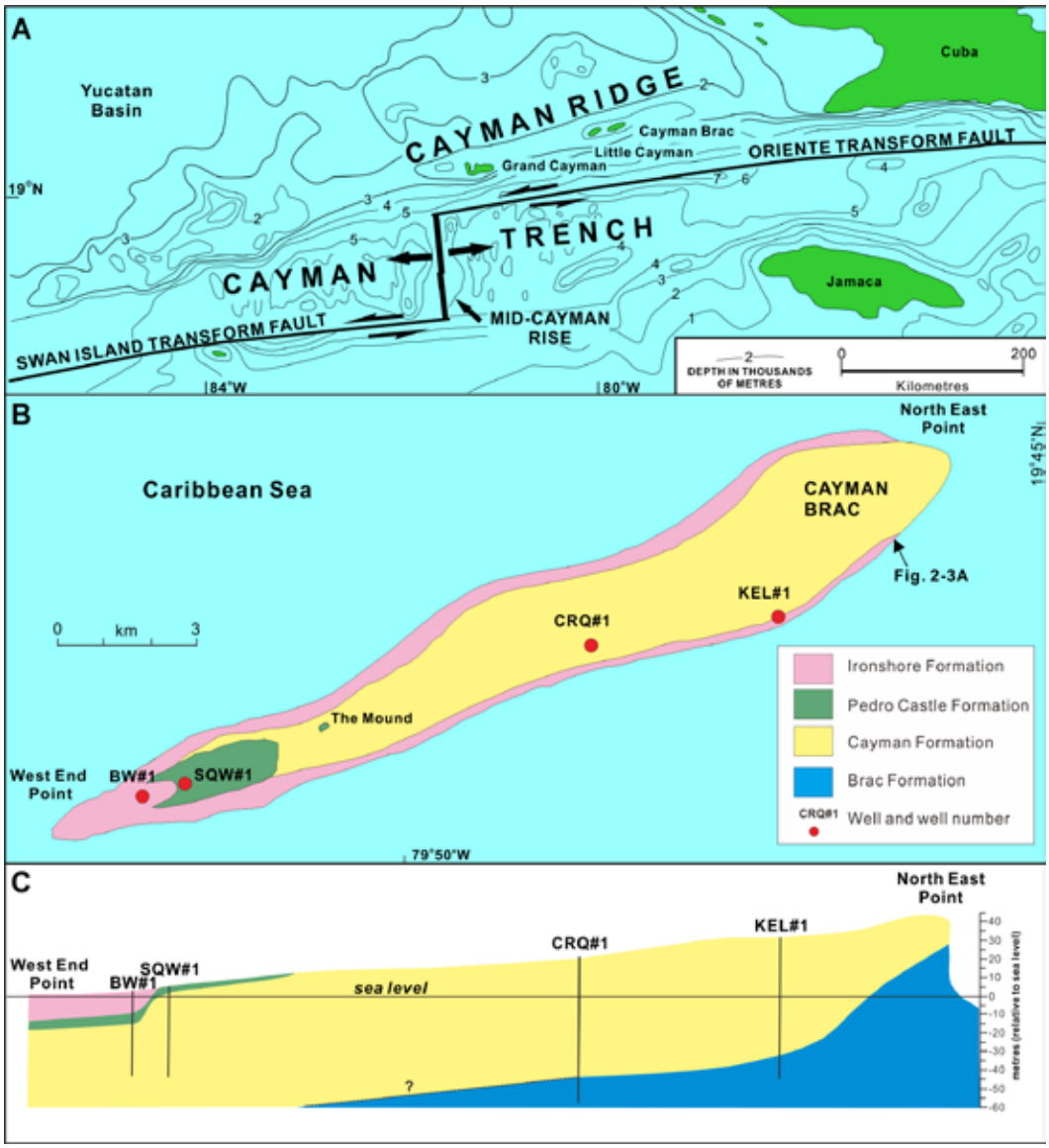

Fig. 2-1. Location and geology of Cayman Brac. A) Tectonic and bathymetric setting of the Cayman Islands. Modified from Jones (1994) and based on maps from Perfit and Heezen (1978) and MacDonald and Holcombe (1978). B) Geologic map of Cayman Brac (modified from Jones, 1994) showing locations of wells BW#1, SQW#1, CRQ#1, and KEL#1. Arrow labelled Fig. 2-3A indicates position of photograph shown in Fig. 2-3A. C) Cross section through Cayman Brac (modified from Jones (2005)).

et al., 1987; Suzuki et al., 2006), evaporated seawater (e.g. Ohde and Elderfield, 1992; Gill et al., 1995; Wheeler et al., 1999), and/or mixed freshwater-seawater regimes (Ward and Halley, 1985; Humphrey, 1988; MacNeil and Jones, 2003). To a large extent, these conflicting interpretations reflect the uncertainties associated with the interpretations of various geochemical proxies. The fractionation behaviour of oxygen isotopes in the dolomite-water system (cf. Humphrey, 2000) and the role(s) that kinetic factors play in trace element concentrations (Vahrenkamp and Swart, 1990, 1994; Wheeler et al., 1999; Suzuki et al., 2006), for example, are still open to debate.

Cayman Brac, the easternmost of the Cayman Islands (Fig. 2-1), offers an ideal natural laboratory for the study of island dolostones because it is geographically isolated by the deep oceanic waters of the surrounding Caribbean Sea. There, the pervasively dolomitized Cayman Formation is at least 100 m thick (Jones et al., 1994b) with much of it being exposed in cliffs that rise to 40 m above sea level. This study uses many different proxies to evaluate the genesis of these dolostones from various perspectives. This integrated approach demonstrates that the finely crystalline dolostones in the Cayman Formation (1) are compositionally heterogeneous, (2) have O isotopic values and Sr contents that are linked to dolomite stoichiometry, (3) probably originated from seawater, and (4) underwent multiple episodes of dolomitization that were ultimately related to changes in sea level. Such interpretations are critical to the understanding of the factors that control the processes that mediate the transformation of limestone to dolostone on isolated oceanic islands. Such conclusions also have important implications for resolving the origin of pervasively dolomitized sequences in older successions.

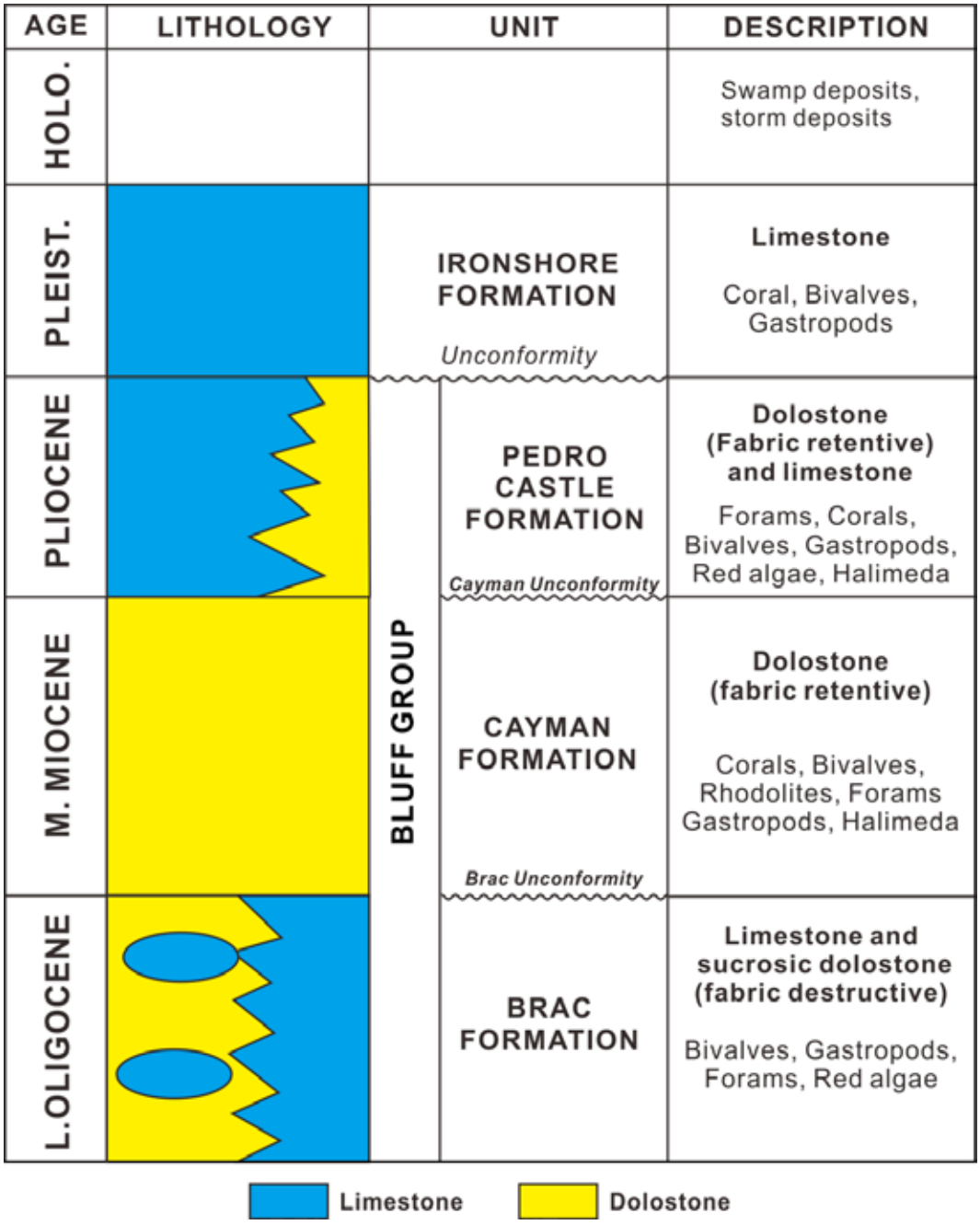

Fig. 2-2. Stratigraphic succession on Cayman Brac (modified from Jones, 1994) showing distribution of dolostones and limestones and dominant biota found in each unit.

2.2. Geological setting

The Cayman Islands, located in the Caribbean Sea to the south of Cuba and northwest of Jamaica, encompass Grand Cayman, Cayman Brac, and Little Cayman (Fig. 2-1A). These islands are located in a tectonically active area with Grand Cayman being located just to the northeast of the Mid-Cayman Rise, which is an active spreading centre with an average opening rate of 11-12 mm yr^{-1} (DeMets and Wiggins-Grandison, 2007) The Oriente Transform Fault extends eastward off the northern end of the spreading centre and the Swan Islands Transform Fault extends westward off it southern end (Fig. 2-1A). The Cayman Trench (also known as the Bartlett Trough), located to the south of the Cayman Islands, is a complex transform fault zone pull apart basin with a maximum water depth of 7686 m. Each of the Cayman islands is located on the Cayman Ridge, possibly on different fault blocks, that lies north of the Orient Transform Fault and extends from the Sierra Maestra of southern Cuba westward towards Honduras (Fig. 2-1A). In effect, Cayman Brac is the surface manifestation of an uplifted fault block that rises 2000-2500 m from the seafloor (Perfit and Heezen, 1978). The upper surface of Cayman Brac, which is 19 km long and 1.5 to 3.0 km wide, slopes gradually from 43 m above sea level (asl) at its east end to sea level at its west end (Fig. 2-1B, C). Cayman Brac is completely isolated by the deep oceanic waters that surround it (Fig. 2-1A).

Although the thickness of the carbonate succession on Cayman Brac is unknown, surface exposures and drilling have shown that it is at least 150 m thick (Fig. 2-1C). Matley (1926) originally assigned all of the exposed Tertiary strata to the Bluff Limestone. Subsequently, Jones et al. (1994a, 1994b) named this succession as the Bluff Group (Fig. 2-2) and defined the constituent, unconformity-bounded formations as the Brac Formation (Upper Lower Oligocene), Cayman Formation (Lower to Middle Miocene), and Pedro Castle

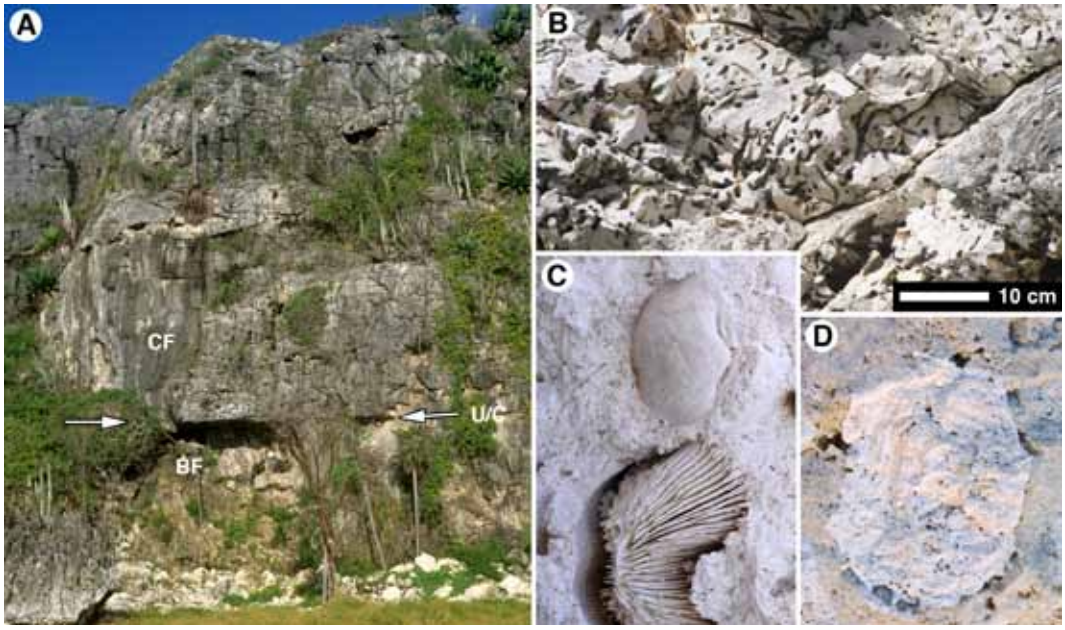

Fig. 2-3. Field photographs of Cayman Formation on Cayman Brac. A) View of cliff face at locality on south coast of Cayman Brac (see Fig. 2-1B for precise location) showing Cayman Formation (CF), Brac Unconformity (U/C), and Brac Formation (BF) with typical grey weathered surfaces and lack of obvious bedding planes. B) Leached Stylophora in finely crystalline dolostone matrix, outcrop near locality CRQ#1 (Fig. 2-1B). C) Leached bivalve (top) and free-living coral (bottom) in finely crystalline dolostone, quarry at locality CRQ#1. D) Dolomitized rhodolith held in finely crystalline dolomite matrix, quarry at locality CRQ#1.

Formation (Pliocene). The Brac Unconformity defines the boundary between the Brac Formation and Cayman Formation whereas the Cayman Unconformity separates the Cayman Formation from the overlying Pedro Castle Formation (Fig. 2-2). Although the paucity of well-defined bedding planes makes it difficult to accurately define the attitude of these strata, it has been estimated that they dip at ~ 0.5^{o} to the west (Jones, 1994). The uplifted core of Cayman Brac is fringed by a low-lying (< 2 m asl) platform that is formed of Late Pleistocene limestones that Matley (1926) assigned to the Ironshore Formation (Fig. 2-1B).

The Brac Formation, exposed only in the basal parts of the sea cliffs at the east end of the island (Fig. 2-1C), is formed of intercalated limestones and

dolostones (Jones, 1994). Similarly, the Pedro Castle Formation, found on the west end of the island, is formed of limestones that have been dolomitized to varying degrees (Jones, 1994; MacNeil and Jones, 2003). Sandwiched between these formations is the Cayman Formation, estimated to be ~ 100 m thick, and formed entirely of dolostone (Figs. 2-1C and 2-2). The succession is so lithologically uniform that it cannot be stratigraphically divided into members or even distinct units and correlation of dolostone exposures on different parts of the island is virtually impossible. These hard dolostones form steep cliff faces with grey weathered surfaces that typically appear massive, display few obvious bedding planes, and are commonly cut by numerous fractures and joints (Fig. 2-3A). Fresh surfaces reveal white, finely crystalline (crystals average 10-20 μm long) fabric-retentive dolostones that commonly contain numerous corals (branching and hemispherical forms), bivalves, gastropods, rhodoliths, *Halimeda* plates, scattered echinoderm plates, red algae biofragments, and foraminifera (mainly benthic) that are held in mudstone to bioclastic grainstone matrices (Fig. 2-3B-D). There is, however, no evidence of reef development. Jones and Hunter (1994b) suggested that the original sediments accumulated on a carbonate bank in water that was probably < 30 m deep. Skeletons originally formed of aragonite (e.g., corals) have been dissolved and are now evident as mouldic porosity (Fig. 2-3B-D). Cavities in the dolostones are commonly lined and/or filled with complex successions of calcite and dolomite cements (Jones, 2004). Caves, which are common in the Cayman Formation, are variously adorned with calcitic speleothems (Tarhule-Lips and Ford, 2004; Jones, 2010, 2011).

2.3. Methods

The samples used in this study were collected from wells BW#1, SQW#1, CRQ#1, KEL#1 and exposures above wells KEL#1 and CRQ#1 (Fig. 2-1).

These wells were located so that different parts of the Cayman Formation could be sampled (Fig. 2-1B). Wells SQW#1 (51.2 m deep) and BW#1 (49.7 m deep) penetrated the basal part of the Pedro Castle Formation, the Cayman Unconformity, and the upper part of the Cayman Formation. In those wells, the Cayman Unconformity was located 3 m asl and 15.4 m below sea level (bsl), respectively (Fig. 2-1C). Section CRQ#1, formed by merging 60.6 m in the well and 15.2 m in quarry walls, includes 64.4 m of the Cayman Formation and 11.4 m of the underlying Brac Formation with the Brac Unconformity being 46.9 m bsl (Fig. 2-1C). Section KEL#1, formed by combining 52.2 m in the well with 21.3 m in the cliff face, includes the basal part of the Cayman Formation and the upper part of the Brac Formation with the Brac Unconformity at 29.3 m bsl (Fig. 2-1C). Drilling was done with a truck mounted drilling rig that used a 10 cm diameter bit with downhole compressed air being used to circulate the groundwater and bring well cuttings to the surface. Samples of well cuttings were collected over 0.75 m intervals. Samples from exposures in the quarry at CRQ#1 and the cliff face at KEL#1 consisted of hand-sized pieces of unweathered dolostones that were collected at 1 m intervals.

The petrography of the dolostones was established by standard thin-section techniques, with each thin section being impregnated with blue epoxy and stained with Alizarin Red-S solution. Selected polished thin sections were examined on a Technosyn Model 8200 Mark II cold-cathode instrument (manufactured by Technosyn Limited, Cambridge, UK) that is mounted on a binocular petrographic microscope equipped with a Canon™ EOS Rebel XS digital single-lens reflex camera (Canon Canada Inc., Ontario, Canada) with a 10.10-megapixel image sensor. The operating voltage was 10-15 kv and gun current level was 550-620 μA.

Scanning electron microscopy (SEM) using a JEOL 6301 field emission

SEM was used to determine the size and morphology of the constituent dolomite crystals, using the procedures outlined by Jones (2005). For this purpose, small fractured samples (typically ~ 1 cm^2) were cut, polished and etched with 30% HCl for 10-15 seconds before being sputter coated with gold and examined on the SEM with an accelerating voltage of 5 kV.

Backscatter electron images (BSEI) that highlight variations in average atomic weights were obtained from polished thin sections that were coated with carbon and analyzed on a JEOL 8900R electron microprobe analysis (EMPA) and operated at 15 kV accelerating voltage. The 1024 x 1024 pixel images were obtained with a beam current of 15nA.

Given that the average length of dolomite crystals in the Cayman Formation is generally < 20 μm (maximum ~ 50 μm), it is impossible to sample individual crystals or individual growth zones in those crystals for geochemical analysis. Thus, all X-ray diffraction (XRD) and geochemical analyses were based on whole-rock samples. For this purpose, small pieces of the dolostones, considered typical of the parent sample, were manually ground into powder (75-150 μm) using an agate mortar and pestle. Each of the two hundred and thirty-three whole-rock samples produced in this manner were then subjected to XRD analysis and those formed of 100% dolomite were subsequently subjected to various other geochemical analyses. XRD analyses were done on a Rigaku Geigerflex 2173 XRD system using Co K_α radiation at the University of Alberta following the protocol developed by Jones et al. (2001). This allows determination of the mol % $CaCO_3$ (hereafter referred to as %Ca) of the dolomite. Following Jones et al. (2001), the dolomite is divided into low-Ca calcian dolomite (LCD – 50-55 %Ca) and high-Ca calcian dolomite (HCD – 55-62 %Ca). The weight % of LCD, weight % of HCD, and the average %Ca were calculated using the methods outlined by Jones et al. (2001).

Oxygen and carbon stable isotopes were determined for 63 samples that were formed of 100% dolomite (as determined by XRD analysis). These samples were reacted with 100% phosphoric acid for 2-3 days at 25°C, following the method of McCrea (1950). All extractions were introduced into a Finnigan-MAT 252 isotope mass spectrometer for analysis. The $\delta^{13}C$ and $\delta^{18}O$ values are reported relative to the Pee Dee Belemnite (PDB) standard normalized to NBS-18 in the per mil (‰) notion. Precision is better than 0.05 ‰ for both isotopes. The oxygen isotope values were not corrected for phosphoric acid fractionation. The concentrations of Sr, Mn, and Fe were determined for 54 samples that were formed entirely of dolomite. For this purpose, ~ 0.2 g of powdered sample was digested by 10 ml 8N HNO_3 and then analyzed on a Perkin Elmer Elan6000 quadrupole ICP-MS at the University of Alberta. Replicate analyses of an internal standard solution indicate an error (1σ) of 0.26% for Sr, 0.22% for Fe, and 0.2% for Mn.

$^{87}Sr/^{86}Sr$ ratios were determined for 45 samples (each 100% dolomite) in the Radiogenic Isotope Laboratory, University of Alberta. Procedures were similar to those described by MacNeil and Jones (2003). All data were normalized to SRM 987 (0.710245). The error margin for these analyses is ± 0.00002.

2.4. Results

2.4.1. Dolomite and calcite distribution

XRD analyses show that most samples from the basal part of the Cayman Formation are formed entirely of dolomite whereas samples from the middle and upper parts are formed of dolomite and variably but generally minor amounts of calcite (Fig. 2-4). A few samples, however, contain significant amounts of calcite. Petrographic analyses show that the calcite is present as small inclusions in the dolomite and/or as a cement (commonly alternating with zones of dolomite) that lines and fills fossil moulds and intergranular/intercrystalline pores.

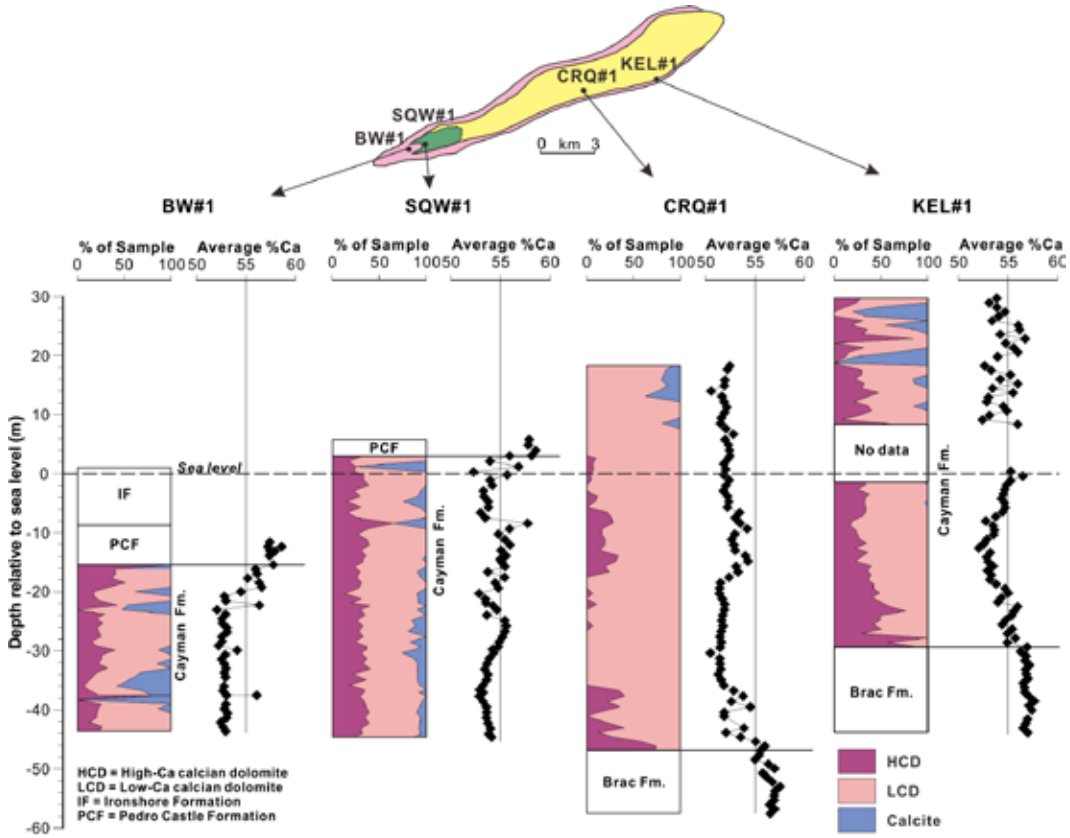

Fig. 2-4. Distribution of calcite, LCD, and HCD and average %Ca of dolostones in Cayman Formation in sections BW#1, SQW#1, CRQ#1, and KEL#1. Datum is modern sea level. Graphs based on XRD analyses of samples collected at 1.5 m intervals in each well.

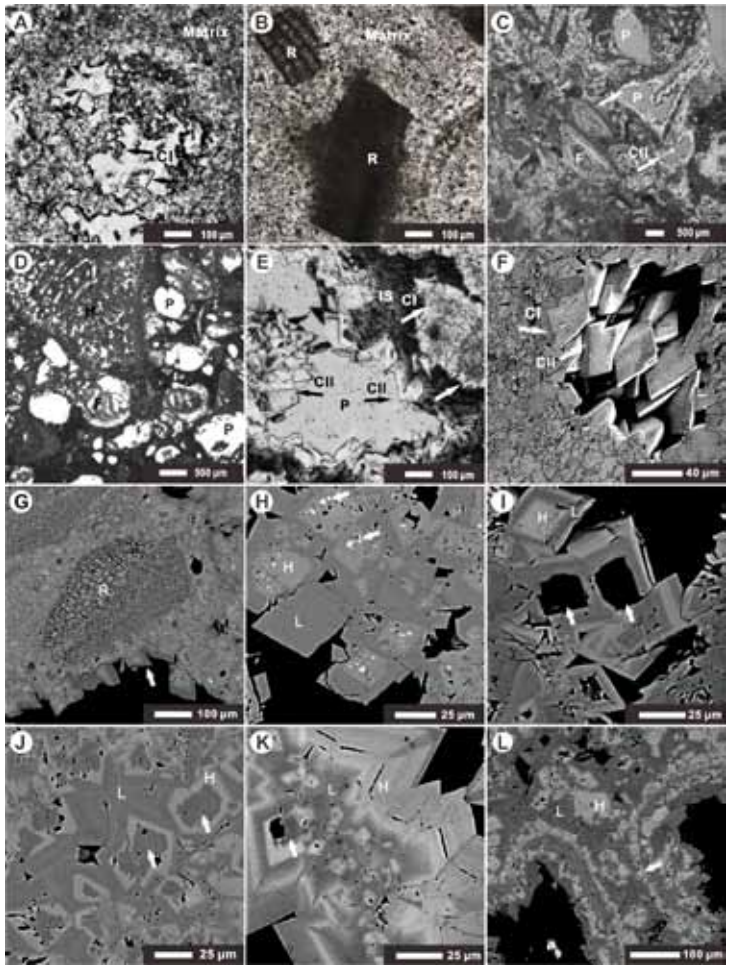

Fig. 2-5. Thin section photomicrographs (A-E), SEM image (F), and backscatter images (G-L) of dolostones from Cayman Formation. Depths are relative to sea level. For backscatter images, dark grey = LCD (L); light grey = HCD (H). (A) CRQ#1, -37.6 m, finely crystalline dolostones. Note that dolomite crystals in more open space show more euhedral habits. Arrows point to CI cement. (B) CRQ#1, -45.3 m, finely crystalline dolostone with crystalline matrix and psudomorphically replaced red algae fragments (R). Note that dolomite crystals have cloudy centres and clear rims. (C) KEL#1, -2.67 m, finely crystalline dolostones. Note pseudomorphically replaced foraminifera (F) and open moldic pores (P). Arrows point to CII cements. (D) CRQ#1, -19.4 m, aphanocrystalline dolostone. Note that Halimeda (H) and some foraminifera (F) were pseudomorphically replaced, whereas some skeletal grains had been leached out, and now show as moldic pores (P). (E) KEL#1, -27.1 m, cavity in finely crystalline dolostone lined with internal sediment (IS) which is following by CII cements. P = pore. Arrows point to CI and CII cements. (F) KEL#1, 17.5 m, SEM image showing CI overgrowth cement and CII cement filling in a pore. (G) KEL#1, -28.6 m, matrix dolomite formed of HCD and red algae (R) is pseudomorphically replaced by LCD and HCD. Note that cements close to pores are encrusted by LCD (arrow). (H) CRQ#1, -45.3 m, euhedral dolomite crystals with HCD cores and LCD cortices. Note calcite inclusions (arrows). (I) BW#1, -31.4 m, euhedral dolomite crystals

(*Continued caption of Fig. 2-5*) with HCD cores and LCD cortices. Note that some crystals with holes in centres (arrows). (J) CRQ#1 -15.7 m, inside-out dolomites (arrows). (K) KEL#1, -5.7 m, bioclast replaced by both HCD and LCD, and encrusted by cements formed of alternating HCD and LCD bands. Note inside-out dolomite crystal (arrow). (L) BW#1, -20.7 m, bioclast replaced by HCD and LCD. Note occurrence of HCD is controlled by precursor's fabrics (arrow).

2.4.2. Dolomite stoichiometry

The average %Ca of the dolostone samples is 50.5 to 57.7 %Ca (n = 233) with most dolostones being formed of LCD and HCD (Fig. 2-4). Although LCD is the most abundant component (75-100%), dolostones formed solely of LCD are found only in BW#1 and CRQ#1 (Fig. 2-4). There is no readily apparent lateral pattern to the distribution of LCD and HCD through the formation (Fig. 2-4). For example, the average %Ca of dolostones in BW#1 and SQW#1, only 1 km apart, cannot be correlated. Stratigraphically, dolostones that are closer to the formation boundaries tend to have higher %Ca (Fig. 2-4).

2.4.3 Petrography

The dolostones are formed of interlocking anhedral to subhedral dolomite

Table 2-1 Cathodoluminescence (CL) features of components of dolostones from Cayman Formation on Cayman Brac.

Type of CL	Components		Features of CL
I	Matrix	aphanocrystalline	Bright red
		Finely crystalline	Moderately bright red
	Allochems		Bright red
		CI	Moderately bright red with zonings
		CII	Bluish grey to dark
II	Finely crystalline matrix		Nonluminescent to dull red
	Allochems		Dull to bright red
		CI	Nonluminescent to dull red
		CII	Nonluminescent

crystals that are up to 50 μm long but typically < 20 μm long (Fig. 2-5A, B). In general, the dolomite crystals in the upper part of the Cayman Formation are smaller than those in the lower part and the crystals nearest to the pores are more euhedral than those located in the groundmass away from the pores (Fig. 2-5A). Most dolomite crystals have cloudy centres encased by clear rims (Fig. 2-5B).

The original fabrics of the precursor limestone are preserved to varying degrees. Biofragments of red algae and echinoderm plates commonly retain their original fabrics (Fig. 2-5B) whereas biofragments originally formed of aragonite (e.g. corals, gastropods, bivalves) have been dissolved and biomolds are all that now remain (Fig. 2-5C and D). Some *Halimeda* plates, originally formed of aragonite, have been pseudomorphically replaced by dolomite with minor dissolution (Fig. 2-5D). Limpid dolomite cements are common in the Cayman Formation on Cayman Brac. Petrographically, they can be divided into two types. Type I is a cement (CI) that typically grew around dolomite crystals in the matrices (Figs. 2-5E and F), is 10-15 μm thick. Type II cement (CII), with crystals 20-60 μm long, fills pores or lines the walls of pores and biomolds (Figs. 2-5E and F).

In dolostones from the basal part of the Cayman Formation, the matrix dolomite tends to be formed largely of unzoned HCD crystals, whereas the allochems have been replaced by LCD (Fig. 2-5G). In samples formed solely of LCD, all of the skeletal components were replaced by LCD. Most of the dolomite crystals, despite their small size, are characterized by various styles of HCD and LCD zoning (Fig. 2-5H-K). Many crystals have a HCD core, commonly with numerous calcite inclusions that are encased by a LCD zone (Fig. 2-5H). In some crystals, preferential dissolution of the HCD cores produced hollow crystals (Fig. 2-5I). Subsequent dolomite precipitation in those hollow crystals (Fig. 2-5J and K) produced inside-out dolomite (cf. Jones, 2007). In some dolomitized bioclasts,

the distribution of HCD follows the fabrics of precursors (Fig. 2-5L).

Based on cathodoluminescence (CL), the dolostones in the Cayman Formation are divided into Type I and Type II (Table 2-1). Type I is characterized by (1) relative homogeneous moderately-bright to bright red CL (Fig. 2-6A) with pseudomorphically replaced allochems (e.g., foraminifera), (2) aphanocrystalline matrices that typically have the brightest luminescence (Fig. 2-6A), (3) finely crystalline matrices that usually have a moderately bright red luminescence (Fig.

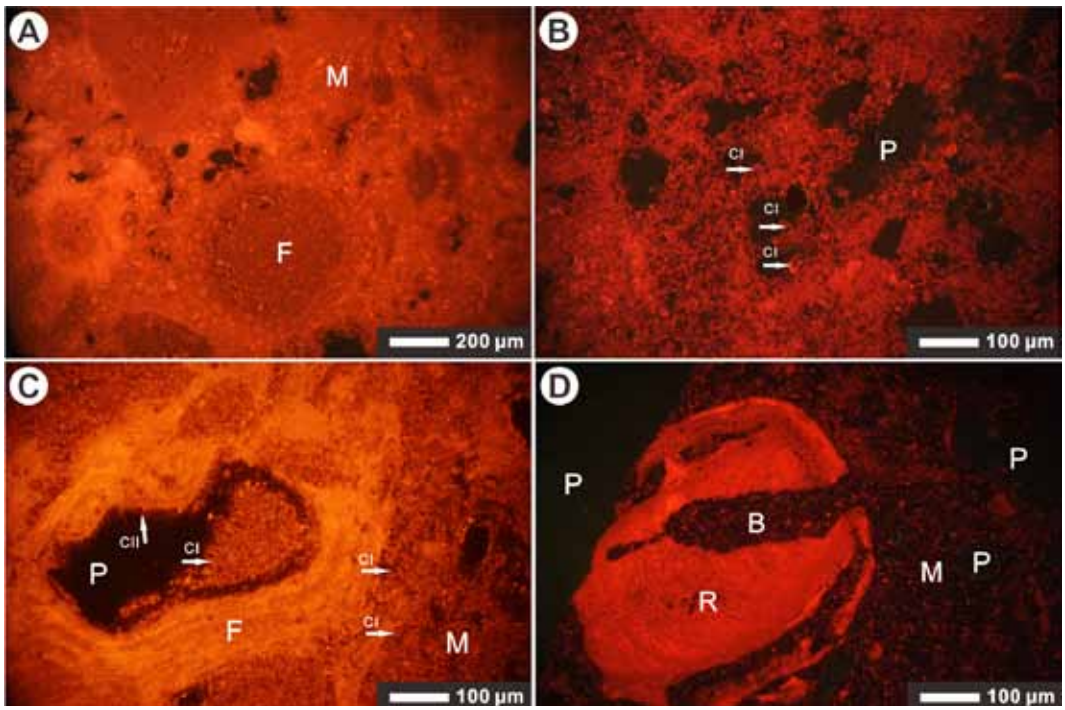

Fig. 2-6. Cathodoluminescence (CL) images of dolostones from Cayman Formation. Depths are relative to sea level. (A) CRQ#1, -4.7 m, aphanocrystalline dolostone showing Type I CL. F = foraminifera, M = matrix. (B) CRQ#1, -19.4 m, finely crystalline dolostone showing Type I CL. Arrows point to CI cement which have brighter CL than centres of euhedral dolomite crystals. P = pore. (C) CRQ#1, -15.7 m, finely crystalline dolostone showing Type I CL. Note that foraminifera (F) has brightest CL, CI has moderately bright CL, and CII shows dark grey CL. P = pore, M = matrix.. (D) KEL#1, -28.6 m, finely crystalline dolostone showing Type II CL. Note that red algae (R) shows bright CL, and matrix (M) and filled burrow (B) show dull CL mottled with some bright spots.

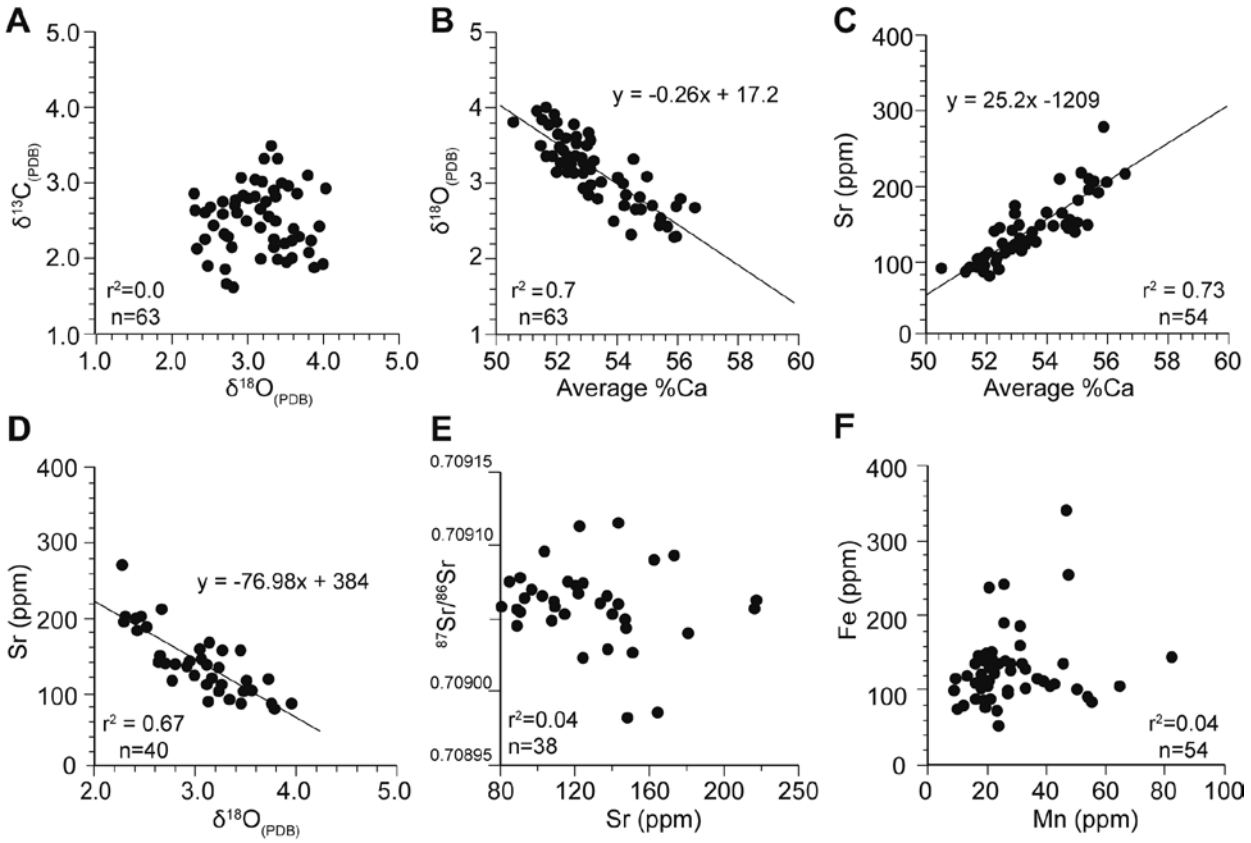

Fig. 2-7. Bivariant graphs showing relationships between various attributes of dolostones from Cayman Formation. A) $\delta^{13}C$ versus $\delta^{18}O$. B) $\delta^{18}O$ versus average %Ca with calculated regression axis. C) Sr content versus average %Ca with calculated regression axis. D) Sr content versus $\delta^{18}O$ with calculated regression axis. E) $^{87}Sr/^{86}Sr$ versus Sr. F) Fe versus Mn.

2-6B), and (4) CI cement has a moderately-bright red CL signature (Fig. 2-6B and C), and CII cement is characterized by a dark grey CL (Fig. 2-6C). Type II dolostones typically have a dull red to nonluminescence CL signature, but there are rare examples in which bright luminescent pseudomorphically-replaced allochems (e.g., red algae) occur in a dark luminescent matrix (Fig. 2-6D). Stratigraphically, Type I is dominant in the middle and upper parts of the Cayman Formation whereas Type II is found only in the lower part of the formation.

2.4.4. Carbon and oxygen stable isotopes

The $\delta^{13}C$ and $\delta^{18}O$ of the dolostones ranges from 1.6 to 3.5‰ (average 2.5‰, n = 63) and from 2.3 to 4.0‰ (average 3.2‰, n = 63), respectively (Appendix 1). There is no correlation between $\delta^{13}C$ and $\delta^{18}O$ (Fig. 2-7A). The $\delta^{18}O$ values of the dolostones are, however, inversely correlated to their average %Ca (Fig. 2-7B).

2.4.5. Strontium and strontium isotope

The Sr content of dolostones from the Cayman Formation, which ranges from 80 to 279 (average 140 ppm, n=54), positively covaries with the average %Ca of the dolomite (Fig. 2-7C) and inversely correlates to their $\delta^{18}O$ (Fig. 2-7D). Dolostones from the Cayman Formation yielded $^{87}Sr/^{86}Sr$ ratios of 0.708982 to 0.709132 (n = 45) with an average of 0.709062 (Appendix 1). There is no correlation between $^{87}Sr/^{86}Sr$ values and the Sr contents of dolostones (Fig. 2-7E).

2.4.6. Iron and Manganese

The Fe content ranges from 52 to 340 ppm with an average of 128 ppm (n = 54) whereas the Mn content ranges from 9 to 82 ppm with an average of 28 ppm (n = 54) (Appendix 1). There is no correlation between the Fe and Mn (Fig. 2-7F).

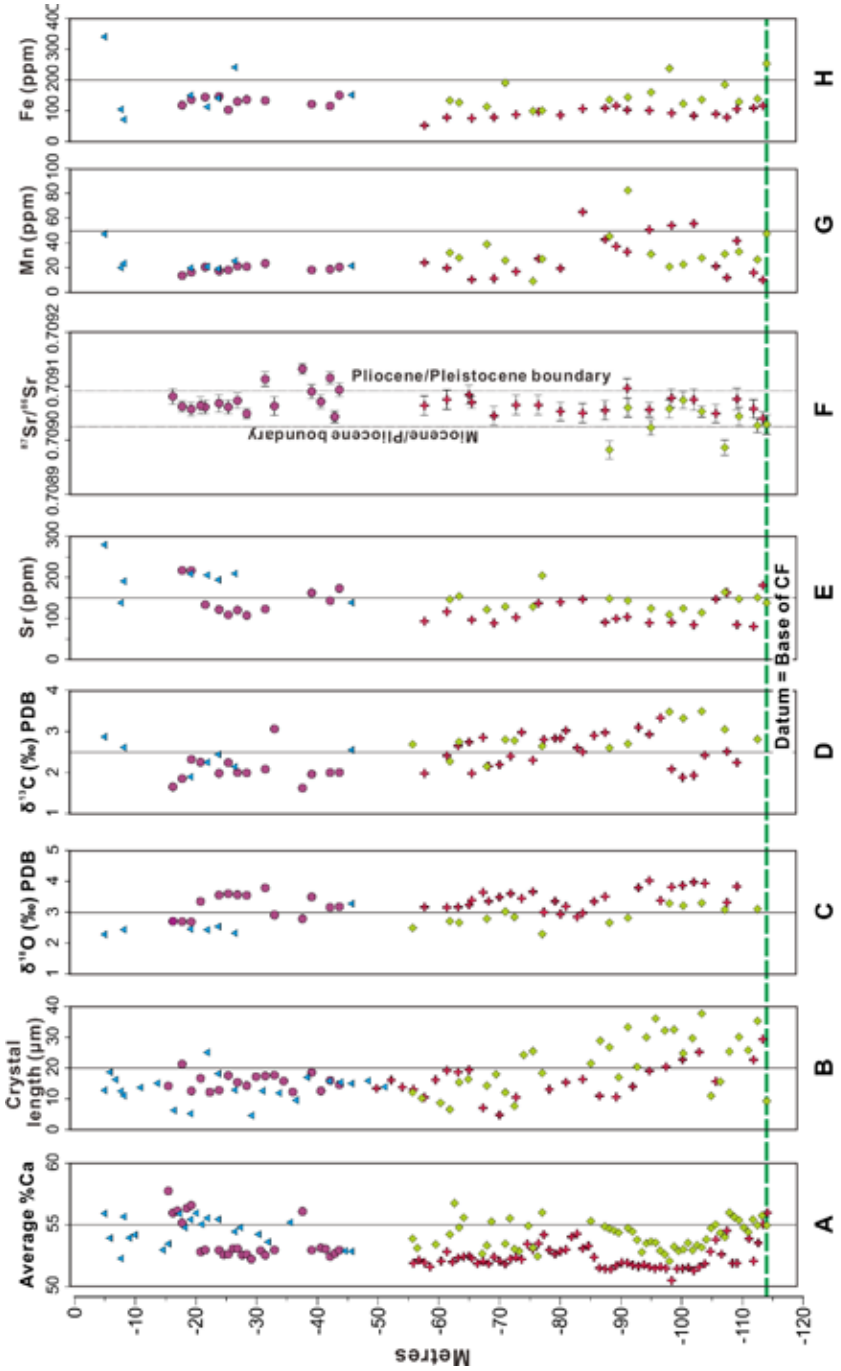

Fig. 2-8. Composite plots, based on successions at BW#1, SQW#1, CRQ#1, and KEL#1, showing stratigraphic variability in average %Ca (A), crystal length (crystal length data for CRQ#1, KEL#1, and SQW#1 first reported by Jones (2005)) (B), $\delta^{18}O$ (C), $\delta^{13}C$ (D), Sr (E), $^{87}Sr/^{86}Sr$ ratio (F), Mn (G), and Fe (H). Datum is base of Cayman Formation.

2.4.7. Stratigraphic trends

In the dolostones from the Cayman Formation on Cayman Brac there is little evidence of systematic stratigraphic variation in the average %Ca (Fig. 2-8A), average crystal length (Fig. 2-8B), $\delta^{18}O$ (Fig. 2-8C), $\delta^{13}C$ (Fig. 2-8D), Sr concentrations (Fig. 2-8E), $^{87}Sr/^{86}Sr$ ratios (Fig. 2-8F), Mn concentrations (Fig. 2-8G), or Fe concentrations (Fig. 2-8H). The only exceptions are the $\delta^{18}O$ (Fig. 2-8C) and the crystal length (Fig. 2-8B) that both become slightly lower towards the top of the formation. In essence, the stratigraphic consistency evident in these geochemical parameters (Fig. 2-8) mimics the stratigraphic and sedimentologic monotony that is so evident in the field (Fig. 2-3).

2.5. Interpretative caveats

Interpretation of the pervasive dolomitized succession that now forms the Cayman Formation must integrate all information relating to the distribution of the dolomite, the stoichiometry of the dolomite, and various geochemical signatures. The challenge is one of translating each of these proxies into parameters that delineate the conditions under which dolomitization took place. Translation of these proxies, however, is not straightforward and interpretations must be mindful of the potential problems that are associated with them.

Three significant problems hinder the interpretation of the dolostones from the Cayman Formation on Cayman Brac.

1. The geochemical characteristics of the precursor limestones are unknown because the formation has been pervasively dolomitized. The calcite now found in the Cayman Formation is there as minute inclusions in some of the dolomite and/or as a cement that lines the pores or cavities in the dolostones.
2. With dolomite crystals < 50 μm long (typically < 20 μm long) and commonly characterized by oscillatory zoned LCD and HCD it is impossible

to sample individual crystals or specific zones in those crystals. The crystals are, for example, smaller than the minimum spot size needed for analysis on the electron microprobe or the minimum beam size used with various laser ablation techniques. Irrespective of the technique used, resultant analyses come from more than one crystal.

3. The dolostones, being formed of both LCD and HCD, are geochemically heterogeneous. The LCD and HCD cannot be analyzed separately (see point 2 above) and examples of dolostones formed solely of LCD or HCD are so rare that information obtained from them could not be considered statistically reliable.

These issues impact all aspects of the data and subsequent interpretations. It must be noted, however, that these issues are true for all island dolostones and that the origin of island dolostones has commonly been debated without even considering many of these issues.

2.5.1. Petrography

The fabric-retentive dolostones of the Cayman Formation are petrographically akin to island dolostones found on the Bahamas (Dawans and Swart, 1988; Vahrenkamp and Swart, 1994), Niue atoll, Pacific Ocean (Wheeler et al., 1999), and Kita-daito-jima atoll, Pacific Ocean (Suzuki et al., 2006). Retention of their original textures indicates that (1) these rocks had not been significantly compacted and/or cemented before the onset of dolomitization, and (2) numerous dolomite nucleation sites must have been present (Sibley, 1982; Sibley et al., 1994). Simulation experiments have shown, for example, that the preservation of original fabrics during dolomitization is largely dependent on the predolomitization diagenesis (Zempolich and Baker, 1993). Pervasive dolomitization also demands highly permeable substrates that would allow the

free passage of the dolomitizing fluids.

Various textures and cathodoluminescence signatures of dolostones in the Cayman Formation indicate that dolomitization was probably a multiple-stage process. The type I and type II cathodoluminescence signatures (Table 2-1 and Fig. 2-6), found in the basal and middle-upper parts of the Cayman Formation, probably reflect differences in the chemical composition of the dolomitizing fluids and/or in redox conditions (cf. Machel, 2000a). The dolomite cements also appear to have formed at different times. Textural evidence indicates that CII formed after CI (Figs. 2-5E, F and 6C). This is clearly evident in some cavities where CII is separated from CI by internal sediment (Fig. 2-5F).

2.5.2. Dolomite stoichiometry

Like most island dolostones, dolostones in the Cayman Formation are formed mainly of calcian dolomite with individual samples having an average %Ca that ranges from 50.5 to 57.7 %Ca (Fig. 2-4). There is no readily apparent correlation between the %Ca of the dolostones with location, depth, or crystal size (Figs. 2-4 and 2-8). The fact that the Cayman Formation was completely dolomitized implies that the dolomitization took place in an open diagenetic environment where a relatively high water/rock ratio existed.

Dolomite stoichiometry has been related to various kinetic factors, including the (1) Mg/Ca ratio of the dolomitizing solutions, (2) rock/water ratio (open or closed diagenetic system), (3) availability of Mg ions, and (4) reaction time with the dolomitizing fluids (Lumsden and Chimahusky, 1980; Sperber et al., 1984; Sibley, 1990; Sibley et al., 1994; Vahrenkamp and Swart, 1994; Budd, 1997; Schubel et al., 2006). Based on high-temperature experiments, Kaczmarek and Sibley (2011) argued that the dolomite stoichiometry reflects the Mg/Ca ratio of the formative waters, albeit in a nonlinear manner. They argued that high Mg/Ca ratios in the dolomitizing fluids will result in shorter induction periods (time for

first appearance of dolomite) and faster dolomitization rates whereas fluids with low Mg/Ca ratios will result in longer induction periods and slower dolomitization rates. All their experiments produced poorly ordered, nonideal dolomites with high solution Mg/Ca ratio fluids producing more Mg-rich dolomites whereas low solution Mg/Ca ratios led to the formation of Ca-rich dolomites.

As yet, it is not possible to directly translate the %Ca of a dolostone to a specific Mg/Ca ratio in the formative fluid. If the relationships developed by Kaczmarek and Sibley (2011) are accepted, then the predominance of LCD (50-55 %Ca) in the Cayman Formation indicates that the fluids that mediated their dolomitization had a high Mg/Ca ratio. Some caution must be attached to this interpretation because (1) some sections of dolostones (e.g., SQW#1) contain more HCD than other sections (e.g., CRQ#1) and (2) some of the original replacive dolomites have been diagenetically modified by the development of hollow dolomite crystals and inside-out dolomite (Fig. 2-5I-K). The issue of scale is also critical because pore-scale variations in pore fluid chemistry would be superimposed on the large-scale fluid characteristics. The oscillatory LCD - HCD zoning (Fig. 2-5K), evident in many dolomite crystals in the Cayman Formation has, for example, been attributed to microscale physiochemical controls (Jones and Luth, 2002).

2.5.3. Carbon and oxygen stable isotopes

2.5.3.1. Carbon isotope

The $\delta^{13}C$ values (1.6 to 3.5‰) of dolostones from the Cayman Formation are compatible with values associated with marine carbonates (see Budd, 1997). There is no evidence of the involvement of any other carbon sources but seawater and the lack of correlation between $\delta^{13}C$ and $\delta^{18}O$ indicates that meteoric water was probably not involved in the dolomitization. It appears, therefore, that the

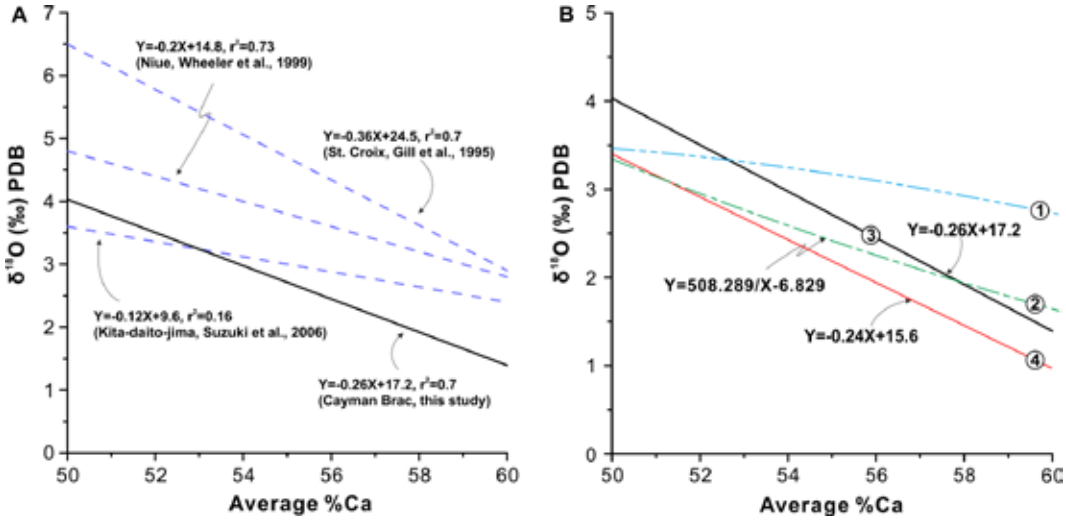

Fig. 2-9. A) Regression lines showing relationship between average %Ca and $\delta^{18}O$ for Tertiary dolostones from various islands. B) Regression equation between average %Ca and $\delta^{18}O$ of Cayman dolostones and corrections of oxygen isotope for dolomite stoichiometry and acid fractionation. Equation #1– regression equation after correcting for both stoichiometric effect and acid fractionation. Equation #2– theoretical equation showing influence of dolomite stoichiometry on its oxygen isotope fractionation, from Chacko and Denies (2008). Equation #3– regression equation from Cayman dolostones. Equation #4–regression equation for Cayman dolostones after acid fractionation correction. See text for details.

$\delta^{13}C$ values were probably inherited from the precursor limestones.

2.5.3.2. Oxygen isotope

The correlation between the $\delta^{18}O$ of the Cayman dolostones and their average %Ca (Fig. 2-7B) is similar to that found in island dolostones on the Bahamas (Dawans and Swart, 1988; Vahrenkamp and Swart, 1994; Gill et al., 1995) and Niue (Wheeler et al., 1999) and Kita-daito-jima (Suzuki et al., 2006) (Fig. 2-9A) in the Pacific Ocean. This correlation has been attributed to extrinsic conditions, such as water temperature and the isotopic composition of the dolomitization fluids (Wheeler et al., 1999; Suzuki et al., 2006), intrinsic factor such as the oxygen isotope fractionation factor, and/or kinetic factors that are largely related

to dolomite precipitation rates (Vahrenkamp and Swart, 1994).

For O isotopes, Ca substitution by Mg will increase the fractionation factor between the carbonate minerals and the water. Although Land (1980) argued that the magnitude of that increase for dolomite is poorly constrained, Tarutani et al. (1969) and Jiménez-López et al. (2004) suggested, respectively, that for high-Mg calcite there was a 0.06‰ to 0.17‰ increase per mol $MgCO_3$. The rate of change between the $\delta^{18}O$ of dolomite and Mg content has also been estimated from the difference in $\delta^{18}O$ between coprecipitated dolomite and calcite (Vahrenkamp and Swart, 1994). Such estimates for $\Delta\delta^{18}O_{dolo\text{-}cal}$ at 25°C, based on experiments and theoretical calculations, include 4 to 7‰ (Northrop and Clayton, 1966; O'Neil and Epstein, 1966; Clayton et al., 1968; Matthews and Katz, 1977), 2.6 to 4‰ (Fritz and Smith, 1970; Schmidt et al., 2005; Vasconcelos et al., 2005), 3‰ (Land, 1980), and 5.08‰ (Chacko and Deines, 2008). Such values translate to 0.05-0.14‰ increase in $\delta^{18}O$ per 1 %Ca increase.

Reported acid fractionation factors, which may also impact the $\delta^{18}O$ derived from calcian dolomite, range from 1.01110 to 1.01186, which corresponds to a difference of 0.84 to 1.59‰ in the $\delta^{18}O$ of calcite and dolomite (Sharma and Clayton, 1965; Land, 1980; Rosenbaum and Sheppard, 1986; Sharma et al., 2002). Although the effect of %Ca on the acid fractionation is uncertain, calcian dolomite probably has a lower acid fractionation factor than ideal dolomite (Aharon et al., 1977; Rosenbaum and Sheppard, 1986; Vahrenkamp and Swart, 1994). If a simple linear relationship between the %Ca of dolomite and the acid fractionation factor is assumed, then a 0.017‰ to 0.032‰ decrease per 1 %Ca is derived. Chacko and Deines (2008) argued that the $\Delta\delta^{18}O_{dolo\text{-}cal}$ of 2.6-4‰ at 25 °C, as derived from low-temperature experiments (Fritz and Smith, 1970; Schmidt et al., 2005; Vasconcelos et al., 2005), was probably an underestimate as they were probably not obtained under equilibrium conditions. Instead, Chacko and

Deines (2008) suggested that the oxygen isotope fractionation factor (α) between carbonate minerals and water can be calculated from equation (1).

$$1000\ln\alpha_{carbonate\text{-}water} = 1000\ln\beta_{carbonate} - 1000\ln\beta_{water} \quad (1)$$

Where β is the reduced partition function ratio of the mineral being analyzed.

If it is assumed that the calcian dolomite is a simple mixture of ideal dolomite layers and "calcite-like" layers (Drits et al., 2005), then the β of calcian dolomite can be expressed by equation (2).

$$1000\ln\beta_{\text{calcian dolomite}} = X_{\text{dolomite}}\ 1000\ln\beta_{\text{ideal dolomite}} + X_{\text{calcite}}\ 1000\ln\beta_{\text{calcite}} \quad (2)$$

Where X_{dolomite} is the molar ratio of dolomite and X_{calcite} is the molar ratio of calcite in the calcian dolomite.

If calcian dolomite formed in equilibrium with seawater with 1.5‰ $\delta^{18}O_{(SMOW)}$ at 25°C (similar to seawater collected from well EEV#2 on Grand Cayman at depth of 100 m, Jones unpublished data), then according to equations (1) and (2), the relationship between the $\delta^{18}O$ of calcian dolomite (in PDB) and %Ca can be expressed by equation (3).

$$\delta^{18}O_{\text{calcian dolomite}} = 508.289/X_{Ca} - 6.829 \quad (3)$$

Where X_{Ca} is the %Ca of calcian dolomite.

According to this relationship, an ideal dolomite (50:50 Ca:Mg) formed in equilibrium with seawater at 25°C should have a $\delta^{18}O$ of 3.3‰ – a figure that is consistent with our data if an acid fractionation factor of 0.8‰ (cf. Land, 1980) is used (equation #2 on Fig. 2-9B). Although the relationship between %Ca and $\delta^{18}O$ is not linear, application of equation (3) for the 50 to 60 %Ca range, yields a ~ 0.17‰ decrease in $\delta^{18}O$ for every 1 %Ca increase (Fig. 2-9B). In order to compare the theoretical equation (#2 on Fig. 2-9B) with the regression equation

derived from our data (#3 on Fig. 2-9B), the regression equation is corrected for the acid fractionation factor under the assumption that the acid fractionation factor of ideal dolomite is 1.0111 ($\delta^{18}O_{(dolomite\text{-}calcite)}$ = 0.8‰) and the acid fractionation factor of dolomite correlates inversely the %Ca of dolomite (#4 on Fig. 2-9B). Following this correction for acid fractionation, however, the dolostone samples with higher %Ca have more negative $\delta^{18}O$ values than the theoretical values (Fig. 2-9B). For dolostones with 60%Ca, for example, there is a 0.6‰ discrepancy between equations 2 and 4 (Fig. 2-9B). This discrepancy may be related to the acid fractionation factor, which might be not linearly related to the %Ca. Aharon et al. (1977), for example, argued that, in terms of acid fractionation behaviour, calcian dolomite behaves more like calcite than dolomite. The acid fractionation correction for dolostones with 60 %Ca, however, is only 0.17‰. Thus, the correlation between the average %Ca of the dolostones and their $\delta^{18}O$ values seems to be only partially related to their phosphoric acid fractionation factor. The rest of the discrepancy may be caused by (1) kinetic effects given that calcian dolomites are general thought to have precipitated faster than ideal dolomite (Vahrenkamp and Swart, 1994), and/or (2) the mixing of different dolomite populations that formed in dolomitizing fluids which had different temperature or distinctly different $\delta^{18}O$ (Wheeler et al., 1999; Suzuki et al., 2006).

Wheeler et al. (1999) argued that a relative uniform change rate in $\delta^{18}O$ with increasing %Ca of calcian dolomite would be expected if this relationship was controlled solely by intrinsic factors. Nevertheless, regression equations relating these two variables, based on samples from different islands, have different slopes (Fig. 2-9A). Thus, the rates of change include 0.20‰ per 1%Ca (Bahamas, Dawans and Swart, 1988), 0.22‰ per 1 %Ca (Bahamas, Vahrenkamp and Swart, 1994), 0.36‰ per 1 %Ca (St. Croix, Gill et al., 1995), 0.20‰ per 1 %Ca (Niue, Wheeler et al., 1999), 0.15‰ per 1 %Ca (Kita-daito-jima, Suzuki et al., 2006),

and 0.26‰ per 1 %Ca (Cayman Brac, this study). Some of this variance may be related to the manner in which samples are processed for analysis. Gill et al. (1995), Wheeler et al. (1999), and Suzuki et al. (2006), for example, used a weak-acid-leaching method for purification of their dolostones. Yui and Gong (2003) suggested that this method may lead to significant errors because of (1) inaccurate estimates of the calcite content of calcareous dolostone and dolomitic limestone, and (2) non-stoichiometric dolomites that are more liable to react with acids than stoichiometric dolomites. For example, the regression equation of Gill et al. (1995) that was based solely on calcian dolomites (56-60 %Ca) has the steepest slope (Fig. 2-9A). This may indicate that the calcian dolomites are more susceptible to the weak-acid-leaching method than the stoichiometric dolomites. The low r^2 (0.15) between %Ca and $\delta^{18}O$ derived by Suzuki et al. (2006) and the positive shift evident in the data of Wheeler et al. (1999) relative to this study could be attributed to the same reason (Fig. 2-9A). Thus, the discrepancies that exist between these values may be related to the analytical methods used in the derivation of the $\delta^{18}O$ values.

2.5.4. Sr content

With < 300 ppm, the Sr contents of dolostones from the Cayman Formation are compatible with most island dolostones (Budd 1997, his Fig.13 and Table 4). The Sr content is controlled by the Sr/Ca ratio of the dolomitizing fluids and the Sr distribution coefficient ($D_{Sr}^{dolomite}$) between the dolomite and the formative fluids (Land, 1980; Banner, 1995; Budd, 1997). Although poorly known, the $D_{Sr}^{dolomite}$ at ambient temperature it is thought to be about half the Sr distribution coefficient of calcite ($D_{Sr}^{calcite}$) (Banner, 1995; Budd, 1997). Banner (1995) suggested that $D_{Sr}^{calcite}$ is 0.03±0.02 for low-temperature diagenetic calcite that forms at slow growth rate. From this it can be estimated that $D_{Sr}^{dolomite}$ should be between 0.015 and 0.025. $D_{Sr}^{calcite}$ is, however, influenced by kinetic factors (Rimstidt et

al., 1998) and Nehrke et al. (2007) suggested that $D_{sr}^{calcite}$ can vary from 0.02 to 0.12 depending on precipitation rates. Based on Bahamian Tertiary dolomites, Vahrenkamp and Swart (1990) suggested that $D_{Sr}^{dolomite}$ is a function of dolomite stoichiometry (0.0118 for ideal dolomite and 0.0507 for dolomite with 60 %Ca) with kinetic factors being responsible. Given modern seawater with molar Sr/Ca = 0.0085 (de Villiers, 1999) and using $D_{Sr}^{dolomite}$ estimates of between 0.015 and 0.025, then the 80 – 279 ppm Sr found in the Cayman Formation dolostones indicates a normal seawater origin.

As reported from many island dolostones, the Sr content of dolostones from the Cayman Formation covaries with their average %Ca (Fig. 2-7C). This relationship has been attributed to (1) $D_{Sr}^{dolomite}$ that is variable due to kinetic factors (e.g., precipitation rates of dolomite) and /or major element composition of dolomite (Vahrenkamp and Swart, 1990), and/or (2) fluctuating Sr/Ca ratios in the dolomitizing fluids (Wheeler et al., 1999; Suzuki et al., 2006). Wheeler et al. (1999) argued that dolomitization of a Sr-rich limestone precursor formed of aragonite and high-Mg calcite would result in Sr-rich calcian dolostones, whereas Sr-poor limestones formed of low-Mg calcite would produce more stoichiometric dolostones. This argument implies that the Sr found in dolostones is partly inherited from the precursor limestones. If that were the case, the $^{87}Sr/^{86}Sr$ values of dolostones should covary with their Sr content because the $^{87}Sr/^{86}Sr$ signatures of dolomitizing fluids (seawater) should be more radioactive than those from the precursor limestones. There is, however, no correlation between the $^{87}Sr/^{86}Sr$ values and Sr contents of dolostones from the Cayman Formation (Fig. 2-7E). Vahrenkamp et al. (1988) suggested that a large dolostone body with relative uniform $^{87}Sr/^{86}Sr$ values yield $^{87}Sr/^{86}Sr$ signatures that reflect the dolomitizing fluids rather than the precusor limestones. It appears, therefore, that the Sr of dolostones from the Cayman Formation were probably inherited from the

dolomitizing fluids.

The Sr/Ca of dolomitizing fluids may be related to the secular fluctuation in the Sr/Ca of seawater. If a $D_{Sr}^{dolomite}$ of 0.02 is assumed, then the 80 to 279 ppm Sr found in the Cayman dolostones indicate that the Sr/Ca of the seawater fluctuated from 0.0084 to 0.0294. Lear et al. (2003), however, argued that since the Neogene seawater has had a Sr/Ca value of < 0.01. Thus, the variation in Sr content of dolostones from the Cayman Formation cannot be attributed entirely to the secular change in Sr/Ca of seawater.

The relative uniform slopes of the regression equations that relate Sr and %Ca for dolostones from different islands (~20-27 ppm per %Ca) indicates that the correlation must be controlled by universal rather than local factors (Fig. 2-7C). Therefore, the variable $D_{Sr}^{dolomite}$ is most probably the major factor causing the correlation between the Sr content of Cayman dolostones and their average %Ca. For dolostones from the Cayman Formation there is a negative correlation ($r^2 = - 0.67$) between the Sr and $\delta^{18}O$ (Fig. 2-7D). Such a correlation indicates that the major element composition of dolomite have important influences on both oxygen isotope fractionation and the Sr partition between dolomite and dolomitization fluids.

2.5.5. Mn and Fe

The low Mn and Fe contents of dolostones from the Cayman Formation are similar to those from other island dolostones (Budd, 1997, his Fig. 17). The Mn and Fe contents in carbonates are generally attributed to (1) their distribution coefficients, (2) the Eh of the diagenetic fluids, (3) the composition of the diagenetic fluid, and/or (4) precipitation rates (Veizer, 1983; Wogelius et al., 1992; Vahrenkamp and Swart, 1994; Budd, 1997; Rimstidt et al., 1998). Although the distribution coefficients of Mn and Fe between dolomite and water are uncertain, they are probably larger than unity (Veizer, 1983). Given the low Fe (2 ppb)

and Mn (0.2 ppb) concentrations in seawater (Drever, 1997), Vahrenkamp and Swart (1994) speculated that the Fe and Mn found in island dolostones were probably inherited from their precursor limestones. For the dolostones found in the Cayman Formation, the lack of correlation between these two cations and their relatively low concentrations indicates that the dolomitizing fluids were either oxidizing and/or had no significant impact on the Fe and Mn in the diagenetic system.

2.6. Dolomitizing fluids and their timing

The nature of the dolomitizing fluid(s) and the age of dolomitization is, by necessity, based on the interpretation and integration of all available data. Such interpretations have to be qualified, wherever possible, by the caveats that are

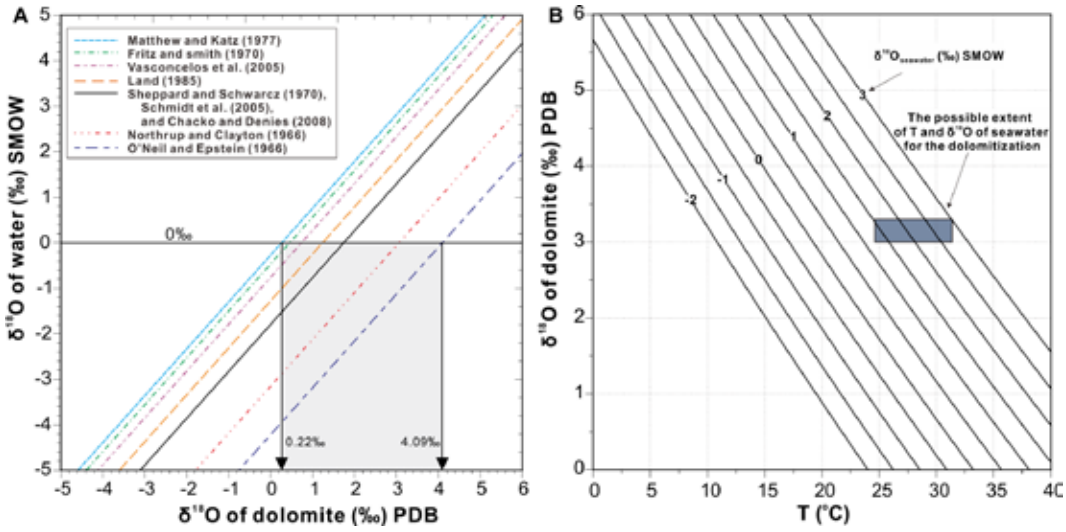

Fig. 2-10. A) Comparison of various oxygen isotope fractionation equations between dolomite and water at 25°C. For $\delta^{18}O$(water) = 0‰, the calculated $\delta^{18}O$(dolomite) by different equations has a discrepancy of ~ 4‰. B) Predicted T and $\delta^{18}O$ of fluids in which Cayman dolostones formed based on oxygen isotope fractionation equation of Chacko and Deines (2008). $\delta^{18}O$ of dolostones have been corrected for acid fractionation and stoichiometric effect (see text for details).

attached to each aspect of the data. Future resolution of those caveats will allow the stratigraphic, petrographic, and geochemical proxies to be more precisely constrained.

2.6.1 Characteristics of dolomitizing fluids

The stoichiometry of the dolomite in the Cayman Formation indicates that the fluids that mediated their formation probably had a high Mg/Ca ratio. This assumes that the relationships postulated by Kaczmarek and Sibley (2011) are accepted and recognizes that early diagenesis may have slightly modified the dolomite stoichiometry that is now calculated from XRD analyses.

The salinity and temperature of the dolomitizing fluids are commonly inferred from the $\delta^{18}O_{(dolomite)}$ by using equations developed from (1) experiments (Northrop and Clayton, 1966; O'Neil and Epstein, 1966; Fritz and Smith, 1970; Sheppard and Schwarcz, 1970; Matthews and Katz, 1977; Schmidt et al., 2005; Vasconcelos et al., 2005), (2) empirical considerations (Land, 1985), or (3) theoretical calculations (Chacko and Deines, 2008). At 25°C, the discrepancy between the $\delta^{18}O_{(dolomite)}$ derived from different equations is up to 3‰ (Fig. 2-10A). Such discrepancies are attributable to (1) uncertainty in extrapolations from high-temperature to low-temperature conditions, (2) stoichiometric effects, (3) disequilibrium, especially for those numbers derived from low temperature experiments, and/or (4) variations in experimental conditions (Chacko and Deines, 2008). This issue is critical because attribution of island dolostones, with similar $\delta^{18}O$ values, to normal seawater or modified seawater (diluted or evaporated) can arise simply because different fractionation values have been used (Humphrey, 2000).

If, as suggested by Wheeler et al. (1999) and Suzuki et al. (2006), the $\delta^{18}O$ values of island dolostones are controlled only by the temperature and isotopic composition of seawater, the correlation between the $\delta^{18}O_{(dolomite)}$ and depth should

echo the physicochemical fluctuation caused by the sea level change. In the dolostones from the Cayman Formation, however, the $\delta^{18}O_{(dolomite)}$ is correlated to the average %Ca (Fig. 2-7B), is not correlated with depth (Fig. 2-8), and displays considerable lateral variation between different wells (Fig. 2-4). Collectively, these considerations indicate that the $\delta^{18}O_{(dolomite)}$ is controlled primarily by dolomite stoichiometry.

After correcting for discrepancies related to dolomite stoichiometry and the acid fractionation factor, the Cayman dolostones with 50.5 to 57.5 %Ca, have $\delta^{18}O_{(dolomite)}$ values ranging from 3.0 to 3.3‰ (equation #1 on Fig. 2-9B). According to the theoretical equation of Chacko and Deines (2008), these dolostones would be in equilibrium with seawater that has a $\delta^{18}O$ of 1.5‰ (SMOW) at 24.5 to 26°C (Fig. 2-10B). Although compatible with modern seawater and consistent with subsurface seawater on Grand Cayman, consideration must be given to the possibility that seawater temperature may have been different when dolomitization took place. Paleotemperature data derived from foraminifera, for example, indicate that Late Miocene to Pliocene seawater might have had warmer than it is today (Zachos et al., 2001; Westerhold et al., 2005). Medina-Elizalde et al. (2008) suggested, for example, that the tropical sea surface temperature (SST) during the Pliocene may have been as high as 31°C and the $\delta^{18}O_{(seawater)}$ may have been 0.3‰ - 0.8‰ higher than present day ocean water. If this was the case, then the dolomitizing fluids that mediated formation of the dolostones in the Cayman Formation were probably near-surface normal seawater that may have had a higher temperature and heavier $\delta^{18}O$ than today (Fig. 2-10B).

2.6.2. Times of dolomitization

If it is accepted that the $^{87}Sr/^{86}Sr$ values were inherited largely from the seawater that mediated their formation (Budd, 1997; Jones and Luth, 2003), then the $^{87}Sr/^{86}Sr$ values can be converted to absolute time using one of the many

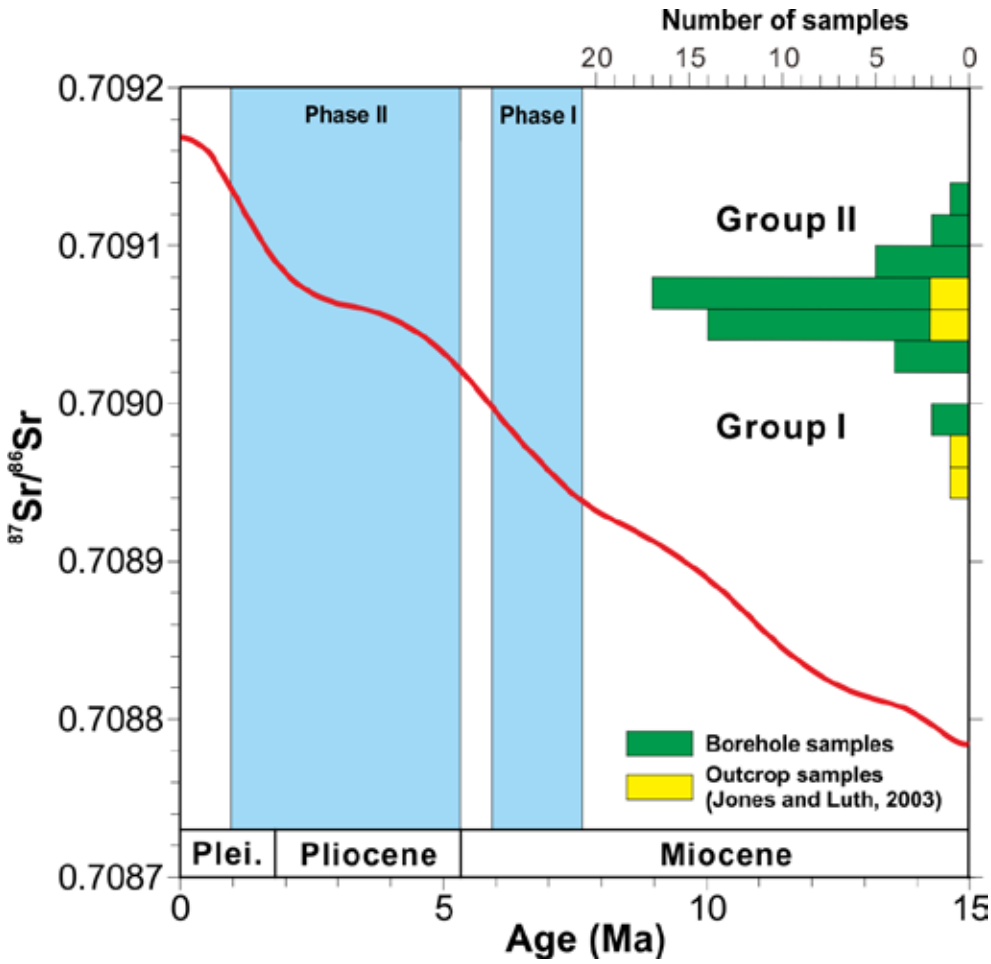

Fig. 2-11. Timing of phase I and II dolomitization, as derived from $^{87}Sr/^{86}Sr$ of dolostones from Cayman Formation (histogram). $^{87}Sr/^{86}Sr$ curve of seawater from McArthur et al. (2001, look-up table version 4:08/03).

curves that have been developed to show its temporal evolution (e.g., Burke et al., 1982; Koepnick et al., 1985; DePaolo and Ingram, 1985; McKenzie et al., 1988; Hodell et al. 1991; Ohde and Elderfield, 1992; Oslick et al., 1994; Swart et al., 2001; McArthur et al., 2001). Although the trends shown on these curves are in general agreement, they commonly differ in detail. Thus, the absolute ages derived from the $^{87}Sr/^{86}Sr$ ratio depend, to some extent, on the curve that is selected for this purpose. Herein, the curve of McArthur et al. (2001) is used

because it is the most recent and is based on a vast amount of data.

The $^{87}Sr/^{86}Sr$ values of dolostones from the Cayman Formation on Cayman Brac range from 0.708982 to 0.709132 (Fig. 2-8). As in any setting, there is the possibility that these ratios may be modified by inheritance from the limestone precursor, detrital input, hydrothermal fluids, and/or ground waters that gain Sr from older rocks (Gill et al., 1995; Fouke et al., 1996; Machel, 2000b; Jones and Luth, 2003). The isolated setting of Cayman Brac, however, means that the sources of the Sr isotope are limited to the carbonate precursor (e.g., Vahrenkamp et al., 1988) and/or the dolomitizing fluid (Jones and Luth, 2003). The former possibility is deemed unlikely because the original limestone were mineralogically heterogeneous, there is no correlation between their Sr contents and $^{87}Sr/^{86}Sr$, and most of the $^{87}Sr/^{86}Sr$ ratios are between 0.709050 and 0.709075 (Fig. 2-7E).

The distribution of the $^{87}Sr/^{86}Sr$ ratios from the dolostones of the Cayman Formation on Cayman Brac can be divided into group 1, with values from 0.70894 to 0.708989, that comes from dolostones in the basal part of the Cayman Formation in KEL#1 and outcrops on the east end of Cayman Brac (Fig. 2-11), and group 2, with values from 0.70902 to 0.70913, that comes from dolostones from the middle and upper parts of the Cayman Formation (Fig. 2-11). Group 2 has a distinct mode between 0.70904 and 0.70908 (Fig. 2-11). Using the $^{87}Sr/^{86}Sr$-time curve of McArthur et al. (2001; Look-Up Table Version 4:08/03), the ratios in Group 1 translate into ages of 6-8 Ma (late Miocene) whereas the ratios in Group 2 give ages of 1-5 Ma (Pliocene to Early Pleistocene) (Fig. 2-11). The modal data in Group 2 yields an age of 2 to 4.5 Ma. The timing of these dolomitization phases agree with those delineated from island dolostones on the Bahamas (Vahrenkamp et al., 1991), on Kita-daito-jima (Ohde and Elderfield, 1992), and Grand Cayman (Jones and Luth, 2003).

The Sr ratio “ages” are consistent with the notion that dolomitization

postdated deposition of the original limestones, which took place in the middle to upper Miocene. Open to debate is (1) the timing of dolomitization relative to the tectonic tilting of Cayman Brac, and (2) if the restriction of the Pedro Castle Formation to the west part of the island resulted from erosion or reflects original depositional patterns (Fig. 2-1). Two models can explain this situation. Model I involved (1) dolomitization of the Cayman Formation, (2) tilting of the island, and (3) deposition of the Pedro Castle Formation on the western part of the island. Model II involved (1) deposition of the Cayman Formation, (2) development of the Cayman Unconformity, (3) deposition of the Pedro Castle Formation over the entire island with dolomitization of the Cayman Formation at the same time, (4) tilting of the island, and (5) removal of the Pedro Castle Formation by erosion from the central and eastern parts of the island. A critical issue with respect to these two models is whether or not there are any indications that the Pedro Castle Formation once covered the entire island. Today, this formation is found on west end of the island and exposures of highly altered (caliche development) limestones belonging to the formation are present around "The Mound", 12 – 16 m above sea level (Fig. 2-1). The notion that the strata developed through model II is also supported by the following considerations.

- The Cayman Formation must have been submerged below sea level at the time of dolomitization.
- The Sr ratio "age" of dolostones in the Cayman Formation indicates that Phase II dolomitization took place during the Pliocene (Fig. 2-11), which is synchronous with the deposition of the Pedro Castle Formation (Fig. 2-2).
- Available evidence indicates that dolomitization of the Cayman Formation on Cayman Brac and Grand Cayman took place at the same time and under similar conditions. There is, however, no evidence for tilting of strata on Grand Cayman (Jones, 1994). Thus, it is reasonable to infer that Cayman

Brac, like Grand Cayman, had not been tilted at the time of dolomitization.

All of the available evidence points to two phases of dolomitization (Fig. 2-11) with phase I in the late Miocene (6 to 8 Ma) being followed by phase II in the Pliocene to Early Pleistocene (1 to 5 Ma).

2.7. Discussion

Island dolostones, irrespective of their locations in the Caribbean Sea and Pacific Ocean, are united by their isolated oceanic settings, their petrographic similarities, and comparable geochemical signatures. In stark contrast, the origin of these dolostones have been variously ascribed to the gravity-controlled reflux brine model (Gill et al., 1995), the hydrothermal convection model (Aharon et al., 1987; Ohde and Elderfield, 1992; Machel, 2000b), or the mixing zone model (Ward and Halley, 1985; Aissaoui et al., 1986; Humphrey, 1988; Gaswirth et al., 2007). This reflects, at least in part, the variable interpretations that have been attached to many of the geochemical proxies derived from the dolostones. Irrespective of the model chosen, pervasive dolomitization requires a source of Mg, a delivery mechanism for moving the Mg to the site of dolomitization, and favourable physiochemical conditions at the site of dolomitization (Morrow, 1982).

Isolated in the Caribbean Sea, the Mg needed for dolomitization of the limestones in the Cayman Formation could only have come from the surrounding Caribbean Sea or from hydrothermal fluids generated from the Mid-Cayman Spreading Centre that is located southwest of Grand Cayman. There is, however, no evidence of hydrothermal fluids being involved in the diagenesis of the carbonate successions found on the Cayman Islands. Thus, the Mg must have been derived from the oceanic waters that surround Cayman Brac.

The circulation of Mg-bearing fluids that mediated formation of island

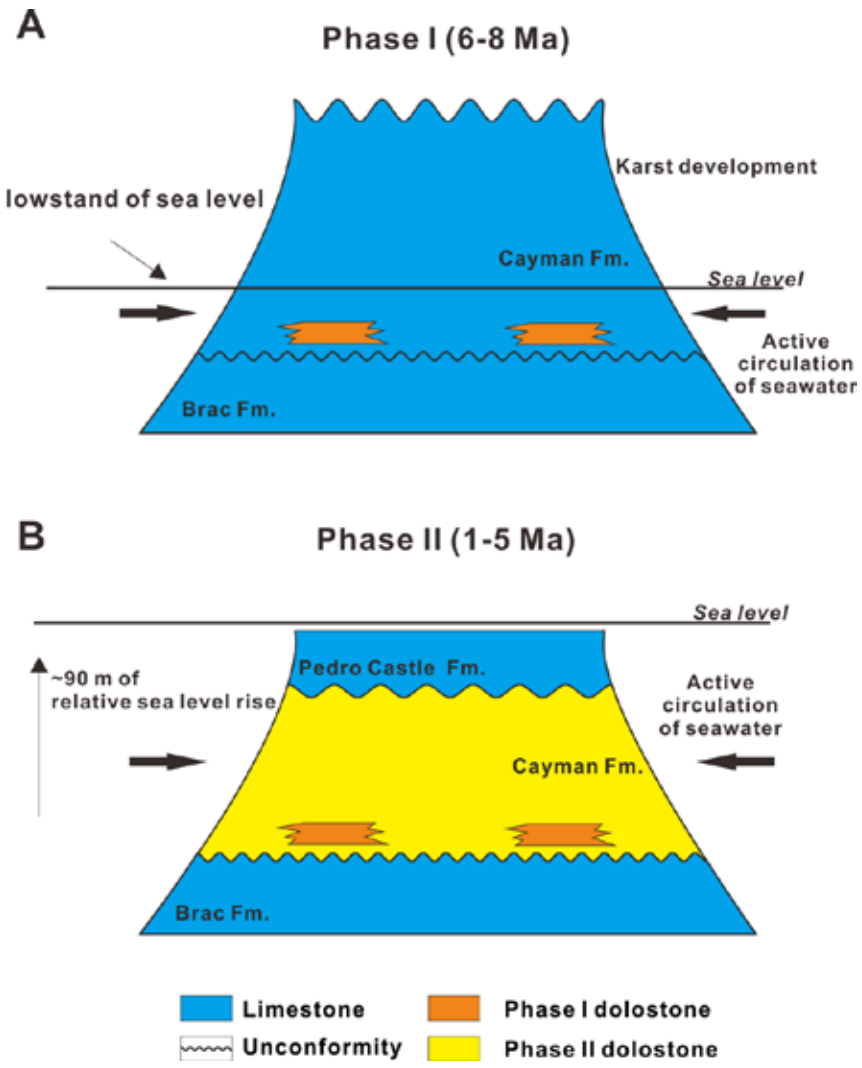

Fig. 2-12. Schematic diagrams showing Phase I and II dolomitization and the linkage between sea level and the timing of dolomitization of Cayman Formation on Cayman Brac.

dolostones was controlled by the hydrology that existed at the time of dolomitization. The reflux, hydrothermal convection, and mixing zone models deemed responsible for the development of island dolostones are characterized by different groundwater circulation patterns that are driven by variable hydrological processes. For the dolostones of the Cayman Formation on Cayman Brac, however, there is no evidence of evaporitic minerals, no evidence of hydrothermal activity, and the stratigraphic distribution of dolostones is inconsistent with the

reflux brine model. Dolomitization of the Cayman Formation on Cayman Brac can, however, be explained if seawater circulated horizontally through the island under the influence of tides and/or onshore currents (Fig. 2-12). Today, much of the saline groundwater on Grand Cayman is, for example, kept in motion by daily tides and at various times, storms. In the east central part of the island, for example, the water table fluctuates in response to daily tides with a lag time of 1 to 4 hours (Ng et al., 1992). This short lag time reflects the transmissive nature of the open carbonate aquifer in the Cayman Formation that is characterized by complex pore networks, fractures, and solution widened joints (Ng et al., 1992). Many of those features developed as karst evolved during periods of exposure. It seems reasonable to assume that tidal influences on Cayman Brac, prior to tilting, were similar to those on Grand Cayman. Indeed, it could be argued that pumping would have been even more effective on Cayman Brac because the island is much narrower than Grand Cayman.

As yet, the exact subsurface conditions needed for dolomitization are poorly known and the mechanism that triggers dolomitization remains elusive. Interpretation of the $\delta^{18}O$ from the dolostones of the Cayman Formation (Fig. 2-10B) indicates that the dolomitization might be related to sea waters that had a higher temperature and salinity than today. The dolostones in the Cayman Formation were produced by multiple episodes of dolomitization. This assertion parallels the conclusions reached for other island dolostones (Budd, 1997; Wheeler et al., 1999; Jones and Luth, 2003; Suzuki et al., 2006) and it has been suggested that dolomitization events may have been synchronous (Budd, 1997). If it is accepted that dolomitization was mediated by seawater, then the precursor limestones must have been bathed in seawater and it follows that regional control(s), such as eustatic changes in sea level, must underpin the dolomitization processes (Budd, 1997; Wheeler et al., 1999; Jones and Luth, 2003; Suzuki et al.,

2006).

Throughout the Miocene and Pliocene there were significant eustatic fluctuates in sea level curves that are largely attributable to glaciations that occurred at different times in the northern and southern hemispheres (e.g., Prentice and Matthews, 1991; Lear et al., 2000; Zachos et al., 2001). Although the general timing and magnitudes of the sea level changes, as derived from various methods, are in general agreement, they differ in detail (Miller et al., 2005; Kominz et al., 2008; Jones and Luth, 2003, their Fig. 16). Such variations mean that it is very difficult to precisely correlate "dolomitization events" with specific highstands or lowstands, especially given the error margins that are associated with the timing of dolomitization events as derived from $^{87}Sr/^{86}Sr$ ratios (e.g., Budd, 1997; Jones and Luth, 2003). The Cayman Unconformity, which forms the upper boundary of the Cayman Formation, has been associated with the Messinian lowstand that resulted from glaciation in the southern hemisphere at the end of the Miocene (Jones and Hunter, 1994a; Jones and Luth, 2003). On Grand Cayman, there is evidence that lowstand was 40 to 90 m below today's sea level (Jones and Hunter, 1994a). Jones and Luth (2003) suggested that karst development that took place during this lowstand was critically important because it enhanced the porosity and permeability of the exposed limestones. Thus, as sea level rose to the next highstand during the Lower Pliocene, sea water was able to move freely through the limestone bedrock and mediate dolomitization. On Cayman Brac, Phase I dolomitization (Late Miocene) caused only incomplete dolomitization of the basal part of the Cayman Formation (Fig. 2-12). A similar situation evolved on Grand Cayman (Jones and Luth, 2003). Phase II dolomitization, associated with a rise in sea level during the Pliocene to Late Pleistocene (Fig. 2-12) completed dolomitization of the Cayman Formation.

On Cayman Brac, the relationship between the Sr isotopic ages of the

dolostones and their stratigraphic positions is similar to that reported from other island dolostones on the Bahamas (Vahrenkamp et al., 1991), Grand Cayman (Jones and Luth, 2003), Kita-daito-jima (Ohde and Elderfield, 1992), and other localities reviewed by Budd (1997). Such similarities support the notion that "island dolomitization events" are fundamentally related to eustatic changes in sea level. Although an attractive and viable possibility, questions remain, largely because the timing of dolomitization during a transgressive-regressive cycle remains debatable and precise dating of these "dolomitizing events" is difficult to establish. Island dolomitization been variously aligned with sea level lowstands, sea level highstands, or periods of aridity (Budd, 1997). This problem arises largely because the error margins associated with the $^{87}Sr/^{86}Sr$ geochronometer are commonly greater than the duration of many of the short-lived sea level highstands that occurred throughout the Pliocene. Thus, it becomes even more difficult to relate the dolomitization events to specific time frames within a given transgressive-regressive cycle (Budd, 1997; Jones and Luth, 2003). It is, for example, generally impossible to know if dolomitization took place during the transgressive phase or highstand phase in one of these cycles. If dolomitization was mediated by seawater, then a stable hydrological regime related to highstand conditions would allow large volumes of seawater to circulate through the limestone bodies (Sibley, 1991). Jones and Luth (2003) suggested that prior to dolomitization, the rocks needed to be diagenetically modified so that large volumes of seawater could easily circulate through the rock body. With specific reference to Grand Cayman, they argued that lowstand conditions would have exposed the island with the carbonates then being subjected to intense karst development that significantly increased the porosity and permeability of the bedrock. Such modifications would have permitted large volumes of seawater to circulate through the bedrock as sea level rose during the next transgressive

cycle. In effect, they suggested dolomitization was genetically related to karst because the karst provided the avenues for circulation of vast quantities of the dolomitizing fluids. The model proposed by Jones and Luth (2003) for dolomitization on Grand Cayman is equally applicable to Cayman Brac. Nevertheless, proof of the linkage between eustacy, karst, and dolomitization "events" remains open to debate, largely because the $^{87}Sr/^{86}Sr$ geochronometer cannot provide the accuracies in dating that are needed.

2.8. Conclusions

The pervasively dolomitized succession embodied in the Cayman Formation on Cayman Brac is an excellent example of "island dolostones", having developed on a small island that is geographically isolated by the deep oceanic waters of the surrounding Caribbean Sea. Analysis of these dolostones, from many different perspectives, produced the following important conclusions.

- The finely crystalline dolostones are formed of LCD and lesser amounts of HCD with individual samples have an average of 50.5 to 57.7 %Ca. There does not appear to be any systematic vertical or lateral patterns to the variance in the dolomite stoichiometry.
- The correlations between the average %Ca and O isotopes and Sr, reflect stoichiometry and kinetic effects rather than fluctuations in the composition of dolomitizing fluids
- The dolomitizing fluids, which probably had a high Mg/Ca ratio, were probably seawater that may have had a slightly higher temperature and heavier $\delta^{18}O$ than modern seawater. Onshore waves and tidal activity was largely responsible for the circulation of those fluids through the precursor limestones.
- A two-episode dolomitization model (6-8 Ma and 1-5Ma) that was related

to the relative sea level rise can reasonably interpret the $^{87}Sr/^{86}Sr$ ratios of dolostones and corresponding petrographic features and geochemical signatures.

The finely crystalline dolostones found in the Cayman Formation on Cayman Brac are extremely similar to other island dolostones found around the Caribbean islands and Pacific atolls in terms of their petrography and geochemistry. Regional control(s) on this process should be responsible for their development although the triggering mechanism is still remaining unknown.

2.9. References

Aharon, P., Kolodny, Y., Sass, E., 1977. Recent hot brine dolomitization in the" Solar Lake," Gulf of Elat, isotopic, chemical, and mineralogical study. Journal of Geology 85, 27-48.

Aharon, P., Socki, R., Chan, L., 1987. Dolomitization of atolls by sea water convection flow: test of a hypothesis at Niue, South Pacific. Journal of Geology 95, 187-203.

Aissaoui, D.M., Buigues, D., Purser, B., 1986. Model of reef diagenesis: Mururoa atoll, French Polynesia. Reef diagenesis, 27-52.

Banner, J.L., 1995. Application of the trace element and isotope geochemistry of strontium to studies of carbonate diagenesis. Sedimentology 42, 805-824.

Budd, D.A., 1997. Cenozoic dolomites of carbonate islands: their attributes and origin. Earth-Science Reviews 42, 1-47.

Burke, W.H., Denison, R.E., Hetherington, E.A., Koepnick, R.B., Nelson, H.F., Otto, J.B., 1982. Variation of seawater $^{87}Sr/^{86}Sr$ throughout Phanerozoic time. Geology 10, 516-519.

Chacko, T., Deines, P., 2008. Theoretical calculation of oxygen isotope fractionation factors in carbonate systems. Geochimica et Cosmochimica Acta 72, 3642-3660.

Clayton, R.N., Jones, B.F., Berner, R.A., 1968. Isotope studies of dolomite formation under sedimentary conditions. Geochimica et Cosmochimica Acta 32, 415-424.

DePaolo, D.J., Ingram, B.L., 1985. Detailed record of Neogene Sr isotope evolution of seawater from DSDP site 590B. Geology 227, 103-106.

Dawans, J.M., Swart, P.K., 1988. Textural and geochemical alternations in Late Cenozoic Bahamian dolomites. Sedimentology 35, 385-403.

DeMet, C., Wiggins-Grandison, M., 2007. Deformation of Jamaica and motion of

the Gonâve microplate from GPS and seismic data. Geophysical Journal International 168, 362-278.

de Villiers, S., 1999. Seawater strontium and Sr/Ca variability in the Atlantic and Pacific oceans. Earth and Planetary Science Letters 171, 623-634.

Drever, J.I., 1997. The geochemistry of natural waters, surface and groundwater environments. Englewood Cliffs, New Jersey (Prentice Hall), 436 pp.

Drits, V.A., McCarty, D.K., Sakharov, B., Milliken, K.L., 2005. New insight into structural and compositional variability in some ancient excess-Ca dolomite. Canadian Mineralogist 43, 1255-1290.

Fouke, B.W., Beets, C., Meyers, W.J., Hanson, G.N., Melillo, A.J., 1996. $^{87}Sr/^{86}Sr$ Chronostratigraphy and dolomitization history of the Seroe Domi Formation, Curaçao (Netherlands Antilles). Facies 35, 293-320.

Fritz, P., Smith, D., 1970. The isotopic composition of secondary dolomites. Geochimica et Cosmochimica Acta 34, 1161-1173.

Gaswirth, S.B., Budd, D.A., Farmer, G.L., 2007. The role and impact of freshwater–seawater mixing zones in the maturation of regional dolomite bodies within the proto Floridan Aquifer, USA. Sedimentology 54, 1065-1092.

Gill, I.P., Moore Jr., C.H., Aharon, P., 1995. Evaporitic mixed-water dolomitization on St. Croix, U.S.V.I. Journal of Sedimentary Research 65, 591-604.

Hodell, D.A., Muller, P.A., Garrido, J.R., 1991. Variations in the strontium isotopic composition of seawater during the neogene. Geology 19, 24-27.

Humphrey, J.D., 1988. Late Pleistocene mixing zone dolomitization, southeastern Barbados, West Indies. Sedimentology 35, 327-348.

Humphrey, J.D., 2000. New geochemical support for mixing-zone dolomitization at Golden Grove, Barbados. Journal of Sedimentary Research 70, 1160-

1170.

Jiménez-López, C., Romanek, C.S., Huertas, F.J., Ohmoto, H., Caballero, E., 2004. Oxygen isotope fractionation in synthetic magnesian calcite. Geochimica et Cosmochimica Acta 68, 3367-3377.

Jones, B., 1994. Geology of the Cayman Islands. In: M.A. Brunt, J.E. Davies (Eds.), The Cayman Islands: Natural history and biogeography. Kluwer, Dordrecht, The Netherlands, pp. 13–49.

Jones, B., 2004. Petrography and significance of zoned dolomite cements from the Cayman Formation (Miocene) of Cayman Brac, British West Indies. Journal of Sedimentary Research 74, 95-109.

Jones, B., 2005. Dolomite crystal architecture: genetic implications for the origin of the Tertiary dolostones of the Cayman Islands. Journal of Sedimentary Research 75, 177-189.

Jones, B., 2007. Inside-out dolomite. Journal of Sedimentary Research 77, 539-551.

Jones, B., 2010. The preferenetial association of dolomite with microbes in stalactites from Cayman Brac, British West Indies. Sedimentary Geology 226, 94-109.

Jones, B., 2011. Stalactite growth mediated by biofilms: example from Nani Cave, Cayman Brac, British West Indies. Journal of Sedimentary Research 81, 322-338.

Jones, B., Hunter, I.G., 1994a. Messinian (late Miocene) karst on Grand Cayman, British West Indies; an example of an erosional sequence boundary. Journal of Sedimentary Research 64, 531-541.

Jones, B., Hunter, I.G., 1994b. Evolution of an isolated carbonate bank during Oligocene, Miocene and Pliocene times, Cayman Brac, British West Indies. Facies 30, 25-50.

Jones, B., Hunter, I.G., Kyser, K., 1994a. Revised stratigraphic nomenclature for Tertiary strata of the Cayman Islands, British West Indies. Caribbean Journal of Science 30, 53-68.

Jones, B., Hunter, I.G., Kyser, K., 1994b. Stratigraphy of the Bluff Formation (Miocene-Pliocene) and the newly defined Brac Formation (Oligocene), Cayman Brac, British West Indies. Caribbean Journal of Science 30, 30-51.

Jones, B., Luth, R.W., MacNeil, A.J., 2001. Powder X-ray diffraction analysis of homogeneous and heterogeneous sedimentary dolostones. Journal of Sedimentary Research 71, 790-799.

Jones, B., Luth, R.W., 2002. Dolostones from Grand Cayman, British West Indies. Journal of Sedimentary Research 72, 559-569.

Jones, B., Luth, R.W., 2003. Temporal evolution of Tertiary dolostones on Grand Cayman as determined by $^{87}Sr/^{86}Sr$. Journal of Sedimentary Research 73, 187-205.

Kaczmarek, S.E., Sibley, D.F., 2011. On the evolution of dolomite stoichiometry and cation order during high-temperature synthesis experiments: An alternative model for the geochemical evolution of natural dolomites. Sedimentary Geology 240, 30-40.

Koepnick, R.B., Burke, W.H., Denison, R.E., Hetherington, E.A., Nelson, H.F., Otto, J.B., Waite, L.E., 1985. Construction of the seawater $^{87}Sr/^{86}Sr$ curve for the Cenozoic and Cretaceous: supporting data. Chemical Geology 58, 55-81.

Kominz, M., Browning, J.V., Miller, K.G., Sugarman, P.J., Mizintseva, S., Scotese, C.R., 2008. Late Cretaceous to Miocene sea level estimates from the New Jersey and Delaware coastal plain coreholes: an error analysis. Basin Research 20, 211-226.

Land, L.S., 1980. The isotopic and trace element geochemistry of dolomite: the state of the art. In: Zenger, D.H., Dunham, J.B., Ethington, R.L. (Eds.), Concepts and Models of Dolomitization, SEPM Special Publication 28, Tulsa, Oklahomano, pp. 87–110.

Land, L.S., 1985. The origin of massive dolomite. Journal of Geological Education 33, 112-125.

Lear, C.H., Elderfield, H., Wilson, P.A., 2000. Cenozoic deep-sea temperartures and global ice volumes from Mg/Ca in benthic foraminiferal calcite. Science 287, 269-272.

Lear, C.H., Elderfield, H., Wilson, P.A., 2003. A Cenozoic seawater Sr/Ca record from benthic foraminiferal calcite and its application in determining global weathering fluxes. Earth and Planetary Science Letters 208, 69-84.

Lumsden, D.N., Chimahusky, J.S., 1980. Relationship between dolomite nonstoichiometry and carbonate facies parameters. In: D.H. Zenger, J.B. Dunham, R.L. Ethington (Eds.), Concepts and Models of Dolomitizatioin. SEPM Special Publication 28, Tulsa, Oklahoma, pp. 123–137.

MacDonald, K.C., Holcombe, T.L., 1978. Inversion of magnetic anomalies and sea-floor spreading in the Cayman Trough. Earth and Planetary Science Letters 40, 407-414.

Machel, H.G., 2000a. Application of cathodoluminescence to carbonate diagenesis. In: M. Pagel, V. Barbin, P. Blanc, D. Ohnenstetter (Eds.), Cathodoluminescence in Geosciences. Springer Verlag, Berlin, pp. 271-301.

Machel, H.G., 2000b. Dolomite formation in Caribbean Islands: Driven by plate tectonics?! Journal of Sedimentary Research 70, 977-984.

MacNeil, A., Jones, B., 2003. Dolomitization of the Pedro Castle Formation (Pliocene), Cayman Brac, British West Indies. Sedimentary Geology 162,

219-238.

Matley, C.A., 1926. The geology of the Cayman Islands (British West Indies), and their relation to the Bartlett Trough. Quarterly Journal of the Geological Society 82, 352-387.

Matthews, A., Katz, A., 1977. Oxygen isotope fractionation during the dolomitization of calcium carbonate. Geochimica et Cosmochimica Acta 41, 1431-1438.

McArthur, J.M., Howarth, R.J., Bailey, T.R., 2001. Strontium isotope stratigraphy: LOWESS Version 3: Best fit to the marine Sr-isotope curve for 0-509 Ma and accompanying look-up table for deriving numerical age. Journal of Geology 109, 155-170.

McCrea, J.M., 1950. On the isotopic chemistry of carbonates and a paleotemperature scale. The Journal of Chemical Physics 18, 849-857.

McKenzie, J.A., Isern, A., Elderfield, H., Williams, A., Swart, P.K., 1988. Strontium isotope dating of paleoceanographic, lithographic and dolomitization events on the northeastern Australia margin, Leg 133. In: J.A. McKenzie, P.J. Davies and A. Palmer-Judson (Eds), Proceedings of Ocean Drilling Program, Scientific Results, pp. 489-498.

Medina-Elizalde, M., Lea, D., Fantle, M., 2008. Implications of seawater Mg/Ca variability for Plio-Pleistocene tropical climate reconstruction. Earth and Planetary Science Letters 269, 585-595.

Miller, K.G., Kominz, M.A., Browning, J.V., Wright, J.D., Mountain, G.S., Katz, M.E., Sugarman, P.J., Cramer, B.S., Christie-Black, N., Pekar, S.F., 2005. The Phanerozoic record of global sea-level change. Science 310, 1293-1298.

Morrow, D.W., 1982. Diagenesis 2. Dolomite-Part 2 Dolomitization models and ancient dolostones. Geoscience Canada 9, 95-106.

Nehrke, G., Reichart, G., Van Cappellen, P., Meile, C., Bijma, J., 2007. Dependence of calcite growth rate and Sr partitioning on solution stoichiometry: Non-Kossel crystal growth. Geochimica et Cosmochimica Acta 71, 2240-2249.

Ng, K.C., Jones, B., Beswick, R., 1992. Hydrogeology of Grand Cayman, British West Indies: a karstic dolostone aquifer. Journal of Hydrology 134, 273-295.

Northrop, D.A., Clayton, R.N., 1966. Oxygen-isotope fractionations in systems containing dolomite. The Journal of Geology 74, 174-196.

O'Neil, J.R., Epstein, S., 1966. Oxygen isotope fractionation in the system dolomite-calcite-carbon dioxide. Science 152, 198-201.

Ohde, S., Elderfield, H., 1992. Strontium isotope stratigraphy of Kita-daito-jima Atoll, North Philippine Sea: Implications for Neogene sea-level change and tectonic history. Earth and Planetary Science Letters 113, 473-486.

Oslick, J.S., Miller, K.G., Ferguson, M.D., Wright, J.D., 1994. Oligocene-Miocene strontium isotopes: stratigraphic revisions and correlations of an inferred glacioeustatic record. Paleoceanography 9, 427-433.

Perfit, M.R., Heezen, B.C., 1978. The geology and evolution of the Cayman Trench. Geological Society of America Bulletin 89, 1155-1174.

Prentice, M.L., Matthews, R.K., 1991. Tertiary ice sheet dynamics: the snow gun hypothesis. Journal of Geophysical Research 96, 6811-6827.

Randazzo, A.F., Zachos, L.G., 1984. Classification and description of dolomitic fabrics of rocks from the Floridan aquifer, USA. Sedimentary Geology 37, 151-162.

Rimstidt, J.D., Balog, A., Webb, J., 1998. Distribution of trace elements between carbonate minerals and aqueous solutions. Geochimica et Cosmochimica Acta 62, 1851-1863.

Rosenbaum, J., Sheppard, S., 1986. An isotopic study of siderites, dolomites and ankerites at high temperatures. Geochimica et Cosmochimica Acta 50, 1147-1150.

Saller, A.H., 1984. Petrologic and geochemical constraints on the origin of subsurface dolomite, Enewetak Atoll: an example of dolomitization by normal seawater. Geology 12, 217-220.

Schmidt, M., Xeflide, S., Botz, R., Mann, S., 2005. Oxygen isotope fractionation during synthesis of CaMg-carbonate and implications for sedimentary dolomite formation. Geochimica et Cosmochimica Acta 69, 4665-4674.

Schubel, K.A., Veblen, D.R., Malone, M.J., 2006. Microstructures and textures of experimentally altered Bahamian ooids: Implications for reaction mechanisms of dolomitization. Carbonates and Evaporites 21, 1-13.

Sharma, S.D., Patil, D.J., Gopalan, K., 2002. Temperature dependence of oxygen isotope fractionation of CO_2 from magnesite-phosphoric acid reaction. Geochimica et Cosmochimica Acta 66, 589-593.

Sharma, T., Clayton, R.N., 1965. Measurement of O^{18}/O^{16} ratios of total oxygen of carbonates. Geochimica et Cosmochimica Acta 29, 1347-1353.

Sheppard, S.M.F., Schwarcz, H.P., 1970. Fractionation of carbon and oxygen isotopes and magnesium between coexisting metamorphic calcite and dolomite. Contributions to Mineralogy and Petrology 26, 161-198.

Sibley, D.F., 1982. The origin of common dolomite fabrics; clues from the Pliocene. Journal of Sedimentary Research 52, 1087-1100.

Sibley, D.F., 1990. Unstable to stable transformations during dolomitization. The Journal of Geology 98, 739-748.

Sibley, D.F., 1991. Secular changes in the amount and texture of dolomite. Geology 19, 151-154.

Sibley, D.F., Nordeng, S.H., Borkowski, M.L., 1994. Dolomitization kinetics of

hydrothermal bombs and natural settings. Journal of Sedimentary Research 64, 630-637.

Sperber, C.M., Wilkinson, B.H., Peacor, D.R., 1984. Rock composition, dolomite stoichiometry, and rock/water reactions in dolomitic carbonate rocks. Journal of Geology 92, 609-622.

Suzuki, Y., Iryu, Y., Inagaki, S., Yamada, T., Aizawa, S., Budd, D.A., 2006. Origin of atoll dolomites distinguished by geochemistry and crystal chemistry: Kita-daito-jima, northern Philippine Sea. Sedimentary Geology 183, 181-202.

Swart, P.K., Elderfield, H., Beets, K., 2001. The $^{87}Sr/^{86}Sr$ ratios of carbonates, phosphorites, and fluids collected during the Bahamas drilling project cores Clino and Unda: implications for dating and diagenesis, Subsurface Geology of a Prograding Carbonate Platform Margin, Great Bahama Bank: Results of the Bahamas Drilling Project. SEPM (Soceity for Sedimentary Geology), pp. 175-185.

Tarhule-Lips, R.F.A., Ford, D.C., 2004. Karst on Cayman Brac. Zeitschrift für Geomorphologie, 136, 69-88.

Tarutani, T., Clayton, R.N., Mayeda, T.K., 1969. The effect of polymorphism and magnesium substitution on oxygen isotope fractionation between calcium carbonate and water. Geochimica et Cosmochimica Acta 33, 987-996.

Vahrenkamp, V.C., Swart, P.K., Ruiz, J., 1988. Constraints and interpretation of $^{87}Sr/^{86}Sr$ ratios in Cenozoic dolomites. Geophysical Research Letters 15, 385-388.

Vahrenkamp, V.C., Swart, P.K., 1990. New distribution coefficient for the incorporation of strontium into dolomite and its implications for the formation of ancient dolomites. Geology 18, 387-391.

Vahrenkamp, V.C., Swart, P.K., Ruiz, J., 1991. Episodic dolomitization of late

Cenozoic carbonates in the Bahamas; evidence from strontium isotopes. Journal of Sedimentary Research 61, 1002-1014.

Vahrenkamp, V.C., Swart, P.K., 1994. Late Cenozoic dolomites of the Bahamas: metastable analogues for the genesis of ancient platform dolomites. In: B. Purser, M. Tucker, D. Zenger (Eds.), Dolomites: A Volume in Honour of Dolomieu: International Association of Sedimentologists, Special Publication, pp. 133–153.

Vasconcelos, C., McKenzie, J.A., Warthmann, R., Bernasconi, S.M., 2005. Calibration of the $\delta^{18}O$ paleothermometer for dolomite precipitated in microbial cultures and natural environments. Geology 33, 317-320.

Veizer, J., 1983. Chemical diagenesis of carbonates: theory and application of trace element technique. In: T.F. Anderson, M.A. Arthur (Eds.), Stable Isotopes in Sedimentary Geology. Society of Economic Paleontologists and Mineralogists Short Course Notes pp. 3-1-3-100.

Ward, W.C., Halley, R.B., 1985. Dolomitization in a mixing zone of near-seawater composition, late Pleistocene, northeastern Yucatan Peninsula. Journal of Sedimentary Petrology 55, 407-420.

Westerhold, T., Bickert, T., Röhl, U., 2005. Middle to late Miocene oxygen isotope stratigraphy of ODP site 1085 (SE Atlantic): New constrains on Miocene climate variability and sea-level fluctuations. Palaeogeography, Palaeoclimatology, Palaeoecology 217, 205-222.

Wheeler, C.W., Aharon, P., Ferrell, R.E., 1999. Successions of late Cenozoic platform dolomites distinguished by texture, geochemistry, and crystal chemistry; Niue, South Pacific. Journal of Sedimentary Research 69, 239-255.

Wogelius, R.A., Fraser, D.G., Feltham, D.J., Whiteman, M.I., 1992. Trace element zoning in dolomite: Proton microprobe data and thermodynamic

constraints on fluid compositions. Geochimica et Cosmochimica Acta 56, 319-334.

Yui, T.F., Gong, S.Y., 2003. Stoichiometry effect on stable isotope analysis of dolomite. Chemical Geology 201, 359-368.

Zachos, J., Pagani, M., Sloan, L., Thomas, E., Billups, K., 2001. Trends, rhythms, and aberrations in global climate 65 Ma to present. Science 292, 686-693.

Zempolich, W.G., Baker, P.A., 1993. Experimental and natural mimetic dolomitization of aragonite ooids. Journal of Sedimentary Petrology 63, 596-606.

CHAPTER 3
ORIGIN OF FABRIC-DESTRUCTIVE DOLOSTONES OF THE BRAC FORMATION[1]

3.1. Introduction

Dolostones of all ages are characterized by fabric-retentive and/or fabric-destructive textures (e.g., Sibley 1991, Budd, 1997, Machel, 2004) that reflect the diagenetic changes associated with dolomitization. The genesis of the fabric-destructive textures, however, remains controversial (Sibley, 1982, Sibley and Gregg, 1987, Gregg et al., 1992, Mazzullo, 1992, Budd, 1997, Choquette and Haitt, 2008, Maliva et al., 2011). Dolostones found on isolated oceanic islands (referred to as "island dolostone" by Budd (1997)) are a perfect candidate for examining this issue because they (1) developed in isolated environments, (2) are relatively young (Cenozoic), and (3) commonly contain both fabric-retentive and fabric-destructive textures. The distribution of dolostones exhibiting these two textures is laterally and vertically variable in most successions of island dolostones. In some successions, however, fabric-destructive dolostones found in the lower part of the sequence are overlain by fabric-retentive dolostones (Dawans and Swart, 1988; Jones, 1994; Wheeler et al., 1999, Ehrenberg et al., 2006). On some islands, the fabric-destructive dolostones are patchily distributed throughout the precursor limestones (Sibley, 1982; Dawans and Swart, 1988; Fouke, 1994; Jones, 1994; Budd, 1997; Wheeler et al., 1999). In contrast, fabric-retentive dolostones are typical of successions that have been completely dolomitized.

The textures of dolostones have commonly been attributed to specific aspects of the dolomitization process, including temperature, the chemical composition of

---

1 This chapter was published as: Zhao, H and Jones, B. 2012, Genesis of fabric-destructive dolostones: A case study of the Brac Formation (Oligocene), Cayman Brac, British West Indies, Sedimentary Geology, 267-268, 36-54.

the dolomitizing fluids, the mineralogy and/or fabric of the precursor limestones (Sibley, 1982; 1991; Sibley and Gregg, 1987; Dawans and Swart, 1988) and/or multiple dolomitization events (Harris and Meyers, 1987; Cander, 1994; Kyser et al., 2002; Machel, 2004; Gaswirth et al., 2007). Such conclusions imply that different processes and/or fluids were responsible for the generation of the different types of dolostones.

The origin of fabric-retentive dolostones found in island dolostone successions has been extensively discussed (e.g., Budd, 1997; Wheeler et al., 1999; Jones and Luth, 2002; MacNeil and Jones, 2003; Suzuki et al., 2006; Zhao and Jones, 2012). By comparison, fewer studies have focused on the fabric-destructive dolostones, largely because surface exposures of this type of dolostone are rare and these rocks can usually be reached only by deep drilling. This is unfortunate because contrasts between the two types of dolostones may provide an opportunity for assessing the factors that controlled their distribution and evolution.

On Cayman Brac (Fig. 3-1) the well-exposed Tertiary succession of limestones and dolostones belongs to the Bluff Group (Fig. 3-2), which encompasses the partly dolomitized Brac Formation (Lower Oligocene), the pervasively dolomitized Cayman Formation (Middle Miocene), and the partly dolomitized Pedro Castle Formation (Pliocene) (Jones et al., 1994a; MacNeil and Jones, 2003). Each formation is unconformity bounded. The contrast and juxtaposition between the fabric-destructive dolostones in the Brac Formation and the fabric-retentive dolostones in the Cayman Formation provides an ideal opportunity for comparing the factors that may control the development of fabric-destructive as opposed to fabric-retentive fabrics in dolostones.

By systematically comparing the petrographic and geochemical features of dolostones in the Brac Formation and Cayman Formation, this study shows that

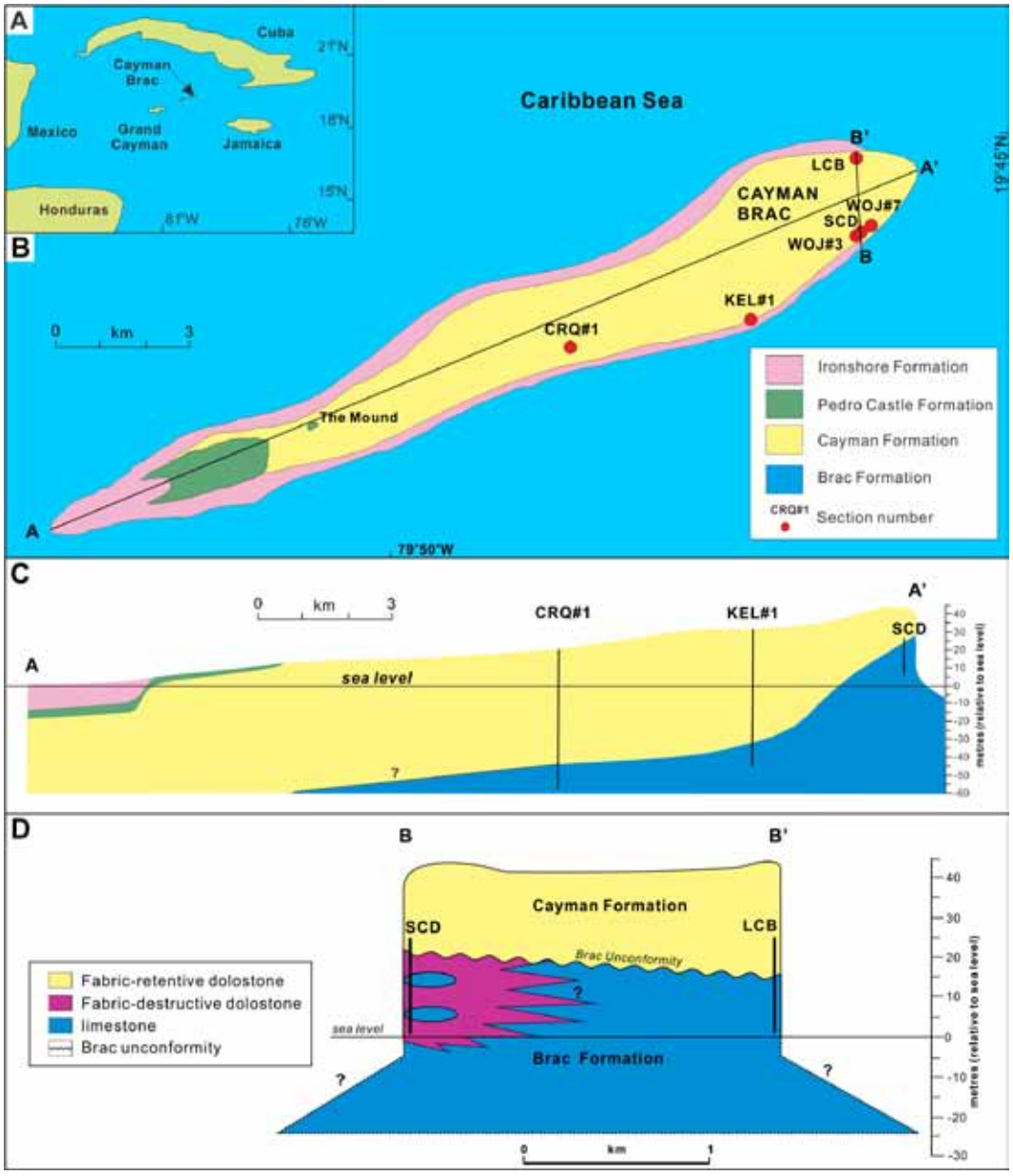

Fig. 3-1. (A) Location of Cayman Brac in the Caribbean Sea. (B) Geological map of Cayman Brac (modified from Jones, 1994) showing locations of CRQ#1, KEL#1, WOJ#3, SCD, WOJ#7, LCB, and two cross sections (A-A' and B-B'). (C) Cross section A – A' (modified from Jones, 2005). (D) Cross section B – B'. Note patchy distribution of fabric-destructive dolostones in the Brac Formation (modified from Uzelman, 2009).

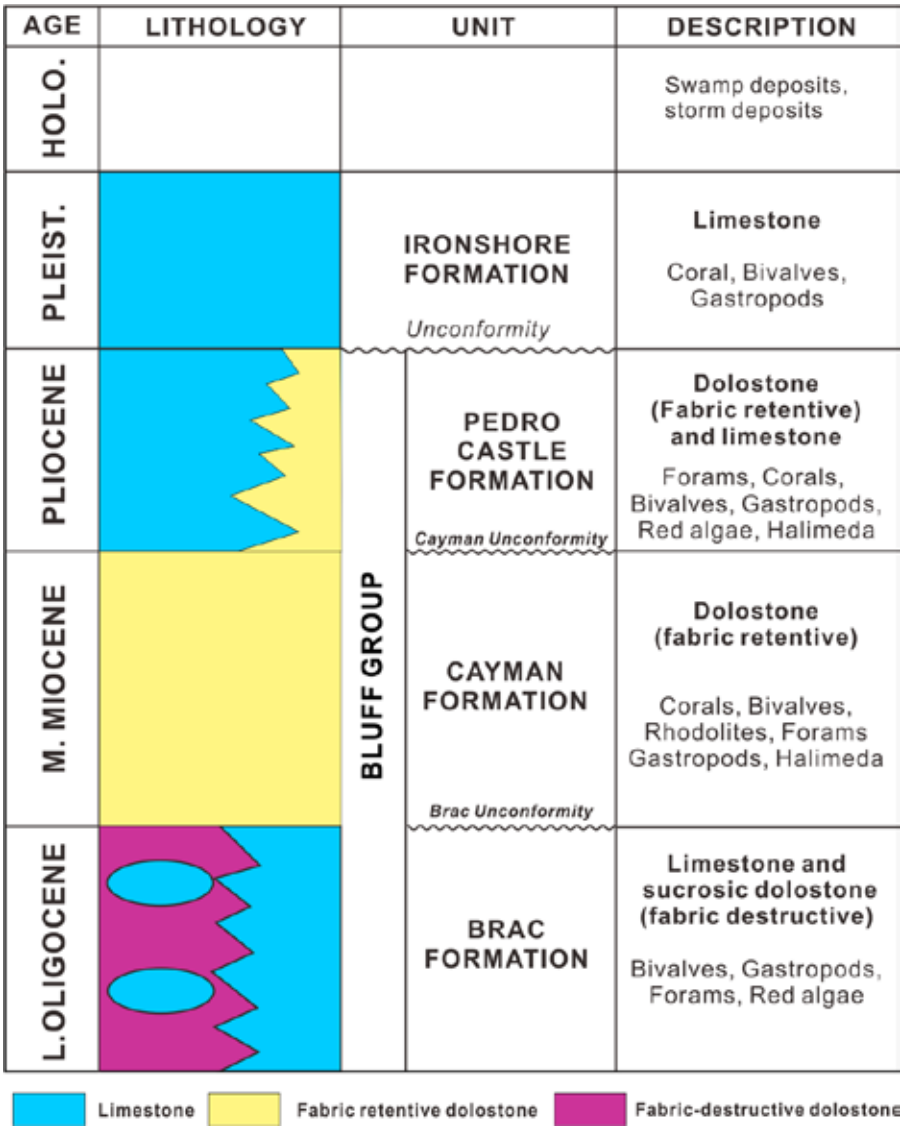

Fig. 3-2. Stratigraphic succession on Cayman Brac (modified from Jones, 1994) showing distribution of dolostones and limestones and dominant biota of each formation.

dolostones with different textures can originate from similar dolomitizing fluids. The dramatic contrast in their textures reflects their different diagenetic pathways. Although based on analysis of Tertiary dolostones, these conclusions have far-reaching implications for the interpretation of dolostones of all ages.

3.2. Geological setting

Cayman Brac, which is 19 km long and 1.5 to 3.0 km wide, is geographically isolated by virtue of deep ocean waters that surround the island. The surface of the island slopes gradually from 43 m above sea level at the northeast end to sea level at the southwest end (Fig. 3-1). The island is located on the Cayman Ridge, which parallels the Oriente Transform Fault that delineates the boundary between the Caribbean Plate and the North American Plate (cf. Jones and Hunter, 1994, their Fig. 3-3). This area has been tectonically active since the Late Eocene (Rosencrantz and Sclater, 1986; Leroy et al., 2000). Recent GPS measurements and seismic data indicate that this area is still tectonically active (DeMets and Wiggins-Grandison, 2007). The Mid-Cayman spreading centre, located southwest of Grand Cayman, is opening at an average rate of ~11-12 mm yr^{-1} (Rosencrantz and Sclater, 1986; Mann et al., 2002).

Exposed on Cayman Brac is a sequence of uplifted Tertiary carbonates that are flanked by a platform formed of Pleistocene limestones (Jones et al., 1994a, 1994b). This is the surface expression of a fault block that is formed of a carbonate succession that sits on volcanic rocks and rises 2000-2500 m from the seafloor (Horsfield, 1975; Perfit and Heezen, 1978; Stoddart, 1980). The carbonate succession is at least 150 m thick (Jones and Hunter, 1994; Jones et al., 1994a, 1994b).

Matley (1926) originally assigned the cliff-formed Tertiary carbonates to the Bluff Limestone and the Pleistocene carbonates that form a low-lying platform

around the island to the Ironshore Formation (Fig. 3-1B). Subsequently, Jones et al. (1994a, 1994b) elevated the Bluff Limestone to group status with the constituent unconformity-bounded formations being the Brac Formation (Upper Lower Oligocene), the Cayman Formation (Lower to Middle Miocene), and the Pedro Castle Formation (Pliocene) (Figs. 3-1 and 3-2). On Cayman Brac, the Brac Formation and the Pedro Castle Formation are formed of limestones and dolostones, whereas the Cayman Formation is formed entirely of dolostones (Jones et al., 1994a, 1994b; Zhao and Jones, 2012).

3.3. Methods

The samples used in this study were collected from outcrops in sections SCD, WOJ#3, WOJ#7 and well cuttings from wells CRQ#1 and KEL#1 (Figs. 3-1 and 3-3). Seventy-five samples were selected to give a complete stratigraphic and geographic coverage of the formation. Each sample was ground into a powder (75-150 μm) with an agate mortar and pestle for X-ray diffraction (XRD) analysis in order to determine their mineralogy. XRD analyses were performed on a Rigaku Geigerflex 2173 XRD system using Co K_{α} radiation at the University of Alberta. For samples containing dolomite, the procedures outlined by Jones et al. (2001) were used to determine the mol % $CaCO_3$ (hereafter referred to as %Ca) of dolomite. Following Jones et al. (2001), the dolomite is divided into low-Ca calcian dolomite (LCD – 50-55 %Ca) and high-Ca calcian dolomite (HCD – 55-62 %Ca). The weight % of LCD, weight % of HCD, and the average %Ca were calculated for dolostones using the methods outlined by Jones et al. (2001).

The petrography was established from large thin-sections (n = 45) that were made from samples that had been collected from outcrop and well cuttings. These samples were carefully selected to give a complete coverage of the formation. All samples were impregnated with blue epoxy. Selected polished thin sections

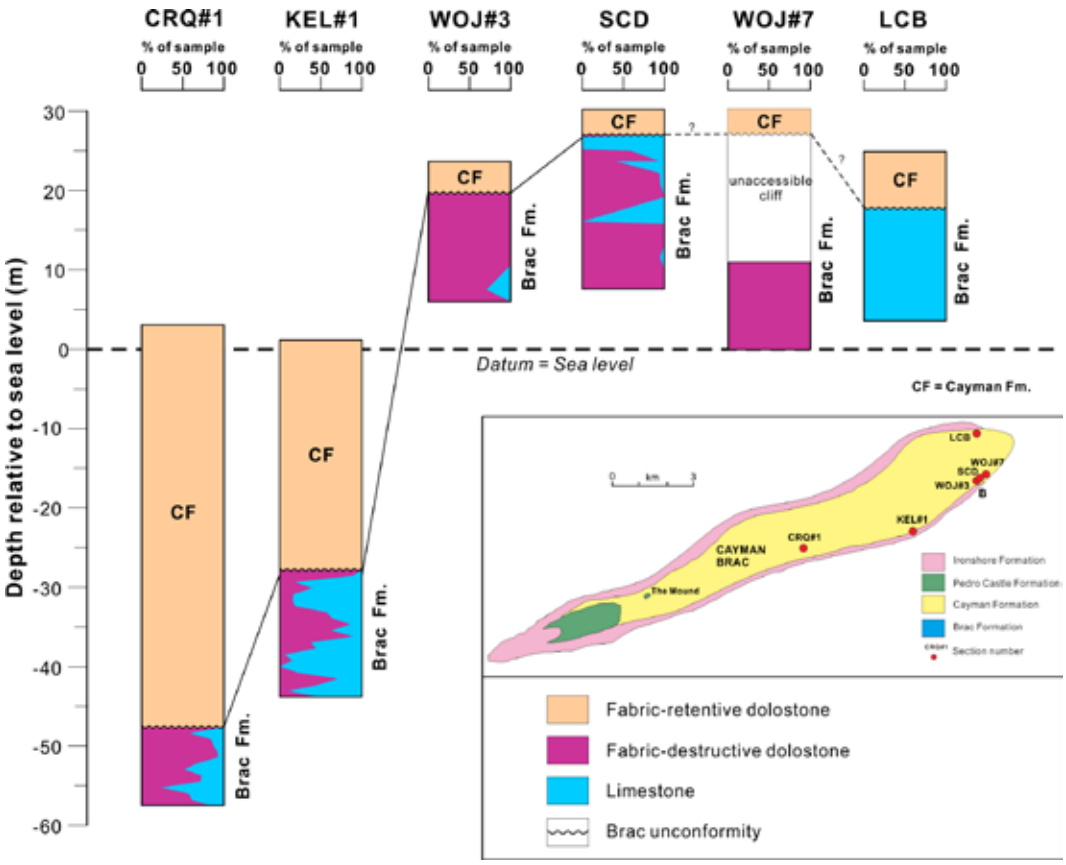

Fig. 3-3. Stratigraphic correlation between wells and outcrops showing the lithology of each section. See the inset map for the distance between sections.

were examined with cathodoluminescence (CL) microscopy. A Technosyn Model 8200 Mark II cold-cathode instrument (manufactured by Technosyn Limited, Cambridge, UK) was mounted on a binocular petrographic microscope equipped with a CanonTM EOS Rebel XS digital single-lens reflex camera (Canon Canada Inc., Ontario, Canada) with a 10.10-megapixel image sensor. Operating voltages were 10-15 kv and gun current levels were at 550-620 µA.

For selected samples (n = 16), the optical percentage of replacive dolomite, cements, and pore spaces was determined from digital images of the thin sections using *ImageJ* software (Fig. 3-4), following the procedure outlined by Grove and Jerram (2011). The thresholds used to distinguish the dolomite cements

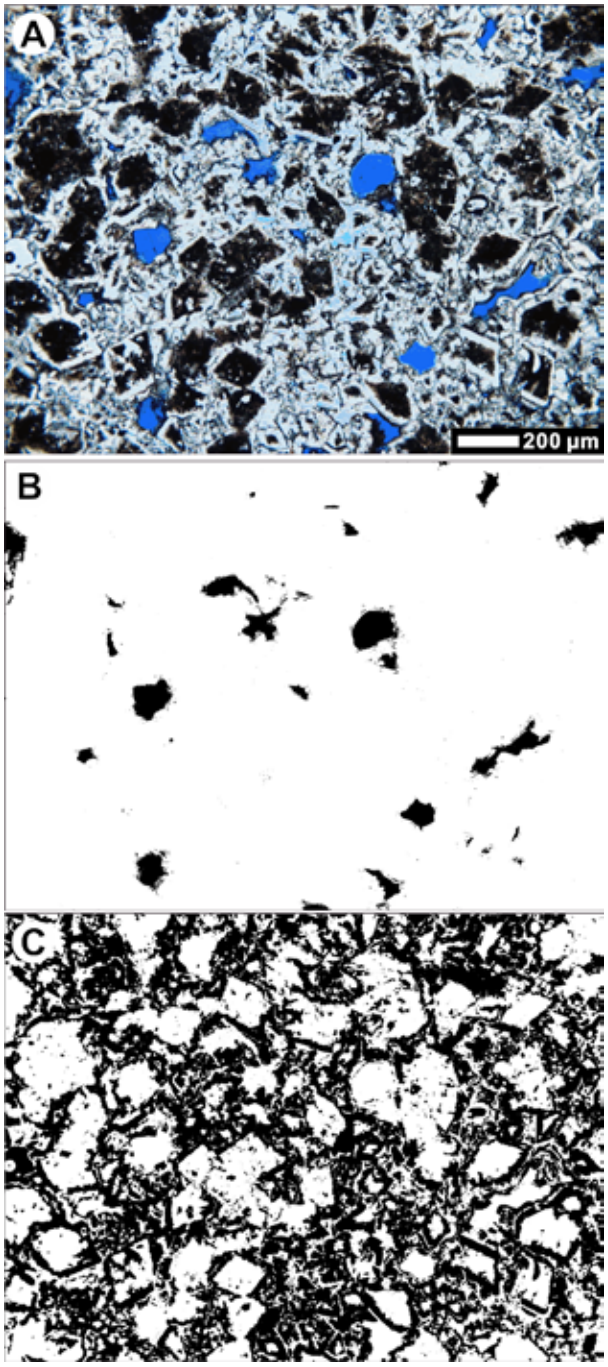

Fig. 3-4. (A) Photomicrograph of a sucrosic dolostone with pore spaces highlighted by blue epoxy. Note the contrast between the cloudy cores of the dolomite crystals (replacive dolomite) and the limpid dolomite (dolomite cement). (B) Same view as (A) but showing only the open pore spaces (black). Optical porosity = 7 %. (C) Same view as (A) but with the pore spaces and cloudy cores of dolomite crystals shown as white, and dolomite cements are black. Optical % of dolomite cement = 47%.

and replacive dolomite were manually defined. This approach is similar to the petrographic digital-image analysis (PIA) used by Gaswirth et al. (2007) for analysis of dolostones from the Ocala Formation and Suwannee Formation of Florida. In order to analyze the relationships between the amount of dolomite cement and the geochemical data of dolostones, the volume of dolomite cement is reported as a percentage of the dolomite (% dolomite cement = [the optical % of dolomite cement/ (the optical % of replacive dolomite + the optical % of dolomite cement)] × 100).

Backscatter electron images (BSEI) were obtained from thin sections that had been polished and coated with carbon before being analyzed on a JEOL 8900R electron microprobe (EMP) that was operated at 15 kV, 15nA. These are 1024 × 1024 pixel images. The concentrations of Ca and Mg were determined using 15 kV accelerating voltage and 10nA beam current.

Oxygen and carbon stable isotopes were obtained from those samples formed of 100% dolomite (n = 41). These analyses were done in the Stable Isotope Laboratory, University of Alberta. The dolostone powers were reacted directly with 100% phosphoric acid for 2-3 days at 25˚C following the protocol outlined by McCrea (1950). All extractions were introduced into a Finnigan-MAT 252 isotope mass spectrometer. Isotope values are reported relative to the PeeDee Belemnite (PDB) standard normalized to NBS-18 in per mil (‰) notation. Precision is better than 0.05 ‰ for $\delta^{18}O$ and $\delta^{13}C$. The oxygen isotope values of the dolostones were not corrected for the phosphoric acid fractionation.

The concentrations of trace elements (Sr, Fe, Mn) of samples formed of 100% dolomite (n = 39) and 100% calcite (n = 5) were determined in the Radio Isotope Laboratory at the University of Alberta. Approximately 0.2 g of powdered sample was digested in 10 ml 8N HNO_3 and then analyzed on a Perkin Elmer Elan6000 quadrupole ICP-MS. Replicate analyses of an internal standard

solution indicate an error (1σ) of 0.26% for Sr, 0.22% for Fe, and 0.2% for Mn.

3.4. Results

3.4.1. The Brac Formation

The Brac Formation, seen only in the vertical to overhanging cliff faces at the east end of the island (Fig. 3-5A, B), is lithologically variable. On the north coast, limestones formed mainly of bioclastic wackestones to grainstones dominate the succession (Fig. 3-5A, C). Large *Lepidocyclina* (up to 32 mm diameter) dominate the biota along with lesser numbers of other foraminifera (e.g., rotalids, milioilids), red algae, and echinoid plates (Fig. 3-5C). Corals, bivalves, and gastropods are absent with the exception of scattered *Porites* fragments in the uppermost part of the formation. This hard limestone, which contains minor amounts of dolomite cement, has low porosity (Fig. 3-5C).

On the south coast, the Brac Formation is formed largely of coarsely crystalline sucrosic dolostone. In some areas there are isolated pods of fossiliferous limestone (Fig. 3-5D), up to 10 m long and 2 m thick, which contain numerous *Lepidocyclina* with scattered bivalves and gastropods. Sucrosic dolostones commonly contain numerous leached *Lepidocyclina* (Fig. 3-5E). The limestones are lithologically akin to the limestones found on the north coast. In wells CRQ#1 and KEL#1, the Brac Formation is formed of interbedded limestones, dolomitic limestones, and fine to medium crystalline dolostones. The limestones are mostly bioclastic wackestones and packstones.

Jones and Hunter (1994) suggested that carbonate sediments that form the Brac Formation were originally deposited on a shallow carbonate bank under a low to moderate energy regime.

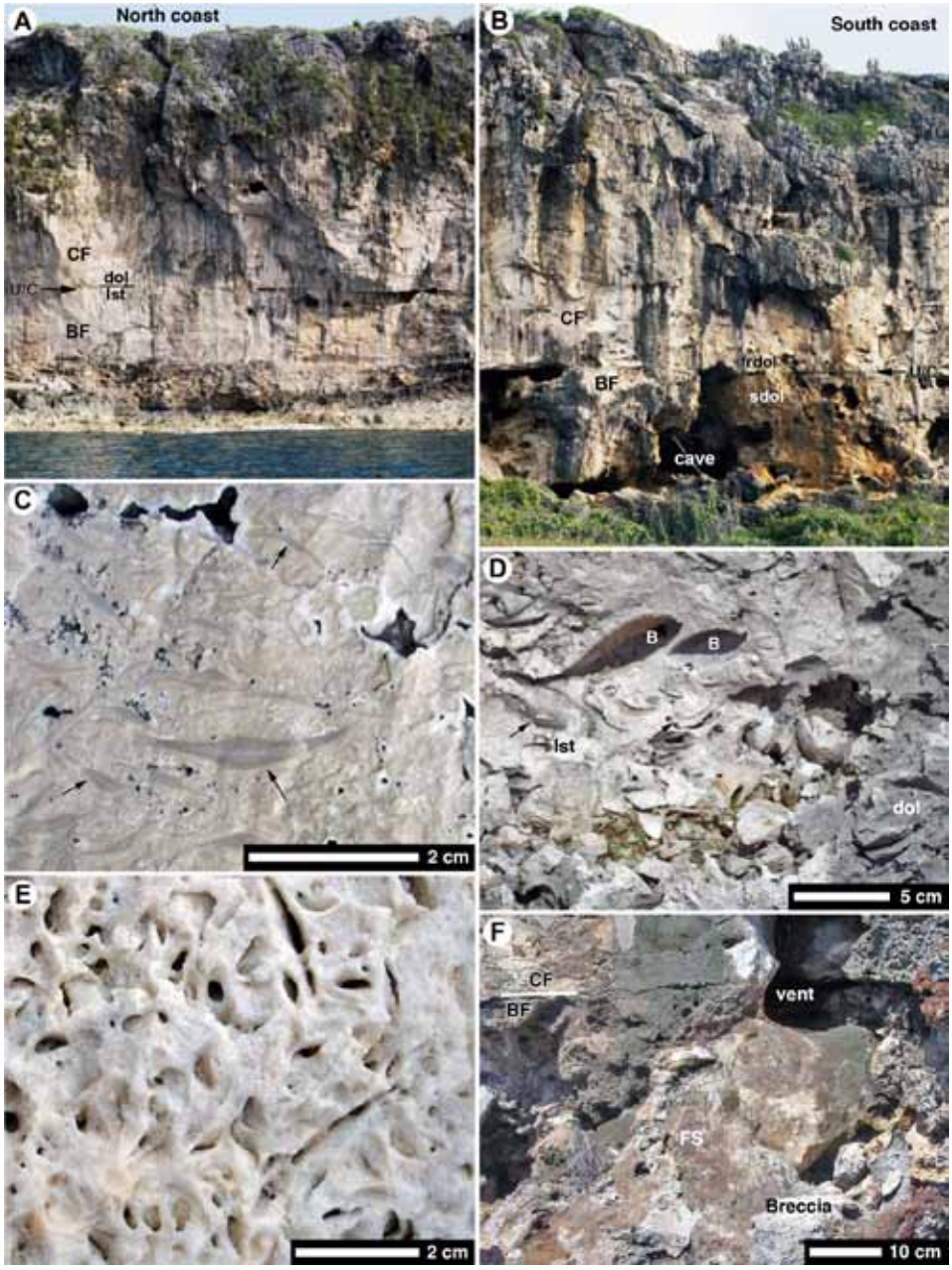

Fig. 3-5. Field photographs of Brac Formation (BF) and Cayman Formation (CF) on the east end of Cayman Brac. (A) Cliff face (~ 35 m high) on the north coast showing the Brac Unconformity (U/C) that separates the dolostones (dol) of the Cayman Formation from the limestones (lst) of the Brac Formation. (B) Cliff face on south coast (~ 30 m high, just east of Great Cave) showing fabric-retentive dolostones (frdol) of the Cayman Formation overlying the sucrosic dolostones (sdol) of the Brac Foramation. Note caves that have flat roofs formed by the Brac Unconformity (U/C). (C) Limestone in the Brac Formation, north coast, showing random sections through large Lepidocyclina (arrows) and small cavities lined with dolomite cement (white). (D) Limestone (lst) pod with leached bivalves (B, arrows) set in sucrosic dolomite (dol), south coast, ~ 3 m below the Brac Unconformity. (E) Sucrosic dolostone with numerous moldic pores formed by

(continued caption of Fig. 3-5) leaching of Lepidocyclina, south coast, ~ 15 m below Brac Unconformity. (F) Scree just below Brac Unconformity (white line) covered with flowstone (FS) that was precipitated from spring waters that flowed from the spring vent located at unconformity.

3.4.2. The Brac Unconformity

The Brac Unconformity, which separates the Brac Formation from the overlying Cayman Formation, is exposed in the cliff faces up to 33 m above sea level at the east end of Cayman Brac (Figs. 3-1 and 3-3). In wells CRQ#1 and KEL#1, it is located at 46.9 m and 29.3 m below sea level, respectively (Fig. 3-3). Based on outcrop and well information, Jones et al. (1994a) suggested that the Brac Unconformity is a karst surface with up to 25 m relief that dips, on average, at ~ 0.5^{o} to west. On the north coast, the finely crystalline dolostones of the Cayman Formation rest directly on top of the limestones of the Brac Formation (Fig. 3-5A), whereas on the south coast they lie on top of the coarsely crystalline sucrosic dolostones of the Brac Formation (Fig. 3-5B). In wells CRQ#1 and KEL#1, the finely crystalline dolostones of the Cayman Formation overlie the partly-dolomitized Brac Formation.

The following features are associated with the Brac Unconformity.

- On the north coast, the flat floor of "Neptune's Lair", which is a cave located in the basal part of the Cayman Formation, is the Brac Unconformity.
- On the south coast, numerous caves including the Great Cave are evident in the Brac Formation (Fig. 3-5B). Although variable in size and shape, all these caves have a flat roof that is the Brac Unconformity (Fig. 3-5B). In the Great Cave, stalactites grow from the base of the Cayman Formation.
- The steep cliffs on the south coast are commonly flanked by scree slopes that formed as the sea cliffs were undercut and collapsed (Jones and Ng,

1988). At one locality, the top of the scree slope is ~ 20 m above sea level with its surface being just below the level of the Brac Unconformity. There, the scree is coated with calcite flowstone that formed from a small spring that emanated from the unconformity (Fig. 3-5F). Although the opening through which the water flowed is still evident, the spring is no longer active.

These observations indicate that the Brac Unconformity is a boundary between two units that have significantly different permeability characteristics.

3.4.3. Petrography of dolomite

3.4.3.1. Optical petrography

The well indurated, finely to coarsely crystalline dolostones found in outcrop (SCD, WOJ3, WOJ7 – Fig. 3-5) are pale tan to white in colour. The coarsely crystalline dolostones are formed largely of interlocking crystals, up to 1.5 mm long, that have regular to irregular-shaped, inclusion-rich dark cores that are encased by clear rims (Fig. 3-6A). With the exception of rare mimetically replaced echinoderm fragments (Fig. 3-6A), all of the original allochems have been obliterated. In some samples, the dolomite crystals were enlarged by the growth of zoned cements (Fig. 3-6B). In the uppermost 5 m of the Brac Formation in section WOJ#3, fabric-retentive finely crystalline dolostones contain pseudomorphically replaced foraminifera and red algae fragments (Fig. 3-6C). In other dolostones, finely crystalline dolostones grade laterally into sucrosic dolostones (Fig. 3-6D).

In the limestone pods exposed in section SCD, numerous subhedral to euhedral dolomite crystals, which replace both the matrix and allochems, float in the limestone groundmass (Fig. 3-6E). Such crystals are typically cloudy and lack clear rims (Fig. 3-6E). In contrast, the dolomite crystals that fill the fractures,

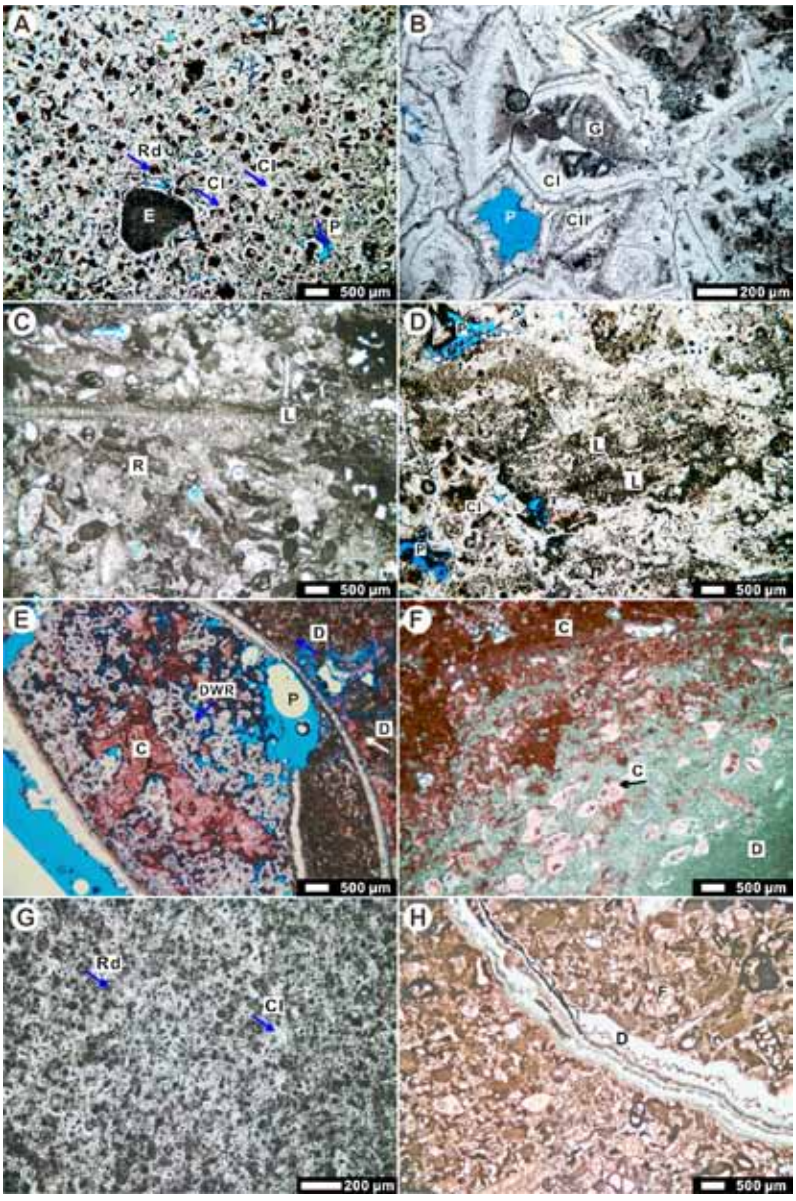

Fig. 3-6. Thin section photomicrographs of limestones and dolostones from the Brac Formation. Depths are relative to the Brac Unconformity (A) WOJ#7, -5.2 m, fabric-destructive dolostone formed of dolomite crystals with cloudy cores and clear rims. Original fabrics of precursors have been obliterated. Only rare bioclasts (e.g., echinoderm plate – E) were mimetically replaced by dolomite. Arrows indicate the replacive dolomite (Rd) and dolomite cement (CI). (B) WOJ#3, -14 m, fabric-destructive dolostone with ghost structures of fossils in the cores of the dolomite crystals (G). Dolomite crystals were enlarged by dolomite overgrowth cements (CI and CII). Occurrence of CII is intimately related to pore spaces (P). (C) WOJ#3, -0.5 m, fabric-retentive dolostone with various pseudomorphically replaced allochems. L = Lepidocyclina, R = red algae. (D) WOJ#3, -9.4 m, dolostone showing transition of fabric-retentive texture (pseudomorphically-replaced Lepidocyclina (L)) to fabric-destructive texture. (E) SCD, -3.3 m, dolomitic limestone stained with Alizarin red-S showing

(continued caption of Fig. 3-6) dolomite crystals floating in the limestone. Note that dolomite crystals with clear rims (DWR) only occur close to pore space (P) whereas dolomite crystals in the groundmass (D) do not have clear rims. (F) SCD, -0.3 m, dolomitic limestone stained with Alizarin-red S. Note that dolomite preferentially replaced the matrix, whereas allochems (e.g., foraminifera) were left intact. D = dolomite, C = calcite. (G) CRQ#1, -5.6 m, finely crystalline equigranular dolostone with no evidence of original fabrics from the precursor limestone, Rd = replacive dolomite, CI = dolomite cement I. (H) KEL#1, -14.8 m, undolomitized foraminifera wackestone with dolomite vein stained with Alizarin red-S. D = dolomite, F = foraminifera

burrows, and vugs have cloudy cores and clean rims (Fig. 3-6E). Locally, the matrix was preferentially dolomitized and allochems were left intact (Fig. 3-6F).

In wells CRQ#1 and KEL#1, the dolostones are composed largely of equigranular, interlocking, anhedral, fine- to medium-crystalline dolomite (20 to 100 μm, average 70 μm) that lack any evidence of precursor textures (Fig. 3-6G). Pores and fractures in the bioclastic limestones are commonly filled with dolomite cement (Fig. 3-6H).

3.4.3.2. Cathodoluminescence

The coarsely crystalline fabric-destructive dolostones are characterized by dull red to bluish grey cathodoluminescence (CL) (Fig. 3-7A). The cloudy cores of the dolomite crystals typically have dull bluish grey-dull red CL, whereas the clear rims show oscillatory zoning with moderately bright red-orange luminescing 'hairline' zones alternating with bluish-grey zones (Fig. 3-7A). Mimetically replaced allochems (e.g., echinoid plates) have dull red luminescence like that in the cores of the sucrosic dolomite crystals (Fig. 3-7A). The interlocking anhedral-subhedral dolomite crystals in the finely-medium crystalline dolostones have the same CL characteristics as their sucrosic counterparts found in outcrop (Fig. 3-7B).

The fabric-retentive, finely crystalline dolostones have a dull red to pinkish-grey CL signature with moderate to bright luminescence zones (Fig. 3-7C).

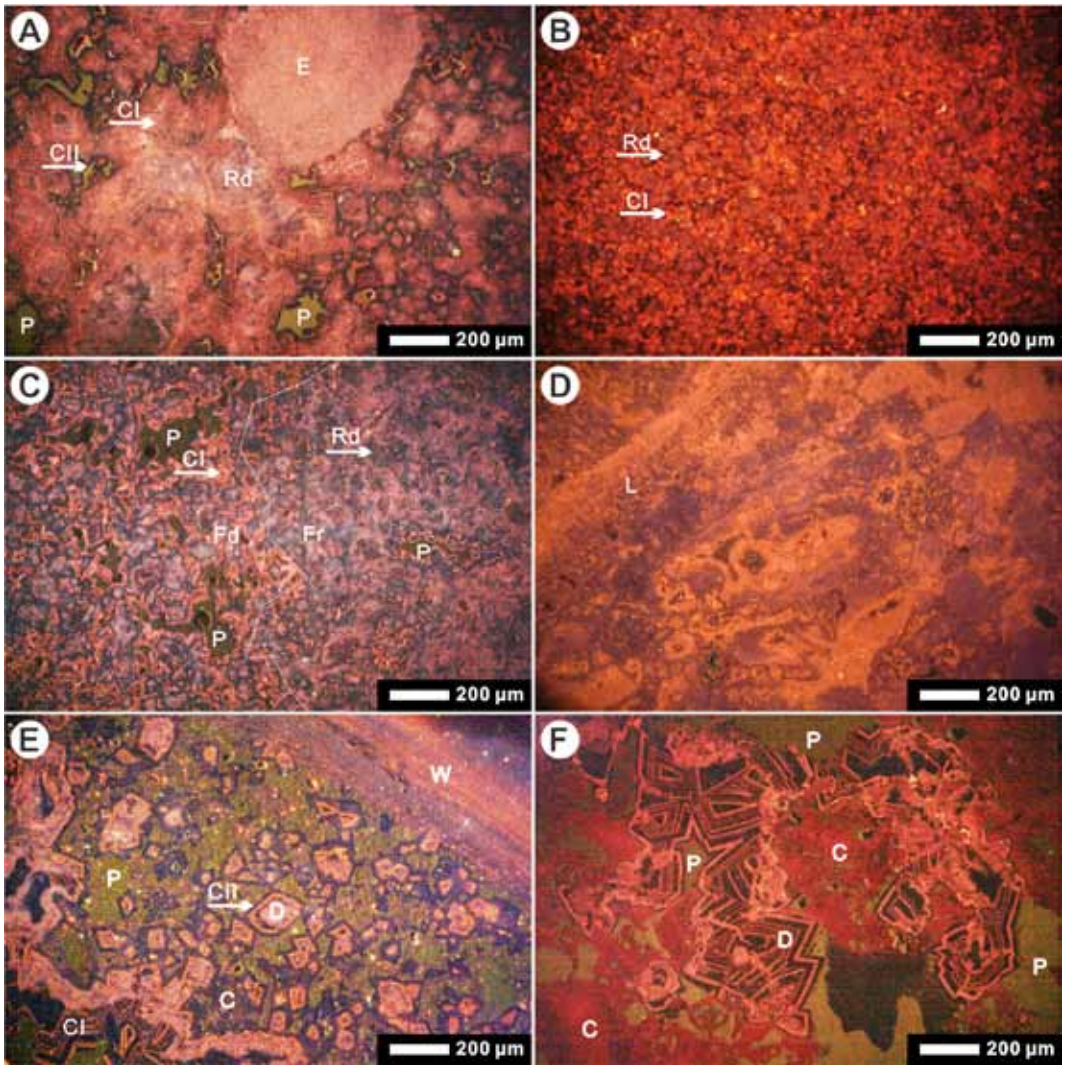

Fig. 3-7. Cathodoluminescence (CL) images of samples from the Brac Formation. Depths are relative to the Brac Unconformity. (A) SCD, -13.9 m, fabric-destructive dolostone showing replacive dolomite (Rd) with dull red to bluish grey luminescence and dolomite cements with zoned luminescence. E = echinoderm plate, CI = dolomite cement I, CII = dolomite cement II. (B) CRQ#1, -10.9 m, finely crystalline equigranular dolostone. Note that replacive dolomites (Rd) show similar CL as those in (A). CI = dolomite cement CI. (C) WOJ#3, -9.1 m, dolostone with mixed fabric-retentive (Fr) and fabric-destructive textures (Fd). Dotted line shows boundary between two textures. Note significant decrease in amount of dolomite cement (CI) from left side to right side. (D) WOJ#3, -0.5 m, fabric-retentive finely crystalline dolostone showing mingled CL luminescence. L = Lepidocyclina. (E) SCD, -10 m, dolomite rhombs in limestone. Note that dolomite rhombs have similar CL luminescence as those in sucrosic dolostones. W = wall of worm tube. D = dolomite, C = calcite, CI = dolomite cement I, CII = dolomite cement II, P = pore. (F) SCD, -10 m, blocky dolomite cement filling pore space in limestone showing zoned CL luminescence. Note that dolomite cement also partially replaces the limestone bedrock. C = undolomitized limestone, D = dolomite cement, P = pore.

Dolostones from just beneath the Brac Unconformity have intercalated bright orange and dull bluish-grey CL luminescence (Fig. 3-7D). Dolomite rhombs floating in the limestone groundmass have the same luminescence features as the sucrosic dolomite crystals found in the fabric destructive dolostones (Fig. 3-7E, F).

The dolomite cements, based on their CL signatures, can be divided into types CI and CII. Volumetrically, CI cements are more abundant than the CII cements. Type CI is zoned with numerous moderately bright red-orange luminescent 'hairline' zones (Fig. 3-7A, B, C, E). This type of cement is found as an overgrowth around dolomite crystals (Fig. 3-7A, B, C) or as blocky dolomite spars filling pore spaces (Fig. 3-7E). Type CII, which is nonluminescent, also developed as an overgrowth (Fig. 3-7A, E). In some samples, Type I zoned CL cements are overlain by Type II dark CL cements (Fig. 3-7A).

3.4.4. Percentage of dolomite cements in the Brac Formation

Using *Image J*, analyses of 16 thin sections, including coarsely crystalline and finely-medium crystalline dolostones, show that the dolostones from the Brac Formation contain 35 to 83% (average = 62%) replacive dolomite, 17 to 47% (average = 32%) dolomite cement, and 0 to 14% (average = 5%) porosity (Table 3-1). For the coarsely crystalline fabric-destructive dolostones, the percentage of dolomite cement is 26 to 54%, whereas, the equigranular finely-medium crystalline dolostones contains 18 to 28% dolomite cement (Table 3-1).

3.4.5. Geochemistry of dolostone in the Brac Formation

3.4.5.1. Dolomite stoichiometry

All the dolostones from the Brac Formation are formed of nonstoichiometric dolomite that contains 55.0 to 57.5 %Ca (average 56.7 %Ca, n = 68) (Appendix 2 and Fig. 3-8A). On backscatter images, the dolomite crystals are typically

Table 3-1. Results of petrographic digital-image analysis. Data derived using ImageJ software, following the procedure outlined by Grove and Jerram (2011) (see text for details).

Sections	Depth (m) (below U/C)	Texture[1]	Optical % porosity	Optical % RD[2]	Optical % DC[3]	% of DC[4]
SCD	-19.4	CC	7	55	38	41
SCD	-13.9	CC	10	49	41	46
WOJ#3	-14.0	CC	12	41	47	54
WOJ#3	-9.4	CC	11	50	39	44
WOJ#3	-9.1	CC	13	50	37	43
WOJ#3	-7.9	CC	5	70	25	26
WOJ#3	-4.9	CC	6	49	45	48
WOJ#7	-22.7	CC	4	61	35	37
WOJ#7	-21.8	CC	3	62	35	36
WOJ#7	-20.0	CC	10	52	38	42
WOJ#7	-17.2	CC	12	53	35	40
CRQ#1	-0.3	FC	0	68	32	32
CRQ#1	-2.5	FC	0	77	23	23
CRQ#1	-5.6	FC	0	73	28	28
CRQ#1	-8.6	FC	0	83	18	18
CRQ#1	-10.2	FC	0	76	24	24

[1] CC = coarsely crystalline, FC = finely to medium crystalline; [2] RD = replacive dolomite; [3] DC = dolomite cement; [4] % of DC = the optical % of dolomite cement/ (the optical %of replacive dolomite + the optical % of dolomite cement) × 100.

homogenous (Fig. 3-9) with no evidence of zoning based on variable atomic weights. The EMPA *in-situ* analyses indicate that the dolomite crystals are composed of a dolomite population with relative uniform %Ca (Fig. 3-9A, B).

3.4.5.2. C and O isotopes

The $\delta^{13}C$ and $\delta^{18}O$ values of the dolostones from the Brac Formation range from 1.5 to 2.9‰ (average 2.3‰, n = 41) and from 2.0 to 3.6‰ (average 2.8‰, n = 41), respectively (Appendix 2, Figs. 3-8B and C, 3-10A). There is no correlation between the $\delta^{13}C$ and $\delta^{18}O$ ($r^2 = 0.2$) values (Fig. 3-10B). The fine to medium crystalline equigranular dolostones are enriched in $\delta^{18}O$ (average 3.2‰, n = 14) relative to the coarsely crystalline sucrosic dolostones (average 2.6‰, n = 27) (Fig. 3-10B).

3.4.5.3. Trace elements

The Sr content in dolostones from the Brac Formation ranges from 150 to 275 ppm (average 206 ppm, n = 39) (Appendix 2 and Fig. 3-8D) whereas the limestones contain 242 to 290 ppm (average 267 ppm, n = 5) (Appendix 2).

The dolostones contain 81 to 263 ppm Fe (average 141 ppm, n = 37) and 2 to 77 ppm Mn (average 18 ppm, n = 37), respectively (Appendix 2 and Fig. 3-8E, F). The limestones contain 83 to 162 ppm Fe (average 113 ppm, n = 5) and 7 to 16 ppm Mn (average 10 ppm, n = 5), respectively (Appendix 2). There is no correlation between the Fe and Mn contents of dolostones ($r^2 = 0.0$) (Fig. 3-11).

3.5. Comparison of dolostones in Brac and Cayman Formations

The dolostones in the Brac Formation and Cayman Formation are distinctly different in terms of their textures and geochemical signals (Table 3-2). Dolostones in the partly dolomitized Brac Formation are dominated by coarsely crystalline fabric-destructive textures (Fig. 3-6). In stark contrast, the overlying

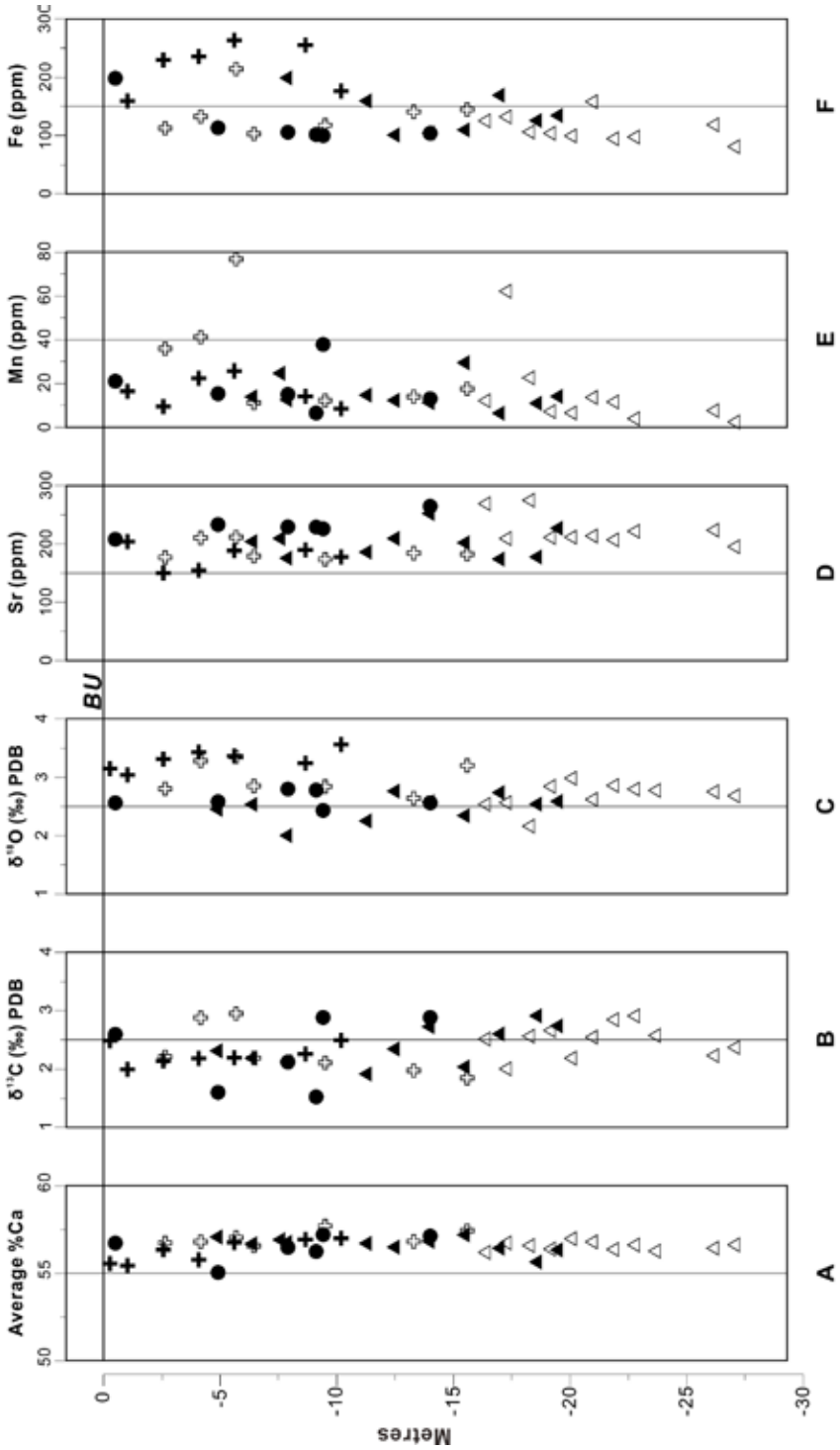

Fig. 3-8. Composite plots, based on successions at SCD, WOJ#3, WOJ#7, CRQ#1, and KEL#1, showing stratigraphic variability in (A) average %Ca, (B), $\delta^{13}C$ (C), $\delta^{18}O$ (D), Sr (E), Mn (F), Fe. Datum is the Brac Unconformity.

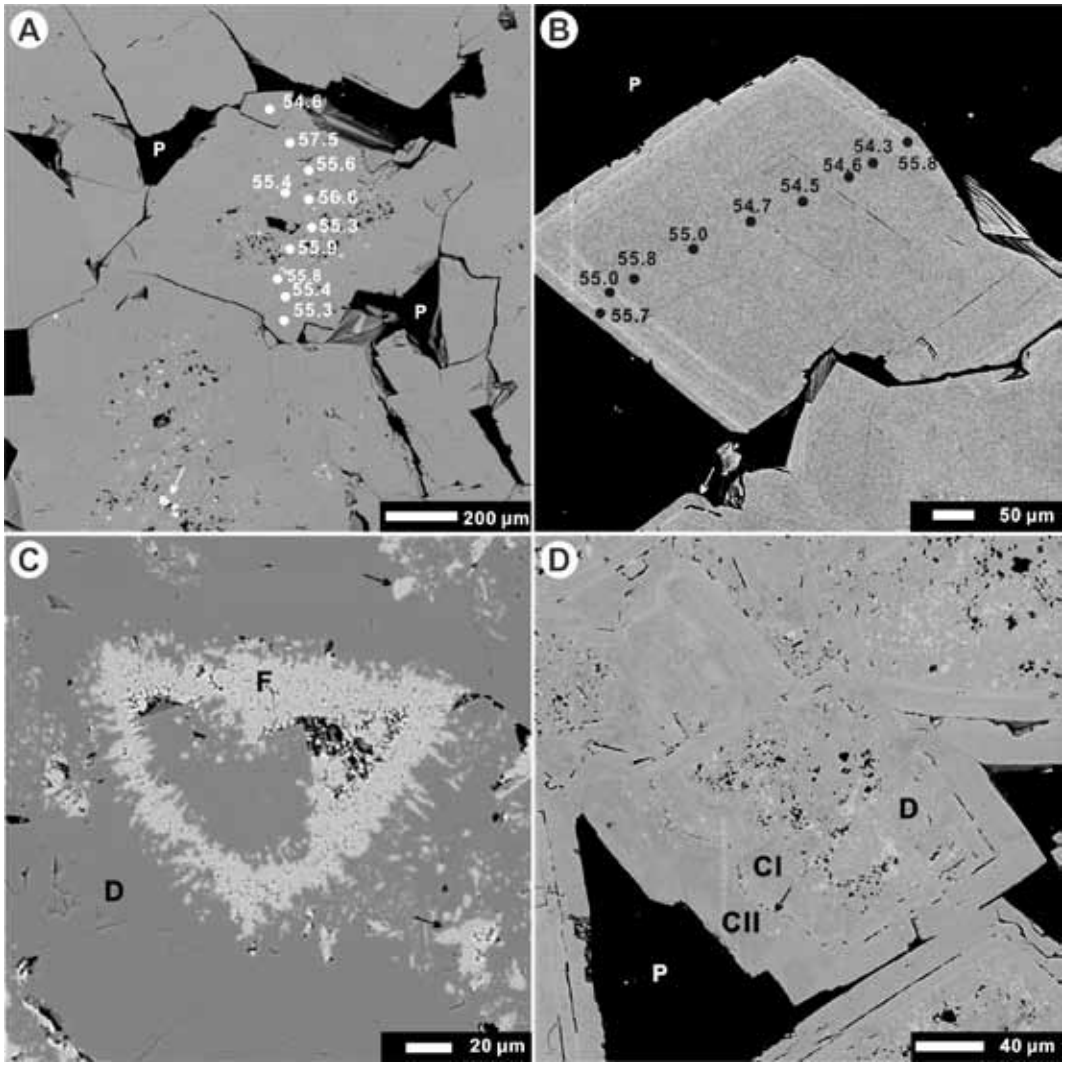

Fig. 3-9. Backscatter images of dolostones from the Brac Formation. Depths are relative to the Brac Unconformity. Numbers on panels A and B show %Ca as determined by microprobe analyses for spots indicated. (A) WOJ#7, -25 m, sucrosic dolomite showing the homogenous distribution of %Ca. (B) WOJ#7, -22.7m, dolomite cement showing homogenous distribution of %Ca (C) CRQ#1, -10.9 m, dolomite cement in partly dolomitized limestone. Note homogenous colour of the dolomite (D). Foraminifera (F) is undolomitized. Arrows point to remnant calcite inclusions. (D) CRQ#1, -0.3 m, finely crystalline equigranular dolostone. Note that dolomite rhomb (D) has colour similar to that of the dolomite cements CI and CII. Arrow indicates irregular boundary between CI and CII.

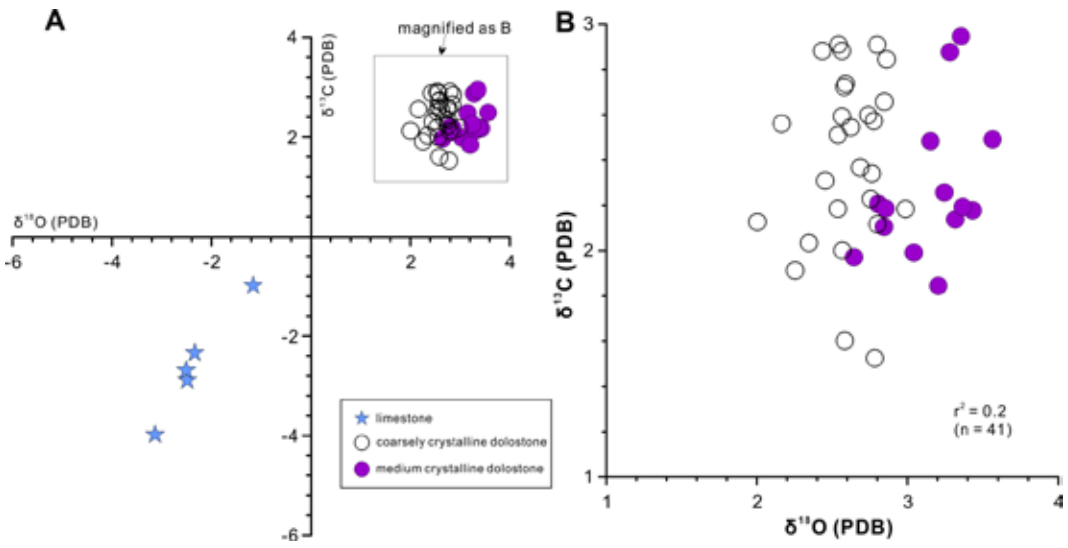

Fig. 3-10. Plots of $\delta^{13}C$ versus $\delta^{18}O$ of medium and coarsely crystalline dolostones from the Brac Formation. Data for limestones from Uzelman (2009).

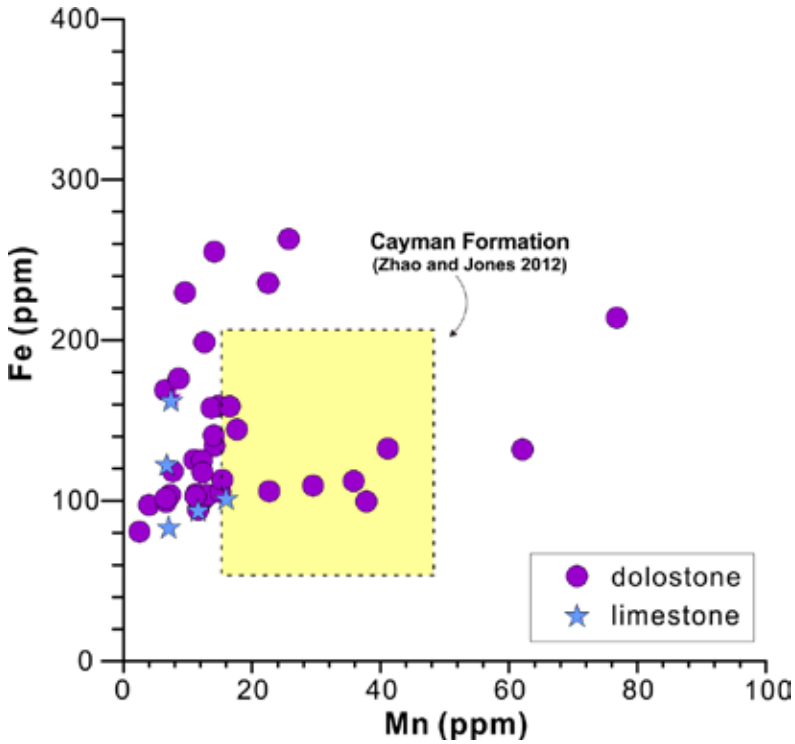

Fig. 3-11. Crossplot of Mn versus Fe content of dolostones from the Brac Formation. Yellow shaded square shows the range of data from dolostones from the Cayman Formation (see Chapter 2).

Table 3-2. Comparison of the Brac Formation and Cayman Formation. Data for the Cayman Formation comes from Zhao and Jones (2012).

	Brac Formation	Cayman Formation
Texture	Fabric-destructive with ghost structures.	Fabric-retentive with numerous biomolds
Crystal size	50-1500 μm	10-20 μm
CL	Bluish grey with hairline zones	Moderate-bright red-orange
Stoichiometry	55 to 57.5 %Ca	50.5 to 57.7 %Ca
$\delta^{13}C$	1.5 to 2.9‰ (average 2.3‰)	1.6 to 3.5‰ (average 2.5‰)
$\delta^{18}O$	2.0 to 3.6‰ (average 2.8‰)	2.3 to 4.0‰ (average 3.2‰)
Sr	150 to 275 ppm (average 206 ppm)	80 to 279 ppm (average 140 ppm)
Fe	81 to 263 ppm (average 141 ppm)	52 to 340 ppm (average 128 ppm)
Mn	2 to 77 ppm (average 18 ppm)	9 to 82 ppm (average 28 ppm)

Cayman Formation is pervasively dolomitized with fabric-retentive dolostones that clearly exhibit the original fabrics of the precursor limestones (Zhao and Jones, 2012). The dolostones from the Brac Formation are characterized by dark CL with various styles of zonings (Fig. 3-7) whereas those from the Cayman Formation are characterized by homogenous bright red CL (Zhao and Jones, 2012).

The dolomite in the Cayman Formation, relative to that in the Brac Formation, tends to be more stoichiometric and has more positive $\delta^{18}O$ (Table 3-2). There are, however, no distinct differences between the $\delta^{13}C$ and Fe content of the dolostones from the two formations (Table 3-2). Dolostones from both formations contain relative low Fe and Mn. The Mn content of dolomite in the Brac Formation is generally less than that in the dolostones from the Cayman Formation (Table 3-2).

3.6. Interpretation of geochemical data

3.6.1. Dolomite stoichiometry

Island dolostones are commonly formed of calcian dolomites with 50-62 % mol $CaCO_3$ (Budd, 1997; Wheeler et al., 1999; Jones et al., 2001; Jones and Luth, 2002; Jones, 2004, 2005, 2007; Suzuki et al., 2006; Gaswirth et al., 2007; Zhao and Jones, 2012). Many of these calcian dolomites are compositionally heterogeneous with two or more populations of dolomites that differ in terms of their %Ca (Wheeler et al., 1999; Jones et al., 2001; Suzuki et al., 2006; Zhao and Jones, 2012). The variable stoichiometry of these sedimentary dolomites may reflect their diagenetic evolution because calcian dolomites, which are less stable than stoichiometric dolomites, are potentially more vulnerable to diagenetic alteration (cf. Sibley et al., 1994; Chai and Navrotsky, 1995). It has been argued, for example, that dolomite stoichiometry reflects the Mg/Ca ratio of the dolomitizing fluid (Lumsden and Chimahusky, 1980; Sass and Katz, 1982; Sperber et al., 1984; Sass and Bein, 1988; Kaczmarek and Sibley, 2011). Any subsequent diagenetic modifications, however, will be controlled by the rock/water ratio in an open or closed system (Sperber et al., 1984). Calcian dolomite, found in many partly dolomitized limestones, has been attributed to formation in a relatively closed dolomitization system characterized by impermeable limestones that impede the introduction of extra allochthonous Mg ions (Sperber et al., 1984). Based on recent high-temperature synthesis experiments, Kaczmarek and Sibley (2011) suggested that the dolomites are always calcian during the initial stage of dolomitization, and the %Ca of dolomite depends on the Mg/Ca ratio of dolomitizing fluids.

Dolostones from the Brac Formation are formed predominantly of HCD (55-57.5 %Ca) (Appendix 2) whereas the dolostones in the overlying Cayman Formation have an average of 50.5 to 57.7 %Ca that reflects the mixed

populations of LCD and HCD (cf. Zhao and Jones, 2012). Backscatter images also show that both sucrosic dolomite crystals and dolomite cements in the Brac Formation are formed of dolomite with relatively uniform %Ca (Fig. 3-9). If the relationships developed by Kaczmarek and Sibley (2011) are accepted, the HCD in the Brac Formation probably evolved from dolomitizing fluids that had a relative lower Mg/Ca ratio compared to those responsible for the formation of the dolostones from the Cayman Formation. Due to the fact that dolomite crystals in the Brac Formation commonly contain calcite inclusions and the precursor limestones were not completely dolomitized (Fig. 3-9A, C), the high %Ca found in the dolostones from the Brac Formation most likely reflects a rock buffering dolomitization system with a relative low water/rock ratio in terms of the Mg/Ca ratio. This conjecture is consistent with the observation in the synthetic experiments that dolomite stoichiometry quickly increases to reach the ideal (Ca:Mg ratio of 50:50) when the calcite has been completely dolomitized (Kaczmarek and Sibley, 2011).

3.6.2. C isotopes

The $\delta^{13}C$ values of the dolostones in the Brac Formation (1.5 to 2.9‰) are significantly different from those of the limestone pods (-2.3 to -4.0 ‰, average -3.0 ‰, n = 4) (Fig. 3-10A). The negative $\delta^{13}C$ of the limestones indicates that freshwater was probably involved in their diagenesis. The alteration of the limestones probably took place as karst developed on the Brac Unconformity during the Late Oligocene and Early Miocene, which predated the onset of the dolomitization. The positive $\delta^{13}C$ values of dolostones in the Brac Formation, which are significantly different from the limestones, must have been completely reset by the dolomitization. Since the $\delta^{13}C$ does not indicate any other carbon sources (e.g., freshwater, organic matter), it must be attributed to seawater. Such an interpretation is consistent with those interpretations derived from the analyses

of other island dolostones (cf. Budd, 1997; Wheeler et al., 1999; Suzuki et al., 2006).

3.6.3. O isotopes

The interpretation of $\delta^{18}O_{(dolomite)}$ from dolostones is controversial because their $\delta^{18}O$ values are influenced by many variables, including the isotopic composition of dolomitizing fluids, temperature, kinetics, and dolomite stoichiometry (Vahrenkamp and Swart, 1994; Budd, 1997; Zhao and Jones, 2012). The correlation between the $\delta^{18}O_{(dolomite)}$ and the %Ca of the dolostones (Fig. 3-12A) from the Cayman Formation (Zhao and Jones, 2012) has also been reported from many island dolostones (Dawans and Swart, 1988; Vahrenkamp and Swart, 1994; Gill et al., 1995; Wheeler et al., 1999; Suzuki et al., 2006). Zhao and Jones (2012) argued that this correlation is caused mainly by the dolomite fractionation factor that varies with the %Ca and the phosphoric acid fractionation factor rather than fluctuations in the chemical composition and/or temperature of the dolomitizing fluids as suggested by Wheeler et al. (1999) and Suzuki et al. (2006).

Compared to the dolostones from the Cayman Formation, the dolostones from the Brac Formation have lower $\delta^{18}O$ and higher %Ca (average 56.7 %Ca) values (Fig. 3-12A). The $\delta^{18}O$ and %Ca values for the dolostones from the Brac Formation generally follow the regression line developed for the dolostones from the Cayman Formation (Fig. 3-12A). Therefore, the relative lower $\delta^{18}O$ of the dolostones from the Brac Formation can be attributed to the influences of dolomite stoichiometry (Zhao and Jones, 2012). As a result, it seems reasonable to infer that the dolostones in the Brac Formation probably developed from dolomitizing fluids (slightly modified seawater) that were similar in composition to those that mediated dolomitization in the Cayman Formation.

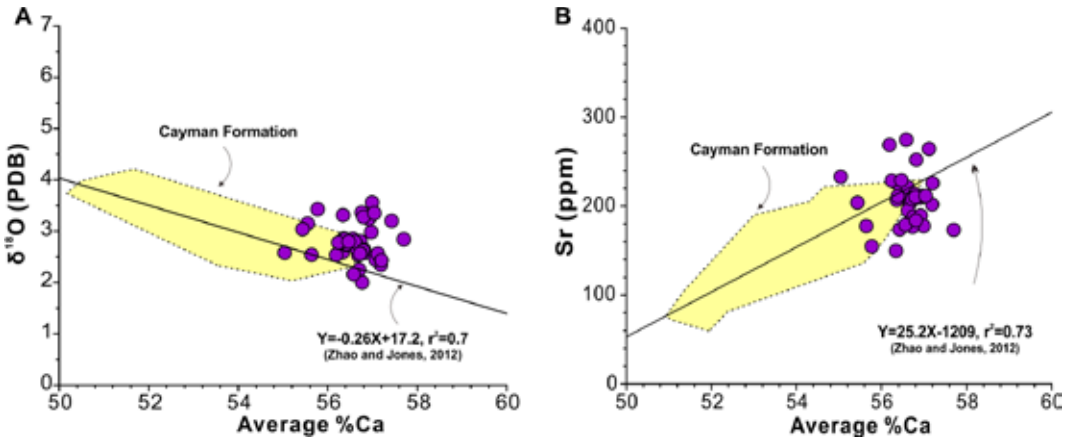

Fig. 3-12. Bivariant graphs showing relationships between average %Ca of dolostones from the Brac Formation with $\delta^{18}O$ and Sr. (A) Average %Ca versus $\delta^{18}O$. (B) Average %Ca versus Sr contents with calculated regression axis. For comparison, the range of data from dolostones from the Cayman Formation (yellow shaded area) and regression equation (solid line) (Zhao and Jones 2012) are shown.

3.6.4. Sr content

The Sr content of dolostones from the Brac Formation (150 to 275 ppm, average 206 ppm, n = 39) is comparable to most island dolostones. Their values are, however, higher than those from the Cayman Formation (Fig. 3-12B). The Sr content of dolostones is influenced by the Sr/Ca ratio of dolomitizing fluids, the Sr content of the precursor calcium carbonates (Land, 1973, 1980; Vahrenkamp and Swart, 1990; Banner, 1995; Wheeler et al., 1999), the major element composition (Ca, Mg) of the dolomite, and kinetic effects (Vahrenkamp and Swart, 1990; Zhao and Jones, 2012). It has been reported that the Sr contents of island dolostones covary with their %Ca from many islands (Bahamas, North Atlantic Ocean, Vahrenkamp and Swart, 1990; Niue, Pacific Ocean, Wheeler et al., 1999; and Kita-daito-jima, North Philippine Sea, Suzuki et al., 2006). This correlation is also apparent in the dolostones from the Cayman Formation on Cayman Brac (Zhao and Jones, 2012). According to the regression equation proposed by Zhao and Jones (2012), dolostones with 55 to 57.5 %Ca that formed in the seawater

should contain 177 to 240 ppm Sr – values that are compatible with the Sr contents of dolostones from the Brac Formation (Fig. 3-12B). Zhao and Jones (2012) argued that the correlation reflects the major element composition of the dolomite and kinetic effects rather than fluctuations in the chemical composition of the dolomitizing fluids. They also pointed out that the Sr content of dolostones from the Cayman Formation, with a range of 80-278 ppm is consistent with dolomitization by seawater-like fluids.

3.6.5. Fe and Mn

The low Fe and Mn contents of dolostones from the Brac Formation are comparable with many other island dolostones (cf. Budd, 1997; Wheeler et al., 1999; Suzuki et al., 2006). The low Fe and Mn contents, combined with a lack of correlation between the two, indicate that no Fe- and Mn-rich fluids were involved into the dolomitization processes and/or that the dolomites formed in an oxidizing environment (Fig. 3-8). Given that the Fe and Mn concentrations in seawater are low (Fe 2 ppb, Mn 0.2 ppb, Drever, 1997), the low Fe and Mn contents of dolostones from the Brac Formation are compatible with a seawater origin for the dolomite.

Relative to the fabric-retentive dolostones in the overlying Cayman Formation, the fabric-destructive dolostones from the Brac Formation have lower Mn (Fig. 3-8), which is consistent with the fact that the dolostones from the Brac Formation have darker CL than those from the Cayman Formation (Zhao and Jones, 2012). This difference in Mn content, however, does not necessarily point to different dolomitizing fluids because the Mn may have been inherited from the precursor limestone rather than the dolomitizing fluid (Vahrenkamp and Swart, 1994). For the Brac Formation, this interpretation is supported by the fact that the Mn content of the limestones is similar to those of the dolostones (Fig. 3-8).

3.7. Timing of dolomitization

The various CL features of different components in the dolostones from the Brac Formation indicate that there were multiple episodes of dolomitization that operated with fluids of different chemical composition and/or under different redox conditions. Interpretation of the petrographic relationships indicates that replacive dolomite was followed by precipitation of CI cements and later CII cements (Figs. 3-7A and 3-9D). Although their absolute timing is unknown, the initial onset of dolomitization in the Brac Formation must have postdated lithification and cementation of limestones. This conjecture is supported by the observations that (1) the limestone pods held in the massive sucrosic dolostones on the south coast have the same diagenetic features as the limestones on the north coast, with both being cemented by blocky calcite spar cements, and (2) dolomite rhombs floating in the limestone pods are most common beside open pores or fractures, which indicates that the transportation of dolomitization fluids was controlled by pre-existing pathways (Fig. 3-6E).

The $^{87}Sr/^{86}Sr$ data of bulk samples from the Brac Formation were reported by Jones et al. (1994a) and Uzelman (2009). Samples containing various amount of calcite have $^{87}Sr/^{86}Sr$ values ranging from 0.70833 to 0.709059 (average 0.708633, n=18). Dolostones formed of 100% dolomite have $^{87}Sr/^{86}Sr$ values ranging from 0.70898 to 0.709054 (average 0.70900, n=4). Limestones formed of 100% calcite have $^{87}Sr/^{86}Sr$ values ranging from 0.70803 to 0.70814 (average 0.70808, n=4) (Fig. 3-13A). Uzelman (2009) argued that the dolomitization of the Brac Formation was a time-transgressive process based on the wide range of $^{87}Sr/^{86}Sr$ values. The $^{87}Sr/^{86}Sr$ values of these samples, however, have a high correlation ($r^2 = 0.94$) with their dolomite content (Fig. 3-13A). This correlation indicates that the broad range of $^{87}Sr/^{86}Sr$ values is most probably caused by the mixture of calcite and dolomite that have different $^{87}Sr/^{86}Sr$ signatures rather than

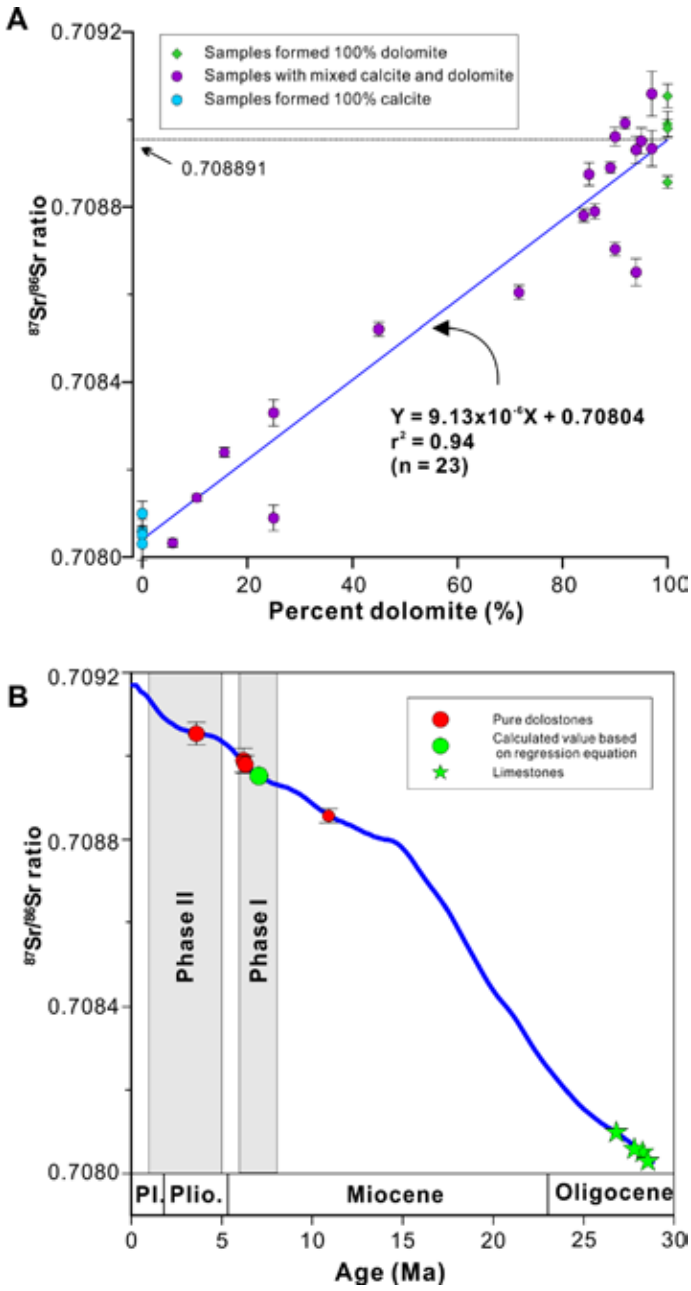

Fig. 3-13. (A) Crossplot of $^{87}Sr/^{86}Sr$ values versus percentage of dolomite in samples (data from Jones et al. (1994a) and Uzelman (2009)) showing correlation between the two variables. Vertical bars indicate ± 2σ of $^{87}Sr/^{86}Sr$ values. (B) Age of dolomitization, as derived from $^{87}Sr/^{86}Sr$ values of pure dolostones and calculated value based on regression equation on (A), $^{87}Sr/^{86}Sr$ curve of seawater from McArthur et al. (2001, look-up table version 4:08/03). For comparison, Phase I and Phase II dolomitization events derived based on dolostones from overlying Cayman Formation by Zhao and Jones (2012) are shown. Vertical bars indicating ± 2σ of $^{87}Sr/^{86}Sr$ values.

various dolomitization events. According to the trend defined by these samples, a dolostone formed of 100% dolomite should have a $^{87}Sr/^{86}Sr$ value of 0.708891 (Fig. 3-13A).

Given the isolated location of Cayman Brac, the Sr can only come from the precursor limestone or the dolomitizing fluids (Jones and Luth, 2003; Zhao and Jones, 2012). Vahrenkamp et al. (1988) argued that the influence of precursor limestones on the $^{87}Sr/^{86}Sr$ of dolostones depends on the mineralogy of the precursors. According to their theoretical modeling, if the precursors were composed of aragonite (~ 7000 ppm Sr), the $^{87}Sr/^{86}Sr$ of dolomite may be partly inherited from the precursor, but if low-Mg calcite (~ 400 ppm Sr) was dominant, then the $^{87}Sr/^{86}Sr$ of dolomite reflects only the dolomitizing fluids. The petrographic features of the Brac Formation indicate that most, if not all, of the aragonite was changed to low-Mg calcite prior to dolomitization. This conjecture is supported by the high correlation between the $^{87}Sr/^{86}Sr$ values of the samples and their dolomite content (Fig. 3-13A). Accordingly, only the $^{87}Sr/^{86}Sr$ age derived from pure dolostones from the Brac Formation should be considered indicative of the dolomitization fluids and hence reflect the true age of dolomitization.

Using the seawater $^{87}Sr/^{86}Sr$-time curve of McArthur et al. (2001: Look-Up Table Version 4: 08/03), the $^{87}Sr/^{86}Sr$ values of three out of four pure dolostones of the Brac Formation are indicative of a Late Miocene (6 - 11 Ma) age (Fig. 3-13B). The $^{87}Sr/^{86}Sr$ value of 0.708891 derived from the regression equation (Fig. 3-13A) indicates a Sr age of 9 Ma (Fig. 3-13B). Compared to the overlying Cayman Formation, the Sr isotope age of dolomitization of the Brac Formation is equivalent to the first episode of dolomitization that was responsible for the dolomitization of the basal part of the Cayman Formation (Fig. 3-13B). There is, however, one sample from just below the Brac Unconformity (0.2 m) with

a $^{87}Sr/^{86}Sr$ of 0.709054 that falls into the range of Phase II dolomitization (Fig. 3-13B). It appears that the second episode of dolomitization (Pliocene) that dolomitized most of the Cayman Formation (Zhao and Jones, 2012) may also have affected the uppermost part of Brac Formation (Fig. 3-13B). This conclusion is consistent with the mixed CL features of samples that came from just below the Brac Unconformity (Fig. 3-7D).

The percentage of dolomite cements in the Brac Formation varies from 18 to 54% (average = 34%). These cements post-dated formation of the dolomite that replaced the matrix of the precursor limestones. The $^{87}Sr/^{86}Sr$ data from Jones et al. (1994a) and Uzelman (2009), which came from whole-rock analyses, are relatively consistent and do not seem to be correlated to the percentage of dolomite cements. This suggests that the formation of the replacive dolomite and dolomite cements was not separated by time intervals sufficient to be detected by the $^{87}Sr/^{86}Sr$ ratios.

3.8. Discussion

3.8.1. Implications for pervasive dolomitization

Although the exact mechanism of dolomitization still remains unclear, it is generally agreed that any dolomitization model must encompass (1) a supply of Mg and CO_3^{2-}, (2) a delivery mechanism, and (3) a dolomite construction site as suggested by Morrow (1982). Land (1985) suggested that the seawater is the most plausible fluid because it contains vast amounts of Mg. There is, however, considerable debate concerning the mechanism by which the Mg and CO_3 ions are delivered to the sites of dolomitization. Many different models haven been proposed with considerations related to the geochemical signatures of the dolostones, hydrological conditions, and the relationship between dolostones and other mineral deposits (cf. Warren, 2000). The geometries of the dolomite bodies

have commonly been connected to various circulation patterns of dolomitizing fluids in order to infer the dolomitization models responsible for their formation (e.g., Wilson et al., 1990; Machel, 2004). Such conjecture typically assumes, however, that there are no barriers to the circulation of the fluids through the precursor limestones.

In the case of Cayman Brac, the pervasively dolomitized Cayman Formation is separated from the underlying, partly dolomitized Brac Formation by an unconformity (Figs. 3-3 and 3-5). The stratigraphic association between dolostones and unconformities has commonly led to notion that the dolomitization might be related to subaerial exposure where the mixing zone dolomitization model was operative (e.g., Harris and Meyers, 1987, Purser et al. 1994). Purser et al. (1994) suggested that the tectonic uplift of a limestone platform could be important for the setup of hydrological circulation of dolomitizing fluids. On Cayman Brac, however, the Brac Unconformity did not seem to exert a direct control on the dolomitization in the Brac Formation. Deposition of sediments that now form the Brac Formation was in the Lower Oligocene (Jones et al., 1994a, b) with dolomitization taking place during the Late Miocene (Fig. 3-13B). The overlying Cayman Formation is early to mid-Miocene in age (Jones et al., 1994a, b). Development of the Brac Unconformity took place during the Late Oligocene to Early Miocene, which is far earlier than the onset of dolomitization of the Brac Formation (Late Miocene). Moreover, the geochemical data derived from the dolostones of the Brac Formation do not indicate the involvement of meteoric water in dolomitization of the Brac Formation.

The permeability contrast across the Brac Unconformity is highlighted by many features that are evident in outcrop (Fig. 3-5B, F). Even on a thin section scale, completely dolomitized coral fragments of the Cayman Formation lie directly on top of the low-porosity limestones of the Brac Formation (Fig.

3-14A). The permeability contrasts between the Brac Formation and Cayman Formation indicate that the limestones in the Brac Formation were lithified and well-cemented before the onset of the dolomitization. The patchy distribution of dolomite in the limestones of the Brac Formation is also indicative of a restricted flow regime that prevented the dolomitizing fluids from reaching all parts of the precursor limestones. This conclusion is also supported by (1) dolomite rhombs being most common in areas close to voids (Fig. 3-6E), and (2) uneven boundaries of replacive-cement dolomite crystal (Fig. 3-14B) indicating the growth of dolomite crystals in the limestone was restricted by the permeability of the precursor. Therefore, the contrast between the dolostones from the Cayman Formation and the Brac Formation most probably reflects differences in their pre-dolomitization diagenesis and the manner in which porosity and permeability developed in each sequence. This may be related to variable karst development, prior to the dolomitization, which produced heterogeneous patterns of porosity and permeability in the precursor limestones, as suggested by Jones and Luth (2003) and Zhao and Jones (2012). Geochemical evidence indicates that the dolostones in the Brac Formation probably formed from seawater-like fluids that were similar to those that mediated formation of the dolostones in the Cayman Formation. There is no evidence to indicate that the chemical composition of the dolomitizing fluids caused the different patterns of dolomitization in the Brac Formation and Cayman Formation.

The dolomitization patterns evident in the Brac Formation and Cayman Formation were controlled largely by the flow patterns of dolomitizing fluids through the original limestones. Limestones, like those in the Brac Formation, that underwent a long pre-dolomitization diagenetic history, have less chance of being pervasively dolomitized. Instead, processes that influenced permeability pathways in the limestones will eventually exert an influence over the distribution

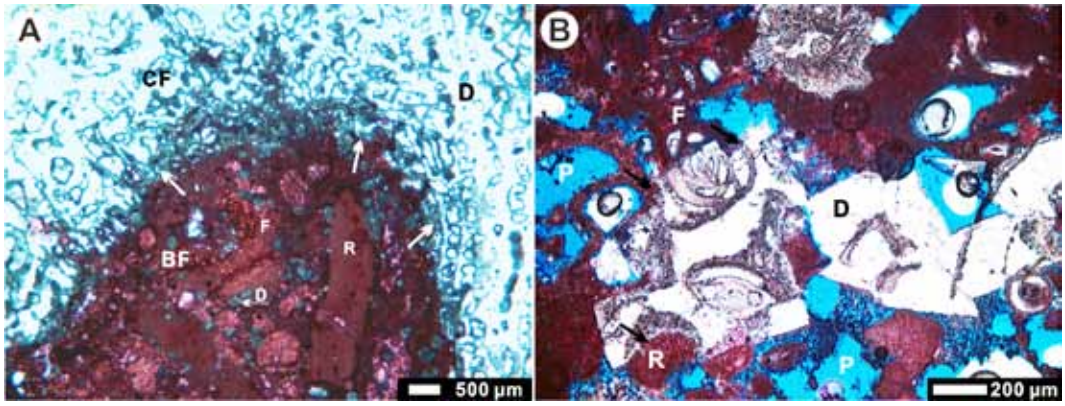

Fig. 3-14. (A) Thin section stained with Alizarin red-S showing sharp contact (arrows) between completely dolomitized Cayman Formation (CF) and limestone of the Brac Formation (BF). R = red algae, D = dolomite. Note the dolomite rhombs (arrow) in the limestone. (B) Thin section stained with Alizarin red-S showing replacive-cement dolomite (D). Note that dolomite boundary is not even due to change in permeability of allochems (arrows). P = pore, D = dolomite, F = foraminifera, R = red algae.

of the dolomite in the limestones.

3.8.2. Origin of fabric-destructive textures in dolostones from the Brac Formation

The co-existence of fabric-retentive and fabric-destructive textures is common in island dolostones (Budd, 1997; Wheeler et al., 1999; Jones, 2005, 2007; Ehrenberg et al., 2006, Suzuki et al., 2006; Zhao and Jones, 2012) and many ancient dolostones (Nichols and Silberling, 1980; Lee and Friedman, 1987; Machel, 2004). The origin of such textures is, however, a matter of controversy. Sibley (1982) suggested that dolostone textures were related to the (1) availability of nucleation sites in the precursor limestones, (2) mineralogy of precursor limestones, and/or (3) chemical composition of the dolomitizing fluids. He also argued that crystals with cloudy cores that contained low-Mg calcite inclusions were probably generated from precursor limestones that were formed of low-Mg calcite. Sibley and Gregg (1987) suggested that the crystal size in the replacive dolomite and the preservation of limestone fabrics during the dolomitization were determined largely by the degree to which the

dolomitizing fluids were supersaturated with respect to dolomite. According to their arguments, coarsely crystalline, fabric destructive dolostones are a product of dolomitization by fluids that are less saturated with respect to dolomite than those responsible for the formation of fabric-retentive dolostones. Based on simulation experiments, however, Zempolich and Baker (1993) argued that the preservation of dolostone textures is related to the pre-dolomitization diagenesis with limestones formed of coarsely crystalline calcite being transformed into dolostones with fabric-destructive textures. Another mechanism that can potentially influence the development of coarsely crystalline fabric-destructive dolostones is recrystallization and/or neomorphism (Machel, 1997). Such recrystallization has been attributed to the thermodynamic stabilization of unstable calcian dolomite and/or the ripening of finely crystalline dolomite – "Ostwald ripening" (Mazzullo, 1992). Recrystallization of this type is generally attributed to dissolution-precipitation processes that also lead to changes in the geochemical signals of the dolomite and destruction of the original textures (Land, 1980, 1985; Mazzullo, 1992). This notion is supported by numerous studies that have demonstrated that recrystallized dolostones have dramatically different geochemical signatures and textures than the dolostones from which they developed (Gregg et al., 1992; Vahrenkamp and Swart, 1994; Malone et al., 1996; Al-Aasm, 2000). Mazzullo (1992) argued that recrystallized dolomites, when compared to the original dolomites, (1) are more stoichiometric, (2) have enlarged crystals, (3) have significantly different geochemical signatures (e.g., $\delta^{18}O$, Sr content), and/or (4) display homogeneous CL signatures.

Dolostones from the Brac Formation are dominated by coarsely crystalline fabric-destructive textures (Fig. 3-6A, B). Many of the dolostones, however, also include small scale, gradual transitions from finely crystalline fabric-retentive dolostone to coarser, more euhedral sucrosic dolostones (Figs. 3-6D and 3-7C).

The fact that the cloudy cores of the crystals in the sucrosic dolomites, which commonly exhibit ghost structures of various fossils, have the same dark bluish grey-dull red CL as the finely crystalline dolostones (Figs. 3-6A, B and 3-7A) indicates that the cores of sucrosic dolomites were probably inherited from the finely crystalline dolostones. The fact that the rims of the large euhedral dolomite crystals are inclusion-free and CL zoned with the bright "hairline" zones that can be correlated from one crystal to another indicates that they probably developed as cements (Fig. 3-7A). Support for this suggestion comes from the dolomite rhombs that float in the limestone pods but only have clear rims if they are located next to or within a cavity (Fig. 3-6E). In many crystals, the clear rims were subsequently overlain by CI and CII cements (Figs, 3-6B, 3-7A, and 3-9D). This interpretation supports Choquette and Hiatt's (2008) assertion that dolomite cement is critical to the development of coarse sucrosic dolostones. Available evidence indicates that the fabric-destructive texture of dolostones in the Brac Formation reflects multiple episodes of cementation as opposed to intrinsic factors related to the mineralogy of the limestone precursors or the degree of supersaturation of dolomitizing fluids as proposed by Sibley (1982) and Sibley and Gregg (1987). In addition, some of the large dolomite crystals found in the limestone pods partly replace the calcite groundmass and partly fill the neighbouring cavity as cement (Fig. 3-14B). Similar replacive-cement crystals have also been reported from the Leduc Formation in Alberta (Murray, 1960), sucrosic dolostones in the Neogene Seroe Domi Formation on Curacao (Fouke, 1994), and sucrosic dolostones in the Avon Park Formation of Florida (Maliva et al., 2011). In the case of the Brac Formation, the precursor limestones had probably been altered to low-Mg calcite prior to the onset of dolomitization. Thus, the replacive-cement dolomite crystals indicate that the mineralogy of the precursor limestones was not a major control on the textures of dolostones.

Geochemical data from dolostones of the Brac Formation are inconsistent with the notion of recrystallization because (1) the dolostones are formed largely of HCD (55 to 57.5 %Ca), (2) there is no correlation between the %Ca and the dolomite fabrics (Fig. 3-8A), (3) the dolostones in the Brac Formation are more Ca-rich than the dolostones in the overlying Cayman Formation (Table 3-2), (4) the $\delta^{18}O$ and Sr signatures of dolostones from the Brac Formation indicate seawater-like dolomitizing fluids, (5) there is no depletion of $\delta^{18}O$ and Sr as would be expected from dolomite recrystallization (cf. Malone et al., 1996; Al-Aasm, 2000) (Fig. 3-10), and (6) zoned crystals, evident with CL, are indicative of original crystals, not ones that have been significantly recrystallized (cf. Mazzullo, 1992).

Dolomite cement forms up to 54% of some sucrosic dolostones in the Brac Formation (Table 3-1). This creates a "space problem" because a rock with 54% porosity could not maintain its integrity and would simply collapse in on itself. These high percentages of cement can only be achieved if there were repeated cycles of dissolution and cementation. Such a cyclic process would also lead to a progressive increase in crystal size and progressive obliteration of the original textures. The mechanism of dissolution is, however, unclear. Choquette and Hiatt (2008) argued that dissolution of the original limestone by fresh water would create the space needed for the dolomite cements (their Fig. 17). Based on the sucrosic dolostones in the Avon Park Formation, Florida, Maliva et al. (2011) argued that the dolomitization was an automorphic process in which the dissolution of precursor limestones happens simultaneously with the dolomitization. As a result, the pore spaces in the sucrosic dolostones were interpreted as a result of dolomitization scavenging the surrounding carbonate according to the local theory of Murray (1960).

In some samples from the Brac Formation the gradual transition from fabric-

retentive textures to fabric-destructive textures is accompanied by significant increases in pore space and cement (Fig. 3-15). This implies that dissolution must have happened before the precipitation of cements. Hence, the force of crystallization (cf. Maliva and Siever, 1988; Maliva et al., 2011) and the local source theory (cf. Murray, 1960) cannot be invoked to explain the formation of pore spaces in the dolostones from the Brac Formation.

Interpretation of the petrographic features of dolostones from the Brac Formation, suggests that these dolostone textures may have evolved in one of two ways.

- The precursor limestone was first replaced by fabric-retentive dolostone. Subsequent dissolution then created spaces in which the cements could be

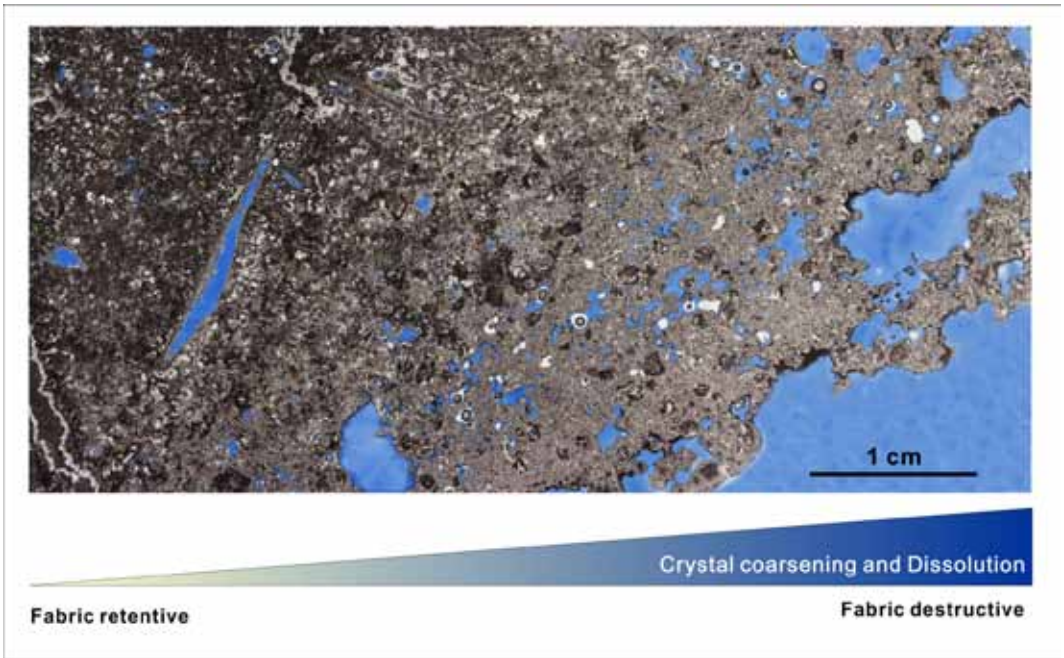

Fig. 3-15. Thin section impregnated with blue epoxy showing the gradual transition from fabric-retentive texture to fabric-destructive texture. Note that coarsening of dolomite crystals is accompanied by an increase in porosity

precipitated. These processes obliterated the original textures and promoted coarsening of the dolomite crystals (Fig. 3-16).

- Initial dolomitization of the low-porosity limestones produced scattered rhombs that seem to float in the limestone matrix. Subsequent dissolution preferentially attacked the limestone matrix and thereby created the spaces where later dolomite cements could be precipitated (Fig. 3-16). Repetition of the dissolution-precipitation cycle through time would progressively reduce the amount of limestone while increasing the amount of dolomite cement.

Both of these processes may have contributed to the development of the fabric-destructive textures evident in the Brac Formation. The operation of these two evolutionary pathways was probably related to the permeability pathways that dictated how the dolomitizing fluids moved through the precursor limestones.

3.8.3. Origin of dolomite cement

Interpretation of geochemical data from the bulk dolostone samples from the Brac Formation indicates that they probably formed from seawater-like dolomitizing fluids. The fine to medium crystalline dolostones, however, have more positive $\delta^{18}O$ values than the coarsely crystalline dolostones (Fig. 3-17A). This disparity cannot be attributed to the stoichiometry effect (Zhao and Jones, 2012) because there are no significant differences between their %Ca (Fig. 3-17B). The fabric-destructive textures in the sucrosic dolostones are the result of multiple dissolution-precipitation episodes during which dolomite cements progressively evolved to form up to 54% of the dolostones (Table 3-1). One possible interpretation is that the dolomite cements precipitated from dolomitizing fluids that had different temperatures and/or different geochemical composition compared to the fluids that mediated development of the replacive dolomites. Under this scenario, it might be expected that the dolostones with large volumes

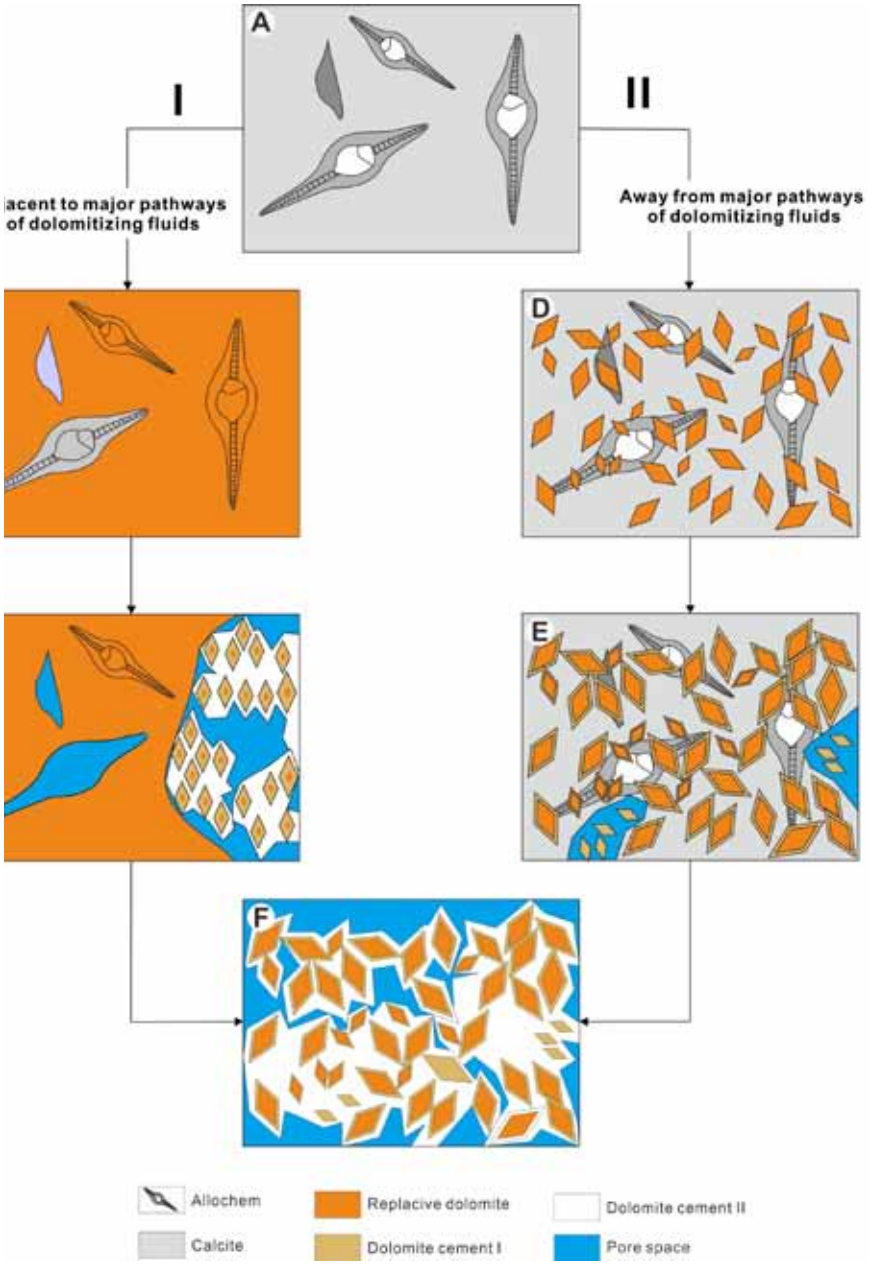

Fig. 3-16. Schematic diagrams showing two possible pathways for the evolution of dolostone textures in the Brac Formation. Pathway I: (A) Limestone with allochems. (B) Fabric-retentive dolostone with pseudomorphically replaced allochems and undolomitized allochems. (C) fabric-retentive dolostone partly modified by dissolution and cementation into fabric-destructive texture. Pathway II: (D) Limestone with floating dolomite rhombs. (E) Partly dissolved limestones with dolomite cements filling in pore spaces or as overgrowth. (F) Fabric-destructive dolostones due to dissolution and cementation.

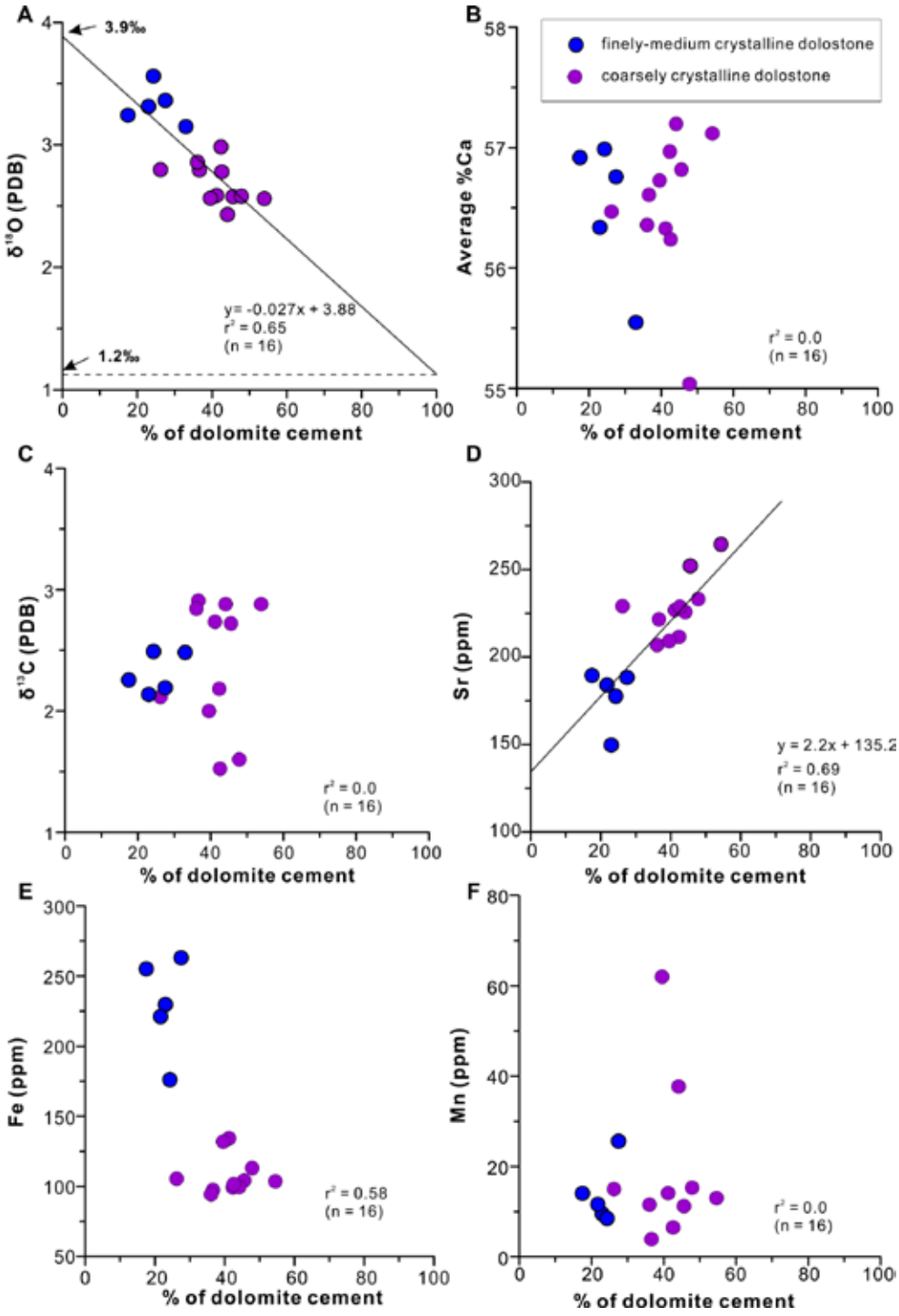

Fig. 3-17. Composite plots showing the relationships between % of dolomite cement and other geochemical attributes of dolostones from the Brac Formation. (A) $\delta^{18}O$, (B) average %Ca, (C) $\delta^{13}C$, (D) Sr, (E) Fe, (F) Mn.

of dolomite cement would have different geochemical features. This conjecture, however, cannot be tested directly because many of the dolomite cements are too thin (< 0.5 mm thick) to be physically separated from the replacive dolomites. Nevertheless, the influences that dolomite cements have on the geochemical composition of bulk dolostones have been reported from many settings (Cander et al., 1988; Fouke, 1994; Humphrey, 2000; Kyser et al., 2002; Gaswirth et al., 2007). Based on studies on Palaeogene sucrosic dolostones from the sub-surface of Florida, Gaswirth et al. (2007) pointed out that the later dolomite cements, which have different CL features from the replacive matrix dolomites, significantly impact the $\delta^{13}C$, $\delta^{18}O$, Na, and Sr values derived from whole-rock analyses. They argued that the negative correlations between the amount of dolomite cements and these geochemical variables arose because the replacive dolomites formed in seawater-like dolomitizing fluids enriched in $\delta^{13}C$, $\delta^{18}O$, Na and Sr, as compared to the dolomite cements, which were precipitated from dilute fluids. In contrast, Kyser et al. (2002) used a two-stage dolomitization model to explain the formation of coarsely crystalline dolomites in the Gambier Limestone, Australia, whereby the replacive dolomite formed from dilute seawater and the dolomite cements that enlarged the pre-existing dolomite crystals, formed from seawater. Development of the dolomite cements made the bulk dolostone samples more enriched in $\delta^{13}C$ and $\delta^{18}O$ compared to silt-sized first generation dolomites (Kyser et al., 2002).

The dolostones from the Brac Formation are petrographically similar to dolostones from Florida (Gaswirth et al., 2007) and Australia (Kyser et al., 2002) in the following respects: (1) the replacive dolomites and the dolomite cements have different CL signatures, (2) there were multiple episodes of dolomite cement precipitation, and (3) the size of dolomite crystals is related to the amount of dolomite cementation. Such comparisons indicate that similar interpretations

could be responsible for the differences in the geochemical signatures of the fine to medium crystalline dolostones and the coarsely crystalline sucrosic dolostones from the Brac Formation. This would imply that the dolomite cements, which form a major part of the sucrosic dolostones, probably formed from waters that had different isotopic composition and/or temperature than the waters that mediated formation of the replacive dolomites. The coarsely crystalline sucrosic dolostones contain more cements than the fine - medium crystalline equigranular dolostones (Table 3-1). The $\delta^{18}O$ values of the dolostones from the Brac Formation covary with the percentage of dolomite cement ($r^2 = 0.65$) (Fig. 3-17A). According to this correlation, the $\delta^{18}O$ of replacive dolomite would be 3.9‰, whereas the dolomite cement would have a $\delta^{18}O$ value of 1.2‰ (Fig. 3-17A). Given that there are no significant differences in the %Ca of replacive dolomite and dolomite cements (Fig. 3-17B), the difference in their $\delta^{18}O$ values most likely reflects the change in the isotopic composition and/or the temperature of dolomitizing fluids rather than the stoichiometric effect (Zhao and Jones, 2012). Zhao and Jones (2012) proposed a two-episode model driven by an increase of relative sea level to interpret the dolomitization of the Cayman Formation. The timing of dolomitization of the Brac Formation is in accordance with their Phase I dolomitization. According to that model, the Brac Formation should be dolomitized by near surface seawater during the Late Miocene. Hence, the more positive $\delta^{18}O$ values of replacive dolomites probably reflect a environment where more evaporation took place. This conjecture is parallel to the conclusion drawn by Wheeler et al. (1999) based on the sucrosic dolostones found on Niue in the Pacific Ocean. The $\delta^{13}C$ values of the fabric-destructive dolostones in the Brac Formation do not covary with the percentage of dolomite cement (Fig. 3-17C), therefore, the lower $\delta^{18}O$ values of dolomite cements indicate a normal seawater origin without significant evaporation rather than involvement of fresh

water. Moreover, the positive correlation between the Sr concentrations and the percentage of dolomite cements in the dolostones from the Brac Formation (Fig. 3-17D) also argues against diluted seawater being the parent fluid for the dolomite cements. As suggested by Gaswirth et al. (2007), dolomite cements precipitated in the mixing zone tend to have lower Sr contents. The fact that the Fe and Mn contents of the two types of dolostones vary over a relative narrow range relative to the percentage of dolomite cement (Fig. 3-7E and F) also indicates that the redox conditions associated with the dolomitizing fluids did not change significantly through the formation of replacive dolomites and dolomite cements. The relative higher Fe content in the fine-medium crystalline dolostones (Fig. 3-7E) might be due to the replacive dolomites inheriting more Fe from the precursor limestone. In comparison with other fabric-destructive dolostones in which two types of dolomitizing fluids (mixed water and seawater) were involved in their formation (e.g., Kyser et al. 2002; Gaswirth et al., 2007), the dolostones found on the Brac Formation provide a case that the fabric-destructive textures of dolostones can form in seawater settings.

3.9. Conclusions

The dolostones from the Brac Formation are characterized by their heterogeneous distribution and the coarsely crystalline fabric-destructive texture that contrasts dramatically with the overlying finely crystalline fabric-retentive dolostones of the Cayman Formation. After examining the dolostones from the Brac Formation and comparing them with the overlying Cayman Formation, the following important conclusions can be drawn:

- The distribution of dolomite in limestones is fundamentally controlled by the pre-existing permeability pathways that dictated the patterns of dolomitizing fluid circulation. Pre-dolomitization diagenesis has an

important influence on the degree of dolomitization.

- Dolomitization of the Brac Formation was probably mediated by seawater. Both replacive dolomite and dolomite cement have same origin, but the seawater responsible for the replacive dolomitization had probably undergone more evaporation than the water from which the dolomite cement was precipitated.
- The fabric-destructive texture of dolostones from the Brac Formation is probably a result of multiple dissolution-precipitation processes rather than the mineralogy of precursor limestones or the chemical composition of dolomitizing fluids. Cementation plays a major role in enlarging dolomite crystals and obliterating the original fabrics of precursors.

This study of the fabric-destructive dolostones from the Brac Formation indicates that the dolostones with various textures can be generated by repeated diagenetic cycles (e.g., dolomitization, dissolution, and cementation). The textures, in themselves, do not necessarily have genetic implications. Hence, caution must be taken when trying to interpret the origin of dolostones based only on their textures. The origin of dolostones can only be resolved following a multidisciplinary approach and the integration of all available information.

3.10. References

Al-Aasm, I.S., 2000. Chemical and isotopic constraints for recrystallization of sedimentary dolomites from the Western Canada sedimentary basin. Aquatic Geochemistry 6, 227-248.

Banner, J.L., 1995. Application of the trace element and isotope geochemistry of strontium to studies of carbonate diagenesis. Sedimentology 42, 805-824.

Budd, D.A., 1997. Cenozoic dolomites of carbonate islands: their attributes and origin. Earth-Science Reviews 42, 1-47.

Cander, H.S., 1994. An example of mixing-zone dolomite, middle Eocene Avon Park Formation, Floridan Aquifer system. Journal of Sedimentary Research 64, 615-629.

Cander, H.S., Kaufman, J., Daniels, L.D., Meyers, W.J., 1988. Regional dolomitization of shelf carbonates in the Burlington–Keokuk Formation (Mississippian), Illinois and Missouri: constraints from cathodoluminescent zonal stratigraphy. Sedimentology and Geochemistry of Dolostones: SEPM, Special Publication 43, 129-144.

Chai, L., Navrotsky, A., 1995. Energetics of calcium-rich dolomite. Geochimica et Cosmochimica Acta 59, 939-944.

Choquette, P.W., Hiatt, E.E., 2008. Shallow-burial dolomite cement: a major component of many ancient sucrosic dolomites. Sedimentology 55, 423-460.

Dawans, J.M., Swart, P.K., 1988. Textural and geochemical alternations in Late Cenozoic Bahamian dolomites. Sedimentology 35, 385-403.

DeMets, C., Wiggins-Grandison, M., 2007. Deformation of Jamaica and motion of the Gonâve microplate from GPS and seismic data. Geophysical Journal International 168, 362-378.

Drever, J.I., 1997. The geochemistry of natural waters, surface and groundwater

environments. Englewood Cliffs, New Jersey (Prentice Hall), 436 pp

Ehrenberg, S., McArthur, J., Thirlwall, M., 2006. Growth, demise, and dolomitization of Miocene carbonate platforms on the Marion Plateau, offshore NE Australia. Journal of Sedimentary Research 76, 91-116.

Fouke, B.W., 1994. Deposition, diagenesis, and dolomitization of Neogene Seroe Domi Formation coral reef limestones on Curaçao, Netherlands Antilles. Natuurwetenschappelijke Studiekring voor het Caraèibisch Gebied (Amsterdam), Amsterdam, 182 pp.

Gaswirth, S.B., Budd, D.A., Farmer, G.L., 2007. The role and impact of freshwater–seawater mixing zones in the maturation of regional dolomite bodies within the proto Floridan Aquifer, USA. Sedimentology 54, 1065-1092.

Gill, I.P., Moore Jr., C.H., Aharon, P., 1995. Evaporitic mixed-water dolomitization on St. Croix, U.S.V.I. Journal of Sedimentary Research 65A, 591-604.

Gregg, J.M., Howard, S.A., Mazzullo, S., 1992. Early diagenetic recrystallization of Holocene (< 3000 years old) peritidal dolomites, Ambergris Cay, Belize. Sedimentology 39, 143-160.

Grove, C., Jerram, D.A., 2011. jPOR: An ImageJ macro to quantify total optical porosity from blue-stained thin sections. Computers & Geosciences 37, 1850-1859.

Harris, D.C., Meyers, W.J., 1987. Regional dolomitization of subtidal shelf carbonates: Burlington and Keokuk Formations (Mississippian), Iowa and Illinois. Geological Society, London, Special Publications 36, 237-258.

Horsfield, W.T., 1975. Quaternary vertical movements in the Greater Antilles. Geological Society of America Bulletin 86, 933-938.

Humphrey, J.D., 2000. New geochemical support for mixing-zone dolomitization

at Golden Grove, Barbados. Journal of Sedimentary Research 70, 1160-1170.

Jones, B., 1994. Geology of the Cayman Islands. In: Brunt, M.A., Davies, J.E. (Eds.), The Cayman Islands: Natural history and biogeography. Kluwer, Dordrecht, The Netherlands, pp. 13–49.

Jones, B., 2004. Petrography and significance of zoned dolomite cements from the Cayman Formation (Miocene) of Cayman Brac, British West Indies. Journal of Sedimentary Research 74, 95-109.

Jones, B., 2005. Dolomite crystal architecture: genetic implications for the origin of the Tertiary dolostones of the Cayman Islands. Journal of Sedimentary Research 75, 177-189.

Jones, B., 2007. Inside-out dolomite. Journal of Sedimentary Research 77, 539-551.

Jones, B., Ng, K. C., 1988. Anatomy and diagenesis of a Pleistocene carbonate breccia formed by the collapse of a seacliff, Cayman Brac, British West Indies. Bulletin of Canadian Petroleum Geology 36, 9-24.

Jones, B., Hunter, I.G., 1994. Evolution of an isolated carbonate bank during Oligocene, Miocene and Pliocene times, Cayman Brac, British west Indies. Facies 30, 25-50.

Jones, B., Hunter, I.G., Kyser, K., 1994a. Stratigraphy of the Bluff Formation (Miocene-Pliocene) and the newly defined Brac Formation (Oligocene), Cayman Brac, British West Indies. Caribbean Journal of Science 30, 30-51.

Jones, B., Hunter, I.G., Kyser, K., 1994b. Revised stratigraphic nomenclature for Tertiary strata of the Cayman Islands, British West Indies. Caribbean Journal of Science 30, 53-68.

Jones, B., Luth, R.W., 2002. Dolostones from Grand Cayman, British West Indies.

Journal of Sedimentary Research 72, 559-569.

Jones, B., Luth, R.W., 2003. Temporal evolution of Tertiary dolostones on Grand Cayman as determined by $^{87}Sr/^{86}Sr$. Journal of Sedimentary Research 73, 187-205.

Jones, B., Luth, R.W., MacNeil, A.J., 2001. Powder X-ray diffraction analysis of homogeneous and heterogeneous sedimentary dolostones. Journal of Sedimentary Research 71, 790-799.

Kaczmarek, S.E., Sibley, D.F., 2011. On the evolution of dolomite stoichiometry and cation order during high-temperature synthesis experiments: An alternative model for the geochemical evolution of natural dolomites. Sedimentary Geology 240, 30-40.

Kyser, T.K., James, N.P., Bone, Y., 2002. Shallow burial dolomitization and dedolomitization of Cenozoic cool-water limestones, southern Australia: geochemistry and origin. Journal of Sedimentary Research 72, 146-157.

Land, L.S., 1973. Holocene meteoric dolomitization of Pleistocene limestones, North Jamaica. Sedimentology 20, 411-424.

Land, L.S., 1980. The isotopic and trace element geochemistry of dolomite: the state of the art. In: Zenger, D.H., Dunham, J.B., Ethington, R.L. (Eds.), Concepts and Models of Dolomitization, SEPM Special Publication 28, Tulsa, Oklahomano, pp. 87–110.

Land, L.S., 1985. The origin of massive dolomite. Journal of Geological Education 33, 112-125.

Lee, Y.I., Friedman, G.M., 1987. Deep-burial dolomitization in the Ordovician Ellenburger Group carbonates, West Texas and southeastern New Mexico. Journal of Sedimentary Research 57, 544-557.

Leroy, S., Mauffret, A., Patriat, P., Mercier de Lépinay, B., 2000. An alternative interpretation of the Cayman trough evolution from a reidentification of

magnetic anomalies. Geophysical Journal International 141, 539-557.

Lumsden, D.N., Chimahusky, J.S., 1980. Relationship between dolomite nonstoichiometry and carbonate facies parameters. In: Zenger, D.H., Dunham, J.B., Ethington, R.L. (Eds.), Concepts and Models of Dolomitizatioin. SEPM Special Publication 28, Tulsa, Oklahoma, pp. 123–137.

Machel, H.G., 1997. Recrystallization versus neomorphism, and the concept of significant recrystallization'in dolomite research. Sedimentary Geology 113, 161-168.

Machel, H.G., 2004. Concepts and models of dolomitization: a critical reappraisal. In Braithwaite, C., Rizzi, G, Drake, G. (Eds.)., The Geometry and Petrogenesis of Dolomite Hydrocarbon Reservoirs. Geological Society of London Special Publication 235, pp. 7-63.

MacNeil, A., Jones, B., 2003. Dolomitization of the Pedro Castle Formation (Pliocene), Cayman Brac, British West Indies. Sedimentary Geology 162, 219-238.

Maliva, R.G., Budd, D.A., Clayton, E.A., Missimer, T.M., Dickson, J.A.D., 2011. Insights into the dolomitization process and porosity modification in sucrosic dolostones, Avon Park Formation (Middle Eocene), east-central Florida, U.S.A. Journal of Sedimentary Research 81, 218-232.

Maliva, R.G., Siever, R., 1988. Diagenetic replacement controlled by force of crystallization. Geology 16, 688-691.

Malone, M.J., Baker, P.A., Burns, S.J., 1996. Recrystallization of dolomite: an experimental study from 50-200°C. Geochimica et Cosmochimica Acta 60, 2189-2207.

Mann, P. Calais, E., Ruegg, J., DeMets, C., Jansma, P. E., Mattioli, G. S., 2002. Oblique collision in the northeastern Caribbean from GPS measurements

and geological observations. Tectonics 21, 1057, 26 pp.

Matley, C.A., 1926. The geology of the Cayman Islands (British West Indies), and their relation to the Bartlett Trough. Quarterly Journal of the Geological Society 82, 352-387.

Mazzullo, S., 1992. Geochemical and neomorphic alteration of dolomite: A review. Carbonates and Evaporites 7, 21-37.

McArthur, J.M., Howarth, R.J., Bailey, T.R., 2001. Strontium isotope stratigraphy: LOWESS Version 3: Best fit to the marine Sr-isotope curve for 0-509 Ma and accompanying look-up table for deriving numerical age. Journal of Geology 109, 155-170.

McCrea, J.M., 1950. On the isotopic chemistry of carbonates and a paleotemperature scale. The Journal of Chemical Physics 18, 849-857.

Morrow, D.W., 1982. Diagenesis 2. Dolomite-Part 2: Dolomitization models and ancient dolostones. Geoscience Canada 9, 95-107.

Murray, R.C., 1960. Origin of porosity in carbonate rocks. Journal of Sedimentary Research 30, 59-84.

Nichols, K., Silberling, N., 1980. Eogenetic dolomitization in the pre-Tertiary of the Great Basin. In: Zenger, D.H., Dunham, J.B., Ethington, R.L. (Eds.), Concepts and Models of Dolomitizatioin. SEPM Special Publication 28, Tulsa, Oklahoma, pp. 237-246.

Perfit, M.R., Heezen, B.C., 1978. The geology and evolution of the Cayman Trench. Geological Society of America Bulletin 89, 1155-1174.

Purser, B., Tucker, M., Zenger, D., 1994. Problems, progress and future research concerning dolomites and dolomitization. In: Purser, B., Tucker, M. Zenger, D. (Eds.), Dolomites: A Volume in Honour of Dolomieu: International Association of Sedimentologists, Special Publication 21, Oxford, pp. 3-20.

Rosencrantz, E., Sclater, J.G., 1986. Depth and age in the Cayman Trough. Earth and Planetary Science Letters 79, 133-144.

Sass, E., Bein, A., 1988. Dolomites and salinity: a comparative geochemical study. In: Shukla, V., Baker, P. A., (Eds.), Sedimentology and Geochemistry of Dolostones. SEPM, Special Publication 43, Tulsa, Oklahoma, pp. 223-233.

Sass, E., Katz, A., 1982. The origin of platform dolomites; new evidence. American Journal of Science 282, 1184-1213.

Sibley, D.F., 1982. The origin of common dolomite fabrics; clues from the Pliocene. Journal of Sedimentary Research 52, 1087-1100.

Sibley, D.F., 1991. Secular changes in the amount and texture of dolomite. Geology 19, 151-154.

Sibley, D.F., Gregg, J.M., 1987. Classification of dolomite rock textures. Journal of Sedimentary Research 57, 967-975.

Sibley, D.F., Nordeng, S.H., Borkowski, M.L., 1994. Dolomitization kinetics of hydrothermal bombs and natural settings. Journal of Sedimentary Research 64, 630-637.

Sperber, C.M., Wilkinson, B.H., Peacor, D.R., 1984. Rock composition, dolomite stoichiometry, and rock/water reactions in dolomitic carbonate rocks. The Journal of Geology 92, 609-622.

Stoddart, D.R., 1980. Geology and geomorphology of Little Cayman. Atoll Research Bulletin 241, 11-16.

Suzuki, Y., Iryu, Y., Inagaki, S., Yamada, T., Aizawa, S., Budd, D.A., 2006. Origin of atoll dolomites distinguished by geochemistry and crystal chemistry: Kita-daito-jima, northern Philippine Sea. Sedimentary Geology 183, 181-202.

Uzelman, B.C., 2009. Sedimentology, diagenesis, and dolomitization of the Brac Formation (Lower Oligocene), Cayman Brac, British West Indies,

Unpublished M. Sc. Thesis, University of Alberta, Canada, 120 pp.

Vahrenkamp, V.C., Swart, P.K., 1990. New distribution coefficient for the incorporation of strontium into dolomite and its implications for the formation of ancient dolomites. Geology 18, 387-391.

Vahrenkamp, V.C., Swart, P.K., 1994. Late Cenozoic dolomites of the Bahamas: metastable analogues for the genesis of ancient platform dolomites. In: Purser, B., Tucker, M. Zenger, D. (Eds.), Dolomites: A Volume in Honour of Dolomieu: International Association of Sedimentologists, Special Publication 21, Oxford, pp. 133–153.

Vahrenkamp, V.C., Swart, P.K., Ruiz, J., 1988. Constraints and interpretation of $^{87}Sr/^{86}Sr$ ratios in Cenozoic dolomites. Geophysical Research Letters 15, 385-388.

Warren, J., 2000. Dolomite: occurrence, evolution and economically important associations. Earth-Science Reviews 52, 1-81.

Wheeler, C.W., Aharon, P., Ferrell, R.E., 1999. Successions of late Cenozoic platform dolomites distinguished by texture, geochemistry, and crystal chemistry; Niue, South Pacific. Journal of Sedimentary Research 69, 239-255.

Wilson, E.N., Hardie, L.A., Phillips, O.M., 1990. Dolomitization front geometry, fluid flow patterns, and the origin of massive dolomite: the Triassic Latemar buildup, northern Italy. American Journal of Science 290, 741-796.

Zempolich, W.G., Baker, P.A., 1993. Experimental and natural mimetic dolomitization of aragonite ooids. Journal of Sedimentary Petrology 63, 596-606.

Zhao, H., Jones, B., 2012. Origin of “island dolostones”: A case study from the Cayman Formation (Miocene), Cayman Brac, British West Indies. Sedimentary Geology 243-244, 191-206.

CHAPTER 4
DISTRIBUTION AND INTERPRETATION OF RARE EARTH ELEMENTS AND YTTRIUM OF CARBONATES[1]

4. 1. Introduction

Many islands throughout the Caribbean Sea and Pacific Ocean are characterized by thick successions of Cenozoic dolostones. Attention has been focused on these "island dolostones" (Budd, 1997) because they are geological young, have not been buried, and their geological histories are known. In an effort to resolve the long-standing debate on how thick successions of limestones can be pervasively dolomitized (i.e., the "dolomite problem"), these dolostones have been examined from many different perspectives (e.g., Varenkamp and Swart, 1994; Budd, 1997; Warren, 2000; Suzuki et al., 2006). Even so, there is still considerable debate regarding the nature of the dolomitizing fluids, the conditions under which dolomitization took place, and the factors that initiated dolomitization. Much of this debate arises because of uncertainties concerning the interpretation of some of the geochemical proxies, including the stable isotope (O and C) values obtained from the dolostones (cf., Budd, 1997; Zhao and Jones, 2012a, b). Some of these issues might be overcome if other proxies derived from the dolostones could also be used for the interpretation of their origin. In this study, we show that rare earth elements (REE) can provide valuable insights into the origin of island dolostones.

The REE in modern seawater, which include 14 elements (lanthanides) and the pseudo lanthanide yttrium (Y), are well known (German and Elderfield, 1990; Piepgras and Jacobsen, 1992; Bertram and Elderfield, 1993; Sholkovitz et al.,

---

1 This chapter has been submitted to *Sedimentary Geology* as: Zhao, H and Jones, B. 2012, Distribution and interpretation of rare earth elements and yttrium in Cenozoic dolostones and limestones on Cayman Brac, British West Indies.

1994; German et al., 1995; Zhang and Nozaki, 1996, 1998; Alibo and Nozaki, 1999; Nozaki and Alibo, 2003). Comparisons of the REE+Y derived from various deposits (including phosphates and carbonates) with the REE+Y of modern seawaters has been used to characterize the composition of ancient seawater (Holser, 1997; Webb and Kamber, 2000; Kamber and Webb, 2001; Shields and Stille, 2001; Miura et al., 2004; Nothdurft et al., 2004; Haley et al., 2005; Bau and Alexander, 2006; Webb et al., 2009; Himmler et al., 2010; Azmy et al., 2011). Such comparisons, however, are commonly problematic because it is not known if the REE+Y patterns derived from the sedimentary rocks are truly representative of the parent seawater. In part, this is because the impact that diagenesis may have had on the REE+Y concentrations in limestones and dolostones is not fully understood.

In this study, attention is focused on the REE+Y distribution throughout the Oligocene to Pleistocene carbonate succession found on Cayman Brac, which is formed largely of dolostones (Fig. 4-1A). Dolostones in the Brac Formation (Lower Oligocene), the Cayman Formation (Miocene), and Pedro Castle Formation (Pliocene) have been well characterized in terms of their stratigraphic setting, petrography, stoichiometry, geochemistry, and isotopic signatures (Jones and Hunter, 1994a; MacNeil and Jones, 2003; Jones, 2004, 2005; Zhao and Jones, 2012a, b). Although dolomitization of the Tertiary succession on Cayman Brac has been attributed to slightly modified seawater (Zhao and Jones, 2012a, b), the exact nature of the dolomitizing fluid and the dolomitizing environment remains open to debate. Critically, this study demonstrates that the REE+Y distributions in the limestones and dolostones of Cayman Brac reveal information that brings further focus to the dolomitization processes that transformed much of the limestone to dolostone. Although based on the dolostones of Cayman Brac, the conclusions reached in this study carry important implications for dolostones of

all ages.

4.2. Geological setting

Cayman Brac (19 km long, 1.5 to 3 km wide) is located on the Cayman Ridge, which lies on the north side of the Oriente Transform Fault that separates the North America Plate from the Caribbean Plate (Fig. 4-1B). Each of the Cayman Islands is an uplifted fault block that rises 2000 – 2500 m from the seafloor (Perfit and Heezen, 1978; Stoddart, 1980). This area has been tectonically active since the Late Eocene (Rosencrantz and Sclater, 1986; Leroy et al., 2000; DeMets and Wiggins-Grandison, 2007). Today, the Mid-Cayman spreading centre, located southwest of Grand Cayman (Fig. 4-1B) continues to open at an average rate of 11–12 mm yr^{-1} (Rosencrantz and Sclater, 1986; Mann et al., 2002).

The carbonate succession on Cayman Brac (Fig. 4-1B) is at least 150 m thick (Jones, 1994). Matley (1926) originally assigned the Tertiary carbonates, which are well exposed in the cliffs around the island, to the Bluff Limestone (Fig. 4-1A). Subsequently, Jones et al. (1994a, b) renamed this succession the Bluff Group, which includes the unconformity bounded Brac Formation, Cayman Formation, and Pedro Castle Formation. The Bluff Group, which forms the uplifted core of the island, is surrounded by a low-lying platform that is formed of Pleistocene limestones that belong to the Ironshore Formation (Fig. 4-1C).

4.3. Stratigraphic succession

4.3.1. The Brac Formation

The Lower Oligocene Brac Formation is exposed in the vertical to overhanging cliffs (up to 45 m high) at the east end of Cayman Brac and was also penetrated by wells CRQ#1 and KEL#1 (Fig. 4-2). The base of the formation is

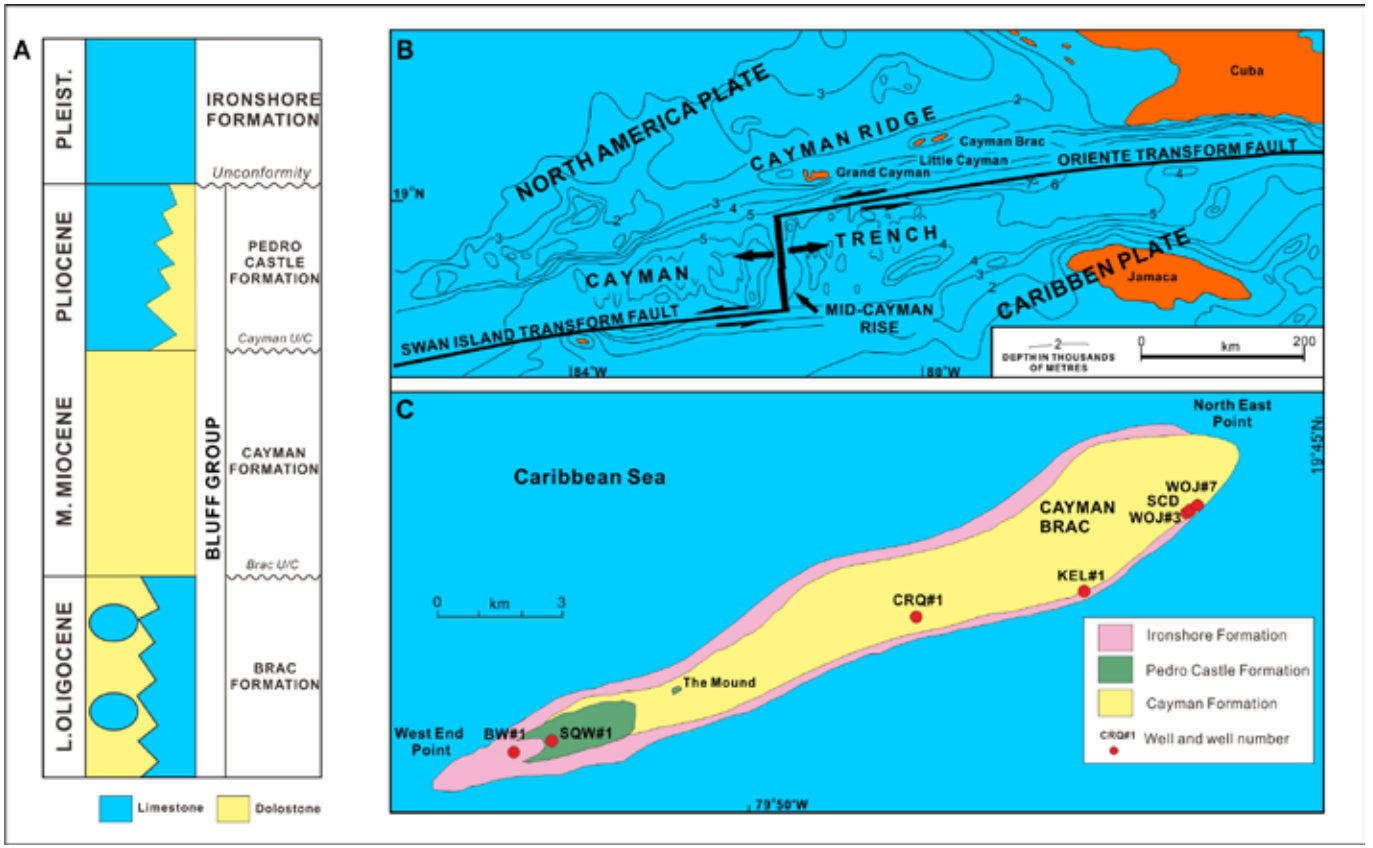

Fig. 4-1. Location and geology of Cayman Brac (A) Stratigraphic succession on Cayman Brac (modified from Jones, 1994) showing distribution of dolostones and limestones. (B) Tectonic and bathymetric setting of the Cayman Islands. Modified from Jones (1994) and based on maps from Perfit and Heezen (1978) and MacDonald and Holcombe (1978). (C) Geological map of Cayman Brac (modified from Jones, 1994) showing locations of BW#1, SQW#1, CRQ#1, KEL#1, WOJ#3, SCD, WOJ#7.

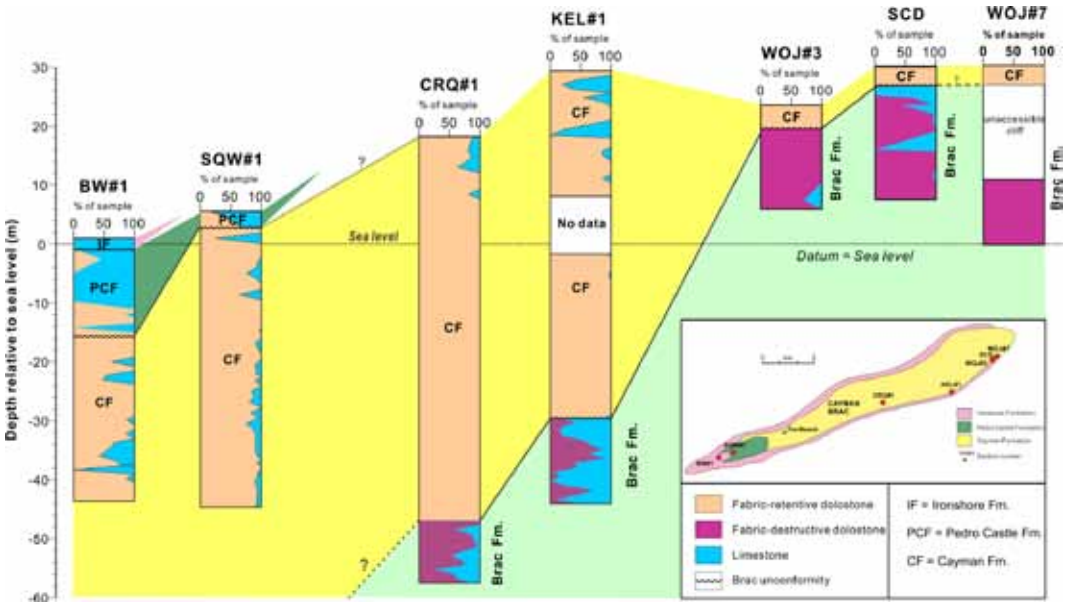

Fig. 4-2. Stratigraphic correlation between wells and outcrops showing the lithology of each section. See the inset map for the distance between sections.

unknown because it is not exposed and has not been found in any of the wells. It is separated from the overlying Cayman Formation by the Brac Unconformity, which ranges from ~ 30 m above sea level on the east end of the island to ~ 47 m below sea level in CRQ #1 (Fig. 4-2). This range in elevation reflects the karst topography that developed on the unconformity and tectonic tilting of the island to the west.

The Brac Formation is lithologically variable. On the north coast, it is formed of limestone that contains numerous large benthic foraminifera with fewer numbers of other foraminifera, red algae, and echinoid plates (Jones, 1994; Zhao and Jones, 2012a). Jones and Hunter (1994a) suggested that these limestones were probably deposited on a shallow (less than 10 m deep), low energy bank. On the south coast, the Brac Formation is characterized by isolated limestone pods (up to 10 m long and 2 m thick) that are surrounded by coarsely

crystalline, fabric-destructive, sucrosic dolostones. The sucrosic dolostones are formed largely of interlocking dolomite crystals, up to 1.5 mm long, with cloudy cores and clear rims. In wells CRQ#1 and KEL#1, the formation is formed of limestones that have been dolomitized to varying degrees. Some of the dolostones in the Brac Formation contain up to 54% (volume) dolomite cement (Zhao and Jones, 2012a). Interpretation of geochemical data and petrographic evidence points to dolomitization being mediated by slightly modified seawater during the Late Miocene (Zhao and Jones, 2012a).

4.3.2. The Cayman Formation

The Cayman Formation on Cayman Brac, which is mostly Middle Miocene in age, is ~ 100 m thick (Jones, 1994). Its base is the Brac Unconformity, whereas its upper boundary is defined by the Cayman Unconformity (Fig. 4-2). On Cayman Brac, this formation is formed largely of finely crystalline, fabric retentive dolostones with anhedral to subhedral dolomite crystals that are typically < 20 μm long (Zhao and Jones, 2012b). These fossil-rich dolostones commonly contain numerous corals, bivalves, gastropods, rhodoliths, Halimeda plates, echinoid plates, red algae, and foraminifera (Zhao and Jones, 2012b). The original sediments probably accumulated on a shallow, submarine bank with a maximum water depth of 30 m (Jones and Hunter, 1994a). Dolomitization of the Cayman Formation was probably achieved through two separate episodes of dolomitization in the Late Miocene and Pliocene that were both mediated by seawater (Zhao and Jones, 2012b).

4.3.3. The Pedro Castle Formation

The Lower Pliocene Pedro Castle Formation is restricted to the western end of Cayman Brac, where it is up to 10 m thick (Fig. 4-2). Much of this formation was eroded from central and eastern parts of the island after tectonic tilting (Zhao

and Jones, 2012b). The base of the formation is the Cayman Unconformity, whereas the upper boundary has been lost to erosion. The Pedro Castle Formation is formed of limestones, dolomitic limestones, and dolostones (MacNeil and Jones, 2003). The original sediments were deposited in environments similar to those for the Cayman Formation (Jones and Hunter, 1994a). The finely crystalline, fabric retentive dolostones from the Pedro Castle Formation are similar to those found in the underlying Cayman Formation. MacNeil and Jones (2003) suggested that dolomitization of the Pedro Castle Formation during the Late Pliocene was mediated by a mixture of freshwater and seawater.

4.3.4. The Ironshore Formation

The Ironshore Formation, up to 6 m thick, forms a low-lying apron around Cayman Brac (Fig. 4-1C) with its landward margin butting against the cliffs that are formed of the Bluff Group. The Ironshore Formation is characterized by limestones that contain numerous corals (commonly still aragonitic), bivalves, gastropods, bivalves, foraminifera, and algae. On Cayman Brac, the exposed part of the Ironshore Formation (Coyne and Jones, 2007) was deposited ~ 125,000 years ago when sea level was ~ 6 m higher than it is today.

4.4. Methods

The 127 samples used in this study came from wells BW#1, SQW#1, CRQ#1, KEL#1, outcrops above wells KEL#1, CRQ#1, BW#1, and SQW#1, and exposed sections SCD, WOJ#3, and WOJ#7 on the east end of Cayman Brac (Figs. 4-1C, 2). For comparison purposes, five samples from the Ironshore Formation (coral and matrix) and two samples of limestone from the Cayman Formation were collected from wells RWP#11 and NSC#1 on Grand Cayman. On Cayman Brac, there is no continuous section through the entire succession and, as yet, no well that has penetrated the entire succession. For the purposes

of this study, however, a composite succession was constructed by using all the information that is currently available. Well BW#1 cut through the Ironshore Formation, the Pedro Castle Formation, and the upper part of the Cayman Formation. Well SQW#1 includes the Pedro Castle Formation and the upper part of the Cayman Formation. The middle and basal parts of the Cayman Formation and the upper parts of Brac Formation are found in wells CRQ#1 and KEL#1. The upper parts of the Brac Formation are also exposed in the outcrops (SCD, WOJ#3 and WOJ#7) at the eastern end of Cayman Brac (Fig. 4-2). The Brac Unconformity is exposed in the cliff faces up to 33 m above sea level at the east end of Cayman Brac (Fig. 4-2). The unconformity is located at 46.9 m and 29.3 m below sea level in wells CRQ#1 and KEL#1, respectively (Fig. 4-2). Correlations between wells coupled with the estimated westerly dip of ~ 0.5^{o} (Jones, 1994) allowed construction of the composite section that is used herein. For the purposes of this paper, the top of the Ironshore Formation is used as a datum, with the positions of all samples being designated relative to that datum. For comparison purposes, the samples of the Ironshore Formation from Grand Cayman are placed at the top of the Ironshore Formation.

Zhao and Jones (2012a, b) described the petrography, isotopic geochemistry (C and O isotopes), and trace element (Sr, Fe, and Mn) concentrations of the dolostones from the Brac Formation and Cayman Formation. In this study, the mineralogy of the whole-rock samples was determined by X-ray diffraction (XRD) analyses. The samples were ground into powders (75-150 μm grain size) with an agate mortar and pestle. XRD analyses were performed on a Rigaku Geigerflex 2173 XRD system using Co Kα radiation at the University of Alberta. XRD was used to determine the mineralogy and the weight percentages of calcite and dolomite. After XRD analyses, ~ 0.2 g of the powdered sample was digested in 10 ml 8 N HNO_3. 1 ml of this solution was then diluted with 8.8 ml deionized

water and 0.1 ml HNO3 and 0.1 ml of an internal standard (Bi, Sc, and In). The diluted solution was introduced into a Perkin Elmer Elan6000 quadrupole inductively coupled plasma mass spectrometer (ICP-MS) for REE and Y analyses. Appropriate oxide interference corrections were applied by running a standard solution (CeO/Ce < 3%) before calibration. One sample was analyzed in duplicate during each analytical run, showing that reproducibility is within ± 2%. The detections limits for REE analyses are from 0.004 ppm for praseodymium (Pr) to 0.05 ppm for lutetium (Lu) (Supplementary Data Table 1). The Fe and Mn concentrations were determined with the REE and Y analyses in order to detect the possible contaminations of Fe- and Mn-hydroxides (Bau et al., 1996).

The REE+Y distribution patterns in the Cayman Brac samples are illustrated by normalizing the REE+Y against the standard Post-Archean Average Shale (PAAS) (McLennan, 1989) and plotting them on a logarithmic scale relative to the atomic numbers of the different elements. The only exception is Y, which is inserted ahead of Ho due to their similarity in atomic radii.

4.5. Results

5.1 Carbonate mineralogy

The carbonates from the Brac Formation, the Cayman Formation, the Pedro Castle Formation, and the Ironshore Formation on Cayman Brac are composed of various combinations of aragonite, calcite and dolomite (Zhao and Jones, 2012a, b) (Fig. 4-2). Samples from the Brac Formation are composed of dolostones, partly-dolomitized limestones, and limestones. Although most samples from the Cayman Formation are pure dolostones, some contain minor amounts of calcite, which is probably a late stage cement. Samples from the Pedro Castle Formation are composed of dolomitic limestones and limestones. The limestones from the Ironshore Formation, which contain no dolomite, are formed of aragonite and

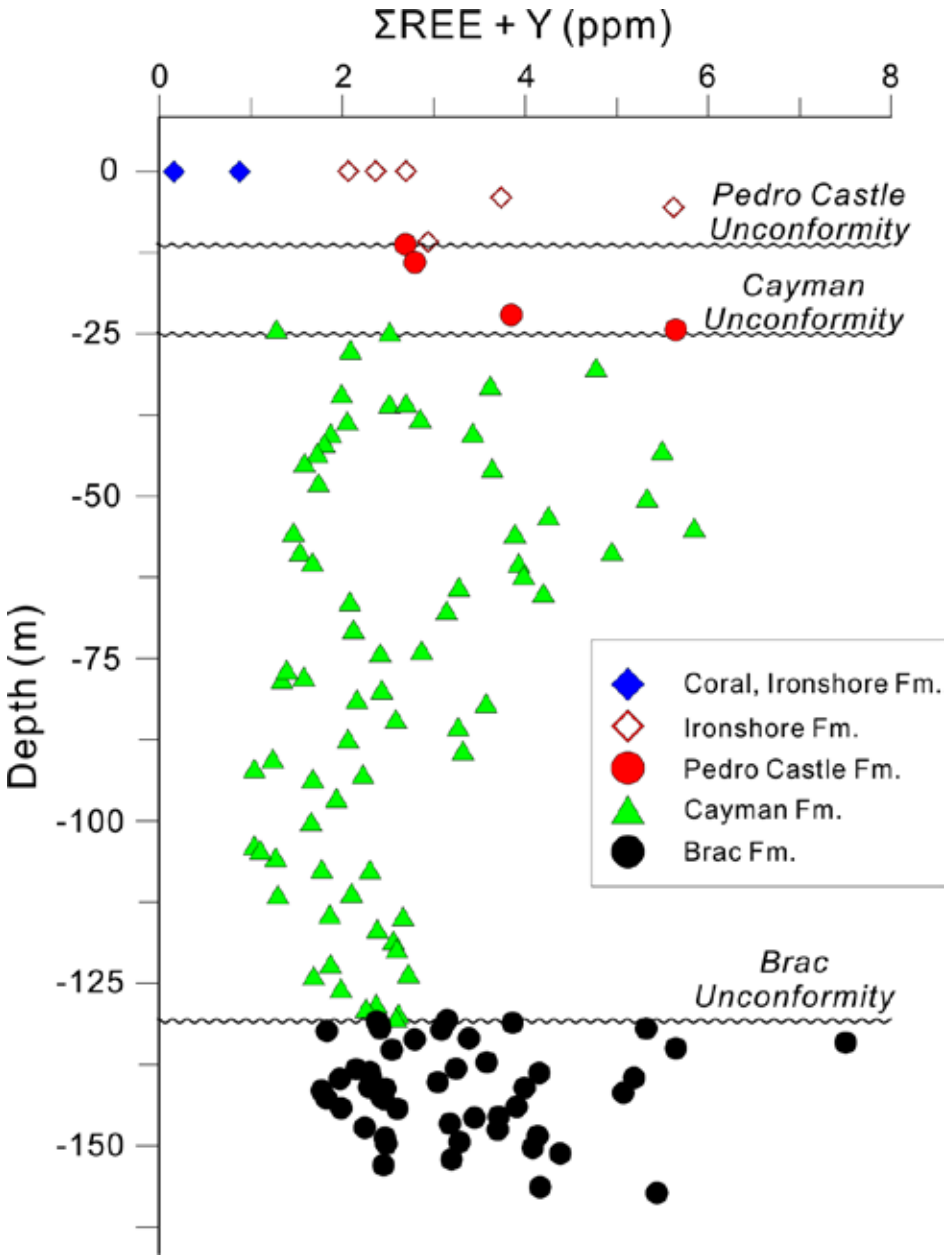

Fig. 4-3. Composite section showing variation in ∑REE (+Y) along with depth.

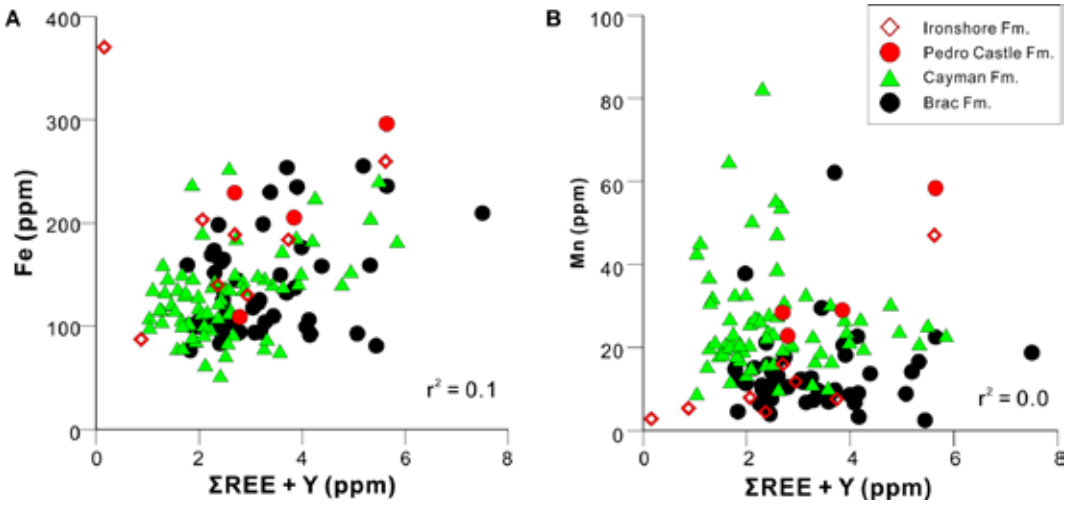

Fig. 4-4. Cross plots showing relationship between ∑REE (+Y) of carbonates and Fe (A) and Mn (B)

calcite.

5.2. Carbonate REE+Y geochemistry

The REE+Y concentrations (∑REE+Y) of limestones and dolostones from the Bluff Group range from 1.0 to 7.5 ppm (average 2.9 ppm, n = 126). In contrast, samples from the Ironshore Formation range from 0.2 to 5.6 ppm (average 2.6, n = 8) with the lowest values being from the two coral samples that are formed of 100% aragonite (average 0.5 ppm, n = 2) (Fig. 4-3). For most samples, the europium (Eu), terbium (Tb), and Lu concentrations are below the detection limits (Supplementary Data Table 1). There are no correlations between ∑REE+Y and sample depths (Fig. 4-3), Fe ($r^2 = 0.1$) or Mn ($r^2 = 0.0$) (Fig. 4-4).

Overall, the shale-normalized REE+Y distribution patterns derived from the carbonates from Cayman Brac are characterized by the following features.

- All samples are heavy-REE (HREE) enriched (average $Dy_N/Sm_N = 1.7$, n = 125), with samples from the Pedro Castle Formation and the Ironshore Formation (average $Dy_N/Sm_N = 2.1$, n = 10) being more enriched in HREE

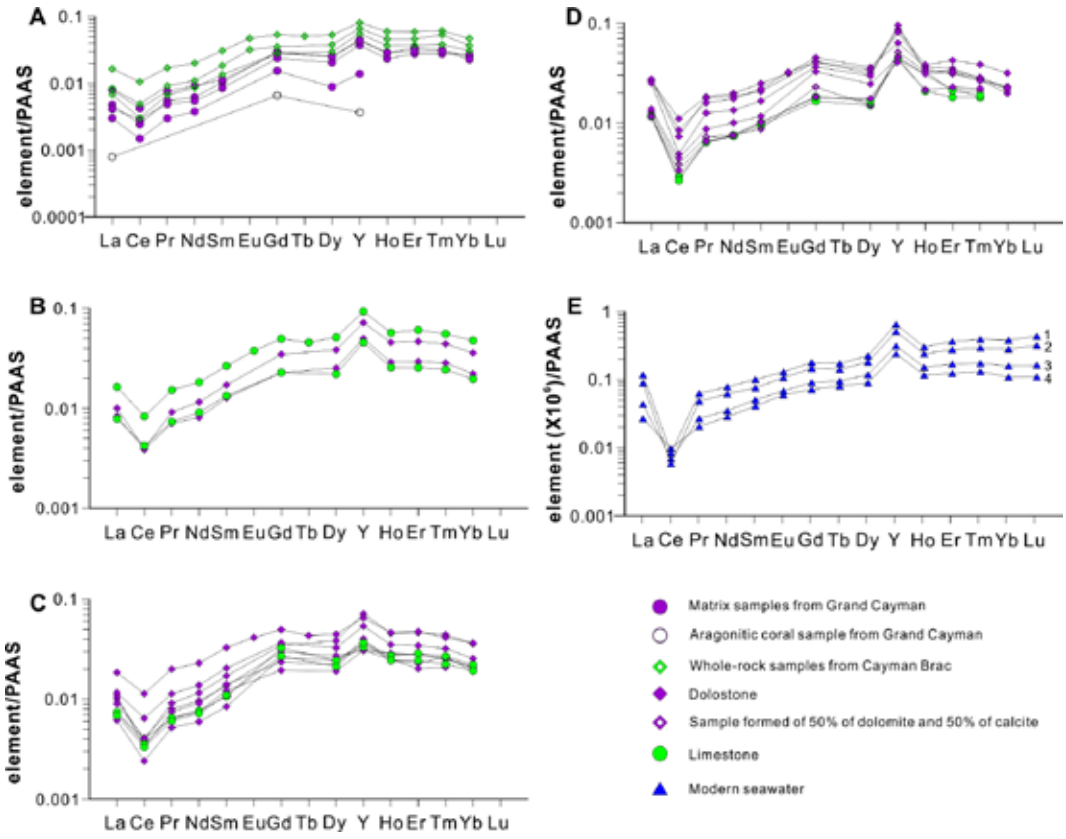

Fig. 4-5. Typical shale-normalized REE +Y patterns of carbonates from each formation of Cayman Brac and shale-normalized REE+Y patterns of modern seawater. (A) Ironshore Formation. Note that most REE+Y elements of aragonitic coral sample (open circles) are below the detection limits. (B) Pedro Castle Formation showing limestone samples and dolostone samples. (C) Cayman Formation showing fabric-retentive dolostone samples (closed diamonds) and limestone samples from Grand Cayman. (D) Brac Formation showing limestone samples, dolostone samples diamonds) and sample formed of 50% of dolomite and 50% of calcite. (E) Modern seawater with various depths (data from Alibo et al. (1999)). 1(1000 m), 2 (599 m), 3 (200 m), and 4 (5 m).

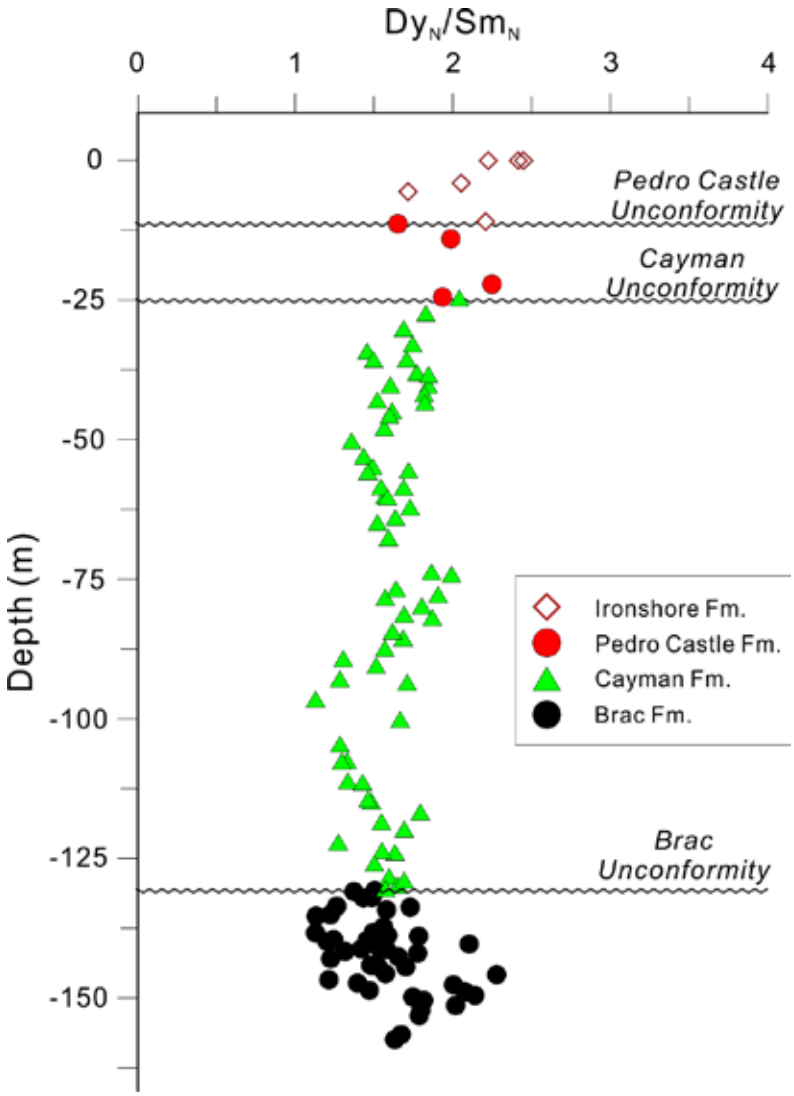

Fig. 4-6. Composite section showing variation in LREE depletion (Dy_N/Sm_N) of carbonates along with depth.

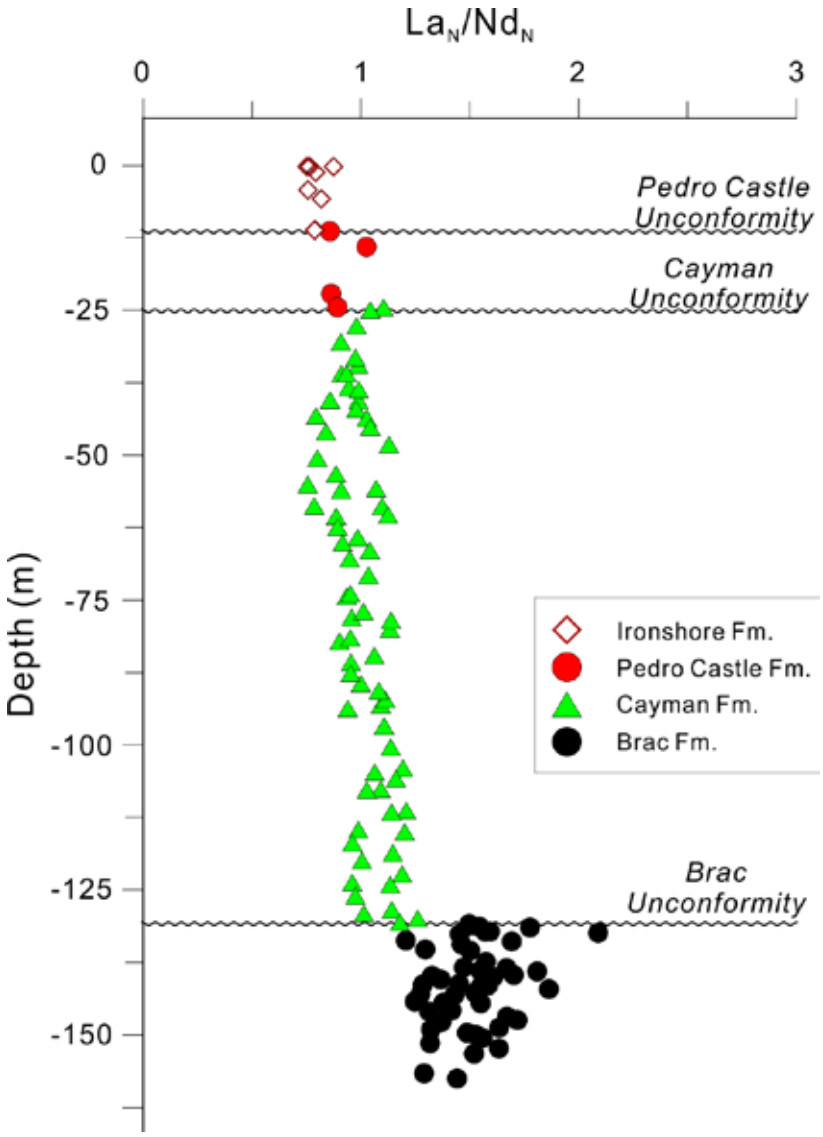

Fig. 4-7. Composite section showing variation in La anomalies (La_N/Nd_N) of carbonates along with depth.

than those from the Cayman Formation and Brac Formation (average Dy_N/Sm_N = 1.6, n = 104) (Fig. 4-6).

- Samples from the Brac Formation have more positive LaN/NdN ratios (1.2 to 2.1, average 1.5, n = 49) than those from the Cayman Formation, Pedro Castle Formation, and Ironshore Formation (0.8 to 1.3, average 1.0, n = 84) (Fig. 4-7).
- Given that anomalous abundance of La in seawater and marine precipitates can produce negative Ce/Ce* values ($Ce^* = 0.5La_N + 0.5Pr_N$), Bau and Dulski (1997) argued that Pr/Pr* ($= Pr_N/(0.5Ce_N + 0.5Nd_N)$ must be greater than 1 if Ce is truly negative. All samples from the four formations on Cayman Brac show true negative Ce anomalies and positive La anomalies

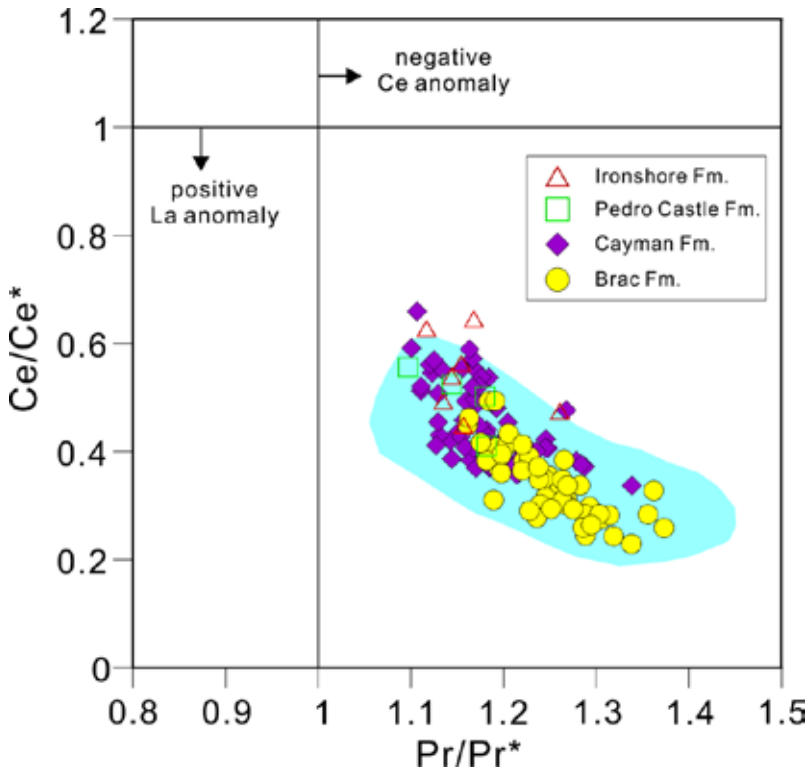

Fig. 4-8. Cross plot showing relationship between Ce/Ce* and Pr/Pr* using the method of Bau and Dulski (1996). Shaded area shows the range of modern seawater (after Nothdurft et al., 2004).

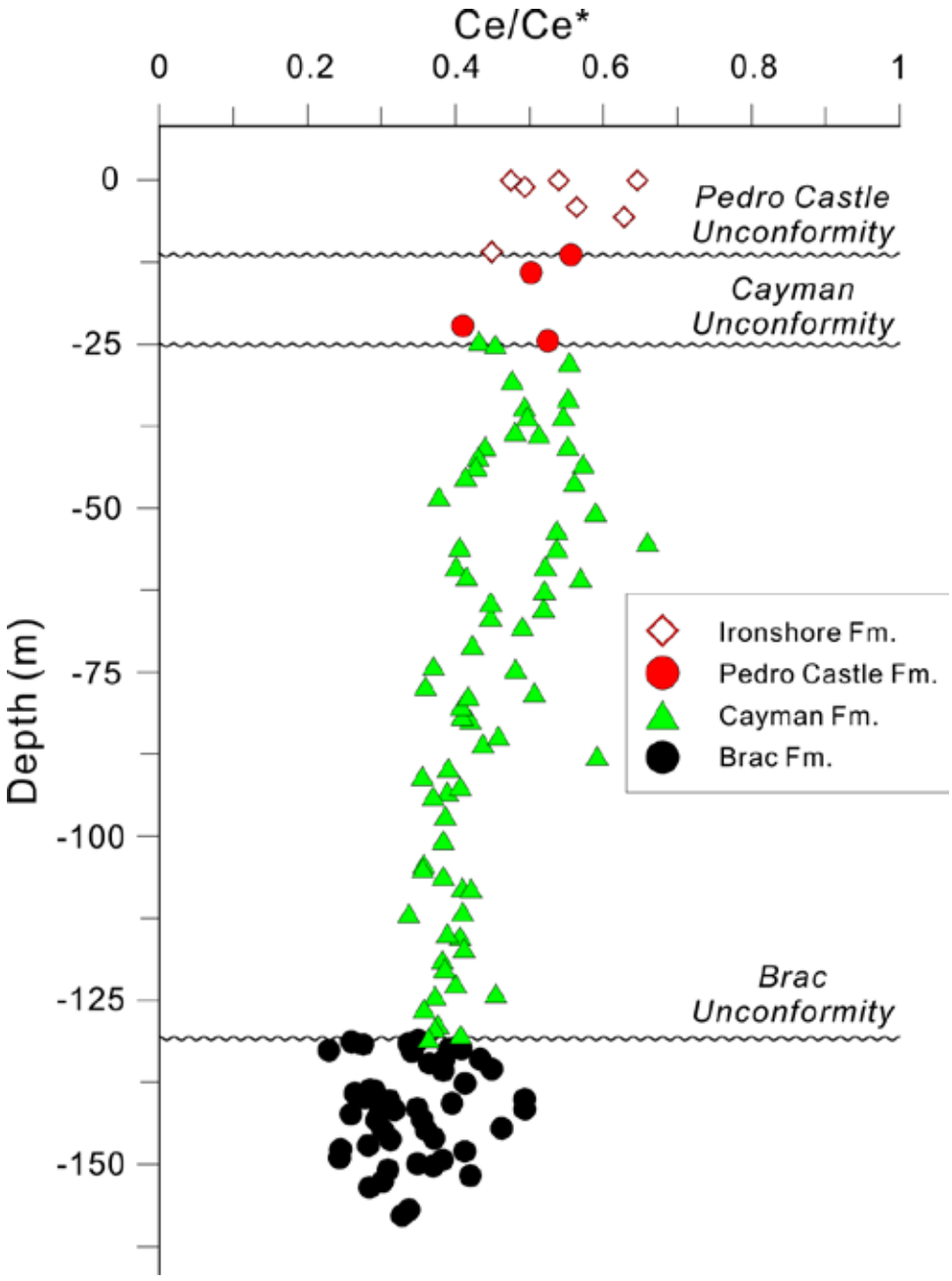

Fig. 4-9. Composite section showing variation in Ce anomalies (Ce/Ce*) of carbonates along with depth.

(Fig. 4-8). Their Ce/Ce* values range from 0.2 to 0.7 (average 0.4, n = 133), which are compatible with modern oxygenated seawater (Fig. 4-9). The samples from the Brac Formation, however, have more negative Ce anomalies (0.2 to 0.5, average 0.3, n = 49) than the overlying formations (0.3 to 0.7, average 0.5, n = 84) (Fig. 4-9).

- All samples show superchondritic Y/Ho molar ratios between 53 and 146 (average 85, n = 86). Samples from the Brac Formation, however, have higher Y/Ho ratios (69 to 146, average 102, n = 32) than those from the Cayman Formation, the Pedro Castle Formation, and the Ironshore Formation (53 to 116, average 75, n = 54) (Fig. 4-10).
- There are no correlations between the dolomite content (weight %) of the samples with their ∑REE+Y, Dy_N/Sm_N, La_N/Nd_N, Ce/Ce*, or Y/Ho (Fig. 4-11).

4.6. Interpretations

Interpretation of the REE data from carbonate succession on Cayman Brac must be considered relative to the geological evolution of the island, which has involved the following stages since the Early Oligocene.

- Lower Oligocene: sea level highstand with deposition of sediments that now form the Brac Formation on a shallow-water bank (Jones and Hunter 1994a; Jones et al., 1994a).
- Upper Oligocene to Early Miocene: sea level lowstand, exposure of Brac Formation leading to lithification and development of Brac Unconformity – a karst surface with at least 25 m of relief (Jones, 1994; Jones and Hunter, 1994a).
- Early to Late Miocene: deposition of sediments that now form the Cayman Formation (Jones, 1994; Jones and Hunter, 1994a; Jones et al., 1994a, b).

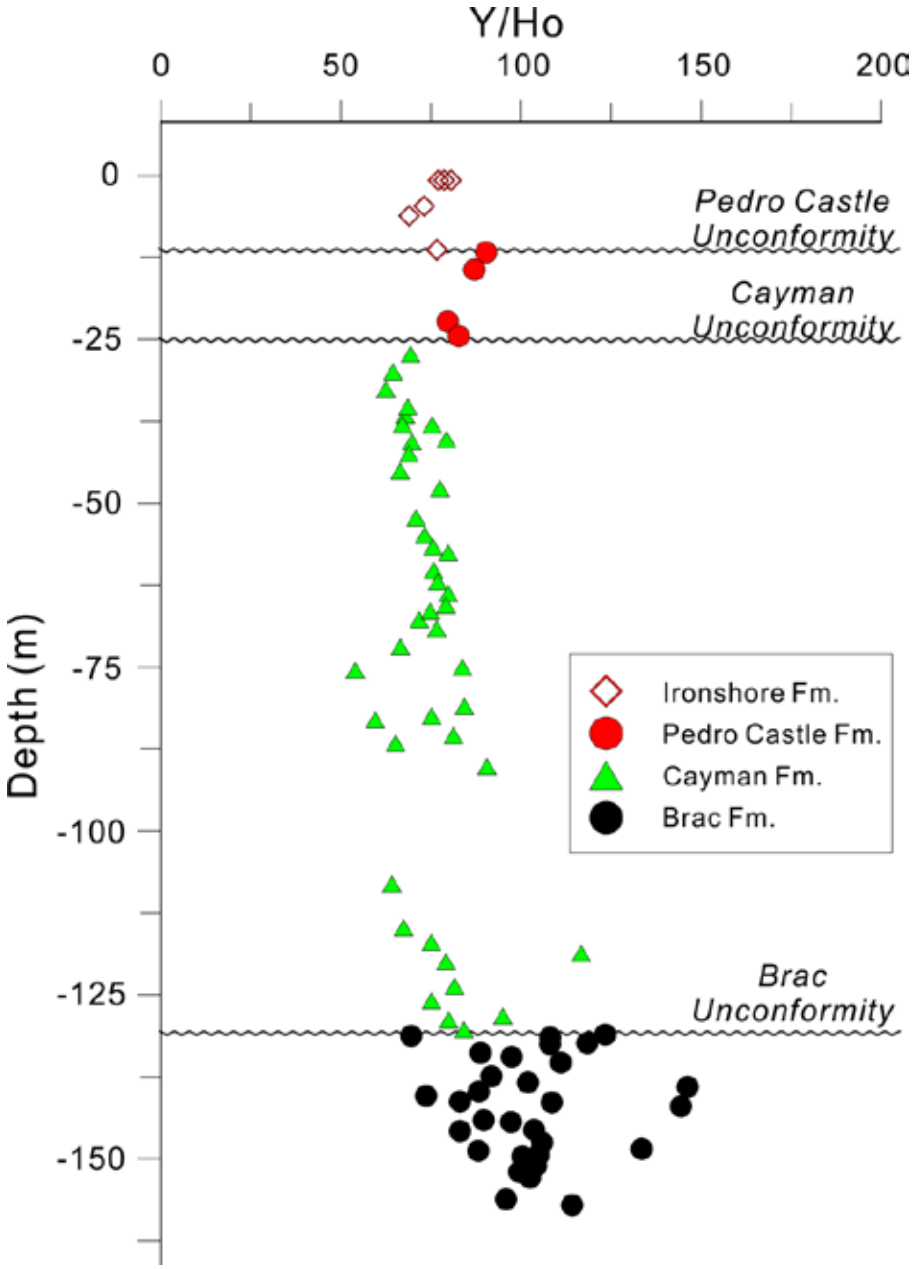

Fig. 4-10. Composite section showing variation in Y/Ho molar ratios of carbonates along with depth.

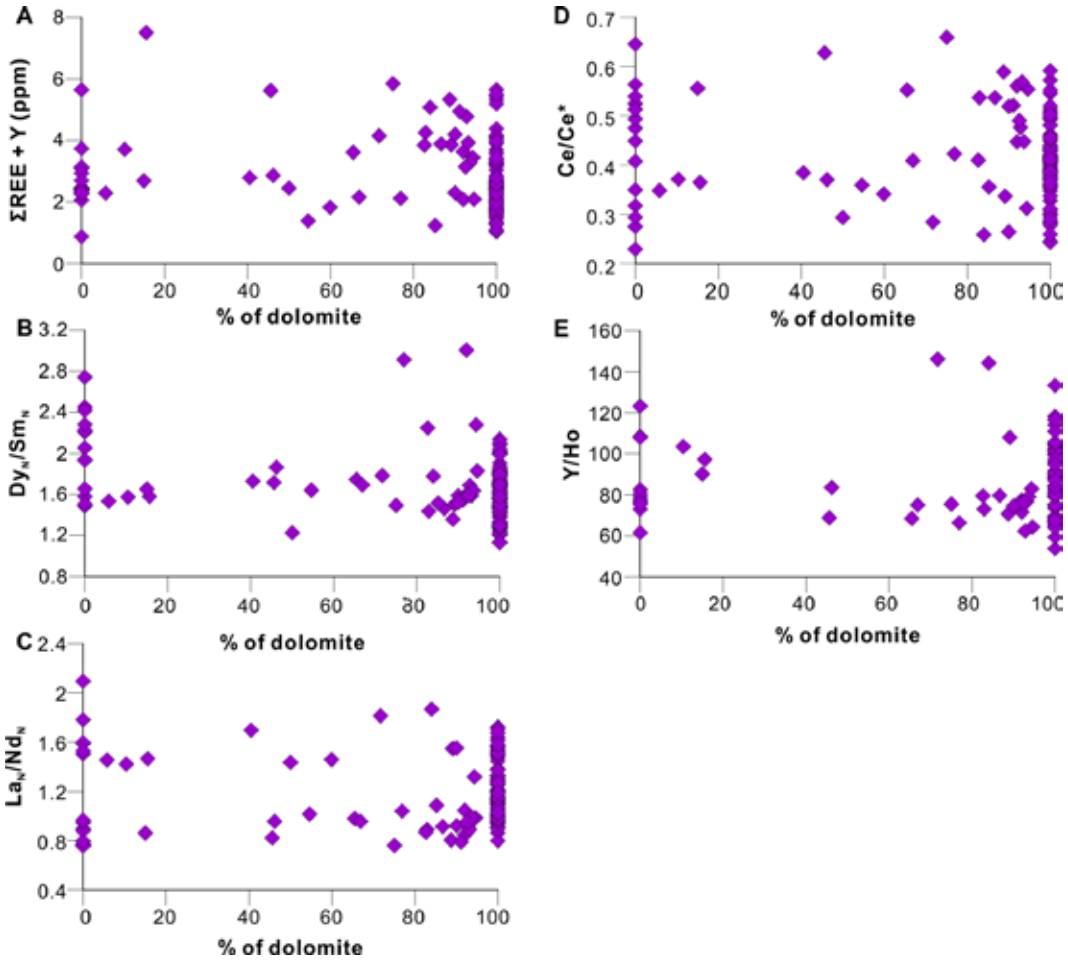

Fig. 4-11. Cross plots showing relationships between dolomite contents of samples and their REE+Y features: (A) ∑REE+Y, (B) Dy_N/Sm_N, (C) La_N/Nd_N, (D) Ce/Ce*, and (E) Y/Ho.

Sediments were deposited on an open bank in waters less than 30 m deep (Jones and Hunter, 1994a). The precise age for the onset of sedimentation is open to debate.

- Late Miocene (Messinian): development of the Cayman Unconformity during the Messinian lowstand, when sea level in this area was at least 40 m below present day sea level (Jones and Hunter, 1994b). Although the total relief of this unconformity is unknown on Cayman Brac, it is at least 40 m on Grand Cayman (Jones and Hunter, 1994b).

- Late Miocene: dolomitization of the Brac Formation and the basal part of the Cayman Formation during the Messinian lowstand or during the transgression that followed that lowstand (Jones and Luth, 2003; Zhao and Jones, 2012a, b).
- Early Pliocene: deposition of sediments, in water less than 30 m deep, that now form the Pedro Castle Formation during the Early Pliocene highstand that was at least 15 m above present day sea level (Jones et al., 1994b).
- Early Pliocene: during the Early Pliocene highstand, the middle and upper parts of the Cayman Formation and parts of the Pedro Castle Formation were dolomitized (MacNeil and Jones, 2003; Jones and Luth, 2003; Zhao and Jones, 2012b).
- Late Pliocene: tectonic tilting of Cayman Brac to the west took place after deposition of the Pedro Castle Formation but before deposition of the Ironshore Formation (Zhao and Jones, 2012b). Today, the Brac Unconformity on the east end of Cayman Brac is up to 30 m above sea level. In well LV#2 on Grand Cayman, the Brac Unconformity is ~120 m below sea level (Jones and Luth, 2003). This suggests that the eastern part of Cayman Brac has been uplifted by ~ 150 m. This figure is also consistent with the thickness of the carbonate succession that overlies the Brac Formation on Cayman Brac.
- Late Pliocene onwards: erosion of upper surface of Cayman Brac with removal of the Pedro Castle Formation from most of the island and development of rugged karst terrain on exposed surface of Cayman Formation (Fig. 4-2).
- Pleistocene: deposition of sediments, during the Sangamon highstand (6 m above present day sea level, ~125,000 years ago) around Cayman Brac that now form a low-lying platform around the island.

4.6.1. REE +Y concentrations in carbonates

Contamination in the form of terrigenous sediment and authigenic minerals (e.g., Fe- and Mn-oxides) can mask the REE+Y signatures of carbonates (e.g., Nothdurft et al., 2004). In the case of Cayman Brac, the possibility of terrigenous contamination of the carbonates is minimal because the island is geographically isolated by the deep oceanic waters that surround it. The only possible sources of terrigeneous contaminants would have been from airborne dust or terra rossa that accumulated on the karst surfaces during periods of exposure. The lack of correlation between ∑REE+Y and the low Fe (<300 ppm) and Mn (< 85 ppm) contents of the Cayman carbonates (Fig. 4-4), however, indicate that there is no contamination due to the presence of Fe- and Mn-hydroxides (cf., Bau et al., 1996).

The ∑REE+Y of samples from the Bluff Group on Cayman Brac (1.0 to 7.5 ppm) and the Ironshore Formation (0.2 to 5.6 ppm) are akin to those found in other Holocene and Pleistocene marine carbonates (Webb and Kamber, 2000; Webb et al., 2009). Factors that potentially influence the ∑REE+Y in carbonates include (1) mineralogy (calcite or aragonite) (Webb et al., 2009), (2) diagenesis (Miura et al., 2004; Azmy et al., 2011), and/or (3) variation in the ∑REE+Y of the seawater from which the carbonates formed (Bertram and Elderfield, 1993; Azmy et al., 2011). Webb et al. (2009) suggested that the ∑REE+Y of carbonates increases as aragonite changes to calcite because the distribution coefficient of REE+Y between calcite and the parent solution is higher than that between aragonite and its parent solutions (Terakado and Masuda, 1988). This is consistent with data from aragonitic corals from the Ironshore Formation (Pleistocene) of Grand Cayman that have a lower ∑REE+Y (average 0.5 ppm, n = 2) than the surrounding matrices that are formed largely of low-Mg calcite (average 2.4 ppm, n = 3) (Fig. 4-3). Samples from the Bluff Group that are

composed of low-Mg calcite and dolomite have a ∑REE+Y (average 2.8 ppm, n = 126), similar to the low-Mg calcite matrices in the limestones from the Ironshore Formation. Given that samples now formed of low-Mg calcite and dolomite were originally aragonitic, the relative higher ∑REE+Y of the carbonates from the Pedro Castle Formation, the Cayman Formation, and the Brac Formation was probably related to their diagenesis.

On Cayman Brac, the Pedro Castle Formation and the Brac Formation have been partly dolomitized, whereas the Cayman Formation has been completely dolomitized (MacNeil and Jones, 2003; Zhao and Jones, 2012a, b). The ∑REE+Y values of the carbonate samples do not, however, correlate with their dolomite contents (Fig. 4-11A). The ∑REE+Y of samples formed of 100% dolomite ranges from 1.0 to 5.6 ppm (average 2.6 ppm, n = 85), whereas those samples with various amount of calcite have a ∑REE+Y ranging from 1.2 to 7.5 ppm (average 3.4 ppm, n = 41). Banner et al. (1988) argued that the dolomitization process, if mediated by seawater-like fluids, would not modify the REE compositions of precursor limestones because the REE concentrations in seawater are very low compared to those in the limestones. Thus, the uniformity of the ∑REE+Y values in the Cayman samples, irrespective of the dolomite content, suggests that the fluid that mediated dolomitization did not significantly modify the REE concentrations in the carbonates. This is consistent with the notion that dolomitization was mediated by seawater.

The dolostones on Cayman Brac are characterized by fabric-retentive and the fabric-destructive textures (MacNeil and Jones, 2003; Zhao and Jones, 2012a, b) and many dolostones, like those in the Brac Formation, contain large amounts (up to 54%, by volume) of dolomite cement (Zhao and Jones, 2012a). There are, however, no significant differences in the ∑REE+Y values between the different types of dolostones (Fig. 4-12). This implies that the fabric retentive dolostones,

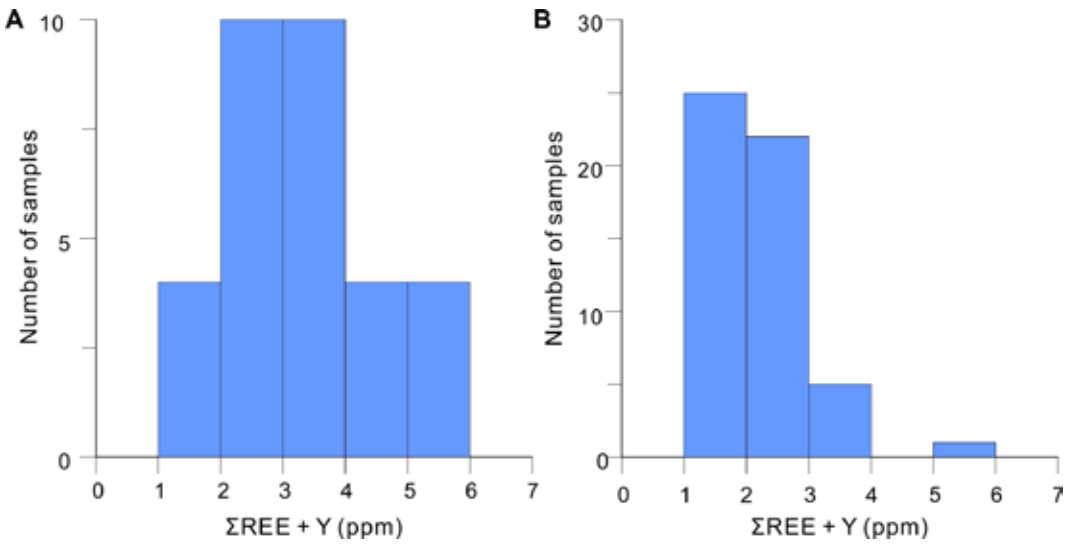

Fig. 4-12. Histograms showing ∑REE +Y of fabric-retentive dolostones (A) and fabric-destructive dolostones

the fabric-destructive dolostones, and the dolomite cements all originated from waters that had similar ∑REE+Y signatures. This suggestion agrees with the conclusion that Zhao and Jones (2012a) reached based on the stable isotope and Sr concentration data from the same rocks.

The carbonate succession on Cayman Brac ranges from Lower Oligocene to Pleistocene (Jones et al., 1994a, b). The fact that the ∑REE+Y values do not correlate with depth (Fig. 4-3) implies that the ∑REE+Y values are not age-related. Samples from the upper part of the Cayman Formation and the upper part of the Brac Formation, however, have the widest ranges of ∑REE+Y values (Fig. 4-3). Although the exact cause for this is not clear, such changes in the ∑REE+Y of these strata might be related to the unconformities that cap the formations. The low ∑REE+Y values associated with the sea water-like REE+Y patterns, however, point to a seawater origin of the REE+Y without significant interference from other REE+Y sources (e.g., Fe- and Mn-oxides). In addition, it appears that pervasive dolomitization did not increase the ∑REE+Y of the carbonates found on

Cayman Brac, which is contrary to the pattern found elsewhere (e.g., Miura et al., 2004; Azmy et al., 2011).

4.6.2. The REE+Y patterns

Irrespective of their age, petrography, and mineralogy, the carbonates on Cayman Brac are characterized by (1) light REE (LREE) depletion relative to HREE, (2) positive La anomalies, (3) negative Ce anomalies (Ce/Ce* <1), and (4) superchondritic Y/Ho molar ratios (> 53). These features are similar to the REE+Y patterns of other marine carbonates (e.g., Webb and Kamber, 2000; Tanaka et al., 2003; Miura et al., 2004; Nothdurft et al., 2004; Webb et al., 2009; Azmy et al., 2011) (Fig. 4-6) and modern seawater (Zhang and Nozaki, 1996; Alibo and Nozaki, 1999; Nozaki and Alibo, 2003). There are, however, subtle differences between the REE+Y patterns of the four formations on Cayman Brac in terms of their LREE depletion, La anomalies, Ce anomalies, and Y/Ho ratios.

4.6.2.1. LREE depletion

LREE depletion, which is a typical feature of the shale-normalized REE+Y patterns of seawater, is caused by the higher affinity of LREE to scavenging processes that are operative in seawater (cf., Byrne and Sholkovitz, 1996). On Cayman Brac, samples from the Cayman Formation and the Brac Formation are less depleted in LREE (average $Dy_N/Sm_N = 1.6$, n = 104) than those from the Ironshore Formation and the Pedro Castle Formation ($Dy_N/Sm_N = 2.1$, n = 10) (Fig. 4-6). A decrease in the LREE depletion of carbonates has been variously attributed to terrigenous contamination (e.g., Nothdurft et al., 2004; Webb et al., 2009), different depositional environments such as estuary versus open ocean (Kamber and Webb, 2001), and/or different diagenetic histories (Mazumdar et al., 2003). For Cayman Brac, variations in the LREE depletion patterns are probably related to differences in the diagenetic processes that affected each

formation. The Dy_N/Sm_N ratios, however, do not vary with the dolomite content of the samples (Fig. 4-11B), suggesting that dolomitization did not have a major influence on the LREE depletion. As indicated by the ∑REE+Y of the samples, the incorporation of REE+Y into carbonates was probably related to early stages of diagenesis, with the alteration of aragonite to calcite being particularly important. Mazumdar et al. (2003) suggested that an increase in alkalinity of the pore waters in the vadose and phreatic zones, which is related to the degradation of organic matter, promotes the uptake of HREE into the carbonate lattice (i.e., increasing the LREE depletion). For the Ironshore Formation and the Pedro Castle Formation, the alteration of aragonite and/or high-Mg calcite to low-Mg calcite (and/or dolomite) may have taken place in a mixed freshwater—seawater environment (MacNeil and Jones, 2003). The role that the meteoric water played in the early diagenesis of the Cayman Formation and the Brac Formation is not clear. Nevertheless, the lower LREE depletion in carbonates from the Cayman Formation and the Brac Formation might indicate less meteoric influence (i.e., more marine) during the alteration of the aragonite and high-Mg calcite in those formations.

4.6.2.2. LaN/NdN ratio

For the carbonate succession on Cayman Brac, the lack of correlation between the dolomite content of the samples and the La_N/Nd_N ratios indicates that dolomitization did not influence the La_N/Nd_N ratios (Fig. 4-11C). The La_N/Nd_N ratios of the samples do, however, increase with depth in the composite section and there is a significant increase in values across the Brac Unconformity (Fig. 4-7). The samples from the Brac Formation have the highest La_N/Nd_N ratios (average 1.5, n = 49), the samples from the Cayman Formation and the Pedro Castle Formation have intermediate La_N/Nd_N ratios (average 1.0, n = 71 and average 0.9, n = 4, respectively), whereas the samples from the Ironshore

formation have the lowest La_N/Nd_N ratios (average 0.8, n = 7) (Fig. 4-7).

This depth-dependent variation in the La_N/Nd_N ratios of carbonates from Cayman Brac must be related to changes in the REE+Y composition of seawater because the ambient seawater is the only source from which the carbonates can take up the REE+Y. This may be due to one of the following options or both.

- Change in the La_N/Nd_N ratios with water depth. In modern seawater, the La_N/Nd_N of seawater increases with depth (Zhang and Nozaki, 1996; Alibo and Nozaki, 1999). In the North Pacific Ocean and South Pacific Ocean the La_N/Nd_N ratios of seawater increases from 0.8 at the surface to 1.5 at a depth of ~ 1000 m.
- Possible secular change in the REE+Y composition of seawater (e.g., Azmy et al., 2011).

On Cayman Brac, the progressive increase in the La_N/Nd_N ratios with depth cannot be attributed to the variations in the original depositional environments because all of the carbonates were deposited in shallow marine environments that were probably less than 30 m deep (Jones and Hunter, 1994a). Thus, the changes in the La_N/Nd_N ratios with depth must be related to post-depositional diagenesis. The La_N/Nd_N ratios (0.8 to 1.2) of the samples from the Cayman Formation, the Pedro Castle Formation and the Ironshore Formation are compatible with those of modern seawater between 0 to 160 m. Miura et al. (2004) suggested that the REE features of carbonates (e.g., Ce/Ce*) may reflect the depth of the seawater in which the early diagenesis took place. There is, however, no evidence that deep-sourced or hydrothermal-altered seawater has ever covered the Cayman carbonates (Zhao and Jones, 2012a, 2012b). Furthermore, if the water depth was responsible for the increasing La_N/Nd_N ratios with depth, the La_N/Nd_N ratios of samples from the Brac Formation (average 1.5, n = 49) would indicate a water depth of 1000 m (Zhang and Nozaki, 1996; Alibo et al., 1999). There is, however,

no evidence to indicate that the Brac Formation was ever covered by seawater of this depth. Thus, the increase in the La_N/Nd_N ratios with depth (Fig. 4-7) may reflect secular change in the REE+Y composition of seawater through time. Unfortunately, little is known about the secular change in the REE+Y composition of seawater (e.g., Azmy et al., 2011).

4.6.2.3. Ce anomalies

Cerium, unlike other REE elements, is redox-sensitive. The oxidation of dissolved Ce3+ to particulate Ce4+ is the dominant process that leads to negative Ce anomalies in seawater (cf., Byrne and Sholkovitz, 1996). All samples of the Cayman carbonates yielded negative Ce anomalies (Ce/Ce* < 1) (Fig. 4-9). The lack of correlation between the dolomite content and the Ce anomalies indicates that dolomitization did not influence the Ce anomalies of the Cayman carbonates (Fig. 4-11C). The Ce/Ce* ratios of carbonates from the Cayman carbonate are compatible with the modern surface seawater (Fig. 4-8), which is interpreted to be indicative of an oxygenated environment in which they formed. The Ce/Ce* ratios of Cayman carbonates do, however, increase with depth (Fig. 4-9). Samples from the Brac Formation have the lowest Ce/Ce* (average 0.3, n = 49), whereas samples from the Cayman Formation and the Pedro Castle Formation have intermediate Ce/Ce* values (average 0.44, n = 72 and average 0.50, n = 4, respectively). The samples from the Ironshore Formation have the highest Ce/Ce* (average 0.54, n = 7). The Ce/Ce*, however, correlates with the LaN/NdN ratios (r2 = 0.64, n = 131) (Fig. 4-13). Hence, the depth-dependent trend found in the Ce/Ce* ratios of the Cayman carbonates is interpreted to reflect the influence of La anomalies on the calculation of Ce anomalies (cf., Bau and Dulski, 1997).

4.6.3.4. Y/Ho ratios

The Y/Ho ratios of samples from Cayman Brac do not show a depth-

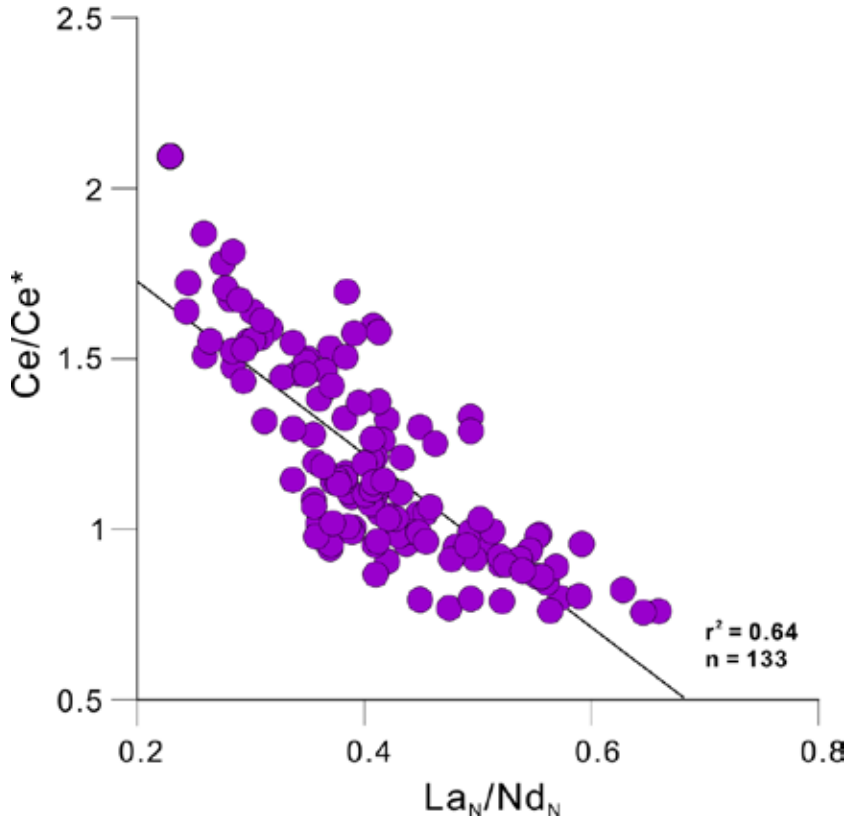

Fig. 4-13. Cross plot showing the correlation between Ce/Ce* and La_N/Nd_N.

dependent trend like the La_N/Nd_N ratios and Ce/Ce* (Fig. 4-10). Although all samples have superchondritic Y/Ho ratios (> 53) that are compatible with a seawater origin (Bau and Dulski, 1997), they vary from formation to formation (Fig. 4-10). The fact that there is no correlation between the dolomite content and the Y/Ho ratios indicates that dolomitization did not impact the Y/Ho ratios of carbonates (Fig. 4-11E). The Y and Ho contents of samples from the Cayman Formation, the Pedro Castle Formation, and the Ironshore Formation are strongly correlated ($r^2 = 0.86$) whereas those of samples from the Brac Formation show a lower degree of correlation ($r^2 = 0.50$) (Fig. 4-14). The high correlation between the Y and Ho contents of samples from the Cayman Formation, the Pedro Castle Formation and the Ironshore Formation indicates that the solutions in which those carbonates were stabilized were similar in terms of their Y/Ho ratios, whereas the

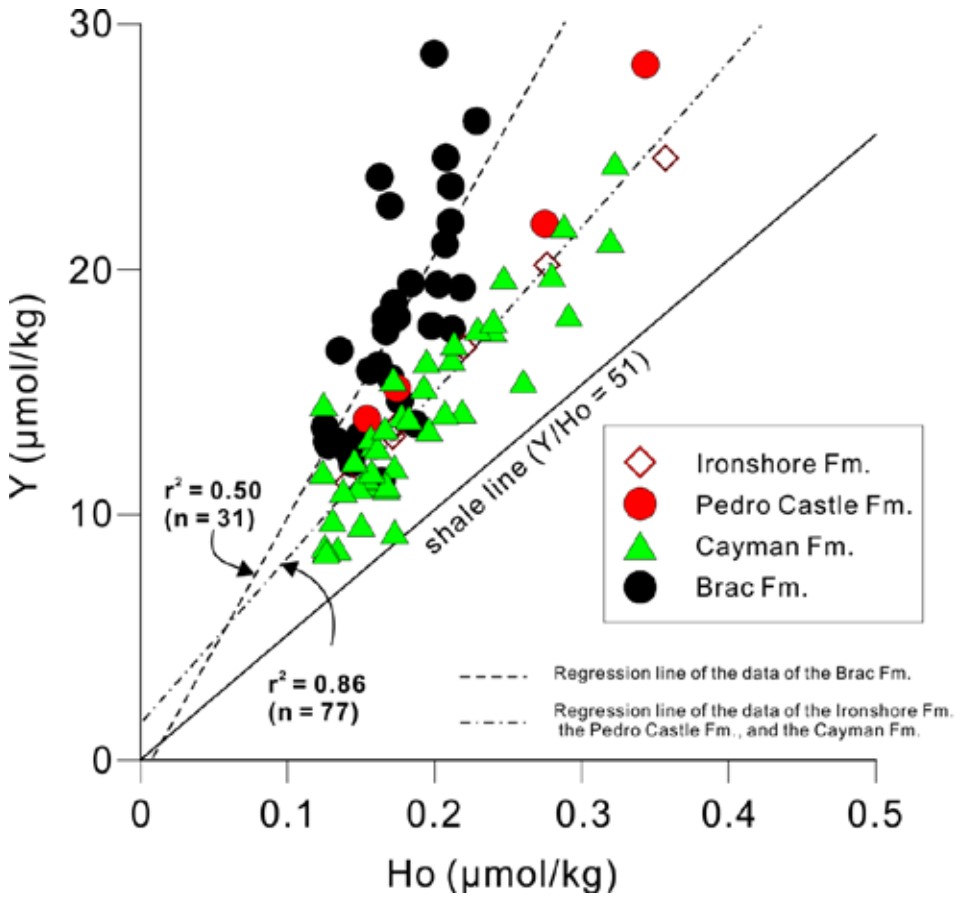

Fig. 4-14. Cross plot showing the relationships between Y and Ho contents of carbonates

higher Y/Ho ratios and the low correlation between Y and Ho contents of samples from the Brac Formation are interpreted to reflect variations in the Y/Ho ratios of seawater. Nozaki et al. (1997) suggested that Y and Ho have short residence times in the ocean (~5100 years for Y and 2700 years for Ho) and that the fractionation between the two elements is controlled largely by scavenging processes related to the Y and Ho complexation on organic and inorganic particles. The Y/Ho ratios of seawater are sensitive to continental contributions and local oceanographic conditions (Mazumdar et al., 2003). The Y/Ho ratios of modern seawater, for example, vary from ocean to ocean (Zhang and Nozaki, 1996; Alibo and Nozaki, 1999; Nozaki and Alibo, 2003). Thus, the variations in the Y/Ho ratios across the

Brac Unconformity probably indicate a long-term change in the Y/Ho ratios of seawater.

4.7. Discussion

4.7.1. Implications for dolomitization of the Cayman carbonates

The influence that dolomitization has on the REE+Y signatures of dolostones is poorly known. Based on Lower Cretaceous dolostones found in Central Tunisia, Tlig and M'Rabet (1985) argued that the shape of REE distribution patterns in dolostones can be preserved even though the REE concentrations may decrease relative to those in the precursor limestones. Supported by the fact that the REE contents of the Tunisian dolostones correlated with their Sr content and $\delta^{18}O$ values, they suggested that this change was related to the low salinity of the dolomitizing fluids. In contrast, Banner et al. (1988) argued that the REE signatures of dolostones in the Mississippian Burlington-Keokuk Formation were inherited from the precursor limestone. This was deemed possible because the REE content of the dolomitizing fluids (seawater) are very low (several ppb) compared to those of limestones (several to tens of ppm). Under this scenario, the REE patterns could only be changed if diagenesis involved a large fluid/rock ratio ($>10^4$). Subsequent research on the REE features of dolostones confirmed the arguments of Banner et al. (1988) that dolomitization does not affect the REE compositions of precursor limestones if dolomitization is mediated by seawater-like fluids (e.g., Devonian dolostones, Canada (Qing and Mountjoy, 1994); Permian dolostones, Japan (Miura et al., 2004); and Paleoproterozoic dolostones, South Africa (Bau and Alexander, 2006)). The REE+Y compositions of limestones can, however, be affected if the dolomitizing fluids are not seawater (e.g., Qing and Mountjoy, 1994; Nothdurft et al., 2004). Nothdurft et al. (2004) reported that the Y/Ho ratios and the LREE depletion of Late Devonian reefal

carbonates in the Canning Basin (Western Australia) decreased as the dolomite content increased. They attributed the changes in the REE patterns during dolomitization to the reducing nature of the dolomitizing fluids that emanated from deeper parts of the basin. Likewise, Qing and Mountjoy (1994) showed that the medium and coarse crystalline dolostones in the Middle Devonian Presqu'ile barrier (Pine Point, Canada) have different REE patterns from the coexisting finely crystalline dolostones that yield typical seawater-like REE patterns. The different REE patterns of the medium and coarsely crystalline dolostones were attributed to different dolomitizing fluids that originated from the deep basin.

Limestones found on Cayman Brac have been dolomitized to different degrees (MacNeil and Jones, 2003; Zhao and Jones, 2012a, b). The textures of the dolostones vary from coarsely crystalline fabric-destructive (Brac Formation) to finely crystalline fabric-retentive (Cayman Formation and Pedro Castle Formation – MacNeil and Jones, 2003; Zhao and Jones, 2012a, b). Based on the geographic and stratigraphic settings, the petrography, their carbon and oxygen stable isotopes, and their trace element characteristics (Sr, Fe, and Mn), Zhao and Jones (2012a, b) argued that the dolomitization of the Cayman Formation and the Brac Formation was mediated by seawater or slightly modified seawater. For the dolostones found in the Pedro Castle Formation, MacNeil and Jones (2003) argued that the dolomitization might have been mediated by slightly diluted seawater. Based on Sr contents and Sr isotope data, however, Machel (2000) argued that dolomitization responsible for the formation of Tertiary dolostones throughout the Caribbean Sea was driven by plate tectonics.

The lack of correlation between the dolomite content of the rocks and the ∑REE+Y and the characteristics of the shale-normalized REE+Y patterns (e.g., La_N/Nd_N, Ce/Ce* and Y/Ho) indicate that the dolomitization did not modify the REE+Y composition of the precursor limestones on Cayman Brac (Fig.

4-11). This suggestion is supported by the fact that no correlations between the diagenesis-sensitive proxies (e.g., $\delta^{18}O$) and the REE+Y compositions of carbonates from Cayman Brac have been found (Fig. 4-15). Hence, our REE+Y data are consistent with the notion of Banner et al. (1988) that dolomitization mediated by seawater does not change the REE+Y composition of the precursor

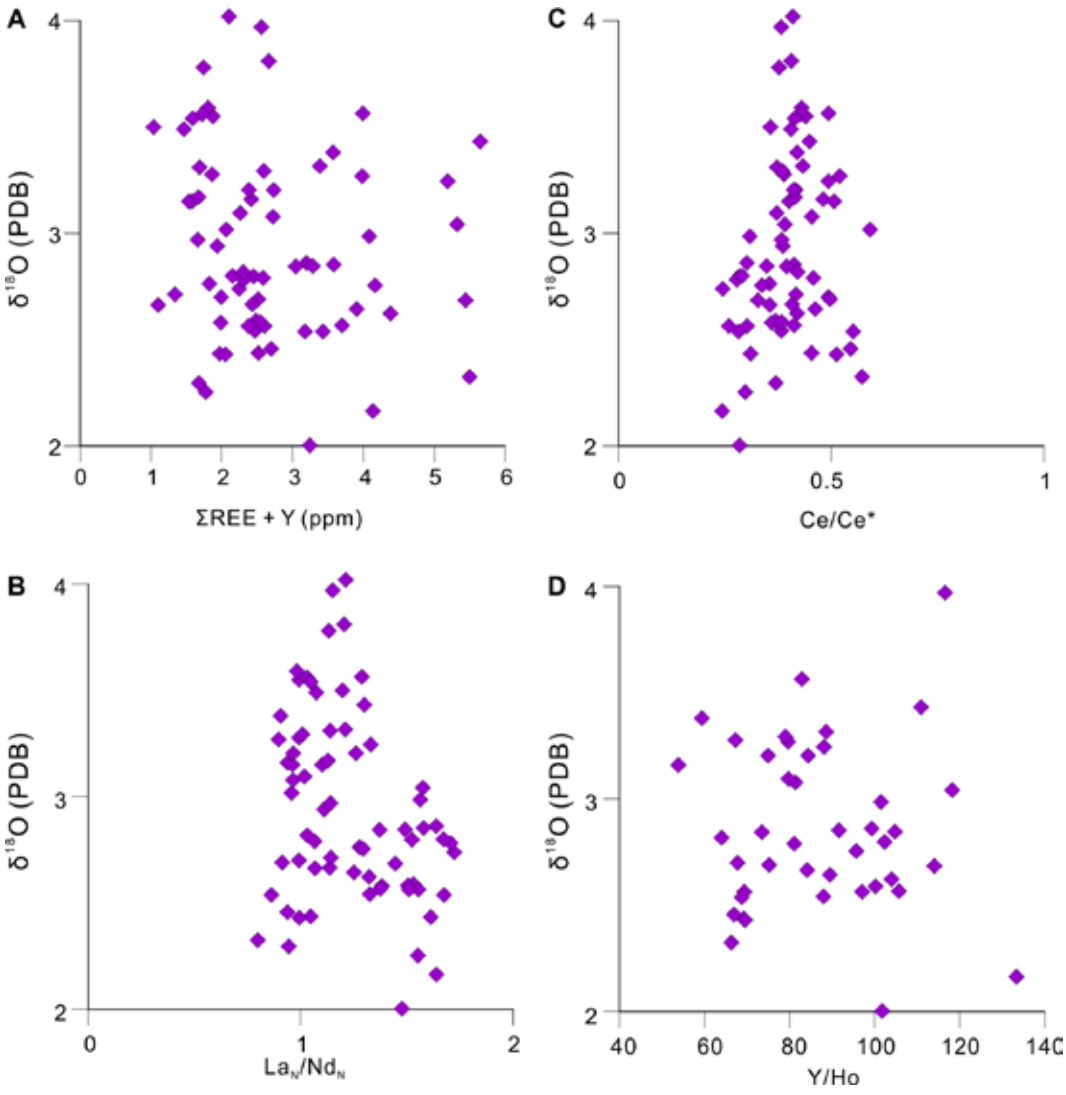

Fig. 4-15. Cross plots showing the relationships between $\delta^{18}O$ of dolostone samples and their REE+Y features: (A) ∑REE+Y, (B) La_N/Nd_N , (C) Ce/Ce*, and (D) Y/Ho.

limestones. There are no indications from the REE data that dolomitization was mediated by hydrothermal-modified seawaters that were related to plate tectonic activity.

4.7.2 Significance of REE+Y features of carbonates and their implications

Ancient limestones and dolostones have commonly been used as proxies for establishing the REE+Y compositions of ancient seawater in which the carbonates formed (e.g., Kawabe et al., 1991; Kamber and Webb, 2001; Mazumdar et al., 2003; Tanaka et al., 2003; Miura et al., 2004; Nothdurft et al., 2004; Bau and Alexander, 2006; Tanaka and Kawabe, 2006; Azmy et al., 2011). They showed that ancient carbonates, irrespective of their age, have REE+Y distribution patterns akin to those found in modern seawaters. By comparing various ancient carbonates and phosphates with modern seawater, Shields and Webb (2004) argued that the REE distribute patterns of seawater has remained the same throughout the Phanerozoic. The REE+Y data from carbonates on Cayman Brac show that the Oligocene to Pleistocene carbonates share features in common with modern seawater (e.g., LREE depletion, positive La anomalies, negative Ce anomalies, superchondritic Y/Ho ratios) (Fig. 4-5), which indicates that the carbonates on Cayman Brac share the REE+Y features of seawater. The composite profiles of La_N/Nd_N and Y/Ho ratios, however, show that there are variations through the succession (Figs. 4-7, 10). Hence, these variations must reflect the subtle changes in the REE+Y composition of seawater in which these carbonates formed.

It has been suggested that the REE+Y composition of carbonates may reflect the water depth under which the early stage of diagenesis took place (Tanaka et al., 2003; Miura et al., 2004). Tanaka et al. (2003) and Miura et al. (2004), for example, tried to estimate water depths for Mesozoic Limestone from the Southern Chichibu Terrain in Japan and Permian limestones and dolostones from

Kuzuu, Japan by comparing their Ce/Ce* ratios with modern seawater. Given that the REE+Y compositions of carbonates are only vulnerable to alteration during the early stage of diagenesis (Webb and Kamber, 2000; Miura et al., 2004; Webb et al., 2009), the REE+Y composition of carbonates must reflect the REE+Y features of the seawater that mediated the early stages of diagenesis (e.g., alteration of aragonite to calcite). In the case of Cayman Brac, however, there is no evidence to indicate that the early stages of diagenesis took place in deep water. Hence, the depth-trend of the La_N/Nd_N ratios in the carbonate succession of Cayman Brac probably reflects a secular change in the REE+Y compositions of seawater. Given that the limestones and dolostones on Cayman Brac have experienced numerous episodes of diagenesis that have included vadose and phreatic diagenesis that was related to the unconformities found throughout the succession (MacNeil and Jones, 2003), and dolomitization (MacNeil and Jones, 2003; Zhao and Jones 2012a, b), the well-preserved REE+Y trends in these carbonates indicate that the behaviours of REE+Y were conservative after mineral stabilization.

The exact causes for the remarkable contrasts in the La_N/Nd_N ratios and Y/Ho ratios across the Brac Unconformity (Figs. 4-7, 10) are unclear. This unconformity, which separates the Brac Formation (Low Oligocene) from the overlying Cayman Formation (Middle Miocene), represents a long period of non-deposition and erosion that lasted throughout the Upper Oligocene and probably into the Lower Miocene (Jones et al., 1994a, b). Thus, the contrasts in various REE+Y elements across this unconformity might be attributed to the secular changes in the REE+Y compositions of seawater during this time period. The secular change in the REE+Y composition of seawater, however, is poorly known. Many factors including the continental charges, the redox condition, and physiochemical conditions may influence the REE+Y composition

of seawater (cf., Byrne and Sholkovitiz, 1996) that is fundamentally controlled by plate tectonics, sea level, and seawater circulation conditions (cf., Byren and Sholkovitiz, 1996; Nozaki et al., 1997). Wang et al. (1993) reported negative Ce/Ce* excursions that were coincident with the Ordovician—Silurian boundary in the Selwyn Basin, northwestern Canada. They attributed this to changes in the circulation and redox conditions. Oceanographic conditions in Caribbean Sea during the transition from Oligocene to Miocene are poorly understood. In order to detect the possible secular changes in the REE+Y composition of seawater, two elements, Sm and Nd, which are only two atomic numbers apart in the REE series, can be used to compare their mass fractionation between samples from the Cayman Formation and the Brac Formation. Given their similar mass, no significant mass fractionation should be expected (Elderfield, 1988). The samarium/neodymium (Sm/Nd) ratios of modern seawater do not systematically change with depth and vary from ocean to ocean (e.g., Atlantic Ocean –0.203 ± 0.009; Indian Ocean –0.196 ± 0.013; Pacific Ocean –0.181 ± 0.024; Bertram and Elderfield, 1993). There is a high correlation between these two elements in samples from the Cayman Formation ($r^2 = 0.97$) and the Brac Formation ($r^2 = 0.92$) (Fig. 4-16). The Sm/Nd ratios of the carbonates from the Brac Formation (average 0.201, n = 45), however, are lower than those from the overlying Cayman Formation (average 0.246, n = 67) (Fig. 4-16). This comparison suggests that variation in the Sm/Nd ratios of the carbonates from the Brac Formation and the Cayman Formation are probably related to secular change in the REE+Y composition of seawater between the Oligocene and Miocene. In contrast, there are no abrupt changes in the La_N/Nd_N, and Y/Ho ratios across the Cayman Unconformity. This comparison suggests that there was no significant change in the REE+Y composition of seawater between the Miocene and Pliocene. Collectively, the REE+Y features of carbonates found on Cayman

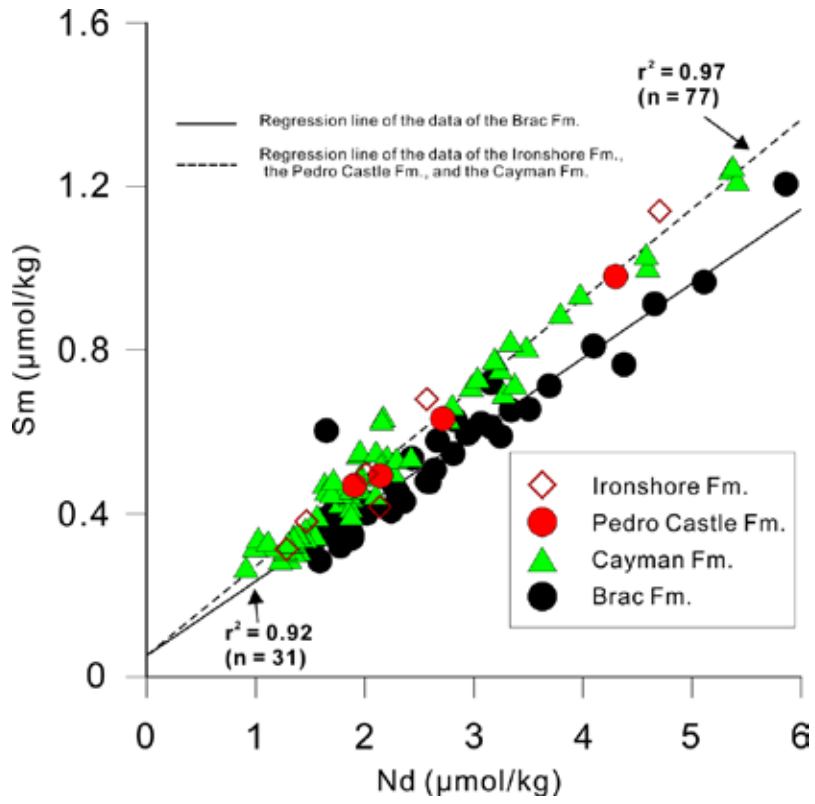

Fig. 4-16. Cross plots Cross plot showing the relationships between Sm and Nd contents of carbonates

Brac indicate that the subtle features of REE+Y patterns of seawater do change through time although the general shale-normalized patterns remain unchanged. More importantly, these changes can be recorded by the carbonates formed in them. Hence, the REE+Y may be a useful tool to decipher the evolution of oceanography and delineate the carbonate stratigraphy.

4.8. Conclusions

The REE+Y signatures of carbonates in the Cenozoic succession can be evaluated in terms of the geological evolution of Cayman Brac. Evaluation of the REE+Y data has led to the following important conclusions.

- Despite their complex diagenetic history, the limestones and dolostones on

Cayman Brac inherited seawater-like REE+Y patterns.

- The fact that the REE+Y signatures were not affected by dolomitization is consistent with the notion that seawater mediated that dolomitization.
- The variations in the La_N/Nd_N, Y/Ho, and Sm/Nd may be indicative of secular change in the REE+Y composition of seawater since the Early Oligocene.

The results of this study show that the REE+Y signatures can be used to support interpretations of dolomitization by seawater and that REE+Y patterns may contain important information about the evolution of the REE+Y signatures of seawater through time. Further work, however, is needed to determine if these conclusions are universally applicable.

4.9. References

Alibo, D.S., Nozaki, Y., 1999. Rare earth elements in seawater: particle association, shale-normalization, and Ce oxidation. Geochimica et Cosmochimica Acta 63, 363-372.

Azmy, K., Brand, U., Sylvester, P., Gleeson, S.A., Logan, A., Bitner, M.A., 2011. Biogenic and abiogenic low-Mg calcite (bLMC and aLMC): Evaluation of seawater-REE composition, water masses and carbonate diagenesis. Chemical Geology 280, 180-190.

Banner, J.L., Hanson, G., Meyers, W., 1988. Rare earth element and Nd isotopic variations in regionally extensive dolomites from the Burlington-Keokuk Formation (Mississippian); implications for REE mobility during carbonate diagenesis. Journal of Sedimentary Research 58, 415-432.

Bau, M., Koschinsky, A., Dulski, P., Hein, J.R., 1996. Comparison of the partitioning behaviours of yttrium, rare earth elements, and titanium between hydrogenetic marine ferromanganese crusts and seawater. Geochimica et Cosmochimica Acta 60, 1709-1725.

Bau, M., Möller, P., Dulski, P., 1997. Yttrium and lanthanides in eastern Mediterranean seawater and their fractionation during redox-cycling. Marine Chemistry 56, 123-131.

Bau, M., Alexander, B., 2006. Preservation of primary REE patterns without Ce anomaly during dolomitization of Mid-Paleoproterozoic limestone and the potential re-establishment of marine anoxia immediately after the"Great Oxidation Event". South African Journal of Geology 109, 81-86.

Bertram, C.J., Elderfield, H., 1993. The geochemical balance of the rare earth elements and neodymium isotopes in the oceans. Geochimica et Cosmochimica Acta 57, 1957-1986.

Budd, D.A., 1997. Cenozoic dolomites of carbonate islands: their attributes and

origin. Earth-Science Reviews 42, 1-47.

Byrne, R., Sholkovitz, E., 1996. Marine chemistry and geochemistry of the lanthanides, Handbook on the Physics and Chemistry of Rare Earths, Elsevier, Amsterdam, volume 23, pp. 497-593.

Coyne, M., Jones, B., 2007. Highstands during Marine Isotope Stage 5: evidence from the Ironshore Formation of Grand Cayman, British West Indies. Quaternary Science Reviews 26, 536-559.

DeMets, C., Wiggins-Grandison, M., 2007. Deformation of Jamaica and motion of the Gonâve microplate from GPS and seismic data. Geophysical Journal International 168, 362-378.

Elderfield, H., 1988. The Oceanic Chemistry of the Rare-Earth Elements [and Discussion]. Philosophical Transactions of the Royal Society of London. Series A, Mathematical and Physical Sciences 325, 105-126.

German, C.R., Elderfield, H., 1990. Rare earth elements in the NW Indian Ocean. Geochimica et Cosmochimica Acta 54, 1929-1940.

German, C.R., Masuzawa, T., Greaves, M.J., Elderfield, H., Edmond, J.M., 1995. Dissolved rare earth elements in the Southern Ocean: Cerium oxidation and the influence of hydrography. Geochimica et Cosmochimica Acta 59, 1551-1558.

Haley, B.A., Klinkhammer, G.P., Mix, A.C., 2005. Revisiting the rare earth elements in foraminiferal tests. Earth and Planetary Science Letters 239, 79-97.

Himmler, T., Bach, W., Bohrmann, G., Peckmann, J., 2010. Rare earth elements in authigenic methane-seep carbonates as tracers for fluid composition during early diagenesis. Chemical Geology 277, 126-136.

Holser, W.T., 1997. Evaluation of the application of rare-earth elements to paleoceanography. Palaeogeography, Palaeoclimatology, Palaeoecology

132, 309-323.

Jones, B., 1994. Geology of the Cayman Islands. In: Brunt, M.A., Davies, J.E. (Eds.), The Cayman Islands: Natural history and biogeography. Kluwer, Dordrecht, The Netherlands, pp. 13–49.

Jones, B., 2004. Petrography and significance of zoned dolomite cements from the Cayman Formation (Miocene) of Cayman Brac, British West Indies. Journal of Sedimentary Research 74, 95-109.

Jones, B., 2005. Dolomite crystal architecture: genetic implications for the origin of the Tertiary dolostones of the Cayman Islands. Journal of Sedimentary Research 75, 177-189.

Jones, B., Hunter, I.G., 1994a. Evolution of an isolated carbonate bank during Oligocene, Miocene and Pliocene times, Cayman Brac, British West Indies. Facies 30, 25-50.

Jones, B., Hunter, I.G., 1994b, Messinian (Late Miocene) karst on Grand Cayman, British West Indies: an example of an erosional sequence boundary. Journal of Sedimentary Research 64, 531-541.

Jones, B., Hunter, I.G., Kyser, K., 1994a. Stratigraphy of the Bluff Formation (Miocene-Pliocene) and the newly defined Brac Formation (Oligocene), Cayman Brac, British West Indies. Caribbean Journal of Science 30, 30-51.

Jones, B., Hunter, I.G., Kyser, K., 1994b. Revised stratigraphic nomenclature for Tertiary strata of the Cayman Islands, British West Indies. Caribbean Journal of Science 30, 53-68.

Jones, B., Luth, R.W., 2003. Temporal evolution of Tertiary dolostones on Grand Cayman as determined by $^{87}Sr/^{86}Sr$. Journal of Sedimentary Research 73, 187-205.

Kamber, B.S., Webb, G.E., 2001. The geochemistry of late Archaean microbial

carbonate: implications for ocean chemistry and continental erosion history. Geochimica et Cosmochimica Acta 65, 2509-2525.

Kawabe, I., Kitahara, Y., Naito, K., 1991. Non-chondritic yttrium/holmium ratio and lanthanide tetrad effect observed in pre-Cenozoic limestones. Geochemical Journal 25, l-44.

Leroy, S., Mauffret, A., Patriat, P., Mercier de Lépinay, B., 2000. An alternative interpretation of the Cayman trough evolution from a reidentification of magnetic anomalies. Geophysical Journal International 141, 539-557.

MacDonald, K.C., Holcombe, T.L., 1978. Inversion of magnetic anomalies and sea-floor spreading in the Cayman Trough. Earth and Planetary Science Letters 40, 407-414.

Machel, H.G., 2000. Dolomite formation in Caribbean Islands: Driven by plate tectonics?! Journal of Sedimentary Research 70, 977-984.

MacNeil, A., Jones, B., 2003. Dolomitization of the Pedro Castle Formation (Pliocene), Cayman Brac, British West Indies. Sedimentary Geology 162, 219-238.

Mann, P., Calais, E., Ruegg, J., DeMets, C., Jansma, P. E., Mattioli, G. S., 2002. Oblique collision in the northeastern Caribbean from GPS measurements and geological observations. Tectonics 21, 1057, 26 pp.

Matley, C.A., 1926. The geology of the Cayman Islands (British West Indies), and their relation to the Bartlett Trough. Quarterly Journal of the Geological Society 82, 352-387.

Mazumdar, A., Tanaka, K., Takahashi, T., Kawabe, I., 2003. Characteristics of rare earth element abundances in shallow marine continental platform carbonates of Late Neoproterozoic successions from India. Geochemical Journal 37, 277-290.

McLennan, S., 1989. Rare earth elements in sedimentary rocks; influence of

provenance and sedimentary processes. Reviews in Mineralogy and Geochemistry 21, 169-200.

Miura, N., Asahara, Y., Kawabe, I., 2004. Rare earth element and Sr isotopic study of the Middle Permian limestone-dolostone sequence in Kuzuu area, central Japan: Seawater tetrad effect and Sr isotopic signatures of seamount-type carbonate rocks. The Journal of Earth Planet Science of Nagoya University 51, 11-35.

Nothdurft, L.D., Webb, G.E., Kamber, B.S., 2004. Rare earth element geochemistry of Late Devonian reefal carbonates, Canning Basin, Western Australia: confirmation of a seawater REE proxy in ancient limestones. Geochimica et Cosmochimica Acta 68, 263-283.

Nozaki, Y., Zhang, J., Amakawa, H., 1997. The fractionation between Y and Ho in the marine environment. Earth and Planetary Science Letters 148, 329-340.

Nozaki, Y., Alibo, D.S., 2003. Dissolved rare earth elements in the Southern Ocean, southwest of Australia: Unique patterns compared to the South Atlantic data. Geochemical Journal 37, 47-62.

Perfit, M.R., Heezen, B.C., 1978. The geology and evolution of the Cayman Trench. Geological Society of America Bulletin 89, 1155-1174.

Piepgras, D.J., Jacobsen, S.B., 1992. The behavior of rare earth elements in seawater: Precise determination of variations in the North Pacific water column. Geochimica et Cosmochimica Acta 56, 1851-1862.

Qing, H., Mountjoy, E.W., 1994. Rare earth element geochemistry of dolomites in the Middle Devonian Presqu'ile barrier, Western Canada Sedimentary Basin: implications for fluid/rock ratios during dolomitization. Sedimentology 41, 787-804.

Rosencrantz, E., Sclater, J.G., 1986. Depth and age in the Cayman Trough. Earth

and Planetary Science Letters 79, 133-144.

Shields, G., Stille, P., 2001. Diagenetic constraints on the use of cerium anomalies as palaeoseawater redox proxies: an isotopic and REE study of Cambrian phosphorites. Chemical Geology 175, 29-48.

Shields, G.A., Webb, G.E., 2004. Has the REE composition of seawater changed over geological time? Chemical Geology 204, 103-107.

Sholkovitz, E.R., Landing, W.M., Lewis, B.L., 1994. Ocean particle chemistry: The fractionation of rare earth elements between suspended particles and seawater. Geochimica et Cosmochimica Acta 58, 1567-1579.

Stoddart, D.R., 1980. Geology and geomorphology of Little Cayman. Atoll Research Bulletin 241, 11-16.

Suzuki, Y., Iryu, Y., Inagaki, S., Yamada, T., Aizawa, S., Budd, D.A., 2006. Origin of atoll dolomites distinguished by geochemistry and crystal chemistry: Kita-daito-jima, northern Phillippine Sea. Sedimentary Geology 183, 181-202.

Tanaka, K., Miura, N., Asahara, Y., Kawabe, I., 2003. Rare earth element and strontium isotopic study of seamount-type limestones in Mesozoic accretionary complex of Southern Chichibu Terrane, central Japan: Implication for incorporation process of seawater REE into limestones. Geochemical Journal 37, 163-180.

Tanaka, K., Kawabe, I., 2006. REE abundances in ancient seawater inferred from marine limestone and experimental REE partition coefficients between calcite and aqueous solution. Geochemical Journal 40, 425-435.

Terakado, Y., Masuda, A., 1988. The coprecipitation of rare-earth elements with calcite and aragonite. Chemical Geology 69, 103-110.

Tlig, S., M'Rabet, A., 1985. A comparative study of the Rare Earth Element (REE) distributions within the Lower Cretaceous dolomites and limestones

of Central Tunisia. Sedimentology 32, 897-907.

Vahrenkamp, V.C, Swart, P.K., 1994. Late Cenozoic dolomites of the Bahamas: metastable analogues for the genesis of ancient platform carbonates. In: Pruser, B., Tucker, M., Zenger, D. (eds.), Dolomites, International Association of Sedimentologists Special Publication 21, p. 133-153.

Wang, K., Chatterton, B.D.E., Attrep Jr, M., Orth, C.J., 1993. Late Ordovician mass extinction in the Selwyn Basin, northwestern Canada: geochemical, sedimentological, and paleontological evidence. Canadian Journal of Earth Sciences 30, 1870-1880.

Warren, J., 2000. Dolomite: occurrence, evolution and economically important associations. Earth-Science Reviews 52, 1-81.

Webb, G.E., Kamber, B.S., 2000. Rare earth elements in Holocene reefal microbialites: a new shallow seawater proxy. Geochimica et Cosmochimica Acta 64, 1557-1565.

Webb, G.E., Nothdurft, L.D., Kamber, B.S., Kloprogge, J.T., Jian-Xin, Z., 2009. Rare earth element geochemistry of scleractinian coral skeleton during meteoric diagenesis: a sequence through neomorphism of aragonite to calcite. Sedimentology 56, 1433-1463.

Zhang, J., Nozaki, Y., 1996. Rare earth elements and yttrium in seawater: ICP-MS determinations in the East Caroline, Coral Sea, and South Fiji basins of the western South Pacific Ocean. Geochimica et Cosmochimica Acta 60, 4631-4644.

Zhang, J., Nozaki, Y., 1998. Behavior of rare earth elements in seawater at the ocean margin: a study along the slopes of the Sagami and Nankai troughs near Japan. Geochimica et Cosmochimica Acta 62, 1307-1317.

Zhao, H., Jones, B., 2012a. Genesis of fabric-destructive dolostones: A case study of the Brac Formation (Oligocene), Cayman Brac, British West Indies.

Sedimentary Geology 267–268, 36-54.

Zhao, H., Jones, B., 2012b. Origin of “island dolostones”: A case study from the Cayman Formation (Miocene), Cayman Brac, British West Indies. Sedimentary Geology 243-244, 191-206.

CHAPTER 5
CONCLUSIONS

5.1 General conclusions

Detailed and carefully analyses of the dolostones found in the Bluff Group on Cayman Brac have produced the following important conclusions:

(1) The distribution of dolomite is variable on Cayman Brac. The Brac Formation is formed of coarsely crystalline dolostones and limestones whereas the Cayman Formation is formed mostly of finely crystalline dolostones.

(2) The dolostones in the Brac Formation are characterized by fabric-destructive textures whereas the dolostones in the Cayman Formation are characterized largely by fabric-retentive textures.

(3) The coarsely crystalline dolostones in the Brac Formation are formed mostly of anhedral to euhedral dolomite crystals (up to 1.5 mm long) that are characterized by dull red to bluish grey cathodoluminescence. In contrast, the finely crystalline dolostones of the Cayman Formation are formed of anhedral to subhedral dolomite crystals that are typically < 20 μm long. These dolostones are characterized by two types of cathodoluminescence: Type I, relative homogeneous moderately-bright to bright red-orange and Type II, dull red to nonluminescence with some bright luminescent pseudomorphically-replaced allochems.

(4) Dolostones found on Cayman Brac are formed mainly of Ca-rich dolomite. The dolostones in the Brac Formation are formed largely of HCD with an average of 55.0 to 57.5%Ca. The dolostones of the Cayman Formation, with average values of 50.5 to 57.7%Ca, typically contain more LCD than HCD. The distribution of the LCD and HCD

varies from section to section with no obvious patterns. The %Ca of the dolomite may be related to the Mg/Ca ratio of the dolomitizing fluids.

(5) The $\delta^{13}C$ of dolostones from the Brac Formation range from 1.5 to 2.9‰ (average 2.3%, n = 41) whereas the $\delta^{13}C$ of dolostones from the Cayman Formation range from 1.6 to 3.5‰ (average 2.5‰, n = 63). These $\delta^{13}C$ values are considered indicative of a marine source of carbon.

(6) The $\delta^{18}O$ of dolostones from the Brac Formation and the Cayman Formation range from 2.0 to 3.6 (average 2.3‰, n = 41) and 2.3 to 4.0‰ (average 3.2‰, n = 63), respectively. The correlation between the $\delta^{18}O$ values and the average %Ca of the dolostones probably reflects the influence that dolomite stoichiometry and kinetic effects have on the $\delta^{18}O$ values of dolostones rather than fluctuations in the composition of the dolomitizing fluids.

(7) The Sr content of dolostones from the Brac Formation and the Cayman Formation ranges from 150 to 275 ppm (average 206 ppm, n = 39) and 80 to 279 ppm (average 140 ppm, n = 54), respectively. The Sr content of the dolostones correlates with their average %Ca and $\delta^{18}O$ values. This correlation is attributed to the influences of dolomite stoichiometry and kinetic effects.

(8) The Fe and Mn contents of dolostones from the Brac Formation range from 81 to 263 ppm (average 141, n = 37) and 2 to 77 ppm (average 17, n = 37), respectively. The Fe and Mn contents of dolostones from the Cayman Formation range from 52 to 340 ppm (average 128 ppm, n = 54) and 9 to 82 ppm (average 28 ppm, n = 54), respectively. The Fe and Mn contents of dolostones from both formations were probably inherited from the precursor limestones. These low Fe and Mn values probably indicate oxidizing dolomitizing fluids.

(9) Integration of all available data indicates that the dolomitizing fluids were probably normal or slightly modified seawater.

(10) Interpretation of the Sr isotopic data indicates a two-episode dolomitization model (6-8 Ma and 1-5 Ma) that may have been related to eustatic changes in sea level. The first episode of dolomitization was responsible for the dolomitization of the Brac Formation and the basal part of the Cayman Formation. The second episode of dolomitization was responsible for the dolomitization of the middle and upper part of the Cayman Formation.

(11) The distribution of the dolomite in the limestones and the evolution of dolostone textures were controlled largely by permeability pathways that governed the circulation patterns of the dolomitizing fluids. The large sucrosic dolomite crystals found on the Brac Formation probably developed as a result of repeated cycles of limestone matrix dissolution and dolomite precipitation.

(12) Dolomitization did not have a significant impact on the REE+Y concentrations in the carbonates on Cayman Brac. This is consistent with the notion that the dolomitizing fluids were seawater or slightly modified seawater.

(13) On Cayman Brac, the REE +Y of the carbonates in the Ironshore Formation, Pedro Castle Formation, and Cayman Formation (e.g. La_N/Nd_N, Ce/Ce*) gradually change with depth and there are marked differences in La_N/Nd_N, Y/Ho and Sm/Nd just below and above the Brac Unconformity. These features may reflect secular changes in the REE+Y composition of seawater.

5.2 Final remarks

The Tertiary dolostones found on Cayman Brac are, in terms of their petrography and geochemistry, compatible with "island dolostones" found on many other islands throughout the Caribbean Sea and the Pacific Ocean. The dolomitization events, based largely on the $^{87}Sr/^{86}Sr$ ratios of the dolostones, are synchronous with many other island dolostones (cf. Budd, 1997). This synchronicity implies that dolomitization was probably related to global as opposed to local factor(s). Dolomitization is thought to be a kinetic process that operates with a high water/rock ratio. The fact that data from Cayman Brac indicate that seawater or slightly modified seawater mediated dolomitization implies that a prolonged period of stable sea level was probably needed so that a stable hydrological circulation of seawater could develop and provide time available for the dolomitization (Sibley, 1991). The results of this study suggest that the two episodes of dolomitization responsible for the formation of the Cayman dolostones were probably related to times when sea-level rose. Although difficult to prove with certainty, it therefore appears that eustatic sea-level change may be responsible for the synchronous "dolomitization events" (e.g., Sibley, 1991; Sun, 1994).

The variation in the REE +Y concentrations of the Tertiary and Pleistocene carbonates from Cayman Brac indicate that secular changes in the REE +Y signatures of ambient seawater may be preserved in island dolostones. However, the factor(s) responsible for the secular changes in the REE composition of seawater is unknown. It might be related to the tectonic events, which affected the terrestrial inputs of REE and the oceanographic conditions (e.g., Sirgudsson et al., 1997). It is also possible, however, that external REE inputs (e.g., aerial dust) may also have contributed to the abrupt changes in the REE patterns of carbonates associated with unconformities (cf. Muhs et al., 2007). Therefore, the change in

the REE+Y patterns of island carbonates may contain important information about the tectonic evolution through time.

5.3 Reference

Budd, D.A., 1997. Cenozoic dolomites of carbonate islands: their attributes and origin. Earth-Science Reviews 42, 1-47.

Muhs, D.R., Budahn, J.R., Prospero, J.M., Carey, S.N., 2007, Geochemical evidence for African dust inputs to soils of western Atlantic islands: Barbados, the Bahamas, and Florida, Journal of geophysical Research 112, F02009.

Sibley, D.F., 1991. Secular changes in the amount and texture of dolomite. Geology 19, 151-154.

Sigurdsson, H., Leckie, R.M., Acton, G.D., 1997. Proceedings of the Ocean Drilling Program, Initial Reports 165: College Station, TX (Ocean Drilling Program)

Sun, S.Q., 1994. A reappraisal of dolomite abundance and occurrence in the Phanerozoic. Journal of Sedimentary Research A64, 364-404.

APPENDICES

Appendix 1. Summary of geochemical data obtained from dolostones of the Cayman Formation on Cayman Brac[a]																
Well	Depth (m)	%Ca of LCD	% LCD	%Ca of HCD	% HCD	Average %Ca	$^{87}Sr/^{86}Sr$ ratio	$^{87}Sr/^{86}Sr$ 2 sigma	Crystal length (μm)			$\delta^{13}C$ (‰ PDB)	$\delta^{18}O$ (‰ PDB)	Sr (ppm)	Mn (ppm)	Fe (ppm)
									Min.	Mean	Max.					
CRQ#1	12.2	51.9	100.0			51.9			8.6	13.1	16.4					
CRQ#1	11.3	52.2	100.0			52.2										
CRQ#1	10.4	51.9	100.0			51.9	0.709064	0.000018	6.8	10.5	14.1	1.98	3.16	93.0	24.0	52.4
CRQ#1	9.4	51.6	100.0			51.6										
CRQ#1	7.6	52.1	100.0			52.1										
CRQ#1	6.7	52.8	100.0			52.8	0.709075	0.000018	9.1	19.2	33.6	2.41	3.15	116.4	19.6	78.7
CRQ#1	5.8	52.0	100.0			52.0										
CRQ#1	4.9	52.3	100.0			52.3			13.6	18.7	25.9	2.65	3.16			
CRQ#1	4.0	52.4	100.0			52.4										
CRQ#1	3.0	52.5	100.0			52.5	0.709084	0.000017	12.7	19.4	35.5	2.74	3.23			
CRQ#1	2.6	51.8	89.9	57.0	10.1	52.3	0.709070	0.000011				1.98	3.38	96.4	10.3	76.0
CRQ#1	1.7	51.5	93.4	56.9	6.6	51.9										
CRQ#1	0.8	51.6	92.3	57.2	7.7	52.0			4.0	7.1	12.0	2.85	3.64			
CRQ#1	-0.2	51.6	95.7	57.3	4.3	51.8						2.15	3.35			
CRQ#1	-1.1	52.1	95.0	58.3	5.0	52.4	0.709045	0.000017						88.5	11.2	78.9
CRQ#1	-2.0	52.1	100.0			52.1			2.8	4.8	7.8	2.19	3.48			
CRQ#1	-2.9	51.8	100.0			51.8										
CRQ#1	-3.8	51.7	88.1	56.5	11.9	52.2						2.40	3.60			
CRQ#1	-4.7	51.9	90.6	56.6	9.4	52.3	0.709065	0.000018	5.3	10.5	19.1			102.4	16.7	87.7
CRQ#1	-5.6	52.2	100.0			52.2						2.98	3.44			
CRQ#1	-6.6	52.4	77.5	57.2	22.5	53.4										
CRQ#1	-7.5	51.7	73.2	56.5	26.8	53.0						2.30	3.66			
CRQ#1	-8.4	52.5	72.2	56.1	27.8	53.5	0.709065	0.000018						137.0	27.2	97.2
CRQ#1	-9.3	53.4	83.5	58.5	16.5	54.2						2.80	3.00			

Appendix 1. Summary of geochemical data obtained from dolostones of the Cayman Formation on Cayman Brac[a] (continued)

Well	Depth (m)	%Ca of LCD	% LCD	%Ca of HCD	% HCD	Average %Ca	$^{87}Sr/^{86}Sr$ ratio	$^{87}Sr/^{86}Sr$ 2 sigma	Crystal length (μm)			$\delta^{13}C$ (‰ PDB)	$\delta^{18}O$ (‰ PDB)	Sr (ppm)	Mn (ppm)	Fe (ppm)
									Min.	Mean	Max.					
CRQ#1	-10.2	52.2	84.0	57.2	16.0	53.0			7.4	13.1	23.5					
CRQ#1	-11.1	51.8	80.4	56.1	19.6	52.6						2.83	3.35			
CRQ#1	-12.0	51.8	80.4	57.0	19.6	52.9	0.709053	0.000017				2.83	2.94	140.1	19.3	86.0
CRQ#1	-13.0	52.5	86.1	55.9	13.9	53.0			11.4	15.4	22.7	3.02	3.18			
CRQ#1	-13.9	52.4	66.6	57.2	33.4	54.0										
CRQ#1	-14.8	52.8	68.6	57.6	31.4	54.3						2.60	2.85			
CRQ#1	-15.7	52.1	80.5	57.2	19.6	53.1	0.709050	0.000018	10.3	16.4	27.9	2.50	2.97	146.5	64.9	106.6
CRQ#1	-16.6	52.2	75.8	56.8	24.2	53.3										
CRQ#1	-17.5	52.4	100.0			52.4						2.90	3.34			
CRQ#1	-18.4	51.5	100.0			51.5			6.8	11.0	18.2					
CRQ#1	-19.4	51.4	100.0			51.4	0.709055	0.000018				2.97	3.50	90.6	42.8	108.6
CRQ#1	-20.3	51.1	93.5	56.1	6.5	51.4										
CRQ#1	-21.2	51.7	100.0			51.7			5.0	10.6	19.1			99.4	37.0	116.3
CRQ#1	-22.1	51.6	89.0	55.1	11.0	51.9										
CRQ#1	-23.0	51.9	100.0			51.9	0.709096	0.000018						103.5	32.8	102.5
CRQ#1	-23.9	51.7	100.0			51.7			6.8	14.0	25.0					
CRQ#1	-24.8	51.6	100.0			51.6						3.10	3.79			
CRQ#1	-25.8	51.4	93.5	56.3	6.5	51.8										
CRQ#1	-26.7	51.6	100.0			51.6	0.709056	0.000013	8.8	19.1	27.9	2.93	4.02	89.3	50.5	101.4
CRQ#1	-27.6	51.5	100.0			51.5										
CRQ#1	-28.5	51.6	100.0			51.6						3.33	3.37			
CRQ#1	-29.4	51.5	100.0			51.5			11.4	20.4	40.9					
CRQ#1	-30.3	50.5	100.0			50.5	0.709078	0.000017				2.08	3.81	90.2	54.0	92.3
CRQ#1	-31.2	51.4	100.0			51.4										
CRQ#1	-32.2	51.5	100.0			51.5			9.1	22.8	45.5	1.88	3.86			

Appendix 1. Summary of geochemical data obtained from dolostones of the Cayman Formation on Cayman Brac[a] (continued)

Well	Depth (m)	%Ca of LCD	% LCD	%Ca of HCD	% HCD	Average %Ca	$^{87}Sr/^{86}Sr$ ratio	$^{87}Sr/^{86}Sr$ 2 sigma	Crystal length (μm)			$\delta^{13}C$ (‰ PDB)	$\delta^{18}O$ (‰ PDB)	Sr (ppm)	Mn (ppm)	Fe (ppm)
									Min.	Mean	Max.					
CRQ#1	-33.1	51.5	100.0			51.5										
CRQ#1	-34.0	51.3	100.0			51.3	0.709075	0.00002				1.93	3.97	84.2	55.5	84.3
CRQ#1	-34.9	51.6	100.0			51.6			13.6	25.2	40.9					
CRQ#1	-35.8	51.9	100.0			51.9						2.42	3.93			
CRQ#1	-36.7	51.5	65.2	55.3	34.8	52.8										
CRQ#1	-37.6	51.9	59.2	56.6	40.8	53.8	0.709049	0.000017	11.4	15.7	20.5			146.9	21.0	89.6
CRQ#1	-38.6	51.4	77.5	56.6	22.5	52.6										
CRQ#1	-39.5	52.8	64.7	57.7	35.3	54.5						2.51	3.31	162.9	11.8	79.0
CRQ#1	-40.4	51.3	87.4	56.1	12.6	51.9										
CRQ#1	-41.1	51.9	100.0			51.9	0.709076	0.00002				2.24	3.83	85.0	41.6	105.8
CRQ#1	-43.1	51.9	59.7	56.9	40.3	53.9										
CRQ#1	-43.8	51.4	87.4	56.7	12.6	52.1	0.709058	0.000017	12.9	22.7	29.4			80.4	15.9	109.2
CRQ#1	-44.6	52.0	71.9	57.4	28.1	53.5										
CRQ#1	-45.3	52.8	42.5	56.7	57.5	55.1	0.709040	0.000013	20.4	29.4	58.8			180.6	9.9	116.3
CRQ#1	-46.1	53.5	26.3	56.9	73.7	56.0										
BW#1	-15.4			57.8	100.0	57.8			6.8	14.2	27.3					
BW#1	-16.2	54.0	60.1	59.0	39.9	56.0	0.709081	0.000014				1.65	2.71			
BW#1	-16.9	53.9	58.6	59.3	41.4	56.1										
BW#1	-17.7	53.0	63.3	58.8	36.7	55.2	0.709062	0.000010	10.9	21.3	40.9	1.85	2.70	216.9	13.5	118.3
BW#1	-18.4	53.5	48.7	59.0	51.3	56.3										
BW#1	-19.2	54.8	65.9	60.1	34.1	56.6	0.709057	0.000013	6.8	12.6	22.7	2.32	2.69	216.3	16.2	136.5
BW#1	-20.7	52.0	82.1	56.6	17.9	52.8	0.709064	0.000016	9.1	16.7	29.6	2.25	3.34			
BW#1	-21.5	51.7	76.2	57.0	23.8	53.0	0.709061	0.000013						133.6	20.4	144.3
BW#1	-23.8	51.5	70.7	56.4	29.3	52.9	0.709068	0.000016	6.8	12.8	21.4	1.98	3.55	121.5	17.2	147.2
BW#1	-24.5	51.5	79.3	56.5	20.7	52.6										

Appendix 1. Summary of geochemical data obtained from dolostones of the Cayman Formation on Cayman Brac[a] (continued)

Well	Depth (m)	%Ca of LCD	% LCD	%Ca of HCD	% HCD	Average %Ca	$^{87}Sr/^{86}Sr$ ratio	$^{87}Sr/^{86}Sr$ 2 sigma	Crystal length (μm)			$\delta^{13}C$ (‰ PDB)	$\delta^{18}O$ (‰ PDB)	Sr (ppm)	Mn (ppm)	Fe (ppm)
									Min.	Mean	Max.					
BW#1	-25.3	51.8	72.4	54.8	27.6	52.6	0.709061	0.000013	6.4	17.6	36.4	2.24	3.59	108.7	18.1	103.1
BW#1	-26.1	52.0	79.1	57.1	21.0	53.1										
BW#1	-26.8	51.9	76.7	57.0	23.3	53.1	0.709073	0.000014	8.6	15.4	28.2	2.00	3.56	120.4	21.2	130.3
BW#1	-27.6	51.2	74.5	56.5	25.5	52.6										
BW#1	-28.4	51.7	85.0	57.5	15.0	52.6	0.709049	0.000009	6.8	14.3	29.6	1.99	3.54	107.4	20.8	136.3
BW#1	-29.1	51.2	80.6	56.5	19.4	52.2										
BW#1	-30.6	51.5	73.5	56.8	26.6	52.9										
BW#1	-31.4	51.2	74.0	56.2	26.0	52.5	0.709113	0.000013	8.2	17.5	33.2	2.08	3.78	122.8	23.3	133.2
BW#1	-32.9	51.3	67.7	56.4	32.3	53.0	0.709063	0.000017	6.8	17.7	32.7	3.06	2.91			
BW#1	-37.5	51.9	20.4	57.2	79.6	56.1	0.709132	0.000010				1.62	2.79			
BW#1	-39.0	51.7	74.2	56.5	25.8	53.0	0.709090	0.000013	8.2	18.6	31.8	1.96	3.49	162.5	18.1	121.5
BW#1	-40.5	52.1	79.0	57.0	21.0	53.1	0.709071	0.000013	5.9	12.6	19.6					
BW#1	-41.3	52.0	79.5	57.0	20.5	53.0										
BW#1	-42.1	51.9	87.1	56.3	12.9	52.4	0.709115	0.000011	7.3	16.0	29.6	2.00	3.15	143.2	18.6	115.9
BW#1	-42.8	51.5	73.4	56.0	26.6	52.7	0.709043	0.000011								
BW#1	-43.6	51.8	76.3	56.7	23.7	52.9	0.709093	0.000013	8.2	14.6	29.1	2.00	3.17	173.1	20.3	150.7
SQW#1	3.0	54.2	66.4	59.4	33.6	55.9			6.8	12.8	27.3	2.869	2.28	279.4	47.2	340.5
SQW#1	2.1	52.8	82.3	59.2	17.7	53.9			7.7	18.7	30.5					
SQW#1	0.3	51.1	76.3	56.0	23.7	52.3			5.9	12.5	20.0			138.1	19.9	104.7
SQW#1	-0.2	54.0	66.8	59.1	33.2	55.7			5.9	11.1	25.0	2.610	2.44	190.6	23.4	71.9
SQW#1	-1.1	52.4	66.0	57.0	34.0	53.9										
SQW#1	-2.0	52.1	61.2	57.4	38.8	54.2										
SQW#1	-6.6	52.1	83.6	57.3	16.4	53.0										
SQW#1	-7.5	52.3	74.0	56.8	26.0	53.5										
SQW#1	-9.3	53.9	61.4	59.1	38.6	55.9										
SQW#1	-10.2	53.3	73.1	58.7	26.9	54.8										

Appendix 1. Summary of geochemical data obtained from dolostones of the Cayman Formation on Cayman Brac[a] (continued)

Well	Depth (m)	%Ca of LCD	% LCD	%Ca of HCD	% HCD	Average %Ca	$^{87}Sr/^{86}Sr$ ratio	$^{87}Sr/^{86}Sr$ 2 sigma	Crystal length (μm)			$\delta^{13}C$ (‰ PDB)	$\delta^{18}O$ (‰ PDB)	Sr (ppm)	Mn (ppm)	Fe (ppm)
									Min.	Mean	Max.					
SQW#1	-11.1	53.2	63.2	59.3	36.8	55.4			2.5	5.2	13.0	1.894	2.46	208.6	19.6	150.6
SQW#1	-12.0	53.9	60.7	59.2	39.3	56.0										
SQW#1	-13.0	53.2	68.8	59.1	31.2	55.0										
SQW#1	-13.9	53.5	64.2	59.3	35.8	55.5			14.3	25.1	38.6	2.247	2.43	205.5	20.7	112.9
SQW#1	-15.7	54.2	76.4	59.4	23.6	55.5			10.9	18.2	31.8	2.440	2.54	194.0	19.0	140.9
SQW#1	-18.4	52.7	68.8	58.4	31.2	54.4			6.8	12.9	22.7	2.139	2.33	209.2	25.4	241.4
SQW#1	-19.4	53.0	71.7	59.4	28.3	54.8										
SQW#1	-22.3	52.4	60.2	57.0	39.8	54.2										
SQW#1	-23.9	51.6	64.8	57.2	35.2	53.6										
SQW#1	-27.6	53.4	66.8	58.8	33.2	55.2										
SQW#1	-36.6	51.3	65.3	55.8	34.7	52.9										
SQW#1	-37.6	51.6	70.6	55.8	29.4	52.8			5.9	15.0	30.0	2.549	3.27	138.6	21.4	151.6
KEL#1	8.4	52.2	34.6	58.0	65.4	56.0			8.2	18.4	32.4	2.642	2.30	204.4	27.0	100.8
KEL#1	9.1	51.9	91.3	57.9	8.7	52.4										
KEL#1	9.9	51.9	73.0	56.5	27.1	53.1			16.5	25.5	41.2			128.7	8.9	99.3
KEL#1	10.7	52.5	59.8	58.6	40.2	54.9										
KEL#1	12.2	52.0	78.5	56.1	21.5	52.9										
KEL#1	13.0	52.0	65.7	55.1	34.3	53.0			3.6	7.7	20.4	2.778	2.85			
KEL#1	13.7	52.8	52.5	58.6	47.5	55.5										
KEL#1	14.5	52.0	70.9	57.1	29.1	53.5			6.5	12.1	23.9	2.8	3.02	128.7	25.8	190.8
KEL#1	16.8	53.5	70.9	59.5	29.1	55.3										
KEL#1	17.5	51.9	70.4	56.8	29.6	53.3			6.7	14.3	43.1	2.146	2.79	121.4	38.9	113.4
KEL#1	18.3	52.1	90.0	57.9	10.0	52.7										
KEL#1	21.3	53.9	68.6	59.4	31.4	55.6										
KEL#1	22.1	54.8	100.0			54.8			6.5	15.4	28.2	2.745	2.67	154.1	27.9	127.0
KEL#1	22.9	52.9	15.7	57.5	84.4	56.8										

Appendix 1. Summary of geochemical data obtained from dolostones of the Cayman Formation on Cayman Brac[a] (continued)

Well	Depth (m)	%Ca of LCD	% LCD	%Ca of HCD	% HCD	Average %Ca	$^{87}Sr/^{86}Sr$ ratio	$^{87}Sr/^{86}Sr$ 2 sigma	Crystal length (μm)			$\delta^{13}C$ (‰ PDB)	$\delta^{18}O$ (‰ PDB)	Sr (ppm)	Mn (ppm)	Fe (ppm)
									Min.	Mean	Max.					
KEL#1	23.6	52.6	69.5	58.0	30.5	54.2			3.5	6.6	13.9	2.27	2.71	146.2	32.1	133.6
KEL#1	25.9	52.4	69.7	55.9	30.3	53.4										
KEL#1	29.0	52.0	75.6	56.5	24.4	53.1										
KEL#1	29.7	52.5	71.4	57.2	28.6	53.9			3.1	12.1	25.0	2.685	2.49			
KEL#1	0.4	54.4	79.9	58.8	20.1	55.3			9.4	21.5	35.3					
KEL#1	-1.9	53.1	66.7	58.3	33.3	54.9										
KEL#1	-2.7	53.2	75.3	59.1	24.8	54.7	0.708982	0.000016	11.3	26.8	48.9	2.596	2.66	147.9	45.4	136.0
KEL#1	-3.4	52.6	62.3	57.8	37.8	54.5										
KEL#1	-4.2	52.5	67.0	58.1	33.0	54.4			8.8	17.0	32.4					
KEL#1	-5.7	53.1	66.1	58.0	33.9	54.7	0.709060	0.000017	16.4	33.3	67.3	2.699	2.82	143.3	82.5	144.0
KEL#1	-6.5	52.8	66.4	57.7	33.7	54.5										
KEL#1	-7.2	52.6	70.1	56.5	29.9	53.8			10.0	20.4	47.1					
KEL#1	-8.0	51.7	80.5	57.1	19.5	52.8										
KEL#1	-8.8	52.6	82.9	58.1	17.1	53.5			15.5	30.0	53.6					
KEL#1	-9.5	52.4	76.8	57.8	23.2	53.6	0.709023	0.000014						124.4	30.9	160.1
KEL#1	-10.3	52.3	74.8	57.2	25.2	53.6			18.2	36.1	90.9					
KEL#1	-11.1	51.8	72.7	55.9	27.3	52.9										
KEL#1	-11.8	51.1	65.5	55.4	34.5	52.6			13.6	32.2	55.5					
KEL#1	-12.6	50.8	77.4	55.8	22.8	52.1	0.709058	0.000017				3.476	3.28	109.3	20.7	237.7
KEL#1	-13.3	51.7	64.1	55.9	35.9	53.2			15.5	32.5	54.6					
KEL#1	-14.1	51.4	71.2	56.6	28.8	52.9										
KEL#1	-14.9	51.9	76.8	56.9	23.2	53.0	0.709074	0.000016	10.9	24.8	59.1	3.321	3.20	124.4	22.5	122.9
KEL#1	-15.6	51.9	60.1	56.0	40.0	53.5										
KEL#1	-16.4	51.4	64.4	55.7	35.6	52.9			11.8	29.7	54.6					
KEL#1	-17.1	51.6	60.3	55.9	39.7	53.3										
KEL#1	-17.9	51.6	63.6	55.9	36.4	53.2	0.709053	0.00001	18.2	37.7	63.6	3.489	3.29	114.1	27.8	136.4

Appendix 1. Summary of geochemical data obtained from dolostones of the Cayman Formation on Cayman Braca (continued)

Well	Depth (m)	%Ca of LCD	% LCD	%Ca of HCD	% HCD	Average %Ca	$^{87}Sr/^{86}Sr$ ratio	$^{87}Sr/^{86}Sr$ 2 sigma	Crystal length (μm)			$\delta^{13}C$ (‰ PDB)	$\delta^{18}O$ (‰ PDB)	Sr (ppm)	Mn (ppm)	Fe (ppm)
									Min.	Mean	Max.					
KEL#1	-18.7	51.9	57.9	56.4	42.1	53.8										
KEL#1	-19.4	52.4	58.1	58.0	41.9	54.7			5.0	11.0	23.5					
KEL#1	-20.2	52.4	51.5	57.8	48.6	55.0										
KEL#1	-21.0	52.0	59.7	57.7	40.4	54.4			6.5	15.6	34.8					
KEL#1	-21.7	51.3	50.3	56.7	49.7	54.0	0.708986	0.000014				3.048	3.08	164.1	31.0	185.3
KEL#1	-22.5	52.7	41.3	58.3	58.7	56.0			11.8	25.4	61.8					
KEL#1	-23.2	51.4	23.4	56.9	76.7	55.6										
KEL#1	-24.0	52.9	50.8	58.0	49.2	55.4	0.709044	0.000017	15.5	30.1	54.6			147.3	32.9	129.3
KEL#1	-24.8	52.3	50.7	57.4	49.3	54.8										
KEL#1	-25.5	52.3	58.2	57.4	41.9	54.4			9.4	25.8	50.4					
KEL#1	-26.3	53.0	49.5	57.9	50.5	55.4										
KEL#1	-27.1	53.6	70.1	58.0	30.0	55.0	0.709027	0.000013	16.4	35.3	64.6	2.807	3.10	150.7	26.5	138.7
KEL#1	-27.8			55.8	100.0	55.8										
KEL#1	-28.6	52.5	42.5	56.8	57.5	55.0	0.709029	0.000018	3.1	9.3	21.2			138.0	47.5	253.2

[a] Crystal lengths are based on the measurement of 50 crystals from each sample. Depth is relative to sea level. See Methods section for explanations of derivation of each parameter.

Appendix 2. Summary of geochemical data obtained from dolostones and limestones from the Brac Formation on Cayman Brac											
Section	Depth (m)[a]	%Ca of LCD	% LCD	%Ca of HCD	%HCD	Average %Ca	$\delta^{13}C$ (‰ PDB)	$\delta^{18}O$ (‰ PDB)	Sr (ppm)	Mn (ppm)	Fe (ppm)
Dolostone											
SCD	-19.4	-	-	56.3	100	56.3	2.7	2.6	227	14.2	134.5
SCD	-18.5	-	-	55.6	100	55.6	2.9	2.5	177.7	11	125.7
SCD	-16.9	54.9	31.1	57.1	68.9	56.4	2.6	2.7	174	6.5	169.2
SCD	-15.4	-	-	57.2	100	57.2	2	2.3	202.1	29.5	109.7
SCD	-13.9	-	-	56.8	100	56.8	2.7	2.6	252.2	11.3	104.4
SCD	-12.4	-	-	56.5	100	56.5	2.3	2.8	209.5	12.4	100.9
SCD	-11.2	-	-	56.7	100	56.7	1.9	2.3	186	14.8	159.4
SCD	-7.8	-	-	56.8	100	56.8	2.1	2	175.6	12.6	198.9
SCD	-6.3	-	-	56.7	100	56.7	2.2	2.5	-	-	-
SCD	-4.8	-	-	57.1	100	57.1	2.3	2.5	-	-	-
WOJ#7	-27	-	-	56.6	100	56.6	2.4	2.7	195.3	2.5	81
WOJ#7	-26.1	-	-	56.4	100	56.4	2.2	2.8	223.6	7.7	118.6
WOJ#7	-23.6	-	-	56.3	100	56.3	2.6	2.8	-	-	-
WOJ#7	-22.7	-	-	56.6	100	56.6	2.9	2.8	221.7	4	97.6
WOJ#7	-21.8	-	-	56.4	100	56.4	2.8	2.9	207	11.6	94.6
WOJ#7	-20.9	-	-	56.8	100	56.8	2.5	2.6	213.7	13.7	158.1
WOJ#7	-20	-	-	57	100	57	2.2	3	211.7	6.6	99.5
WOJ#7	-19.1	-	-	56.4	100	56.4	2.7	2.8	211.1	7.3	103.9
WOJ#7	-18.2	-	-	56.6	100	56.6	2.6	2.2	274.9	22.7	106.1
WOJ#7	-17.2	-	-	56.7	100	56.7	2	2.6	209.3	62.1	132.2
WOJ#7	-16.3	-	-	56.2	100	56.2	2.5	2.5	269	12.2	125.3
WOJ#3	-14	-	-	57.1	100	57.1	2.9	2.6	264.6	13.1	103.9
WOJ#3	-9.4	-	-	57.2	100	57.2	2.9	2.4	225.9	37.8	99.8
WOJ#3	-9.1	-	-	56.2	100	56.2	1.5	2.8	228.9	6.6	101.8
WOJ#3	-7.9	-	-	56.5	100	56.5	2.1	2.8	229.2	15.1	105.7

Appendix 2. Summary of geochemical data obtained from dolostones and limestones from the Brac Formation on Cayman Brac (continued)											
Section	Depth (m)[a]	%Ca of LCD	% LCD	%Ca of HCD	%HCD	Average %Ca	$\delta^{13}C$ (‰ PDB)	$\delta^{18}O$ (‰ PDB)	Sr (ppm)	Mn (ppm)	Fe (ppm)
Dolostone											
WOJ#3	-4.9	-	-	55	100	55	1.6	2.6	233.3	15.4	113.3
WOJ#3	-0.5	50.6	6.6	57.2	93.4	56.7	2.6	2.6	208	21.1	198.2
CRQ#1	-0.3	53	26.9	56.5	73.1	55.6	2.5	3.2	-	-	-
CRQ#1		54	32.2	56.1	67.9	55.4	2	3	204.2	16.5	159.1
CRQ#1	-2.5	-	-	56.3	100	56.3	2.1	3.3	149.9	9.6	229.9
CRQ#1	-4.1	53.3	27	56.7	73	55.8	2.2	3.4	155	22.5	235.8
CRQ#1	-5.6	-	-	56.8	100	56.8	2.2	3.4	188.5	25.7	263.3
CRQ#1	-8.6	-	-	56.9	100	56.9	2.3	3.2	189.7	14.1	255.3
CRQ#1	-10.2	-	-	57	100	57	2.5	3.6	177.8	8.6	176.3
KEL#1	-2.6	-	-	56.7	100	56.7	2.2	2.8	176.8	35.8	112.5
KEL#1	-4.1	-	-	56.8	100	56.8	2.9	3.3	210.4	41.1	132.7
KEL#1	-5.7	-	-	57	100	57	2.9	3.4	211.7	76.8	214.2
KEL#1	-6.4	-	-	56.6	100	56.6	2.2	2.9	179	11.2	103
KEL#1	-9.5	-	-	57.7	100	57.7	2.1	2.8	173.5	12.3	117.9
KEL#1	-13.3	-	-	56.8	100	56.8	2	2.6	184.1	14	141
KEL#1	-15.6	-	-	57.4	100	57.4	1.8	3.2	182.3	17.7	144.7
Limestone											
SCD	-1.8	-	-	-	-	-	-2.9	-2.5	278.1	11.6	93.8
SCD	-1.5	-	-	-	-	-	-4	-3.1	290.4	16	101.1
SCD	-0.8	-	-	-	-	-	-2.3	-2.3	262.7	7	83.2
SCD	-0.3	-	-	-	-	-	-2.7	-2.5	261.3	6.7	122.3
KEL#1	-11.8	-	-	-	-	-		-1.2	242.2	7.4	162.3
[a] depth is relative to the Brac Unvonformity											

Appendix 3. Summary of rare earth elements and yttrium data obtained from Cenozoic carbonate samples on Cayman Brac and Grand Cayman[a]

Units	Sections	Depth (m)	% of calcite	% of dolomite	Y (ppm)	La (ppm)	Ce (ppm)	Pr (ppm)	Nd (ppm)	Sm (ppm)	Eu (ppm)	Gd (ppm)	Tb (ppm)	Dy (ppm)	Ho (ppm)	Er (ppm)	Tm (ppm)	Yb (ppm)	Lu (ppm)
The Brac Formation	SCD	7.6	0	100	1.14	0.44	0.27	0.06	0.26	0.06	-	0.08	-	0.08	0.02	0.06	0.01	-	-
	SCD	8.5	0	100	1.11	0.41	0.27	0.06	0.27	0.05	-	0.11	-	0.09	0.02	0.07	0.01	-	-
	SCD	10.1	0	100	1.00	0.49	0.19	0.06	0.25	0.06	-	0.08	-	0.07	-	0.05	0.01	-	-
	SCD	11.6	5.7	94.3	1.56	0.55	0.30	0.08	0.37	0.07	-	0.15	-	0.14	0.03	0.10	0.01	0.06	-
	SCD	13.1	0	100	0.87	0.36	0.22	0.05	0.23	0.06	-	0.08	-	0.07	-	0.05	0.01	-	-
	SCD	14.6	0	100	0.86	0.30	0.19	0.05	0.21		-	0.09	-	0.07	-	0.06	0.01	-	-
	SCD	15.8	0	100	0.78	0.37	0.18	0.05	0.21	0.05	-	0.07	-	0.06	-	-	-	-	-
	SCD	16.1	100	0	1.21	0.45	0.23	0.06	0.25	0.05	-	0.08	-	0.07	0.02	0.05	0.01	-	-
	SCD	19.2	0	100	1.41	0.64	0.30	0.09	0.38	0.09	-	0.11	-	0.11	0.03	0.08	0.01	-	-
	SCD	23.7	59.5	40.5	1.38	0.49	0.31	0.06	0.26	0.05	-	0.11	-	0.07	-	0.06	0.01	-	-
	SCD	25.0	40.1	59.9	0.91	0.32	0.18	0.05	0.20	-	-	0.07	-	0.05	-	0.04	-	-	-
	SCD	25.2	100	0	1.66	0.54	0.18	0.05	0.23	0.04	-	0.10	-	0.10	0.03	0.08	0.01	0.06	-
	SCD	25.4	100	0	1.01	0.49	0.32	0.06	0.27	0.05	-	0.08	-	0.07	-	0.05	0.01	-	-
	SCD	26.1	100	0	1.35	0.41	0.18	0.05	0.20	-	-	0.09	-	0.06	-	0.05	0.01	-	-
	SCD	26.7	100	0	1.48	0.56	0.32	0.08	0.33	0.07	-	0.12	-	0.09	0.02	0.07	0.01	-	-
	WOJ#7	0.0	0	100	2.32	1.03	0.58	0.16	0.63	0.11	-	0.19	-	0.16	0.04	0.12	0.02	0.09	-
	WOJ#7	0.9	0	100	1.72	0.74	0.43	0.12	0.51	0.10	-	0.17	-	0.14	0.03	0.10	0.01	0.08	-
	WOJ#7	4.3	0	100	1.16	0.44	0.21	0.06	0.25	0.05	-	0.11	-	0.08	0.02	0.06	0.01	-	-
	WOJ#7	5.2	0	100	1.43	0.60	0.29	0.07	0.33	0.07	-	0.11	-	0.11	0.03	0.08	0.01	0.06	-
	WOJ#7	6.1	0	100	1.95	0.70	0.51	0.11	0.47	0.09	-	0.18	-	0.15	0.03	0.11	0.01	0.07	-
	WOJ#7	7.0	0	100	1.87	0.75	0.37	0.10	0.42	0.09	-	0.14	-	0.14	0.03	0.09	0.01	0.06	-
	WOJ#7	7.9	0	100	1.55	0.54	0.32	0.08	0.32	0.06	-	0.13	-	0.11	0.03	0.08	0.01	0.06	-
	WOJ#7	8.8	0	100	2.01	0.79	0.30	0.10	0.43	0.09	-	0.13	-	0.11	0.03	0.08	0.01	0.06	-
	WOJ#7	9.8	0	100	1.73	0.57	0.41	0.09	0.37	0.07	-	0.15	-	0.12	0.03	0.09	0.01	0.06	-
	WOJ#7	10.7	0	100	1.45	0.66	0.30	0.08	0.35	0.08	-	0.10	-	0.08	-	0.06	0.01	-	-

Appendix 3. Summary of rare earth elements and yttrium data obtained from Cenozoic carbonate samples on Cayman Brac and Grand Cayman[a] (continued)

Units	Sections	Depth (m)	∑ REE+Y	Dy_N/Sm_N[e]	La_N/Nd_N[e]	Ce/Ce*	Pr/Pr*	Y/Ho (molar)	Sm/Nd (molar)	Fe (ppm)	Mn (ppm)
The Brac Formation	SCD	7.6	2.5	1.7	1.5	0.4	1.2	100.2	0.211	134.5	14.2
	SCD	8.5	2.5	2.1	1.3	0.4	1.2	88.0	0.181	125.7	11.0
	SCD	10.1	2.2	1.4	1.7	0.2	1.3	-	0.227	169.2	6.5
	SCD	11.6	3.4	2.3	1.3	0.3	1.3	82.9	0.184	109.7	29.5
	SCD	13.1	2.0	1.5	1.4	0.4	1.2	-	0.228	104.4	11.3
	SCD	14.6	1.8	-	1.3	0.4	1.2	-	-	100.9	12.4
	SCD	15.8	1.8	1.3	1.6	0.3	1.3	-	0.233	159.4	14.8
	SCD	16.1	2.5	1.6	1.6	0.3	1.2	108.4	0.202	164.7	7.5
	SCD	19.2	3.2	1.5	1.5	0.3	1.3	101.8	0.217	198.9	12.6
	SCD	23.7	2.8	1.7	1.7	0.4	1.3	-	0.180	94.2	10.5
	SCD	25.0	1.8	-	1.5	0.3	1.3	-	-	76.6	4.5
	SCD	25.2	3.1	2.7	2.1	0.2	1.3	107.9	0.179	93.8	11.6
	SCD	25.4	2.4	1.5	1.6	0.4	1.2	-	0.185	101.1	16.0
	SCD	26.1	2.4	-	1.8	0.3	1.3	-	-	83.2	7.0
	SCD	26.7	3.1	1.5	1.5	0.3	1.2	123.2	0.196	122.3	6.7
	WOJ#7	0.0	5.4	1.6	1.4	0.3	1.4	114.1	0.175	81.0	2.5
	WOJ#7	0.9	4.2	1.7	1.3	0.3	1.3	95.7	0.187	92.5	3.3
	WOJ#7	4.3	2.4	1.8	1.5	0.3	1.4	102.4	0.203	97.6	4.0
	WOJ#7	5.2	3.2	1.8	1.6	0.3	1.3	99.3	0.208	94.6	11.6
	WOJ#7	6.1	4.4	2.0	1.3	0.4	1.2	104.0	0.182	158.1	13.7
	WOJ#7	7.0	4.1	1.8	1.6	0.3	1.3	101.5	0.203	99.5	6.6
	WOJ#7	7.9	3.3	2.1	1.5	0.3	1.3	104.8	0.181	103.9	7.3
	WOJ#7	8.8	4.1	1.5	1.6	0.2	1.3	133.4	0.203	106.1	22.7
	WOJ#7	9.8	3.7	2.0	1.4	0.4	1.2	105.7	0.186	132.2	62.1
	WOJ#7	10.7	3.2	1.2	1.7	0.3	1.3	-	0.220	125.3	12.2

Appendix 3. Summary of rare earth elements and yttrium data obtained from Cenozoic carbonate samples on Cayman Brac and Grand Cayman[a] (continued)

Units	Sections	Depth (m)	% of calcite	% of dolomite	Y (ppm)	La (ppm)	Ce (ppm)	Pr (ppm)	Nd (ppm)	Sm (ppm)	Eu (ppm)	Gd (ppm)	Tb (ppm)	Dy (ppm)	Ho (ppm)	Er (ppm)	Tm (ppm)	Yb (ppm)	Lu (ppm)
The Brac Formation	WOJ#3	6.0	0	100	0.25	0.06	0.29	0.06	-	0.09	-	0.09	0.02	0.06	0.01	-	-	2.6	1.7
	WOJ#3	7.5	50	50	0.22	0.06	0.28	0.06	-	0.07	-	0.06	-	0.05	0.01	-	-	2.5	1.2
	WOJ#3	10.6	0	100	0.96	0.40	0.19	0.05	0.22	0.05	-	0.06	-	0.05	-	-	-	-	-
	WOJ#3	10.9	0	100	1.16	0.48	0.21	0.05	0.25	0.05	-	0.06	-	0.06	-	-	-	-	-
	WOJ#3	12.1	0	100	1.04	0.45	0.20	0.05	0.24	0.06	-	0.06	-	0.05	-	-	-	-	-
	WOJ#3	15.1	0	100	1.15	0.51	0.32	0.07	0.30	0.06	-	0.07	-	0.06	-	-	0.01	-	-
	WOJ#3	19.5	0	100	1.01	0.40	0.17	0.05	0.24	0.09	-	0.11	-	0.10	0.03	0.08	0.02	0.08	-
The Cayamn Formation	CRQ#1	-47.6	0	100	2.18	1.05	0.68	0.14	0.59	0.12	0.03	0.19	-	0.15	0.03	0.09	0.01	0.06	-
	CRQ#1	-49.1	0	100	1.18	0.66	0.51	0.11	0.48	0.10	-	0.14	-	0.10	0.02	0.07	0.01	-	-
	CRQ#1	-50.7	0	100	2.08	1.08	0.84	0.17	0.74	0.15	0.04	0.20	-	0.15	0.03	0.10	0.01	0.07	-
	CRQ#1	-54.5	28.3	71.7	2.11	0.78	0.35	0.09	0.38	0.08	-	0.14	-	0.11	0.03	0.08	0.01	-	-
	CRQ#1	-55.2	0	100	1.71	1.01	0.88	0.16	0.67	0.14	0.03	0.21	-	0.17	0.04	0.10	0.01	0.06	-
	CRQ#1	-56.8	0	100	1.30	0.77	0.68	0.13	0.53	0.11	-	0.16	-	0.13	0.03	0.08	0.01	0.06	-
	CRQ#1	-57.5	16	84	2.56	0.96	0.39	0.11	0.46	0.09	-	0.17	-	0.14	0.03	0.09	0.01	0.06	-
	KEL#1	-29.3	10.9	89.1	1.60	0.77	0.43	0.10	0.44	0.09	-	0.13	-	0.12	0.03	0.08	0.01	0.05	-
	KEL#1	-32.4	84.4	15.6	3.09	1.40	0.85	0.19	0.85	0.18	0.05	0.27	0.04	0.24	0.06	0.17	0.02	0.12	-
	KEL#1	-35.4	0	100	1.39	0.72	0.49	0.10	0.41	0.08	-	0.12	-	0.11	0.03	0.07	0.01	0.05	-
	KEL#1	-37.0	10	90	1.08	0.44	0.19	0.06	0.25	0.06	-	0.08	-	0.08	-	0.06	0.01	-	-
	KEL#1	-38.5	0	100	1.22	0.53	0.35	0.08	0.34	0.06	-	0.15	-	0.11	0.03	0.09	0.01	0.06	-
	KEL#1	-39.2	94.2	5.8	1.09	0.39	0.23	0.05	0.24	0.06	-	0.09	-	0.08	-	0.06	0.01	-	-
	KEL#1	-40.8	100	0	1.17	0.44	0.21	0.06	0.26	0.06	-	0.09	-	0.08	-	0.06	0.01	-	-
	KEL#1	-42.3	0	100	1.57	0.64	0.52	0.10	0.46	0.11	-	0.15	-	0.14	0.03	0.09	0.01	0.08	-
	KEL#1	-43.8	89.6	10.4	1.60	0.65	0.41	0.09	0.41	0.09	-	0.14	-	0.13	0.03	0.09	0.01	0.06	-
	KEL#1	-44.6	0	100	1.08	0.47	0.34	0.07	0.33	0.07	-	0.12	-	0.09	0.02	0.07	0.01	0.05	-
	CRQ#1	18.3	8	92	1.00	0.22	0.19	0.04	0.19	0.04	-	0.12	-	0.11	0.03	0.07	0.01	0.05	-

Appendix 3. Summary of rare earth elements and yttrium data obtained from Cenozoic carbonate samples on Cayman Brac and Grand Cayman[a] (continued)											
Units	Sections	Depth (m)	∑ REE+Y	Dy_N/Sm_N[e]	La_N/Nd_N[e]	Ce/Ce*	Pr/Pr*	Y/Ho (molar)	Sm/Nd (molar)	Fe (ppm)	Mn (ppm)
The Brac Formation	WOJ#3	6.0	1.6	0.3	1.2	97.1	0.199	103.9	13.1	1.15	0.51
	WOJ#3	7.5	1.4	0.3	1.3	-	0.210	92.7	8.6	1.17	0.46
	WOJ#3	10.6	2.0	1.2	1.6	0.3	1.2	-	0.215	99.8	37.8
	WOJ#3	10.9	2.3	1.2	1.7	0.3	1.2	-	0.205	101.8	6.6
	WOJ#3	12.1	2.2	1.1	1.7	0.3	1.2	-	0.222	105.7	15.1
	WOJ#3	15.1	2.5	1.1	1.5	0.4	1.2	-	0.205	113.3	15.4
	WOJ#3	19.5	2.4	1.4	1.5	0.3	1.3	69.4	0.366	198.2	21.1
The Cayamn Formation	CRQ#1	-47.6	5.3	1.4	1.6	0.4	1.2	118.2	0.198	159.1	16.5
	CRQ#1	-49.1	3.4	1.3	1.2	0.4	1.2	88.6	0.195	229.9	9.6
	CRQ#1	-50.7	5.6	1.2	1.3	0.4	1.2	110.9	0.189	235.8	22.5
	CRQ#1	-54.5	4.2	1.8	1.8	0.3	1.3	146.1	0.192	91.5	9.0
	CRQ#1	-55.2	5.2	1.5	1.3	0.5	1.2	88.1	0.196	255.3	14.1
	CRQ#1	-56.8	4.0	1.4	1.3	0.5	1.2	82.9	0.193	176.3	8.6
	CRQ#1	-57.5	5.1	1.8	1.9	0.3	1.4	144.2	0.194	92.8	8.8
	KEL#1	-29.3	3.9	1.5	1.5	0.3	1.3	108.0	0.202	137.0	20.5
	KEL#1	-32.4	7.5	1.6	1.5	0.4	1.2	97.3	0.206	209.5	18.7
	KEL#1	-35.4	3.6	1.6	1.6	0.4	1.2	91.6	0.194	149.6	6.9
	KEL#1	-37.0	2.3	1.6	1.6	0.3	1.3	-	0.237	151.7	9.9
	KEL#1	-38.5	3.0	2.1	1.4	0.4	1.2	73.5	0.182	117.9	12.3
	KEL#1	-39.2	2.3	1.5	1.5	0.3	1.2	-	0.235	173.4	10.9
	KEL#1	-40.8	2.4	1.7	1.5	0.3	1.3	-	0.209	162.3	7.4
	KEL#1	-42.3	3.9	1.5	1.3	0.5	1.2	89.5	0.228	234.8	18.1
	KEL#1	-43.8	3.7	1.6	1.4	0.4	1.2	103.5	0.222	253.7	9.7
	KEL#1	-44.6	2.7	1.7	1.3	0.4	1.2	84.4	0.189	144.7	17.7
	CRQ#1	18.3	2.1	3.0	1.0	0.4	1.2	71.6	0.222	68.5	28.0

Appendix 3. Summary of rare earth elements and yttrium data obtained from Cenozoic carbonate samples on Cayman Brac and Grand Cayman[a] (continued)

Units	Sections	Depth (m)	% of calcite	% of dolomite	Y (ppm)	La (ppm)	Ce (ppm)	Pr (ppm)	Nd (ppm)	Sm (ppm)	Eu (ppm)	Gd (ppm)	Tb (ppm)	Dy (ppm)	Ho ppm)	Er (ppm)	Tm (ppm)	Yb (ppm)	Lu (ppm)
The Cayman Formation	CRQ#1	14.0	23.1	76.9	0.99	0.24	0.19	0.05	0.20	0.05	-	0.12	-	0.11	0.03	0.08	0.01	0.06	-
	CRQ#1	10.4	0	100	0.83	0.34	0.33	0.07	0.33	0.08	-	0.14	-	0.13	0.03	0.08	0.01	0.06	-
	CRQ#1	6.7	0	100	0.55	0.24	0.23	0.05	0.22	0.05	-	0.09	-	0.09	-	0.05	0.01	-	-
	CRQ#1	2.6	0	100	1.37	0.47	0.38	0.09	0.46	0.12	0.03	0.18	-	0.18	0.04	0.12	0.02	0.09	-
	CRQ#1	-1.1	0	100	1.27	0.46	0.39	0.09	0.43	0.11	-	0.15	-	0.15	0.04	0.10	0.01	0.08	-
	CRQ#1	-4.7	0	100	1.38	0.50	0.36	0.09	0.44	0.11	-	0.12	-	0.12	0.03	0.08	0.01	0.07	-
	CRQ#1	-8.4	0	100	0.94	0.35	0.25	0.06	0.28	0.07	-	0.08	-	0.08	-	0.06	0.01	0.05	-
	CRQ#1	-12.0	0	100	0.85	0.32	0.22	0.05	0.26	0.06	-	0.07	-	0.06	-	0.04	-	-	-
	CRQ#1	-15.7	0	100	0.77	0.25	0.17	0.04	0.20	0.05	-	0.07	-	0.06	-	0.04	0.01	-	-
	CRQ#1	-19.4	0	100	0.53	0.18	0.12	0.03	0.14	-	-	0.04	-	-	-	-	-	-	-
	CRQ#1	-21.2	0	100	0.68	0.19	0.13	0.03	0.14	-	-	0.05	-	0.04	-	-	-	-	-
	CRQ#1	-23.0	0	100	0.94	0.24	0.18	0.04	0.19	0.05	-	0.07	-	0.06	-	-	-	-	-
	CRQ#1	-26.7	0	100	1.05	0.31	0.23	0.05	0.23	0.06	-	0.07	-	0.07	-	0.04	-	-	-
	CRQ#1	-30.3	0	100	1.34	0.38	0.28	0.07	0.28	0.07	-	0.09	-	0.09	-	0.05	0.01	-	-
	CRQ#1	-34.0	0	100	1.29	0.35	0.25	0.06	0.27	0.07	-	0.10	-	0.09	0.02	0.06	0.01	-	-
	CRQ#1	-37.6	0	100	0.94	0.28	0.20	0.05	0.21	0.05	-	0.07	-	0.06	-	-	-	-	-
	CRQ#1	-39.5	0	100	0.79	0.25	0.17	0.04	0.19	0.05	-	0.08	-	0.07	-	0.04	-	-	-
	CRQ#1	-43.8	0	100	1.04	0.37	0.25	0.07	0.28	0.07	-	0.11	-	0.09	0.02	0.06	0.01	-	-
	CRQ#1	-45.3	0	100	1.15	0.43	0.31	0.07	0.30	0.07	-	0.12	-	0.09	-	0.06	0.01	-	-
	BW#1	-17.7	0	100	0.76	0.30	0.29	0.06	0.27	0.07	-	0.09	-	0.08	0.02	0.05	0.01	-	-
	BW#1	-19.2	0	100	1.02	0.33	0.33	0.07	0.32	0.08	-	0.11	-	0.10	0.03	0.07	0.01	0.05	-
	BW#1	-21.5	0	100	1.25	0.35	0.34	0.07	0.33	0.08	-	0.12	-	0.12	0.03	0.08	0.01	0.07	-
	BW#1	-23.8	0	100	0.87	0.25	0.21	0.05	0.22	0.05	-	0.08	-	0.08	-	0.06	0.01	-	-
	BW#1	-25.3	0	100	0.86	0.23	0.19	0.04	0.21	0.05	-	0.08	-	0.08	-	0.05	0.01	-	-
	BW#1	-26.8	0	100	0.79	0.24	0.19	0.04	0.20	0.05	-	0.08	-	0.08	-	0.05	0.01	-	-

Appendix 3. Summary of rare earth elements and yttrium data obtained from Cenozoic carbonate samples on Cayman Brac and Grand Cayman[a] (continued)											
Units	Sections	Depth (m)	∑ REE+Y	Dy_N/Sm_N[e]	La_N/Nd_N[e]	Ce/Ce*	Pr/Pr*	Y/Ho (molar)	Sm/Nd (molar)	Fe (ppm)	Mn (ppm)
The Cayman Formation	CRQ#1	14.0	2.1	2.9	1.0	0.4	1.2	66.4	0.222	62.9	26.3
	CRQ#1	10.4	2.4	2.0	0.9	0.5	1.2	53.8	0.222	52.4	24.0
	CRQ#1	6.7	1.6	1.9	1.0	0.5	1.1		0.230	78.7	19.6
	CRQ#1	2.6	3.6	1.9	0.9	0.4	1.1	59.4	0.242	76.0	10.3
	CRQ#1	-1.1	3.3	1.7	1.0	0.4	1.2	65.0	0.239	78.9	11.2
	CRQ#1	-4.7	3.3	1.3	1.0	0.4	1.2	90.4	0.242	87.7	16.7
	CRQ#1	-8.4	2.2	1.3	1.1	0.4	1.2	-	0.251	97.2	27.2
	CRQ#1	-12.0	1.9	1.1	1.1	0.4	1.1	-	0.241	86.0	19.3
	CRQ#1	-15.7	1.7	1.7	1.1	0.4	1.2	-	0.227	106.6	64.9
	CRQ#1	-19.4	1.0	-	1.2	0.4	1.3	-	-	108.6	42.8
	CRQ#1	-21.2	1.3	-	1.2	0.4	1.2	-	-	116.3	37.0
	CRQ#1	-23.0	1.8	1.3	1.1	0.4	1.2	-	0.257	102.5	32.8
	CRQ#1	-26.7	2.1	1.3	1.2	0.4	1.2	-	0.253	101.4	50.5
	CRQ#1	-30.3	2.7	1.5	1.2	0.4	1.2	-	0.236	92.3	54.0
	CRQ#1	-34.0	2.6	1.5	1.2	0.4	1.3	116.6	0.235	84.3	55.5
	CRQ#1	-37.6	1.9	1.3	1.2	0.4	1.2	-	0.250	89.6	21.0
	CRQ#1	-39.5	1.7	1.6	1.1	0.4	1.3	-	0.247	79.0	11.8
	CRQ#1	-43.8	2.4	1.6	1.1	0.4	1.3	94.8	0.235	109.2	15.9
	CRQ#1	-45.3	2.6	1.7	1.3	0.4	1.2		0.213	116.3	9.9
	BW#1	-17.7	2.0	1.5	1.0	0.5	1.2	67.8	0.241	118.3	13.5
	BW#1	-19.2	2.5	1.5	0.9	0.5	1.2	75.2	0.245	136.5	16.2
	BW#1	-21.5	2.9	1.8	0.9	0.5	1.2	79.1	0.234	144.3	20.4
	BW#1	-23.8	1.9	1.8	1.0	0.4	1.2	-	0.224	147.2	17.2
	BW#1	-25.3	1.8	1.8	1.0	0.4	1.1	-	0.234	103.1	18.1
	BW#1	-26.8	1.7	1.8	1.0	0.4	1.2	-	0.243	130.3	21.2

Appendix 3. Summary of rare earth elements and yttrium data obtained from Cenozoic carbonate samples on Cayman Brac and Grand Cayman[a] (continued)

Units	Sections	Depth (m)	% of calcite	% of dolomite	Y (ppm)	La (ppm)	Ce (ppm)	Pr (ppm)	Nd (ppm)	Sm (ppm)	Eu (ppm)	Gd (ppm)	Tb (ppm)	Dy (ppm)	Ho (ppm)	Er (ppm)	Tm (ppm)	Yb (ppm)	Lu (ppm)
The Cayman Formation	BW#1	-28.4	0	100	0.74	0.22	0.17	0.04	0.19	0.05	-	0.07	-	0.07	-	0.05	-	-	-
	BW#1	-31.4	0	100	0.82	0.26	0.17	0.04	0.20	0.05	-	0.07	-	0.07	-	0.05	0.01	-	-
	BW#1	-39.0	0	100	0.66	0.21	0.16	0.04	0.18	0.04	-	0.06	-	0.06	-	0.04	0.01	-	-
	BW#1	-42.1	0	100	0.69	0.23	0.17	0.04	0.18	0.05	-	0.07	-	0.07	-	0.04	-	-	-
	BW#1	-43.6	0	100	0.75	0.25	0.19	0.04	0.19	0.05	-	0.07	-	0.07	-	0.05	0.01	-	-
	SQW#1	0.3	0	100	0.64	0.19	0.15	0.03	0.15	-	-	0.06	-	0.06	-	-	-	-	-
	SQW#1	-0.2	0	100	1.06	0.33	0.28	0.06	0.28	0.07	-	0.12	-	0.12	0.03	0.08	0.01	0.06	-
	SQW#1	-2.9	5.43	94.57	0.77	0.30	0.33	0.06	0.27	0.06	-	0.11	-	0.10	0.02	0.06	0.01	-	-
	SQW#1	-5.6	7.2	92.8	1.61	0.68	0.68	0.16	0.66	0.15	0.04	0.24	0.03	0.21	0.05	0.14	0.02	0.10	-
	SQW#1	-8.4	34.52	65.48	1.26	0.52	0.57	0.11	0.47	0.10	0.03	0.17	-	0.15	0.03	0.10	0.01	0.07	-
	SQW#1	-11.1	0	100	1.00	0.37	0.40	0.08	0.35	0.08	-	0.14	-	0.12	0.03	0.08	0.01	0.06	-
	SQW#1	-13.9	0	100	0.78	0.30	0.29	0.06	0.27	0.06	-	0.11	-	0.09	0.02	0.06	0.01	-	-
	SQW#1	-15.7	0	100	1.20	0.47	0.53	0.11	0.49	0.11	-	0.17	-	0.15	0.03	0.09	0.01	0.07	-
	SQW#1	-18.4	0	100	1.88	0.69	0.86	0.17	0.77	0.19	0.05	0.27	0.04	0.24	0.05	0.15	0.02	0.11	-
	SQW#1	-21.2	8.03	91.97	1.46	0.44	0.51	0.10	0.47	0.11	-	0.17	-	0.15	0.03	0.10	0.01	0.07	-
	SQW#1	-25.8	11.25	88.75	1.76	0.71	0.90	0.18	0.78	0.18	0.04	0.23	0.03	0.21	0.05	0.14	0.02	0.10	-
	SQW#1	-28.5	17.08	82.92	1.56	0.57	0.64	0.13	0.57	0.14	0.03	0.19	-	0.17	0.04	0.11	0.02	0.08	-
	SQW#1	-30.3	24.96	75.04	2.16	0.66	0.96	0.17	0.78	0.19	0.05	0.26	0.04	0.24	0.05	0.15	0.02	0.12	-
	SQW#1	-31.2	13.33	86.67	1.51	0.52	0.56	0.11	0.50	0.12	-	0.17	-	0.15	0.04	0.10	0.01	0.08	-
	SQW#1	-34.0	8.89	91.11	1.94	0.59	0.66	0.14	0.66	0.16	0.04	0.22	0.03	0.20	0.05	0.14	0.02	0.11	-
	SQW#1	-35.8	6.81	93.19	1.56	0.48	0.56	0.11	0.48	0.12	0.03	0.18	-	0.17	0.04	0.11	0.01	0.08	-
	SQW#1	-37.6	0	100	1.75	0.46	0.48	0.10	0.46	0.12	-	0.18	-	0.17	0.04	0.12	0.02	0.09	-
	SQW#1	-39.5	6.35	93.65	1.35	0.45	0.39	0.09	0.40	0.10	-	0.15	-	0.14	0.03	0.09	0.01	0.08	-
	SQW#1	-40.4	9.96	90.04	1.59	0.57	0.59	0.12	0.55	0.13	0.03	0.19	-	0.17	0.04	0.12	0.01	0.09	-
	SQW#1	-43.1	7.46	92.54	1.24	0.43	0.42	0.09	0.40	0.10	-	0.15	-	0.13	0.03	0.09	0.01	0.07	-

Appendix 3. Summary of rare earth elements and yttrium data obtained from Cenozoic carbonate samples on Cayman Brac and Grand Cayman[a] (continued)

Units	Sections	Depth (m)	∑ REE+Y	Dy_N/Sm_N[e]	La_N/Nd_N[e]	Ce/Ce*	Pr/Pr*	Y/Ho (molar)	Sm/Nd (molar)	Fe (ppm)	Mn (ppm)
The Cayman Formatioin	BW#1	-28.4	1.6	1.6	1.0	0.4	1.2	-	0.251	136.3	20.8
	BW#1	-31.4	1.7	1.6	1.1	0.4	1.2	-	0.253	133.2	23.3
	BW#1	-39.0	1.5	1.7	1.1	0.4	1.2	-	0.235	121.5	18.1
	BW#1	-42.1	1.5	1.7	1.1	0.4	1.2	-	0.247	115.9	18.6
	BW#1	-43.6	1.7	1.6	1.1	0.4	1.2	-	0.252	150.7	20.3
	SQW#1	0.3	1.3	-	1.1	0.4	1.2	-	-	104.7	19.9
	SQW#1	-0.2	2.5	2.0	1.0	0.5	1.2	69.2	0.246	71.9	23.4
	SQW#1	-2.9	2.1	1.8	1.0	0.6	1.2	64.3	0.222	92.0	15.1
	SQW#1	-5.6	4.8	1.7	0.9	0.5	1.3	62.3	0.218	141.1	30.5
	SQW#1	-8.4	3.6	1.7	1.0	0.6	1.2	68.4	0.212	173.2	30.4
	SQW#1	-11.1	2.7	1.7	0.9	0.5	1.1	66.9	0.222	150.6	19.6
	SQW#1	-13.9	2.1	1.8	1.0	0.5	1.1	69.6	0.212	112.9	20.7
	SQW#1	-15.7	3.4	1.6	0.9	0.6	1.1	68.7	0.213	140.9	19.0
	SQW#1	-18.4	5.5	1.5	0.8	0.6	1.2	66.3	0.232	241.4	25.4
	SQW#1	-21.2	3.6	1.6	0.8	0.6	1.1	77.4	0.233	138.4	16.8
	SQW#1	-25.8	5.3	1.4	0.8	0.6	1.2	70.7	0.224	205.2	21.0
	SQW#1	-28.5	4.3	1.4	0.9	0.5	1.2	73.1	0.236	225.0	19.8
	SQW#1	-30.3	5.8	1.5	0.8	0.7	1.1	75.5	0.232	182.4	23.0
	SQW#1	-31.2	3.9	1.5	0.9	0.5	1.2	79.7	0.232	186.4	26.7
	SQW#1	-34.0	4.9	1.5	0.8	0.5	1.2	75.6	0.226	153.5	23.9
	SQW#1	-35.8	3.9	1.6	0.9	0.6	1.1	76.7	0.246	141.8	23.8
	SQW#1	-37.6	4.0	1.7	0.9	0.5	1.1	79.7	0.244	151.6	21.4
	SQW#1	-39.5	3.3	1.6	1.0	0.4	1.2	79.0	0.238	146.5	22.8
	SQW#1	-40.4	4.2	1.5	0.9	0.5	1.2	74.7	0.235	183.5	26.9
	SQW#1	-43.1	3.1	1.6	1.0	0.5	1.2	76.5	0.229	149.3	32.7

Appendix 3. Summary of rare earth elements and yttrium data obtained from Cenozoic carbonate samples on Cayman Brac and Grand Cayman[a] (continued)

Units	Sections	Depth (m)	% of calcite	% of dolomite	Y (ppm)	La (ppm)	Ce (ppm)	Pr (ppm)	Nd (ppm)	Sm (ppm)	Eu (ppm)	Gd (ppm)	Tb (ppm)	Dy (ppm)	Ho (ppm)	Er (ppm)	Tm (ppm)	Yb (ppm)	Lu (ppm)
The Cayman Formation	CRQ#1	8.4	0	100	0.86	0.20	0.14	0.04	0.19	0.05	-	0.07	-	0.07	-	0.05	0.01	-	-
	CRQ#1	9.9	0	100	0.52	0.16	0.11	0.03	0.12	-	-	0.05	-	0.04	-	-	-	-	-
	CRQ#1	11.4	14.8	85.2	0.61	0.16	0.11	0.03	0.13	0.04	-	0.06	-	0.05	-	0.04	0.01	-	-
	CRQ#1	14.5	0	100	0.84	0.28	0.32	0.06	0.26	0.07	-	0.09	-	0.09	-	0.06	0.01	-	-
	CRQ#1	17.5	0	100	1.14	0.34	0.29	0.06	0.28	0.08	-	0.11	-	0.11	0.03	0.08	0.01	0.06	-
	CRQ#1	20.6	33.1	66.9	0.99	0.25	0.20	0.05	0.24	0.07	-	0.10	-	0.10	0.02	0.07	0.01	0.06	-
	CRQ#1	22.1	0	100	1.17	0.30	0.22	0.05	0.24	0.07	-	0.10	-	0.10	0.03	0.08	0.01	0.06	-
	CRQ#1	23.6	0	100	0.59	0.21	0.16	0.04	0.16	0.05	-	0.07	-	0.06	-	-	-	-	-
	CRQ#1	25.1		54.6	0.71	0.16	0.11	0.03	0.14	0.05	-	0.07	-	0.07	-	0.05	0.01	-	-
	CRQ#1	28.2	53.8	46.2	1.45	0.30	0.21	0.06	0.28	0.08	-	0.12	-	0.13	0.03	0.10	0.01	0.08	-
	KEL#1	-2.7	0	100	0.46	0.18	0.12	0.03	0.15	0.05	-	0.06	-	0.06	-	-	-	-	-
	KEL#1	-5.7	0	100	0.85	0.36	0.29	0.07	0.31	0.10	-	0.11	-	0.10	0.02	0.07	0.01	-	-
	KEL#1	-9.5	0	100	0.58	0.21	0.13	0.04	0.16	0.05	-	0.06	-	0.06	-	-	0.01	-	-
	KEL#1	-12.6	0	100	0.76	0.27	0.20	0.05	0.24	0.07	-	0.09	-	0.08	0.02	0.06	0.01	-	-
	KEL#1	-14.9	0	100	1.05	0.31	0.23	0.06	0.28	0.07	-	0.11	-	0.11	0.03	0.07	0.01	0.06	-
	KEL#1	-17.9	0	100	1.13	0.34	0.25	0.06	0.30	0.08	-	0.12	-	0.12	0.03	0.08	0.01	0.06	-
	KEL#1	-21.7	0	100	1.20	0.34	0.29	0.06	0.31	0.09	-	0.12	-	0.12	0.03	0.08	0.01	0.06	-
	KEL#1	-24.0	0	100	0.87	0.27	0.18	0.05	0.25	0.07	-	0.10	-	0.09	0.02	0.06	0.01	-	-
	KEL#1	-27.1	0	100	0.98	0.31	0.21	0.06	0.27	0.07	-	0.11	-	0.10	0.02	0.07	0.01	0.05	-
	KEL#1	-28.6	0	100	1.09	0.41	0.26	0.07	0.31	0.08	-	0.11	-	0.10	0.02	0.07	0.01	0.05	-
	NSC#1	-57.3	100	0	0.99	0.26	0.26	0.05	0.25	0.06	-	0.13	-	0.10	0.02	0.07	0.01	0.05	-
	NSC#1	-60.0	100	0	0.90	0.28	0.28	0.06	0.26	0.06	-	0.15	-	0.11	0.03	0.08	0.01	0.06	-
The Pedro Castle Formation	BW#1	-12.4	17.35	82.65	1.94	0.38	0.31	0.08	0.39	0.09	-	0.16	-	0.18	0.05	0.13	0.02	0.10	-
	BW#1	-14.6	100	0	2.52	0.63	0.66	0.13	0.62	0.15	0.04	0.23	0.04	0.24	0.06	0.17	0.02	0.13	-
	SQW#1	5.5	85	15	1.24	0.30	0.34	0.06	0.31	0.07	-	0.11	-	0.10	0.03	0.07	0.01	0.06	-
	SQW#1	2.8	0	100	1.35	0.32	0.31	0.06	0.27	0.07	-	0.11	-	0.12	0.03	0.08	0.01	0.06	-

Appendix 3. Summary of rare earth elements and yttrium data obtained from Cenozoic carbonate samples on Cayman Brac and Grand Cayman[a] (continued)

Units	Sections	Depth (m)	∑ REE (+Y)	Dy_N/Sm_N[e]	La_N/Nd_N[e]	Ce/Ce*	Pr/Pr*	Y/Ho (molar)	Sm/Nd (molar)	Fe (ppm)	Mn (ppm)
The Cayamn Formation	CRQ#1	8.4	1.7	1.7	0.9	0.4	1.2	-	0.254	100.8	27.0
	CRQ#1	9.9	1.0	-	1.1	0.4	1.2	-	-	99.3	8.9
	CRQ#1	11.4	1.2	1.5	1.1	0.4	1.2	-	0.296	117.2	15.5
	CRQ#1	14.5	2.1	1.6	1.0	0.6	1.1	-	0.252	190.8	25.8
	CRQ#1	17.5	2.6	1.6	1.1	0.5	1.2	81.1	0.281	113.4	38.9
	CRQ#1	20.6	2.2	1.7	1.0	0.4	1.2	75.0	0.291	114.2	27.3
	CRQ#1	22.1	2.4	1.8	1.1	0.4	1.2	84.1	0.277	127.0	27.9
	CRQ#1	23.6	1.3	1.6	1.1	0.4	1.2	-	0.282	133.6	32.1
	CRQ#1	25.1	1.4	1.6	1.0	0.4	1.2	-	0.324	147.0	21.4
	CRQ#1	28.2	2.9	1.9	1.0	0.4	1.2	83.6	0.283	136.1	21.0
	KEL#1	-2.7	1.1	1.3	1.1	0.4	1.3	-	0.333	136.0	45.4
	KEL#1	-5.7	2.3	1.3	1.0	0.4	1.2	64.0	0.294	144.0	82.5
	KEL#1	-9.5	1.3	1.4	1.1	0.3	1.3	-	0.299	160.1	30.9
	KEL#1	-12.6	1.9	1.5	1.0	0.4	1.2	67.3	0.266	237.7	20.7
	KEL#1	-14.9	2.4	1.8	1.0	0.4	1.1	75.0	0.252	122.9	22.5
	KEL#1	-17.9	2.6	1.7	1.0	0.4	1.2	79.0	0.262	136.4	27.8
	KEL#1	-21.7	2.7	1.6	1.0	0.5	1.1	81.4	0.292	185.3	31.0
	KEL#1	-24.0	2.0	1.5	1.0	0.4	1.2	75.0	0.282	129.3	32.9
	KEL#1	-27.1	2.3	1.7	1.0	0.4	1.2	79.8	0.246	138.7	26.5
	KEL#1	-28.6	2.6	1.6	1.2	0.4	1.2	84.0	0.242	253.2	47.5
	NSC#1	-57.3	2.3	1.9	0.9	0.5	1.1	75.5	0.238	105.9	9.1
	NSC#1	-60.0	2.3	2.3	1.0	0.5	1.2	61.5	0.219	108.8	8.3
The Pedro Castle Formation	BW#1	-12.4	3.8	2.2	0.9	0.4	1.2	79.5	0.233	205.2	29.0
	BW#1	-14.6	5.6	1.9	0.9	0.5	1.1	82.6	0.228	296.2	58.4
	SQW#1	5.5	2.7	1.7	0.9	0.6	1.1	90.1	0.230	229.3	28.4
	SQW#1	2.8	2.8	2.0	1.0	0.5	1.2	86.9	0.246	108.9	22.8

Appendix 3. Summary of rare earth elements and yttrium data obtained from Cenozoic carbonate samples on Cayman Brac and Grand Cayman[a] (continued)

Units	Sections	Depth (m)	% of calcite	% of dolomite	Y (ppm)	La (ppm)	Ce (ppm)	Pr (ppm)	Nd (ppm)	Sm (ppm)	Eu (ppm)	Gd (ppm)	Tb (ppm)	Dy (ppm)	Ho (ppm)	Er (ppm)	Tm (ppm)	Yb (ppm)	Lu (ppm)
The Ironshore Formation	BW#1	-2.1	100	0	1.79	0.32	0.39	0.08	0.37	0.10	0.03	0.16	-	0.18	0.05	0.13	0.02	0.10	-
	BW#1	-3.6	54.38	45.62	2.18	0.63	0.84	0.15	0.68	0.17	0.05	0.25	0.04	0.25	0.06	0.17	0.02	0.13	-
	BW#1	-8.9	100	0	1.50	0.26	0.24	0.06	0.29	0.07	-	0.13	-	0.14	0.04	0.11	0.02	0.09	-
	RWP#11 (M) [b]	-3.8	100	0	1.21	0.18	0.19	0.05	0.21	0.06	-	0.14	-	0.12	0.03	0.10	0.01	0.07	-
	RWP#11 (M) b	-4.6	100	0	1.01	0.16	0.23	0.04	0.19	0.05	-	0.11	-	0.10	0.02	0.08	0.01	0.08	-
	RWP#11 (M) [b]	-6.7	100	0	1.17	0.31	0.34	0.07	0.31	0.06	-	0.13	-	0.12	0.03	0.09	0.01	0.06	-
	RWP#11 (C) [c]	-9.8	100d	0	0.10	0.03	-	-	-	-	-	0.03	-	-	-	-	-	-	-
	RWP#11 (C) [c]	-15.1	100d	0	0.37	0.12	0.12	0.03	0.13		-	0.07	-	0.04	-	-	-	-	-

Appendix 3. Summary of rare earth elements and yttrium data obtained from Cenozoic carbonate samples on Cayman Brac and Grand Cayman[a] (continued)

Units	Sections	Depth (m)	∑ REE+Y	Dy_N/Sm_N [e]	La_N/Nd_N [e]	Ce/Ce*	Pr/Pr*	Y/Ho (molar)	Sm/Nd (molar)	Fe (ppm)	Mn (ppm)
The Ironshore Formation	BW#1	-2.1	3.7	2.1	0.8	0.6	1.2	73.0	0.265	183.7	7.6
	BW#1	-3.6	5.6	1.7	0.8	0.6	1.1	68.8	0.242	259.7	47.0
	BW#1	-8.9	2.9	2.2	0.8	0.4	1.2	76.6	0.247	130.0	11.7
	RWP#11 (M) [b]	-3.8	2.4	2.5	0.8	0.5	1.3	78.5	0.260	139.5	4.5
	RWP#11 (M) [b]	-4.6	2.1	2.4	0.8	0.6	1.2	80.4	0.244	203.3	7.9
	RWP#11 (M) [b]	-6.7	2.7	2.2	0.9	0.5	1.1	76.9	0.194	188.7	15.9
	RWP#11 (C) [c]	-9.8	0.2	-	-	-	-	-	-	370.5	2.8
	RWP#11 (C) [c]	-15.1	0.9	-	0.8	0.5	1.1	-	-	87.2	5.3

[a] Except for NSC#1 and RWP#11 that are located on Grand Cayman, the rest of sections are from Cayman Brac. Depth is relative to sea level. See Methods section for explanations of derivation of each parameter

[b] M-Matrix

[c] C-Coral

[d] formed of 100% of aragonite

[e] N-shale normalized

Detection limits (ppm): Fe (3.7), Mn (0.03), Y (0.02), La (0.03), Ce (0.03), Pr (0.004), Nd (0.03), Sm (0.04), Eu (0.03), Gd (0.03), Tb (0.03), Dy (0.03), Ho (0.02), Er (0.04), Tm (0.006), Yb (0.05), Lu (0.04).

- below the detection limit